

Modulating cell behaviour through biomimetic multilayers of natural and semi-synthetic glycosaminoglycans

Dissertation
zur Erlangung des
Doktorgrades der Naturwissenschaften (Dr. rer. nat.)

der

Naturwissenschaftliche Fakultät I – Biowissenschaften –

der Martin-Luther-Universität
Halle-Wittenberg,

vorgelegt

von M.Sc. Neha Aggarwal

geb. am 16.02.1984 in Palwal, India

Gutachter: Prof. Dr. Thomas Groth
Prof. Dr. Karsten Mäder
Prof. Dr. Manuel Salmeron-Sanchez

Datum der öffentlichen Verteidigung: 17.06.2014

To My Family

Contents

Table of Contents

| | |
|--|-----------|
| ABSTRACT | 6 |
| ZUSAMMENFASSUNG | 8 |
| Chapter 1 | 10 |
| Introduction | 10 |
| 1.1 Background..... | 10 |
| 1.2 Basics of cell adhesion on biomaterial surfaces..... | 11 |
| 1.3 Cell growth on biomaterial surfaces | 16 |
| 1.4 Surface modification of biomaterials..... | 17 |
| 1.4.1. Layer-by-layer (LBL) Assembly | 18 |
| 1.4.1.1. General potential of LBL in biomedical applications | 19 |
| 1.4.1.2. Effects of deposition conditions on multilayer properties | 21 |
| 1.4.1.3. LBL films prepared by blending of polyelectrolytes | 24 |
| 1.4.1.4. Controlling protein adsorption and cellular responses on LBL films | 24 |
| 1.4.2. Polyelectrolytes used during this study | 26 |
| 1.4.2.1. Polycations | 26 |
| 1.4.2.2. Polyanions | 28 |
| 1.5 Motivation..... | 30 |
| 1.6 Overview of thesis and summary of papers | 31 |
| 1.7. References..... | 43 |
| Chapter 2 | 63 |
| Tuning cell adhesion and growth on biomimetic polyelectrolyte multilayers by variation of pH during layer-by-layer assembly | 63 |
| 2.1. Abstract..... | 63 |
| 2.2. Introduction..... | 64 |
| 2.3. Materials and Methods..... | 65 |
| 2.3.1. Materials | 65 |
| 2.3.2. Polyelectrolyte Multilayer (PEM) Assembly | 66 |
| 2.3.3. Physical Characterization of Multilayers | 66 |
| 2.3.4. Biological Investigations | 68 |
| 2.4. Results and Discussion..... | 69 |
| 2.4.1. Measurements of Wetting Properties During Multilayer Formation | 69 |
| 2.4.2. Measurements of Multilayer Growth | 71 |
| 2.4.3. Studies of Multilayer Surface Topography by Atomic Force Microscopy (AFM) | 76 |
| 2.4.4. Adhesion and Growth of C2C12 Cells on Multilayers | 77 |
| 2.5. Conclusion | 82 |
| 2.6. Acknowledgements | 83 |
| 2.7. References..... | 83 |
| Chapter 3 | 86 |
| Synthesis of novel cellulose derivatives and investigation of their mitogenic activity in the presence and absence of FGF2 | 86 |
| 3.1. Abstract..... | 86 |
| 3.2. Introduction..... | 86 |
| 3.3. Experimental | 88 |
| 3.3.1. Cellulose materials for chemical modification | 88 |
| 3.3.2. Synthesis of cellulose sulfates (CS) | 88 |
| 3.3.3. Oxidation of CS | 89 |

| | | |
|---|---|------------|
| 3.3.4. | Carboxymethylation of CS | 89 |
| 3.3.5. | Characterization of reaction products | 90 |
| 3.3.6. | Preparation of solutions of heparin and cellulose derivatives for biological experiments 90 | |
| 3.3.7. | Cell culture..... | 91 |
| 3.3.8. | Cytotoxicity assay..... | 91 |
| 3.3.9. | Investigation of mitogenic effects of cellulose derivatives on 3T3-L1 fibroblasts | 91 |
| 3.4. | Results and discussion | 92 |
| 3.4.1. | Synthesis of CS | 92 |
| 3.4.2. | Oxidation of CS | 95 |
| 3.4.3. | Carboxymethylation of CS | 95 |
| 3.4.4. | Cytotoxicity measurements | 99 |
| 3.4.5. | Screening investigation on mitogenic effects of cellulose derivatives in the presence of FGF2 101 | |
| 3.4.6. | Concentration-dependent effects of cellulose derivatives on 3T3 cell proliferation in the presence of exogenous FGF2 | 103 |
| 3.4.7. | Concentration-dependent effects of cellulose derivatives on 3T3 cell proliferation in the absence of exogenous FGF2..... | 106 |
| 3.5. | Summary and conclusions | 109 |
| 3.6. | Acknowledgment | 109 |
| 3.7. | References..... | 109 |
| Chapter 4..... | | 114 |
| Study on multilayer structures prepared from heparin and semi-synthetic cellulose sulfates as polyanions and their influence on cellular response..... | | 114 |
| 4.1. | Abstract..... | 114 |
| 4.2. | Introduction..... | 115 |
| 4.3. | Experimental Section | 118 |
| 4.3.1. | Materials | 118 |
| 4.3.2. | Synthesis of cellulose sulfates (CS) | 118 |
| 4.3.3. | Characterization of cellulose sulfate (CS) and heparin | 119 |
| 4.3.4. | Polyelectrolyte Multilayer Formation | 119 |
| 4.3.5. | Characterization of Multilayer | 120 |
| 4.3.5.1. | Measurement of mass adsorption and multilayer growth:..... | 120 |
| 4.3.5.2. | Water contact angle and zeta potential measurements | 121 |
| 4.3.6. | Biological Investigations | 122 |
| 4.3.6.1. | Cell culture..... | 122 |
| 4.3.6.2. | Cell adhesion and spreading..... | 122 |
| 4.3.6.3. | Cell morphology..... | 123 |
| 4.3.6.4. | Cell growth measurements..... | 123 |
| 4.4. | Results and Discussion..... | 124 |
| 4.4.1. | Cellulose sulfates and heparin..... | 124 |
| 4.4.2. | Characterization of multilayer formation..... | 126 |
| 4.4.2.1. | Measurement of fibronectin adsorption by QCM-D | 130 |
| 4.4.3. | Water contact angle (WCA) and zeta potential measurements | 131 |
| 4.4.4. | Adhesion and growth of C2C12 cells on multilayers | 134 |
| 4.5. | Conclusion | 140 |
| 4.6. | Acknowledgements | 141 |
| 4.7. | References..... | 141 |
| 4.8. | Supporting Information..... | 147 |
| Chapter 5..... | | 149 |
| Effect of molecular composition of heparin and cellulose sulfate on multilayer formation and cell response..... | | 149 |
| 5.1. | Abstract..... | 149 |
| 5.2. | Introduction..... | 150 |

| | |
|---|------------|
| 5.3. Materials and Methods..... | 152 |
| 5.3.1. Materials..... | 152 |
| 5.3.2. Synthesis of cellulose sulfate (CS)..... | 153 |
| 5.3.3. Characterization of cellulose sulfate (CS) and heparin..... | 153 |
| 5.3.4. Polyelectrolyte multilayer assembly..... | 154 |
| 5.3.5. Characterization of multilayer properties..... | 154 |
| 5.3.5.1. <i>Measurement of multilayer growth and mass.....</i> | 154 |
| 5.3.5.2. <i>Water contact angle and surface zeta potential measurements.....</i> | 156 |
| 5.3.6. Biological studies..... | 157 |
| 5.3.6.1. <i>Cell culture.....</i> | 157 |
| 5.3.6.2. <i>Measurement of cell adhesion and spreading.....</i> | 157 |
| 5.3.6.3. <i>Cell morphology.....</i> | 157 |
| 5.3.6.4. <i>Growth of C2C12 cells.....</i> | 158 |
| 5.4 Results and Discussion..... | 158 |
| 5.4.1. Synthesis of cellulose sulfate and analysis of chemical compositions..... | 158 |
| 5.4.2. Characterization of multilayer formation..... | 161 |
| 5.4.3. Measurements of wetting properties..... | 166 |
| 5.4.4. Measurement of zeta potentials..... | 168 |
| 5.4.5. Adhesion and growth of C2C12 cells on multilayers..... | 170 |
| 5.5. Conclusions..... | 176 |
| 5.6. Acknowledgements..... | 176 |
| 5.7. References..... | 176 |
| Chapter 6..... | 182 |
| Multilayer films by blending heparin with semi-synthetic cellulose sulfates: Physico-chemical characterisation and cell responses..... | 182 |
| 6.1. Abstract..... | 182 |
| 6.2. Introduction..... | 182 |
| 6.3. Materials and Methods..... | 185 |
| 6.3.1. Characterization of multilayer properties..... | 186 |
| 6.3.2. Biological Investigations..... | 187 |
| 6.4 Results and Discussion..... | 188 |
| 6.4.1. Multilayer growth measurement..... | 188 |
| 6.4.2. Measurements of wetting properties..... | 194 |
| 6.4.3. Adhesion measurements and morphological studies of C2C12 cells on multilayers..... | 195 |
| 6.5. Conclusions..... | 199 |
| 6.6. Acknowledgements..... | 199 |
| 6.7. References..... | 200 |
| 6.8. Supplementary Information..... | 205 |
| Chapter 7..... | 206 |
| Conclusions and Outlook..... | 206 |
| Acknowledgements..... | 209 |
| Abbreviations..... | 210 |
| Publication list with declaration of self contribution..... | 213 |
| Curriculum Vitae..... | 215 |
| Eidesstattliche Erklärung..... | 217 |

ABSTRACT

Controlling the surface properties is a key aspect in the field of biomaterials. Among the available surface modification techniques, a simple yet facile technique, called layer-by-layer (LBL) method, has been widely exploited due to its numerous applications including the biomedical field. LBL technique, based on the alternate adsorption of oppositely charged polyelectrolytes (PEL) onto charged surfaces, has been applied here to design multilayers of heparin (HEP) and cellulose sulfates (CS) as polyanions on glass as model substrate to obtain control over cell adhesion and growth. First studies were carried out with HEP and chitosan (CHI), which showed that a change of pH value during multilayer formation affected not only multilayer assembly and surface properties, but also adsorption of fibronectin (FN) and subsequent adhesion and growth of cells. Since HEP is a natural glycosaminoglycan with limited abundance, semi-synthetic cellulose derivatives were synthesized and studied towards their toxicity, interaction with fibroblast growth factor (FGF-2) and cell growth. CS with higher degree of sulfation were found to be as bioactive as HEP having significant mitogenic activity. Two different CS with high (CS2.6) and intermediate (CS1.6) sulfation degree were chosen as polyanions, along with HEP, and combined with CHI as polycation for assembling multilayers. A comparative study was executed using either HEP, CS1.6 or CS2.6 to study the effect of different molecular compositions of the polyanions on bulk and surface properties of multilayers along with effects on behaviour of C2C12 cells. The characterization process revealed differences in specific growth patterns, hydration, and surface properties of multilayers in dependence on the type of polyanions that also affected FN adsorption and cellular responses. Since the layer deposition conditions affect multilayer properties, here the pH variation during polyanion adsorption was used as tool to tailor the properties of HEP and CS1.6 multilayers. The results showed that changing pH (acidic to basic) strongly affected the bulk and surface properties of HEP-based multilayers as well as FN adsorption and cellular behaviour. These effects strongly differed on multilayers prepared at different pH conditions. In contrast, CS1.6 multilayers were not as pH responsive as HEP-based multilayers. They did not exhibit strong differences in their physical and biological characteristics when assembled at different pH conditions. Further, they positively affected cell interactions. In a final step, multilayers were prepared by blending HEP with CS as polyanions and a preferential incorporation of HEP was found, displacing CS despite their higher degree of sulfation. However, it apparently improved the bioactivity of HEP-containing multilayers formed at acidic pH. Overall, the present thesis aimed to investigate the effect of molecular composition

of polyanions and pH variation during formation of polyelectrolyte multilayers (PEM) to control cellular behaviour on multilayer coated substrates. It was proven that not only HEP, but also semi-synthetic CS as polyanions along with CHI as polycation are candidates for multilayer formation with high bioactivity that could be of great interest for different biomedical applications.

ZUSAMMENFASSUNG

Die gezielte Anpassung von Biomaterialien an unterschiedliche Anwendungen wird häufig durch eine Modifizierung der Oberflächeneigenschaften erreicht. Neben anderen Methoden zur Oberflächenmodifizierung findet in jüngster Zeit die sogenannte Layer-by-Layer (LBL) Methode zunehmend Verwendung im Bereich der Biomaterialforschung. Die LBL-Methode, welche durch die abwechselnde Adsorption von Polyelektrolyten charakterisiert ist, wurde hier genutzt, um Multischichten aus Heparin (HEP) oder Zellulosesulfaten (CS) als Polyanionen auf Glas als Modellsubstrat herzustellen. Die so hergestellten Polyelektrolyt-Schichten sollen eine gezielte Steuerung von Zelladhäsion und Zellwachstum ermöglichen. Erste Versuche mit HEP als Polyanion und Chitosan als Polykation zeigten, dass eine Änderung des pH-Wertes während der Adsorption des Polyanions sowohl die Schichtbildung als auch deren Oberflächeneigenschaften beeinflussen, wodurch sich die Adsorption von Fibronectin und das anschließende Zellwachstum beeinflussen ließ. Da es sich bei HEP um ein natürliches Glykosaminoglykan handelt, welches nur in begrenzter Menge verfügbar ist, wurden halbsynthetische CS synthetisiert und hinsichtlich Toxizität, ihrem Einfluss auf das Bindungsvermögen von FGF-2 (fibroblast growth factor-2) und des Wachstums von Fibroblasten untersucht. Dabei zeigten CS mit einem höheren Sulfatierungsgrad eine erhöhte Bindung von FGF-2 und eine Verstärkung des Zellwachstums in ähnlicher Weise wie HEP. Zusammen mit Chitosan als Polykation wurden deshalb neben HEP auch ein hochsulfatiertes CS (CS2.6) und ein CS mit mittlerem Sulfatierungsgrad (CS1.6) als Polyanion für die Formierung von Multischichten verwendet. Die Charakterisierung der Multischichten mit den ausgewählten Polyanionen offenbarte Unterschiede hinsichtlich der Oberflächeneigenschaften, der Masse und des Wassergehaltes der Multischichten, was Auswirkungen auf die Adsorption von Fibronectin und die Wechselwirkung mit C2C12 Myoblasten hatte. Da auch die Beschichtungsbedingungen eine entscheidende Rolle auf die Adsorption von Polyelektrolyten haben, wurden unterschiedliche pH-Werte während der Adsorption der Polyanionen HEP und CS1.6 verwendet. Im Fall des HEP zeigte sich, dass ein Wechsel vom sauren zum basischen Milieu einen erheblichen Einfluss auf die resultierenden Volumen- und Oberflächeneigenschaften der Multischichten hatte. Dieser unterschiedliche Einfluss spiegelte sich auch bei der Adsorption von Fibronectin und im Zellverhalten wieder. Im Gegensatz dazu zeigten die Multischichten mit CS1.6 keine derartige Beeinflussung hinsichtlich ihrer physikalischen und biologischen Eigenschaften durch eine Änderung des pH-Wertes. Zusätzlich wurden auch Multischichten hergestellt, bei

denen HEP und CS gleichzeitig als Gemisch während der Formierung der Multischichten mit Chitosan als Polykation eingesetzt wurden. Die Untersuchungen zeigten eine bevorzugte Einlagerung von HEP anstelle von CS in die Multischichten, obwohl wegen des höheren Sulfatgehalts der CS das Gegenteil erwartet wurde. Zudem zeigte sich, dass die Bioaktivität der HEP-Schichten erhöht war, wenn die Multischichten im sauren Milieu hergestellt wurden. Zusammenfassend kann festgestellt werden, dass eine Änderung des pH-Wertes während der Ausbildung von Polyelektrolyt-Schichten eine Kontrolle von Proteinadsorption und des Zellverhaltens ermöglicht, was für die Beschichtung von Implantaten und Scaffolds im Bereich des Tissue Engineering nutzbar ist. Zudem konnte gezeigt werden, dass neben HEP auch halbsynthetische CS als Polyanionen zusammen mit Chitosan als Polykation die Bildung bioaktiver Multischichtsystemen ermöglicht, die in unterschiedlichen biomedizinischen Applikationen eingesetzt werden können.

Chapter 1

Introduction

1.1 Background

In the past years, the field of implantable biomaterials and tissue engineered constructs has gained an increasing attention due to the limited accessibility of autografts as well as the immune response and the considerable problems associated with allografts [1]. Once implanted, a biomaterial's fate is strongly dependent on various parameters such as its localization in the tissues, size and shape as well as its surface and bulk properties [2]. The design of biomaterials with nanoscale precision and controlling their properties (bulk and surface) is a great challenge for scientists and engineers working in the field of biomaterials and regenerative medicine. The bulk properties are important for the overall properties of the material, especially the mechanical/ viscoelastic properties. However, surface properties are also of chief importance, since the material surface forms an interface between the material and the host tissue [3]. Surface properties influence subsequent tissue and cellular events including protein adsorption, cell adhesion and inflammatory responses, each of which are important for tissue remodelling [4, 5]. Once a biomaterial is implanted, a cascade of events occurs at the interface that is initiated by its interaction with the surroundings that contains a number of bioactive species [6-8]. The complex series of events that occurs in dependence on surface properties of the biomaterial and the surrounding environment is crucial for understanding the biocompatibility of the implant biomaterial. Surface properties like wettability, surface charge, topography etc. influence the adsorption of plasma proteins that, in turn, dictate cellular events which will establish a communication between the material surface and cell interior processes affecting its tissue compatibility [2] [9-11]. Currently, considerable efforts are being made in the direction of biomaterial surface functionalization that are generally used in tissue engineering (TE) and biomedical applications to render them with biological functionalities [12, 13]. Further, biomaterials are constantly developed by adding required features for improvement of biocompatibility involving their biodegradability, bioactivity etc. and efforts to avoid the undesirable reactions like foreign body reaction (FBR) or stress shielding. Biomaterials can be classified in three generations; first as bioinert materials, second as bioactive and biodegradable materials, and third as materials specifically designed to stimulate certain cellular responses [14]. Biomaterials used for TE generally belong to the latter one, designed to mimic the extracellular matrix (ECM) and to host cells

similar to their natural environment. These biomaterials are designed with biophysical and biochemical cues that direct cellular interactions [13] [15, 16]. Hence, the understanding of cellular interaction at the interface of biomaterials is important [8]. In general, the biomaterial should promote cellular events for the successful incorporation of implants [17]. The initial cell-biomaterial interaction is a multi-step paradigm initiated by adsorption of proteins from the surrounding fluids followed by cellular events like cell adhesion, spreading and polarization [18, 19]. The adsorption of proteins is of ultimate importance since it determines cell behaviour that is important for the constructive cell response, which, in turn, will be beneficial for wound healing and tissue integration [20, 21].

1.2 Basics of cell adhesion on biomaterial surfaces

Cell adhesion is a fundamental process that is extremely important for functionality of cells and proper arrangement of tissues. Hence, it is a prerequisite for the majority of biomedical applications in TE [12, 13]. When cells attach to the substratum, they form connections to the internal cytoskeleton through specific cell receptors like integrins that connect the extracellular space with the intracellular cytoskeleton. As a result, signaling molecules among other cell adhesion mechanisms help to translate the genetic information into the complex three-dimensional patterns of cells in tissues [22, 23]. It was found that the degree of cell spreading and shape of cells depends on strength of cell adhesion to the substrate [24] and that the shape of cells is the regulator of cellular functions [25, 26].

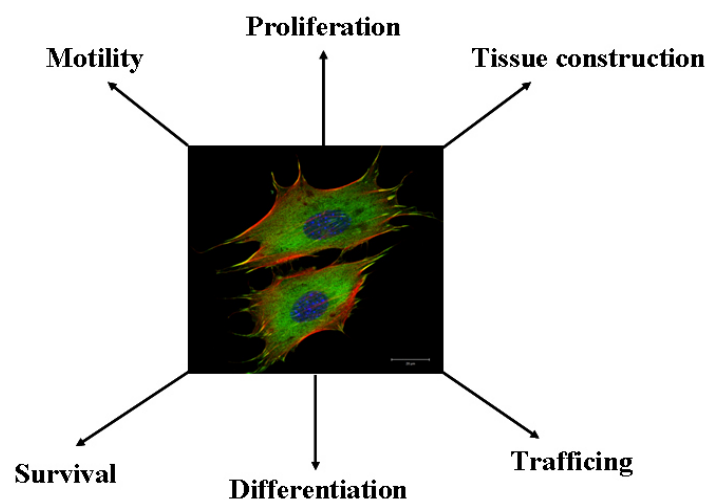


Figure 1.1: Impact of cell adhesion on different cellular processes (adapted from [15]).

Attractive forces for cell adhesion on substratum can be both long and short range. Long range interactions are represented by Coulomb or electrostatic forces that are dependent on the charges of both, cell surface and substrate [27]. Cell surfaces are predominantly negatively charged, whereas the charge of a substrate can vary resulting in repulsive or attractive forces between cells and material surfaces [27, 28]. Additionally, the presence of salt ions influences the degree of interactions, too. At high ionic strength, the charges on cells and surfaces may get shielded to a certain extent, whereas at lower salt concentration the electrostatic forces act at longer distances [29]. Attractive forces include also van-der-Waals forces, hydrogen bonding, hydrophobic and acid-base interactions. Short-range forces can also be repulsive and are exerted by hydration forces that are caused by the presence of bound water molecules on polar moieties. Further, steric hindrance generated by presence of hydrophilic mobile molecules on the material or cell surface is a repulsive barrier. More details on physics of cell adhesion are described elsewhere [27, 28]. It was found during basic studies on cell adhesion that surface charge strongly influences the adhesion of cells. Adhesion is promoted by positively charged surfaces while the negative ones reduce cell adhesion [27, 28]. At low ionic strength, cell adhesion is weak on a negatively charged substrate. This effect is altered by high ionic strength. Cell adhesion is strong at high salt concentration as electrostatic repulsion becomes negligible due to charge shielding and van-der-Waals forces start to dominate [29]. On the other hand, to prevent cell adhesion, effect of binding water to polar surfaces has been exploited. Water molecules bind to the head groups of phospholipids like phosphatidylcholine. Functionalization of surfaces with such phospholipids was used to prepare adhesion-preventing materials [30, 31]. The same effect can also be achieved by the immobilisation of hydrophilic macromolecules like poly (ethylene glycol) (PEG), which leads to a steric repulsion inhibiting cell attachment [32, 33]. Besides the physico-chemical properties of material surfaces, surface topography influences the cell adhesion, too, and it was found that roughened surfaces generally promoted cell adhesion to a higher extent [34, 35]. Lastly but importantly, the viscoelastic properties of the substrata are being sensed by the cells, too. Cell adhesion might get inhibited by soft flexible substrata while stiff surfaces may promote it [36-38]. However, certain cell types like neuronal cells prefer soft substrata [39]. Additionally, cell adhesion and spreading behaviour differs for the cells of different origin (exoderm, mesoderm or endoderm) [40, 41].

At physiological conditions, cells never directly contact with the biomaterial surface due to the presence of proteins in the surrounding fluids. This holds also for the majority of *in vitro* culture conditions, especially when serum is used as an ingredient of culture media.

Additionally, most of the cells secrete a multitude of proteins [42]. Therefore, before cells come in contact with the biomaterial surfaces, proteins are transported to the surface by diffusion or convection [43]. When a biomaterial is exposed to a biosystem, protein adsorption takes place instantaneously. The diffusion process, which is dependent on the bulk concentration and diffusion coefficient, is mainly responsible for the initial arrival of smaller proteins [44]. However, larger proteins that have higher affinity to the biomaterial surface subsequently dominate the next stage [45]. The conditions for protein adsorption are principally the same like cell adhesion. Indeed, the physicochemical properties such as chemistry, presence of certain atoms or chemical functional groups (e.g. carbon, amino groups, or hydroxyl groups), surface energy, wettability, size and curvature controls the adsorption of proteins [46-49]. Since proteins are the copolymers of amino acids, most of them carry acid and basic groups as well as hydrophilic and hydrophobic moieties. Hence, they are both amphoteric and amphiphilic. Depending on the isoelectric point (pI) of proteins, they might be positively or negatively charged at physiological conditions [50]. The electrostatic state of proteins is determined by pH and ionic strength. When pH is equal to the pI, the charges are balanced. At high pH conditions, proteins are negatively charged ($\text{pH} > \text{pI}$) and they are positively charged at low pH. Additionally, even the net charge of proteins is negative it may carry positively charged residues and vice versa [51]. The body fluids contain various types of proteins which differ in amino acids content, structure (secondary and tertiary) and size [52]. Consequently, proteins are capable of interacting with different type of material surfaces, except on highly hydrophilic surfaces with tight water binding [31] or having coverage with hydrophilic macromolecules like PEG that creates a repulsive layer [32, 33] [53]. Conformation of proteins can be altered by apolar or highly charged surfaces due to structural rearrangements upon adsorption to minimize the free Gibbs energy of the system [52]. The mechanism and driving forces that are involved in these rearrangements are described in detailed elsewhere [50] [52] [54]. Such conformational changes in proteins can lead to undesirable effects like activation of blood clotting as well as denaturation of epitopes for cell binding receptors or might also expose other domains that may provide signals for inflammation [55-58]. On the other hand, highly hydrophilic surfaces may allow only traces of proteins to get adsorbed, which might be desirable for blood contacting applications but not favourable for colonization of implants or scaffolds with tissue cells [50]. Hence, a prediction of orientational and conformational rearrangements that occur during protein adsorption on to material surfaces would very helpful to control cellular responses [21] [59-61].

It has been shown that adhesion of cells is linked to the presence and conformation of specific adhesive proteins on the material surface [62]. Attachment proteins such as fibronectin (FN), fibrinogen (FNG) and vitronectin (VN) belong to blood plasma and could adsorb on material surfaces [43]. The ECM, which surrounds cells in tissues, consists of structural proteins like collagen (COL), adhesive proteins and glycosaminoglycans (GAG) [63]. These proteins provide attachment to cellular receptors and transmit signals important for survival, growth and differentiation [64, 65]. Cell adhesion receptors are the transmembrane glycoproteins that mediate specific cell-cell and cell-ECM interactions. The members of this class of proteins are integrins, cadherins, IG-super family, selectins and proteoglycans (syndecans) [63]. The intracellular parts of these adhesion receptors are connected with the signalling molecules that transduce signals initiated at cell surface by the adhesion receptors for the further cellular events [23] [66]. Integrin receptors as transmembrane proteins are heterodimers of non-covalently associated α and β subunits [63]. So far, 18 α and 8 β subunits have been identified in mammalian cells that are known to form 24 distinct family members [64]. There are specific cellular receptors for different ECM proteins such as integrin $\alpha v \beta 3$ for VN and the integrin $\alpha 5 \beta 1$ for FN. The integrin $\alpha v \beta 3$ is part of the focal adhesion (FA) contacts, usually located in the cell periphery as a flat and elongated structure while, $\alpha 5 \beta 1$ is part of the fibrillar adhesion, more centrally located, and consists of extracellular FN fibrils [67]. Integrins play a very important role in development, organization, maintenance and repair of tissues by providing anchorage and activating signals that in turn direct cell growth, migration and differentiation [68]. The activation and clustering of integrins initiates a cascade of biochemical events known as integrin signalling via different signalling molecules (Figure 1.2). Integrins contribute to signal transmitting either from ECM into the cell (outside-in signalling), or in the other direction, from inside of the cells to regulate the extracellular binding activity towards matrix proteins (inside-out signalling) [69].

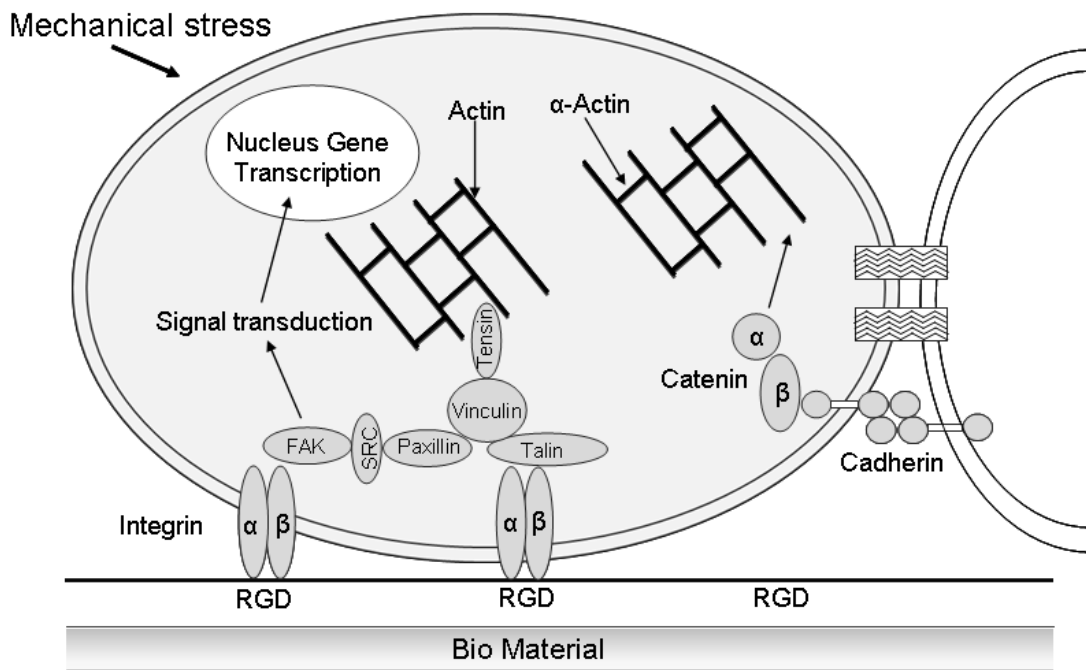


Figure 1.2: Illustration of the cell adhesion complex. Proteins like vinculin, talin, paxillin, tensin anchor to integrin to mediate the cell behaviour (adapted from [70])

The ability of a biomaterial in context of its role in normal cell survival and growth can be tested as these signalling events are a tool to for biocompatibility assessment. By means of immunocytochemical methods, investigations in the last few years have revealed the relationship between biomaterial surface properties and the distribution and quantity of focal contacts. Examples include evaluation of focal contacts distribution (labelled with vinculin) on substrates with different roughness [70], and actin filaments (F-actin) cytoskeleton reorganization on various substrata [71].

The ECM contributes to the assembly of tissues and affects this process of tissue integration from individual cells at both receptor and cytoskeleton levels. The adhesion mediated signalling is dependent on the ability of cells to sense the chemical and physical properties [72].

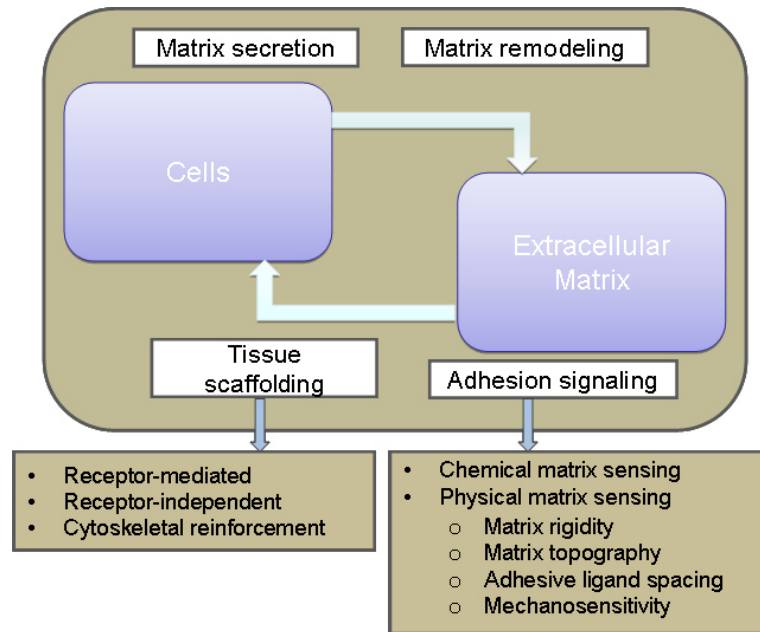


Figure 3: Dynamic cross-talk between cells and ECM (adapted from [72])

1.3 Cell growth on biomaterial surfaces

Cell adhesion and spreading are important prerequisites for cell growth and differentiation [26]. Well organized FA established during the progression of cell spreading, will contribute to integrin mediated signalling processes. This signalling connects numerous proteins like FAK (focal adhesion kinase), MAP (mitogen activated proteins) kinase, bone-specific transcription factor Runx2/Cbfa1, Ras homolog gene family member (Rho) family, conduct the signal transduction machinery, lead to organization of cytoskeletal structures and contractile activity and finally, to the progression of cell cycle, or various commitments of the cells [69] [73].

Growth factors like fibroblast growth factor (FGF), epidermal growth factor (EGF) induces proliferation of different cells by forming complexes with their corresponding receptors. [74, 75]. Fan and coworkers proposed the incorporation of epidermal growth factor (EGF) into a synthetic matrix surface that increased survival of mesenchymal stem cells (MSC) [76]. EGF activated intracellular signals via the extracellular-regulated kinase (ERK) and Akt pathways [77, 78]. These signals promoted migration, adhesion, proliferation and survival in various cell types [75] [77] [79]. Besides, diverse in vitro investigations of cell behaviour on scaffolds made of COL, hyaluronan (HA), gelatin (GEL), chitosan (CHI), chondroitin sulphate (CHS), fibrin etc., have also proved an optimal effect on cell viability, proliferation and differentiation [80, 81].

1.4 Surface modification of biomaterials

Many contemporary materials that possess very useful physical and chemical properties, makes them attractive for biomedical applications. However, their clinical use can hamper some undesirable side effects, which are caused by uncontrolled protein adsorption and subsequent conformational changes. Since, only the surfaces of materials are in intimate contact with the surrounding biological environment, it is very important to modify the surface of the materials upto a size scale of few nano to micrometers. Surface properties of a material are directly related to in vitro biological performance such as protein adsorption and cellular responses, which are necessary for tissue remodelling [4]. The aim is to fully develop the biological model for surface science in a highly complex and interactive in vivo biological environment. Thus lot of efforts are being dedicated to engineer new forms of biomimetic surfaces by using a combination of cells, surface engineering and materials together with suitable biochemical and biophysical factors [40]. Until now, numerous methods of surface modification have been developed to improve the biocompatibility of (biodegradable) polymers and other biomaterials. Typically, modifications can either alter the atoms, compounds, or molecules on the existing surface chemically or physically. In addition, coating with different materials can lead to specially modified surfaces [82]. Principally, surface modification techniques can be divided into two categories: physical and chemical. Physical techniques involved surface coating [83, 84], vapour deposition [85] and surface self assembly methods [86, 87]. Physical interactions related to these techniques are electrostatic interaction, van-der-Waals force, hydrogen bonding, hydrophobic interaction, etc. Physical techniques are often simple, which generally do not require large and expensive equipments. To this end thin film coatings by surface self-assembly methods deposited on the bulk materials offer great potentials. Therefore enormous efforts are being dedicated in engineering new biocompatible forms of biomimetic surfaces. Designing of thin films with controlled properties along with maintenance of the bioactivity of embedded molecules and adjusting their delivery is thus a great challenge. The importance of thin films does not only exist in biomedical field but also in many other areas such as electronics, optical devices, sensors and catalysts [88]. The use of thin films for a given application is motivated by a number of factors. In many cases, their use is generated from a desire to only modify the surface and keeping the bulk properties of the underlying material preserved, for instance, when an anti-fog coating is applied to a mirror or a non-stick coating on a pan

As a result, several techniques have thus been developed to design thin films at the molecular level. In the second half of the 20th century, two techniques dominated the thin films research

area: Langmuir–Blodgett (LB) [89] and self-assembled monolayers (SAMs) [90, 91]. These two sorts of films have shown a remarkable capability for immobilization of proteins and cells as well as subsequent applications in biocatalysis, controlled drug delivery, etc [90-92] [93]. However certain intrinsic drawbacks of both methods limit their applicability. The limitations associated with Langmuir–Blodgett deposition include the requirement of expensive instrumentation and long fabrication periods for preparation of the biomolecule films along with the disadvantage of the type of the molecules (amphiphilic) that can be embedded in the films. For SAMs, the disadvantages are due to the low loading capacity of films because of their monolayer nature and the need for the presence of thiols on the substrate (e.g., for only noble metals or silanes) in order to deposit [87]. A very considerable alternative to LB deposition and SAMs called layer-by-layer (LBL) assembly was introduced by Decher, Hong and co-workers in 1992 [94] for preparing structure-controlled thin films for biological applications.

1.4.1. Layer-by-layer (LBL) Assembly

The concept of thin film fabrication via alternating deposition of two oppositely charged species was firstly introduced by R. K. Iler in 1966 [95]. Based on his work, Decher and co-workers introduced the concept of creating multilayers of oppositely charged polymers/polyelectrolytes (PEL)-thus introducing the “polyelectrolyte multilayers” (PEM) [94] [96]. Ever since, the PEM research field has greatly expanded and thousands of publications have been reported where the deposition of PEM by LBL method have been employed. This self-assembly-driven surface modification method allows the construction of nano-scaled thin films onto substrates of any geometry (simple two-dimensional surfaces to more complex three-dimensional scaffolds and implants. In general, the alternate adsorption of PEL is typically driven by electrostatic attraction and subsequent ion pairing on to a charged substrate [97, 98]. As ion pairing is probably the most abundant driving force applied during the multilayer assemblies, other interactions are also involved in PEM assembly that include van-der-Waals forces, hydrogen bonding, hydrophobic interactions etc [99-101]. During the pioneering work by Schlenoff, the concept of intrinsic, (i.e., PEL of opposite charge) versus extrinsic (i.e., counterions) charge matching was introduced [98] [102]. However, it has been also described in literature that the multilayers formation is not only driven by the electrostatic interactions but also by the gain in entropy due to the release of counter-ions [103, 104]. The strength of the various interactions involved in multilayer

formation process might be influenced by certain other intrinsic factors such as the molecular weight, size, charge density etc of the PEL and by environmental conditions like temperature, pH and ionic strength of the solvent (described in details in the following section). Variation of one or more parameters can lead to desired interactions and properties of resulting multilayer films. This easy to perform strategy offers a fine control on designing the properties of material surface/structures, which are robust in physiological environment [99] [104, 105]. Figure 1.4 shows a schematic of the LBL fabrication method using PEL, where a positively charged substrate is dipped into a polyanion solution followed by rinsing and dipping into a polycation solution. The process is repeated several times until the desired number of layers is assembled. Each step of layer deposition is followed by washing/rinsing steps which are done to remove the loosely bound material. Washing steps are necessary to avoid complex formation between weakly adsorbed PEL and the next adsorbing layer.

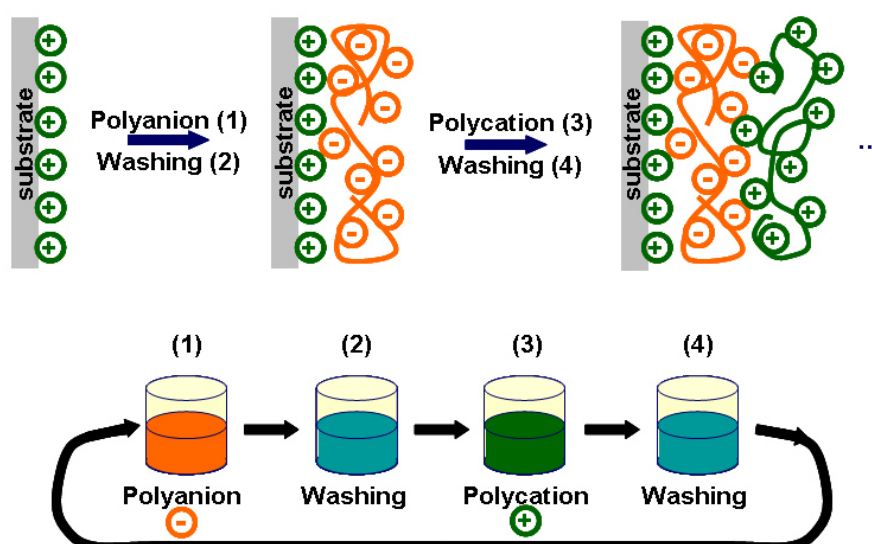


Figure 1.4: The multilayer build-up process using the LbL method [96].

1.4.1.1. General potential of LBL in biomedical applications

A large variety of charged specimen are suitable for being adsorbed as multilayers that range from nanoparticles [106, 107], carbon nanotubes [108, 109], and synthetic polymers [110] to biogenic polysaccharides [111, 112], polypeptides [113-115], nucleic acids [116, 117] and viral components [118, 119]. In the past years, a lot of attention has been given to synthetic PEL, poly(styrene sulfonate)/poly(allylamine hydrochloride) (PSS/PAH) system has been

widely investigated [4]. It has been found that the thickness of (PSS/PAH) multilayer system can be precisely varied from few nanometers to few tens of nanometers [120]. Various cell types of cells such as endothelial cells, fibroblasts, osteoblasts, and hepatocytes [121-124] have been cultured on (PSS/PAH) films and in general these films supported cell adhesion growth. Additionally, a study by Guillaume-Gentil et al. using human MSCs, showed that (PSS/PAH) films on conductive indium tin oxide (ITO) electrodes can be used as a platform for growing viable cell sheets [125]. Another synthetic multilayer system, poly(acrylic acid)/ poly(allylamine hydrochloride) (PAA/PAH) films, initially developed by Rubner and his co-workers has also been studied in detail [110] [126]. The potential of (PAA/PAH) films for wound healing in cornea was investigated by Hajicharalambous and Rajagopalan et al [127]. During their studies by using corneal epithelial cells as cellular models, they found that cells undergone proliferation and migrated to the wound location. Nanoscale porous films were created that significantly enhanced the corneal epithelial cellular response. The well organized actin cytoskeleton and vinculin FA were found in cells present on nanoscale environment. Their studies suggested that the physical environment plays a defining role in guiding cell behaviour.

However for the biomedical applications, many biopolymers like proteins, glycosaminoglycans (GAG) and DNA represent polyelectrolytes and can be applied to generate biomimetic multilayers on biomaterial surfaces with imprinted biological information [87] [97] [128]. In past years, several scientists have focused their research on using different polysaccharides for multilayer coatings, for example, HA, CHS, HEP, COL, CHI etc [112] [129-133]. These films made from natural polymers render compositional uniqueness, such as initiating specific cellular responses and provides both mechanical and biochemical signals. COL I is a major protein of fibrous connective tissues that provides mechanical support to the other tissues. COL is also a natural ligand for several cell receptors of the integrin family [134]. HA, CHS and HEP belong to the family of GAG that are made of disaccharide repeating units with a derivative of amino sugar such as glucosamine or galactosamine and an uronic acid. They are negatively charged due to the presence of carboxylate and sulfate groups [134]. HA and CHS are highly hydrated polymers surrounded by respectively ~20 and ~30 water molecules per disaccharide unit respectively by interaction through hydrogen bonds [135]. Importantly they both are the ingredients of the pericellular coat (glycocalyx) which play a major role in interaction of cells with their environment [136]. HEP is known for its anticoagulation activity as it binds specifically to antithrombin III, which accelerates the subsequestration of thrombin [137] and it is often applied as

anticoagulant coating of blood contacting devices [130] [138]. Additionally, HEP possesses a high affinity towards adhesive proteins (e.g. FN) and growth factors (e.g. bone morphogenic proteins (BMP)) interacting via specific HEP-binding domains [139]. Biopolymer-based multilayers are advantageous as they can specifically interact with living cells. The incorporation of biomolecules and bioavailability as well as the possibility of biodegradability due to presence of specific enzymes in tissues and biological fluids renders them with exclusive applications in the biomedical field.

1.4.1.2. Effects of deposition conditions on multilayer properties

Multilayer structure, growth and mechanical and other properties are controlled by the solution deposition conditions including PEL concentrations, type of PELs (their molecular weight, charge density etc) adsorption time, temperature, ionic strength and pH of the solution. There are also other conditions which can have influence on the film deposition like rinsing time, substrate charge density etc [140]. Changing the ionization of the PEL changes the chemical functionality of the molecule. Hence, it is reasonable that these changes affect the morphology and thickness of the assembled multilayer films. Generally, the PEL are long chains and the ionic charge is homogeneously distributed. Counter ions, usually through addition of salts, neutralize some fractions of the charges and reduce the repulsive forces among the PEL chain segments. By adsorbing polyions from salt solutions of varying electrolyte concentrations, film thickness can be tailored over a wide range [141]. During high salt conditions, polyion charges are screened leading to more coiled structures and smaller radius of gyration. Therefore adsorption of smaller coils will occupy lower surface area per chain, resulting into a larger density of segments and consequently higher thickness of the layer [128]. Many authors have shown in their studies that the thickness of CHI/HEP multilayers is affected by the ionic strength of the deposition solution [142] [143]. Another and important way to manipulate the charge and conformation of the PEL is to adjust the pH of the PEL solution [110] [144, 145]. This is specifically applicable for weak PEL as they dissociate in dependence on the solution pH. The linear charge density of weak PEL is sensitive to pH change and can vary considerably with change in pH when operating near the pKa value of the PEL [144]. Hence, a weak polycation tends to adsorb as a thin layer with a flat chain conformation when it is highly charged at acidic pH (highly protonated) and as thicker, more coiled structures when it is less charged (alkaline pH) [144] [146]. Vice versa, the same applies to the weak polyanions for opposite pH values (Figure 1.5). When both,

polycation and polyanion, are weak PEL, the pH of the dipping solution can be used to control the charge density of the adsorbing polymer, the pre-adsorbed polymer (i.e. the surface charge density) or both [110] [144]. This provides a great flexibility over the assembly of multilayers and the ability to tailor the thickness, ionic cross-link density and conformation of the adsorbed PEL as layers [141].

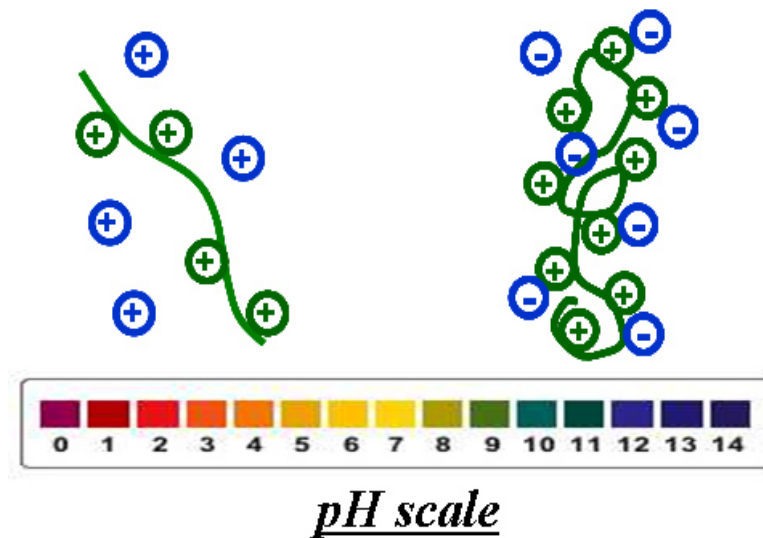


Figure 1.5: Polyelectrolyte structure (weak polycation) at different pH values. The structure is more extended and elongated at acidic values whereas it is more coiled and loopy at alkaline values. The same holds for weak polyanions at opposite pH values.

Furthermore, the temperature of the PEL solutions also affects the film morphology, since the solubility of the polymers as well as the shape of the polymer chains are influenced [147] [148]. It was found that a temperature increase resulted in a rise of the internal roughness of the multilayer systems after exceeding a certain salt concentration of the solutions, which also led to the formation of thicker layers [147]. Additionally, the results of high salt and low temperature combination were similar to that of low salt and high temperature [147]. Previous studies showed that film properties can be also tailored using thermoresponsive PEL. Films prepared from PEL closer to their lower critical solubility temperature resulted into smoother surfaces than films prepared far below this temperature [148].

In addition, the applied PEL pair for the multilayer construction influences the film structure. In literature, there have been mainly two types of film growth reported. The film thickness and adsorbed amount increase either linearly or exponentially with the number of layers as

thoroughly described by Picart [149] and von Klitzing [103]. In general, the strong synthetic PEL gives rise to linearly growing multilayers, whereas an exponential-like growth can be found for some weak natural PEL, mainly polysaccharides or polypeptides [103] [150, 151]. The observed exponential growth was explained by the diffusion theory, where at least one of the two PEL diffuses within the film [150]. According to this theory, the adsorbed amount of a PEL in a given deposition step not only depends on the amount of the oppositely charged PEL in the outermost layer, but also on the amount of free diffusing PEL available for complexation within the multilayer film. Diffusion of the PEL (fluorescently labelled) within very thick films (several μm) during their build-up was visualized by the confocal laser scanning microscopy (CLSM) technique [152, 153]. It has been suggested that linear growth can be turned into an exponential growth if the LBL conditions are changed so that the intermolecular forces/interactions are weakened enough between the PEL [154].

Surface properties such as surface charge, wettability and morphology are also dependent on the deposition conditions and have their influence on the interactions with the surrounding environment. The surface charge of the multilayer films can be tailored using either polyanion or polycation as the outermost layer which, in turn, results in negative or positive surface net charge [97] [128]. Another surface charge controlling parameter is the pH adjustments of the PEL, especially if weak ones are present [128]. The charges of such weak PEL are adjustable as the degree of dissociation of their functional groups depends on their pKa value [128]. Hence the overall surface charge can be controlled that later on and may have an impact on the protein adsorption and initial cellular events. Furthermore, the wetting properties of multilayer surfaces also depend on the deposition conditions. Many of the commonly used PEL (e.g. PSS) have a hydrophobic hydrocarbon chain as a backbone [128]. The charges on the PEL are present due to attached functional groups. If these charges are screened, may at high ionic strength, the hydrophobic character becomes dominant [128] that reduces the wettability of the surface. In addition to that, the rigidity of the multilayers is also influenced by the ionic strength as well as the type of PEL used [97] [128]. During the assembly of multilayers, low salt concentration leads to the stretched conformation of the PEL (due to high intramolecular repulsion forces between the charged functional groups) and the multilayers appear more rigid. Vice versa, at high ionic strength, the layers tend to be more flexible due the coiled conformation of the PEL as the high salt concentration screens the charges and the PEL chains are more like coils and appear more soft [128]. Therefore, rigidity of the multilayers can be controlled which tend to also affects the cell behaviour [36]. As described previously, the protein adsorption from the surrounding fluids depends on the characteristics

of the material surfaces [155] and consequently protein adsorption, cell adhesion and other related events are strongly influenced by the molecular composition of the material surface coatings. Therefore, surface modification by application of LBL technique can be a versatile tool to tailor the biocompatibility of the materials.

1.4.1.3. LBL films prepared by blending of polyelectrolytes

The conditions during the film construction and also the intrinsic properties of the PEL that are used in the formation of multilayers dictate the bulk properties of these films. Hence, controlling the chemical composition of multilayer films provides a further possibility of tuning their physical properties. With this as a goal, an innovative enhancement in LBL technique for tuning of film properties by blending of either polyanions or polycations has been introduced recently [156, 157]. Such blend films offer new possibilities for the modulation of film thickness, morphology and secondary structure [156] [158], degradation rates, protein adsorption or even mechanical properties [159]. A number of studies have reported the blending technique and its ability to enhance the functionality of the LBL films [160, 161]. When designing a PEL blend film, the control over the chemical composition of the film is of chief importance, as it is the origin of the desired, intrinsic and surface properties of the films. In many cases, preferential incorporation of one of the two PEL in the film has been reported. For example, the study on blends of polyanion (HA-PSS) built with poly-L-lysine (PLL) had shown the preferential adsorption of PSS over HA and also anomalous evolution of film thickness [162]. Stability of films prepared from several low molecular weight species was also improved by blending them with PSS [163]. Caruso et al. has provided a wide overview about the different aspects and utilities of the blends in multilayers so far [160], although details of PEL arrangement within such films are still unresolved and are difficult to investigate. Additionally, Cruzier et al. showed how blending could improve the biological aspects. Their studies demonstrated the ability of HA-HEP blend films as potential growth factor reservoir and probed the bioactivity of these films by measuring the alkaline phosphatase (ALP) activity of C2C12 cells [161].

1.4.1.4. Controlling protein adsorption and cellular responses on LBL films

Controlling protein adsorption and cellular behaviour on surfaces is one of the critical and important steps during development of a biomedical device. Adsorption of proteins on LBL films is a complex phenomenon attributed to electrostatic forces, hydrogen bonding,

hydrophobic interactions and hydrophilic repulsion [164-166]. A number of studies have shown the effect of multilayer surface charge on the adsorption behaviour of different proteins (serum albumin, FNG etc) [164] [166-169]. These studies showed that proteins strongly interact with LBL films regardless of the sign for both the multilayer surface and the proteins. When the sign of charges was similar, a monolayer of proteins was adsorbed due to hydrogen bonding and hydrophobic interactions. Whereas, when charges on protein and multilayer surface were opposite, electrostatic interactions became dominant and led to the adsorption of a thicker layer of proteins. Wittmer et al. added a final FN layer to PLL/ dextran sulfate (DS) films and found that higher amount of protein was observed on positively charged PLL ending films [170]. Cells were larger and more symmetrically spread on FN-coated films. Another study by Kirchhof and colleagues has used preadsorption of FN to enhance the cell adhesion that was strongly pH dependent on CHI/HEP multilayers [111] [131]. However, Salloum et al. exploited the hydrophilic repulsions to minimize the protein adsorption through fabrication of LBL films of a diblock-co-polymer comprising a hydrophilic poly(ethylene oxide) block [164].

The flexible properties of multilayers have fostered studies on the influence of these properties on cell behaviour. Synthetic PEL like PSS, PAA or PAH have been widely used for cell studies on multilayers. In most cases, the cell attachment to the layer surface was mediated by electrostatic interactions, and more indirectly by adsorption of serum proteins. Apart from films of synthetic polymers, cell behaviour has been studied widely on multilayers from natural ECM components. Multilayers of ECM proteins, GAG and other polysaccharides have been subjected for cell studies and it was observed that cellular responses were dependent on both properties of layers (thickness, hydration and mechanical properties) and cell type. For example, most cells are known to adhere poorly on hydrated surfaces and materials that are soft [171]. This was observed for different cells on films of PLL/HA [172, 173], CHI/HA [86, 174] or PLL/PGA (poly(L-glutamic acid)) [175]. However, certain cell types prefer to adhere on soft substratum, like neuronal cells on COL/HA films [176]. Niepel et al. showed that surface wettability, surface charge and lateral structures of PEI/HEP multilayers were controlled by pH variation of HEP solution which also led to the modulation of fibroblast adhesion [112]. Another way to improve cell adhesion on multilayers is grafting peptides that are known to interact with specific cellular receptors. For instance, the RGD (arginine-glycine-aspartate) sequence, which is a central integrin-binding region present on fibronectin and collagen. Multilayers that exhibit poor adhesion properties can be very well use for such grafting functionalization. This was applied using poly(allylamine

hydrochloride) (PAH)-RGD and poly(L-glutamic acid) (PGA)-RGD for improvement of cell attachment [175] [177].

1.4.2. Polyelectrolytes used during this study

1.4.2.1. Polycations

(a) Poly (ethyleneimine) (PEI)

Poly (ethyleneimine) (PEI) is a highly water soluble, cationic synthetic polymer generated from the ethyleneimine monomer where every third atom is a nitrogen. It exists as a branched polymer as well as in linear form. PEI is generally available in a broad range of molecular weights M_w , from <1000 Da to 1.6×10^3 kDa. It was found that high M_w PEI lead to increased cytotoxicity [178, 179], where as low M_w PEI demonstrated a low cytotoxicity in cell culture studies [179-182]. PEI is a strongly alkaline molecule and approximately 20% of nitrogen atoms are protonated under physiological conditions [183]. As result it can change its ionization state over a broad range of pH.

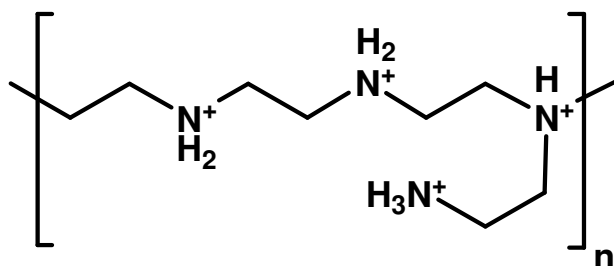


Figure 1.6: Molecular structure of Poly (ethyleneimine)

PEI is widely used as a transfection agent as it condenses DNA into a globular nanostructure that can be internalized by the cells via endocytosis [184]. On the other hand, PEI has often been used in the field of PEL multilayers. Mostly it is used as a precursor uniform anchoring layer during LbL assembly to provide better bonding to the underlying substrate [185, 186]. The degree of dissociation of PEI, as weak polycation, is dependent on the pH of the solution and the reported pK_a value is around 8.3 [187].

(b) Chitosan

Chitosan (CHI) is a GAG and represents a co-polymer of N-acetylglucosamine and glucosamine linked via 1-4-beta glycosidic bonds produced by deacetylation of chitin. Chitin is a natural mucopolysaccharide present in arthropods and is composed of $\beta(1\rightarrow4)$ -D-glucosamine units with a variable degree of N-acetylation (DA) [188]. The N-acetyl group distribution along the polymeric backbone may control the solubility. Chitin (DA~1) is insoluble in aqueous solutions. When the average DA is lower than approximately 0.5, the polymers are called CHI and become soluble in aqueous solutions in the presence of acids like acetic acid [189]. This is related to the fact that protonation of amino groups of glucosamine residues contributes to the disruption of hydrogen bonding. This is followed by solvation of cationic sites and leads to the solubilisation when the balance between solvent/ polymer and polymer/ polymer interactions becomes favourable. This limit is tightly related to the intrinsic pKa of CHI [190]. The DA influences the various properties of CHI like its solubility and biodegradability [191].

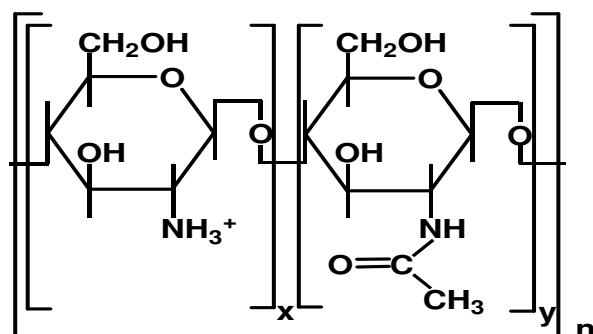


Figure 1.7: Structural formula of chitosan

The primary amines make CHI a weak PEL. It has an intrinsic pKa varying from 6.46 to 7.32 [192]. The charge density and pH of the solution influences the conformation of the CHI chains [193]. Increase in solution pH or ionic strength reduces the charge density of chitosan which in turn results in reduction in chain dimensions corresponding to collapse of the polymer [194]. CHI possesses remarkable antimicrobial activity and promotes wound healing through a number of mechanisms [195, 196]. Hence, it is not surprising that CHI has been applied in different studies as polycation during multilayer formation [142, 143] [197].

1.4.2.2. Polyanions

(a) Heparin

Heparin (HEP), the most sulfated GAG, represents a strong polyanion, composed of either β -D-glucuronic acid or α -D-iduronic acid and 2-N-sulfo-glucosamine connected by a 1-4-glycosidic linkage. Generally, HEP has three different functional groups, sulphate monoesters, sulphamido groups and carboxylate groups [198]. The first two are highly acidic and have pKa values ranging from 0.5 to 1.5 while the third one is less acidic with a pKa value of 3.13 [198].

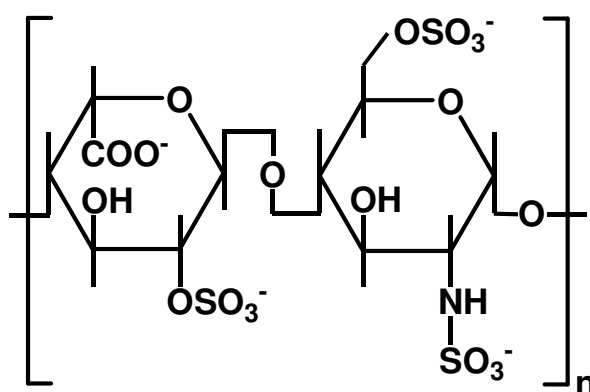


Figure 1.8: Structural formula of Heparin

HEP has the highest negative charge density of any known biological polyanion, due to the presence of carboxyl and sulfonate groups [199]. It interacts with a large variety of proteins that regulate adhesion, growth and differentiation of cells [200]. It is also commonly known for its anti-thrombogenic activity [201]. The biological activity and the degree of sulfation of HEP are dependent on the animal source of extraction [202]. Due to the high affinity of heparin towards several growth factors [203], it is often incorporated into the hydrogels [204] and also recently used in making multilayer coatings on biomaterial surfaces [129] [131].

However, the use of HEP has certain draw-backs. The isolation of HEP from animal sources, e.g., porcine intestinal mucosa or bovine lung limits its availability in larger quantities and also leads to substantial chemical heterogeneity and variability of physiological activity [200]. Therefore, previous studies were conducted to replace HEP by modification of more abundantly occurring polysaccharides like cellulose to achieve heparinoid features as cellulose sulfates (CS) [205-207].

(b) Cellulose sulfates

The naturally occurring HEP exhibits various molecular compositions which results into different biological responses [208-210]. Therefore a wide variety of GAG-analogues have been derived by sulfating other abundantly available natural polysaccharides. For example, cellulose as a renewable resource has been exploited for the synthesis of a number of derivatives like carboxymethyl cellulose, cellulose acetate and cellulose sulfate (CS) [211-214]. In contrast to cellulose, cellulose sulfates (CS) are the water soluble derivatives and thus exhibit diverse biological effects such as enzymatic degradability and anticoagulant activity [214, 215]. CS has been widely used in biotechnology and pharmaceuticals to encapsulate enzymes and cells [216-218], as inhibitors for HIV viruses and anticoagulant effectors [205] [219, 220]. CS were prepared previously by regioselective sulfation of cellulose to achieve molecular similarity and bioactivity to HEP [207], particularly with respect to interaction with growth factors and cells. It was also found that CS with high substitution degree could bind to growth factors and promotes proliferation [221], while CS with intermediate sulfation degree had shown significant binding with BMP-2 and increased osteogenic activity in C2C12 cells [222].

Different strategies have been developed to prepare CS with different substitution patterns. CS can be synthesized through either heterogeneous or homogeneous sulfation of cellulose with solvents like N,N-dimethylformamide (DMF), pyridine, dimethyl sulfoxide, N₂O₄·DMF system as well as ionic liquids. Different sulfating agents such as SO₃, chlorosulfuric acid and SO₃-DMF complex have also been applied [214] [223, 224].

Additionally, protocols for cellulose sulfation as acetosulfation or as homogeneous sulfation in ionic liquids have been introduced [213] [221] [225, 226]. During our studies, synthesis of cellulose derivatives was carried out either as acetosulfation of cellulose or as direct sulfation of cellulose with different degrees of substitution with sulfate (DS_S). CS containing carboxyl (CO) or carboxymethyl (CM) groups were also synthesized. The characterization was done by nuclear magnetic resonance and Raman spectroscopy. The details are described elsewhere [207] [222] [227].

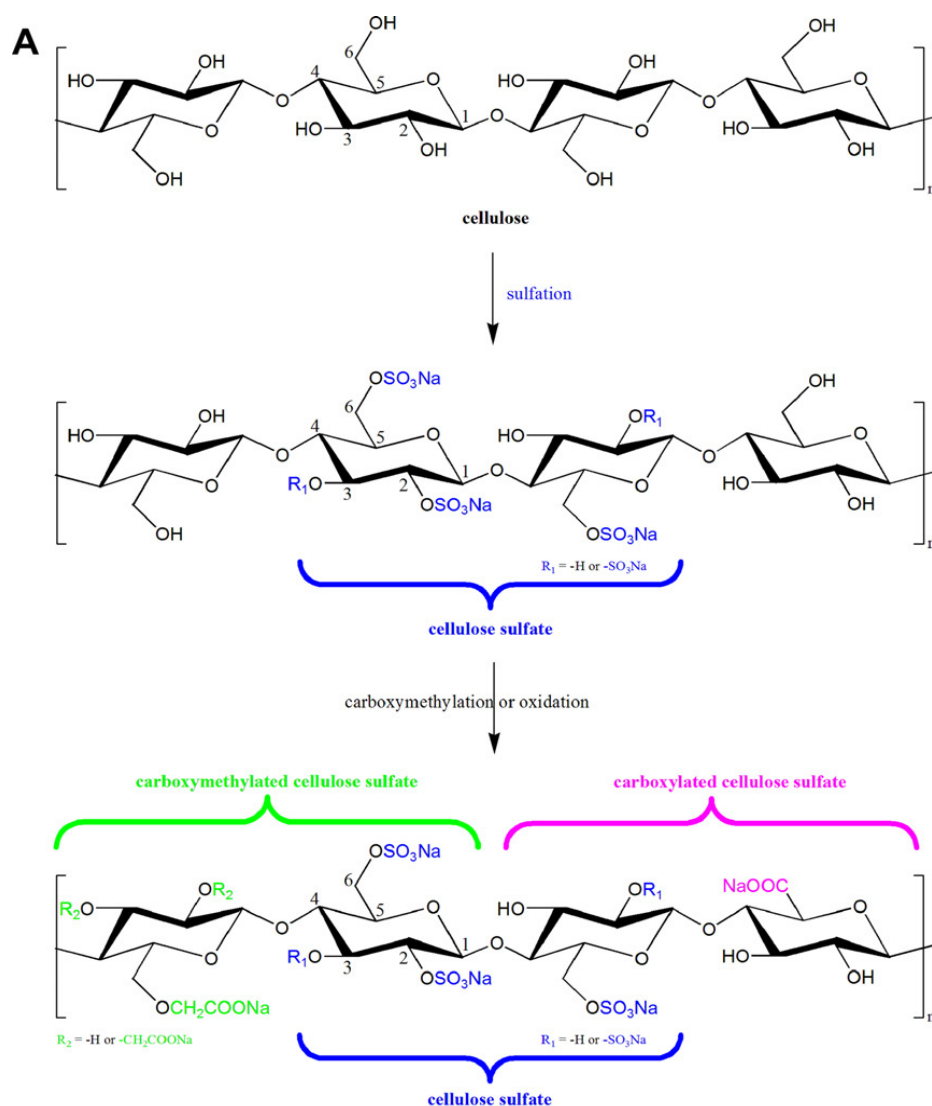


Figure 1.9: Chemical synthesis of cellulose sulfate, carboxymethylated cellulose sulfate and carboxylated cellulose sulfate [222]

1.5 Motivation

In the field of biomedical materials, TE, and regenerative medicine constant efforts are being made in designing and development of functional nanostructured materials at the molecular level with specific bioactivity. This study was aimed to develop biomimetic surfaces with possible biospecific cues to obtain control over cell adhesion and growth by exploiting the layer-by-layer (LBL) technique. The main focus was on developing multilayers using different polyanions with varying chemical composition (sulfate groups) paired with CHI and studying the effect of distinct molecular compositions on the multilayer formation process, protein adsorption and cellular responses. Novel CS with controlled degree of sulfation (DS_s) were synthesized and they demonstrated a significant FGF2-induced proliferation of 3T3 cells

and even stronger mitogenic effects than HEP. Since natural based HEP exhibits certain limitations, hence using these bioactive CS with heparinoid features as components of multilayers was a strong motivation with intentions of replacing HEP.

Multilayers of CHI paired with either HEP or semi-synthetic CS that possessed a higher sulfation degree than HEP were assembled. Such multilayers were particularly of interest due to presence of different functional groups on HEP and CS, as HEP contains sulfate as well as carboxylic groups, whereas CS were having only sulfate groups. The study was aiming to interpret how the different degree of sulfation, presence or lack of carboxylic groups influences multilayer properties as well as to interpret the type of interactions that are involved in formation of multilayers (ion pairing to others such as hydrogen bonding etc.). Additionally, the influence of such distinct multilayer properties on protein adsorption (FN) and behaviour of C2C12 cells was investigated.

Since deposition conditions of multilayer formation influence the properties (physico-chemical and biological) of PEM, pH variation was used here as a tool to tailor the multilayer characteristics and their bioactivity. Multilayers of HEP and one of the CS were assembled at different pH conditions (acidic & basic) to study the effect of pH change on multilayer properties (bulk and surface) as well as on protein adsorption and bioactivity.

Overall, the present study was attempted to design multilayered surfaces with varying molecular composition on glass as model substrate, exploiting different pH conditions to guide adhesion and growth of C2C12 skeletal muscle cells.

1.6 Overview of thesis and summary of papers

This thesis consists of five papers as chapters 2-6. Out of five papers, four are published and one accepted.

Nano-structured multilayers of natural HEP and semi-synthetic cellulose sulfates were prepared on glass as model surfaces and explored physico-chemically and biologically. As also outlined in the introduction, deposition conditions influences the properties of multilayers. Therefore, the effect of pH variation on layer characteristics (in terms of physico-chemical and biological aspects) was studied in detail in the current work. Multilayers of HEP and CHI were constructed at different pH conditions, where the HEP solution was applied at pH 4, pH 9, or at pH 4 during the formation of the first layers followed by pH 9 during the last steps of the multilayer assembly (annotated pH 4+9). These multilayers showed distinct properties and

also different cell behavior. As illustrated before, naturally occurring glycosaminoglycans (e.g. HEP) exhibit certain drawback and to this end cellulose derivatives were made and characterized to exploit them as promising candidates for replacement of HEP in different biomedical applications. In this perspective, a series of cellulose derivatives with defined substitution patterns of sulfate, carboxylate and carboxymethyl groups were prepared. These derivatives were examined for their cytotoxicity and mitogenic activity by modulation of 3T3 fibroblast proliferation with or without exogenous fibroblast growth factor (FGF-2). It was found that none of the derivatives were toxic. Highly sulfated CS strongly promoted FGF2-induced proliferation while CS with intermediate degree of sulfation exerted stronger mitogenic effects than HEP in the absence of FGF2. On the other hand, CO and CM did not show any significant promoting effects of on cell proliferation despite the structure of CO showed similarities to HEP. On the basis of this detailed study executed over these derivatives, middle and highly sulfated CS were chosen for further exploration of their bioactivity when surface immobilized in multilayers. Therefore, these two (middle and highly sulfated) CS along with HEP were applied as polyanions paired with CHI to construct PEL multilayer thin films on the model substrate glass. However, also to study the influence of deposition conditions, later on multilayers of HEP and middle sulfated CS were deposited under acidic (pH 4) and basic (pH 9) conditions of the adsorbing solutions. Another important aspect in the field of multilayers is the blending of PELs (polyanions/polycations) prior to film deposition to improve the properties of the layers. This possibility, by blending of HEP with CS was also explored during the course of this thesis work. Following is the summery of this complete study which includes the different objectives of the research and the achieved results in form of five papers.

Summary – paper I (chapter 2)

The first paper was aimed to delve into the effects of pH variation onto the physico-chemical properties and bioactivity of multilayers. Multilayer coatings from HEP and CHI were prepared at different pH to allow control of layer mass and surface properties, as well as protein adsorption, cell adhesion and growth. During the fabrication of multilayer films, the HEP solution was applied at varied pH values including pH 4, pH 9, or at pH 4 during the formation of the first layers followed by pH 9 during the last steps of the multilayer assembly (denoted pH 4+9). This study demonstrated a method to alternate between ion pairing and hydrogen bonding by varying the pH of the HEP solution from 4 to 9 that also led to

differences in both layer mass and adhesivity for C2C12 myoblast cells. A unique finding of this study was that a flip of pH from 4 to 9 allowed the formation of thicker multilayers with a high adhesivity for cells.

As it was found that the multilayers assembled by applying the HEP solution at pH 9 were significantly more cell adhesive and supported growth of C2C12 cells to a higher extent than layers assembled at pH 4 (cells adhered and grew poorly). However, the pH 4+9 condition improved cell adhesion and growth to a similar level as the PEM with HEP applied at pH 9. Therefore, this could be applied as a potential system for controlled release of growth factors in different tissue engineering applications.

The PEM of CHI and HEP fabricated at different pH conditions were characterized by several methods. Water contact angles (WCA) between CHI and HEP layers changed alternately which correlates to the change in the composition of the terminal layer. The WCA results showed distinct pH-dependent changes in wettability with high differences between CHI and HEP terminal layers prepared at pH 4, while the differences were smaller for multilayers where the HEP was added at pH 9 or by the pH 4+9 sequence. The difference in WCA between the layers at pH 4 were larger which indicated a dominance of either CHI or HEP in the outer layers after the corresponding coating step. In contrast, the WCA differences between CHI and HEP layers were smaller during the adsorption of HEP at pH 9. In this case the previously adsorbed CHI is not charged at pH 9 and, hence, other mechanisms than ion pairing were expected to be responsible for the adsorption of HEP. Hydrogen bonding was assumed here as it was also reported for HEP/CHI interaction with FTIR studies by Dong et al.[228]. Likewise, a distinct change in surface wettability was seen as the pH of the HEP solution is changed from 4 to 9 after the formation of 7th layer. The 8th layer (assembled at pH 9) became less hydrophilic than the ones assembled at pH 4. The WCA were even higher than compared to layers exclusively formed at pH 9, which pointed to a dominance of CHI in the outermost layers for systems formed at pH 9 as well as at pH 4+9 condition.

Surface plasmon resonance (SPR) and quartz crystal microbalance with dissipation monitoring (QCM-D) investigations allowed both the measurement of adsorbed quantities of PEL and also an estimation of the water content of the layers. Both techniques showed differences in the biomolecular mass adsorption and hydration during the multilayer build-up at different pH conditions. Exponentially growing multilayers were obtained when the HEP solution was kept at pH 4, while only a slight linear mass increase was observed for multilayers prepared where the HEP solution was kept at pH 9. At pH 4, when ion pairing

should dominate due to the protonation of CHI amino groups, more mass was adsorbed at each step, while lower mass increase observed at pH 9 indicated the dominance of hydrogen bonding [228]. PEM formed at the pH 4+9 condition showed an arrest of mass increase upon switching from pH 4 to pH 9 (QCM-D), while a further increase of layer mass was evident by SPR. The calculated QCM-D layer masses were much larger than those measured by SPR, particularly for the pH 4 and pH 4+9 regime. This indicated a substantial amount of water bound to these layers. In contrast, multilayers prepared at the pH 9 regime had a lower water content since only a small layer growth was observed with QCM-D. The ability of such multilayers to adsorb proteins was also measured by QCM-D by exposing the terminal HEP layer (12th layer) to FN for 1 hour. FN was chosen as a model protein to illustrate adsorption of adhesive proteins from serum that are important prerequisites for cells to adhere on material surfaces. The results showed that multilayers prepared at pH 9 had a higher affinity to FN followed by pH 4+9 layers, whereas pH 4 layers did not supported FN adsorption.

Atomic force microscopy (AFM) displayed a distinct surface morphology for each of the pH conditions with the smoothest granular surface topography for the multilayers prepared at pH 4 and the roughest globular structure when the HEP solution was applied at pH 9, while the pH 4+9 condition showed intermediate structures.

The different multilayers were exposed to serum containing culture medium for subsequent studies with C2C12 mouse myoblast cells. The pH during multilayer formation showed a great effect on cell adhesion and spreading. In the case of pH 4 multilayers, in general, cells were round. In contrast, elongated and well spread C2C12 cells were found on multilayers prepared at pH 9. On pH 4+9 layers more cells adhered with a more spread phenotype that was similar to the pH 9 conditions. Quantitative data (obtained by analysis of phase contrast images) on cell adhesion and spreading also confirmed the qualitative observations. The higher adhesion and spreading of cells on pH 9 and pH 4+9 multilayer systems were in accordance with the findings on FN adsorption.

The results of cell proliferation study revealed that cell spreading was improved on multilayers prepared at pH 4 although cell number was considerably lower. The cell coverage after 1 and 3 days was lowest on pH 4 multilayers followed by pH 4+9 and pH 9 layers. C2C12 cells were almost confluent after 3 days of culture on pH 9 layers and, hence, these layers are more proliferation supporting than pH 4 ones. The pH 4+9 layer setup also presented higher coverage of the surface with cells if compared with pH 4 layers which was in accordance with the cell adhesion results.

This work showed that multilayer coatings made from HEP (a strong PEL) and CHI (a weak PEL) can be used to affect adhesion and growth of C2C12 cells by simple adjustment of pH of HEP solution during multilayer assembly. This had a great effect on wetting properties of multilayers, their layer mass, water content and surface topography. Furthermore, the pH variation also influenced the subsequent adsorption of adhesive proteins like FN and adhesion and growth of cells. Therefore, multilayer systems prepared by variation of pH might be very useful to support initial cell attachment and growth, while at the same time providing additional functions, such as reservoirs and delivery systems for growth factors and similar molecules.

Summary – paper II (chapter 3)

The aim this following work was focused on synthesis of semi-synthetic cellulose derivatives and to explore the bioactivity of these cellulose derivatives by realizing their ability to cooperate with growth factors such as FGF-2 and modulate the growth of cells in comparison with the HEP.

GAG like HEP or HEP sulfate interact with growth factors and plays pivotal roles in regulating cell proliferation and differentiation. Furthermore, GAG such as HEP not only prolong the half-life of growth factors, but can also directly control the proliferation of cells by modulating the cellular production of growth factors [229, 230]. Since naturally occurring HEPs differ greatly regarding their molecular composition, their biological activity depends on the source, too [200]. Therefore, synthetic routes to prepare substances with controlled heparinoid activity are attractive for a variety of biomedical applications. Cellulose is one of the most abundant natural occurring polysaccharides. CS have been synthesized by variety of methods and in contrast to cellulose, CS showed highly improved solubility in water and better enzymatic degradability. This study introduced novel routes of cellulose derivatisation to obtain defined substitution patterns with sulfate, carboxylate and also carboxymethyl groups. CS were synthesized through aceto-sulfation as well as direct sulfation, whereas CS containing CO or CM groups were prepared by TEMPO oxidation from low sulfated CS or by carboxymethylation with chloroacetic acid. CM groups with the methyl group as spacer element in CM were intended to enhance the potential steric accessibility of the carboxyl groups for interaction with FGF2. All derivatives were water soluble. A series of CS from low to high sulfation degree were prepared along with three types of CO and four types of CM

from different CS as starting materials. The derivatisation was characterized by nuclear magnetic resonance and Raman spectroscopy.

Cytotoxicity measurements were performed with all the derivatives on 3T3-L1 fibroblast cells. All derivatives were non-toxic for 3T3 fibroblast cells. Most of the derivatives showed little but not significant reduction in cell viability. The derivatives were also investigated regarding their mitogenic activity by modulation of 3T3 fibroblast proliferation with or without exogenous FGF-2. For the CS, the degree of sulfation in both positions (6-*O* and 2-*O*) played an important role in the enhancement of the mitogenic activity of FGF-2. Additionally, in previous studies by Zhang et al. it was shown that CS with maximum sulfation at *O*-6-position and intermediate to high sulfation at *O*-2 position could accomplish a binding of FGF-2 [221]. With an increase in 6-*O* sulfation up to 1.0, the proliferation increased up to 120 % of the control (10 ng ml⁻¹ FGF2) and a further increase of sulfation at 2-*O*-position continuously increased the proliferation up to 160% of the control. In contrast to the finding with CS, only some of the carboxylated and carboxymethylated derivatives possessed a small mitogenic activity. Moreover, the mitogenic activity was not related to the degree of carboxylation or carboxymethylation as was observed for the degree of sulfation. The results confirmed that a higher degree of sulfation obviously provoked the enhanced mitogenic activity and also indicated that an increase in DS_{COO} (DS values of carboxyl groups) led to impaired proliferation, which was an unexpected finding if compared with HEP that possesses a similar DS_{COO}.

Additionally, concentration-dependent effects of cellulose derivatives on 3T3 cell proliferation in the presence of exogenous FGF-2 were tested. All CS yielded results compared with HEP at a concentration of 1 mg ml⁻¹ and increased the growth of 3T3 cells up to 195% compared with the control, which was DMEM with 10 ng ml⁻¹ FGF-2 alone. The highest mitogenic activity was found for HEP (215% compared with the control), but only at a concentration of 100 µg ml⁻¹. However, derivative CS-1.94 showed a remarkable mitogenic activity over the whole concentration range which was in correlation to the difference in degree of derivatisation and site. The reasons for the mitogenic property might be due to the prolonged life time of FGF-2 as well as the increased binding of FGF-2 to its receptor by CS, as also shown by Pye et al. for heparan sulfate oligosaccharides, where an increased sulfation was linked to elevated cell growth [231]. Later on, studies by Weltrowski et al. have shown that CS increased the stability of FGF-2 towards proteases alone or in contact with cells that might release MMPs (matrix metalloproteinases) [232].

Another experiment was done where direct impact of the cellulose derivatives on the proliferation of 3T3-L1 fibroblasts was studied at the same concentrations as in the former experiments but without addition of FGF-2. The middle sulfated derivative CS-1.57 showed highest mitogenic activity at the lower concentration range. The mitogenic activity of CS-1.57 even at lower concentrations exceeded that of HEP by far. Surprisingly, the highest sulfated CS-1.94 yielded a slight increase only at 1 mg ml⁻¹ (131% of the FGF-2 control). Comparable to the results with the addition of FGF-2, CS-1.94 showed almost a constant mitogenic activity over the whole concentration range. But CS with lower degree of derivatisation, especially at 2-*O*-position led to higher mitogenic activity without FGF-2, even at relatively low concentrations. Hence, it was speculated that a certain degree of 2-*O*-sulfation can foster the mitogenic activity of the cellulose derivatives. With the exception of CM-1.09, all of the carboxylated and carboxymethylated CS did not show any promoting effect on cell growth. The results show that the mitogenic effects of the cellulose derivatives in the absence of exogenous growth factors depend highly on derivatisation, especially the degree of sulfation. Surprisingly none of the carboxylated CS expressed a remarkable mitogenic activity even their structure shows some similarities to HEP and this might be because their DS_S was probably not high enough to become potent mitogenic inducers. CS with intermediate and high DS_S possessed a mitogenic activity far exceeding that of HEP, which makes these materials alone, or more specifically, together with FGF-2, highly interesting. This study indicated that CS represented highly effective alternative to HEP in tissue culture applications as supplements to media, but more importantly as component of scaffolds, able to bind, protect and control the release of growth factors.

Summary – paper III (chapter 4)

The investigations of CS properties and their biological responses when applied as thin film coatings were aimed here. A comparative study on multilayers prepared from high (CS2.6) and middle sulfated CS (CS1.6) along with HEP was done to depict effect of chemical composition of polyanions (presence of sulfate groups and absence of carboxylic groups) on multilayer properties and their bioactivity.

The ‘optical’ mass of the multilayers, measured by SPR, showed little differences in the total mass adsorbed irrespective of which polyanion was used. In the case of the CHI-HEP multilayer system, the layer growth was exponential. Multilayer mass of both CS systems (CHI-CS1.6 and CHI-CS2.6) was slightly larger, but with a different growth pattern. The CS

graphs appeared staircase-like indicating more mass adsorption during the CS1.6 and CS2.6 deposition as compared to CHI. In contrast, 'acoustic' mass, calculated from QCM-D, showed the lowest mass and dissipation values for CS2.6 multilayers (highest sulfation degree) indicating the formation of stiffer layers compared to HEP and CS1.6 layers, who resulted in higher mass and dissipation values. The layer masses obtained from the QCM-D data were much larger than the corresponding masses measured by SPR, which indicated the hydrated nature of CHI-HEP multilayers. In contrast, the acoustic mass of CHI-CS2.6 layers was also very low and pointed to a highly condensed nature of these films. The dissipation values for the CHI-HEP system showed alternately increased values upon addition of CHI followed by strongly decreased values upon addition of HEP. The decrease of dissipation values after addition of HEP indicates a stiffening of the multilayer system. Such alternating changes in the dissipation curves were absent for the CHI-CS1.6 and CHI-CS2.6 systems. For the CHI-CS1.6 system, there was an almost linear increase, whereas the dissipation values remained almost constant in case of CHI-CS2.6, pointing again to the formation of highly condensed layers. The relative water content of these multilayers was calculated by comparison of layer mass calculated from SPR and QCM-D measurements. The staircase growth pattern observed for CS based multilayers indicated the dominating presence of CS in the CHI-CS1.6 and CHI-CS2.6 layer systems (unlike CHI-HEP system) that also draws the attention towards the fact that they contain only sulfate groups and no carboxylic groups like HEP. Dominance of sulfate groups over carboxylic groups in ion pairing has been observed previously by others, too [129].

QCM-D measurements were also used to measure the adsorption of FN on the terminal polyanion layer to investigate the protein adsorption abilities (FN possesses HEP-binding domains). FN adsorption was very low and not detectable on the CHI-HEP layers as found in the previous Paper I, whereas both CHI-CS multilayers showed significant adsorption of FN. However, the quantity adsorbed on CHI-CS1.6 was higher compared to CHI-CS2.6 multilayers.

Water contact angle (WCA) and zeta potential measurements were executed to determine wettability and surface charge of HEP and CS multilayers. Both measurements indicated formation of more distinct layers using HEP as polyanion, while the employment of CS1.6 and CS2.6 resulted into more fuzzy intermingled multilayers. CHI-HEP multilayers showed alternating values with lower WCA for HEP and higher for CHI and these differences in WCA values pointed to the formation of more separated layers of CHI-HEP system. In contrast, no such alternating WCA values were observed for CHI-CS1.6 or very low

differences were seen for CHI-CS2.6 system which hinted towards the formation of more intermingled multilayers. These observations were further affirmed by the zeta potential measurements.

The biological behaviour of HEP and CS based multilayer films was studied by cell adhesion and growth experiments with C2C12 cells. The cell count and cell spreading (cell size) was significantly lower on the CHI-HEP multilayer system compared to both CS terminated multilayers, which was also in correlation with the lack of FN adsorption on CHI-HEP. The proliferation of C2C12 cells on different corresponding multilayer systems was studied after incubation periods of 24 and 72 h. On both CHI-HEP and CHI-CS1.6 layers, cells showed a reduced degree of spreading and a tendency to form bulky aggregates in contrast to cells seeded on CHI-CS2.6 layers, where cells had a more spread phenotype. The speculated reason might be the hydration of HEP and CS1.6 layers during the long term culture affecting the growth and phenotypes of the cells. From the above observations, one can conclude that multilayer coatings prepared from three different polyanions (HEP, CS1.6, CS2.6) can be used to attain multilayer systems with specific growth patterns, hydration, mechanical properties as well as fibronectin adsorption and cellular responses.

Summary – paper IV (chapter 5)

In continuation with the investigations of CS, this work was focused on the preparation of PEL multilayers at different pH conditions using HEP or middle sulfated CS as the polyanion and CHI as a polycation. The multilayers were prepared at pH 4 and 9 in analogy to paper I and shall help in understanding the effects of deposition conditions on the properties and bioactivity of the multilayers of CS along with HEP. This study provided the opportunity to learn whether a CS with slightly higher degree of sulfation and molecular weight but lack of carboxylic group would behave similarly to HEP regarding film formation, surface properties and bioactivity towards protein adsorption, cell adhesion and proliferation.

PEM were again characterized by SPR, QCM-D, WCA and zeta potential measurements. Biological behavior of these multilayers was studied regarding FN adsorption and adhesion/ proliferation of C2C12 myoblast cells.

Layer growth and dry mass were higher for both polyanions at pH 4. Layers grew exponentially and ion pairing occurred due to protonation of CHI at pH 4 [142]. On the other hand, at pH 9 condition only a low increment of layer mass was observed. Here, ion pairing was replaced by hydrogen bonding since the amino groups of the previously adsorbed CHI

are not protonated at pH 9. In contrast, a different behaviour was observed for CHI-CS multilayer systems. CS as polyanion resulted also in high layer growth and mass at pH 9 (difference between pH 4 and 9 was moderate), indicating a much stronger effect of hydrogen bonding between CHI and CS. Also the growth pattern suggested a higher mass increase by CS, but lower with CHI. Findings of QCM-D measurements were in correlation with SPR studies for the CHI-HEP system, whereas CHI-CS had shown some discrepancy. In strong contrast to the CHI-HEP system, the layer mass at pH 9 regimes was higher than at pH 4 for the CHI-CS system. The calculated water content of these layers at pH 9 was higher than at pH 4, which indicates the reason for higher layers mass at pH 9. The CHI-CS multilayers at pH 4 were supposed to be more condensed due to electrostatic cross-linking than CHI-CS at pH 9, where hydrogen bonding might have anticipated. Further, the sulfate groups from CS and amino groups from CHI coupled counter ions and water, respectively. This showed that hydrogen bonding in the CHI-CS system might be an important parameter during multilayer formation.

QCM-D studies were also used to measure the adsorption of FN on the terminal polyanion layer to investigate the protein adsorption abilities of these layers. CHI-HEP multilayers prepared at pH 9 had a higher affinity to FN as compared to those prepared at pH 4, which showed apparently no measurable FN adsorption. On the other hand, FN adsorption was seen for both of the CHI-CS systems, but was higher for CHI-CS multilayers prepared at pH 4.

The wettability of CHI-HEP multilayers was alternating with lower WCA for HEP and higher for CHI at both pH regimes. The differences were greater for multilayers prepared at pH 4 than those at pH 9. Such differences in WCA between the CHI and HEP layers solely represent the characteristics of terminal layer and indicated the formation of more distinct layers without or less intermingling of PEL during the fabrication of such multilayer systems. On the other hand, no such alternating WCA values were observed in CHI-CS multilayer systems formed at both pH 4 and 9 which indicated that CS was rather integrating into CHI layers than forming well separated layers.

These observations were further supported by the zeta potential measurements of the terminal CHI and polyanion (HEP or CS) layers prepared at pH 4 and pH 9, which also indicated the formation of more separated layers in case of CHI-HEP multilayers prepared at pH 4 whereas more intermingled, fuzzy multilayers formed by CHI-CS at both pH conditions and CHI/HEP at pH 9.

Cell adhesion studies were performed to study the effect of multilayer composition, prepared from different polyanions and at different pH conditions on adhesion and growth of C2C12 cells. The cell behaviour was highly dependent on pH for the CHI-HEP multilayers and was closely related to FN adsorption. The number of adhering cells and their spreading was significantly lower on CHI-HEP multilayers prepared at pH 4 condition as compared to the layers fabricated at pH 9 condition as also found in paper I. The lower cell adhesion and spreading on pH 4 layers was correlated to FN adsorption. In contrast, properties of CHI-CS layers did not show such strong dependency on pH value, where cell adhesion and spreading was high on multilayers prepared either at pH 4 or pH 9. Cell growth was studied also on terminal polyanion layers for 24 and 72 h and cell growth was lower on terminal HEP layers compared to CS terminal layers, which was closely related to FN adsorption on HEP terminal layers and also to the findings of adhesion studies. In case of CHI-HEP system, pH 9 multilayers showed more surface cell coverage by cells as compared to pH 4 multilayers, supported by the quantitative measurements as well. C2C12 cell growth showed low dependence on pH during formation of CHI-CS multilayers

The results of this study show that CS is an attractive candidate for multilayer formation that does not depend strongly on pH during multilayer formation. In addition, such multilayer system also represents a good substrate for cell interactions. Moreover, CS possessed a high bioactivity to promote adhesion and growth of cells on multilayers in addition to their ability to bind growth factors provides them with huge advantages for designing bioactive coatings for tissue engineering and implantology.

Summary – paper V (chapter 6)

PEL multilayers prepared via facile LBL technique offers the creation of a wide range of biomaterial coatings with potential adjustment of bioactivity towards proteins and cells. An enhancement of such versatile and useful technique was achieved by application of blended PEL during fabrication of multilayer films [160]. After exploring the potentials of semi-synthetically derived CS, a comparative study was conducted on physical and biological multilayer film properties prepared from HEP, semi-synthetic CS and their blends.

PEL multilayers were fabricated at pH 4 by blending HEP with either the intermediately sulfated cellulose (CS1.6) or highly sulfated cellulose (CS2.6) as polyanions paired with CHI as polycation. The different systems were designated as CHI-HEP, CHI-CS1.6, CHI-CS2.6, the blend of HEP and CS1.6 as CHI-(HEP+CS1.6) while the blend of HEP and CS2.6 as

CHI-(HEP+CS2.6). Multilayers growth was again monitored by SPR and QCM-D, whereas surface wettability was determined by WCA measurements. Both SPR and QCM-D showed clear differences in the multilayer growth patterns of the different polyanion systems. An exponential layer growth was visible for the CHI-HEP multilayer system as also shown before. Both multilayer systems of CS (CHI-CS1.6 and CHI-CS2.6) showed slightly larger adsorbed mass as well as different increment behaviour (staircase growth curves) compared to the CHI-HEP system, which was also shown in the previous paper III. Indeed, the CHI-(HEP+CS1.6) multilayer system expressed an exponential growth similar to CHI-HEP system, whereas a staircase-like pattern was achieved with the CHI-(HEP+CS2.6) (similar to the pure CS systems).

The overall adsorbed mass increment (including water content) measured by QCM-D for each type of multilayer system (except for CHI-CS2.6 system, where layers seemed to be highly condensed as also shown in paper IV) was much larger than the corresponding mass measured by SPR, which indicated that a substantial amount of water was coupled within these multilayer systems. Both blend systems [CHI-(HEP+CS1.6) and CHI-(HEP+CS2.6)] showed oscillating dissipation values similar to the CHI-HEP system. The result of SPR and QCM-D indicated that HEP was capable to displace CS also with a high sulfation degree (CS2.6) during multilayer formation. This pointed to an important role of carboxylic groups (HEP) with amino groups (CHI) WCA measurements showed an alternating trend of WCA values for CHI-(HEP+CS1.6) like the CHI-HEP system, which indicated again a dominating incorporation of HEP over CS1.6. The changes in the WCA of CHI-CS2.6 multilayers were also very small which also pointed towards the formation of intermingled multilayers. While for the system of CS2.6 blended with HEP (CHI-(HEP+CS2.6)), an oscillating trend of WCA similar to CHI-HEP system was found. These observations again pointed to the dominating presence of HEP in CHI-(HEP+CS2.6) multilayers, which is in line with the multilayer growth data from SPR and QCM-D.

C2C12 cells were plated on the different multilayer surfaces (terminal polyanion, 8th layer) to reveal the effect of multilayer molecular composition on the cell attachment and morphology. The cell count as well as the cell spreading (cell size) were found to be significantly lower on both CHI-HEP and CHI-(HEP+CS1.6) multilayer systems in comparison to the other three CHI-CS1.6, CHI-CS2.6 and CHI-(HEP+CS2.6) systems. On the other hand, as shown in the previous paper, CHI-CS1.6 multilayers were capable of FN adsorption and supported cell adhesion and growth. Similar to the CHI-CS1.6, CHI-CS2.6 multilayer systems promoted also significantly cell adhesion and spreading. In case of blend multilayers, the

CHI-(HEP+CS1.6) multilayer system also did not support cell adhesion and spreading, very much similar to CHI-HEP multilayers, which again indicated the dominating presence of HEP over CS1.6. In contrast, the CHI-(HEP+CS2.6) multilayers provided the superior surface for cell attachment and spreading. The reason for such behaviour was speculated as the conformation of HEP in the ternary system of CHI-(HEP+CS2.6), which might be quite different than in the other systems [CHI-HEP and CHI-(HEP+CS1.6)]. Both (HEP and CS2.6) might have contributed in promotion of cell adhesion as CS2.6 was also found to support cell attachment. The morphology of C2C12 cells also supported the results of quantitative measurements. The CHI-(HEP+CS2.6) multilayers expressed most well developed FA with well-organized actin stress fibres.

During this comparative study, it was found that blending of HEP with two different CS resulted in multilayers that differ dramatically in their bioactivity. This work was also beneficial as HEP is a natural GAG with limited abundance and CS represent potential alternative materials in making bioactive surface coatings. Hence, CS might be used as diluting agent of HEP in blends, thereby merging the useful properties of both natural and semi-synthetic PEL. Overall, the blending of PEL with different bioactivity in multilayer coatings can provide additional possibilities to regulate multilayer properties and their biological response.

1.7. References

1. Salgado, A.J., O.P. Coutinho, and R.L. Reis, *Bone Tissue Engineering: State of the Art and Future Trends*. Macromolecular Bioscience, 2004. **4**(8): p. 743-765.
2. Anderson, J.M., *Biological responses to materials*. Annual Review of Materials Research, 2001. **31**: p. 81-110.
3. Castner, D.G. and B.D. Ratner, *Biomedical surface science: Foundations to frontiers*. Surface Science, 2002. **500**(1-3): p. 28-60.
4. Boudou, T., et al., *Multiple Functionalities of Polyelectrolyte Multilayer Films: New Biomedical Applications*. Advanced Materials, 2010. **22**(4): p. 441-467.
5. Stevens, M.M. and J.H. George, *Exploring and engineering the cell surface interface*. Science, 2005. **310**(5751): p. 1135-1138.
6. Remes, A. and D.F. Williams, *Immune response in biocompatibility*. Biomaterials, 1992. **13**(11): p. 731-743.

7. Tang, L., T.A. Jennings, and J.W. Eaton, *Mast cells mediate acute inflammatory responses to implanted biomaterials*. Proceedings of the National Academy of Sciences, 1998. **95**(15): p. 8841-8846.
8. Williams, D.F., *On the mechanisms of biocompatibility*. Biomaterials, 2008. **29**(20): p. 2941-2953.
9. Tzoneva, R., N. Faucheux, and T. Groth, *Wettability of substrata controls cell-substrate and cell-cell adhesions*. Biochimica Et Biophysica Acta-General Subjects, 2007. **1770**(11): p. 1538-1547.
10. Hench, L.L. and I. Thompson, *Twenty-first century challenges for biomaterials*. Journal of The Royal Society Interface, 2010. **7**(Suppl 4): p. S379-S391.
11. Planell, J., et al., *Materials Surface Effects on Biological Interactions*, in *Advances in Regenerative Medicine: Role of Nanotechnology, and Engineering Principles*, V.P. Shastri, G. Altankov, and A. Lendlein, Editors. 2010, Springer Netherlands. p. 233-252.
12. Shin, H., S. Jo, and A.G. Mikos, *Biomimetic materials for tissue engineering*. Biomaterials, 2003. **24**(24): p. 4353-4364.
13. Groth, T., et al., *Development of bioactive surface coatings for tissue engineering applications*. Internal Medicine 2007-2008. **15-16**: p. 7-9.
14. Hench, L.L. and J.M. Polak, *Third-Generation Biomedical Materials*. Science, 2002. **295**(5557): p. 1014-1017.
15. Groth, T., et al., *Chemical and Physical Modifications of Biomaterial Surfaces to Control Adhesion of Cells*, in *Advances in Regenerative Medicine: Role of Nanotechnology, and Engineering Principles*, V.P. Shastri, G. Altankov, and A. Lendlein, Editors. 2010, Springer Netherlands. p. 253-284.
16. Niepel, M., et al., *Generic Methods of Surface Modification to Control Adhesion of Cells and Beyond*, in *Biomaterials Surface Science*. 2013, Wiley-VCH Verlag GmbH & Co. KGaA. p. 441-467.
17. Griffith, L.G. and G. Naughton, *Tissue engineering - Current challenges and expanding opportunities*. Science, 2002. **295**(5557): p. 1009-+.
18. Grinnell, F., *Focal Adhesion Sites and the Removal of Substratum-Bound Fibronectin*. Journal of Cell Biology, 1986. **103**(6): p. 2697-2706.

19. Altankov, G., et al., *Development of Provisional Extracellular Matrix on Biomaterials Interface: Lessons from In Vitro Cell Culture*, in *Advances in Regenerative Medicine: Role of Nanotechnology, and Engineering Principles*, V.P. Shastri, G. Altankov, and A. Lendlein, Editors. 2010, Springer Netherlands. p. 19-43.
20. Vogel, V. and G. Baneyx, *The tissue engineering puzzle: A molecular perspective*. Annual Review of Biomedical Engineering, 2003. **5**: p. 441-463.
21. Robert, A.L., *Biomaterials: Protein-Surface Interactions*, in *Encyclopedia of Biomaterials and Biomedical Engineering*. 2013, Taylor & Francis. p. 1-15.
22. Gumbiner, B.M., *Cell Adhesion: The Molecular Basis of Tissue Architecture and Morphogenesis*. Cell, 1996. **84**(3): p. 345-357.
23. Yamada, K.M. and B. Geiger, *Molecular interactions in cell adhesion complexes*. Current Opinion in Cell Biology, 1997. **9**(1): p. 76-85.
24. Huang, S. and D.E. Ingber, *The structural and mechanical complexity of cell-growth control*. Nat Cell Biol, 1999. **1**(5): p. E131-E138.
25. Altankov, G., F. Grinnell, and T. Groth, *Studies on the biocompatibility of materials: Fibroblast reorganization of substratum-bound fibronectin on surfaces varying in wettability*. Journal of Biomedical Materials Research, 1996. **30**(3): p. 385-391.
26. Huang, S. and D.E. Ingber, *Shape-Dependent Control of Cell Growth, Differentiation, and Apoptosis: Switching between Attractors in Cell Regulatory Networks*. Experimental Cell Research, 2000. **261**(1): p. 91-103.
27. Bongrand, P., C. Capo, and R. Depieds, *Physics of cell adhesion*. Progress in Surface Science, 1982. **12**(3): p. 217-285.
28. Vitte, J., et al., *Regulation of cell adhesion*. Clin Hemorheol Microcirc, 2005. **33**(3): p. 167-88.
29. Trommler, A., D. Gingell, and H. Wolf, *Red blood cells experience electrostatic repulsion but make molecular adhesions with glass*. Biophysical Journal, 1985. **48**(5): p. 835-841.
30. Israelachvili, J. and H. Wennerstrom, *Role of hydration and water structure in biological and colloidal interactions*. Nature, 1996. **379**(6562): p. 219-225.
31. Iwasaki, Y., et al., *Competitive adsorption between phospholipid and plasma protein on a phospholipid polymer surface*. J Biomater Sci Polym Ed, 1999. **10**(5): p. 513-29.

32. Lee, J.H., J. Kopecek, and J.D. Andrade, *Protein-resistant surfaces prepared by PEO-containing block copolymer surfactants*. *J Biomed Mater Res*, 1989. **23**(3): p. 351-68.
33. Tziampazis, E., J. Kohn, and P.V. Moghe, *PEG-variant biomaterials as selectively adhesive protein templates: model surfaces for controlled cell adhesion and migration*. *Biomaterials*, 2000. **21**(5): p. 511-520.
34. Zhu, X., et al., *Effects of topography and composition of titanium surface oxides on osteoblast responses*. *Biomaterials*, 2004. **25**(18): p. 4087-4103.
35. Kommireddy, D.S., et al., *Stem cell attachment to layer-by-layer assembled TiO₂ nanoparticle thin films*. *Biomaterials*, 2006. **27**(24): p. 4296-4303.
36. Pelham, R.J. and Y.-l. Wang, *Cell locomotion and focal adhesions are regulated by substrate flexibility*. *Proceedings of the National Academy of Sciences*, 1997. **94**(25): p. 13661-13665.
37. Crouzier, T., et al., *Presentation of BMP-2 from a Soft Biopolymeric Film Unveils its Activity on Cell Adhesion and Migration*. *Advanced Materials*, 2011. **23**(12): p. H111-H118.
38. Richert, L., et al., *Improvement of Stability and Cell Adhesion Properties of Polyelectrolyte Multilayer Films by Chemical Cross-Linking*. *Biomacromolecules*, 2003. **5**(2): p. 284-294.
39. Saha, K., et al., *Substrate Modulus Directs Neural Stem Cell Behavior*. *Biophysical Journal*, 2008. **95**(9): p. 4426-4438.
40. Langer, R. and J.P. Vacanti, *Tissue Engineering*. *Science*, 1993. **260**(5110): p. 920-926.
41. Ryan, P.L., et al., *Tissue spreading on implantable substrates is a competitive outcome of cell-cell vs. cell-substratum adhesivity*. *Proceedings of the National Academy of Sciences*, 2001. **98**(8): p. 4323-4327.
42. Senger, D.R., D.F. Wirth, and R.O. Hynes, *Transformed mammalian cells secrete specific proteins and phosphoproteins*. *Cell*, 1979. **16**(4): p. 885-893.
43. Jauregui, H.O., *Cell adhesion to biomaterials. The role of several extracellular matrix components in the attachment of non-transformed fibroblasts and parenchymal cells*. *ASAIO Trans*, 1987. **33**(2): p. 66-74.

44. Andrade, J.D., V. Hlady, and A.P. Wei, *Adsorption of Complex Proteins at Interfaces*. Pure and Applied Chemistry, 1992. **64**(11): p. 1777-1781.
45. Meyer, U., et al., *Basic reactions of osteoblasts on structured material surfaces*. Eur Cell Mater, 2005. **9**: p. 39-49.
46. Groth, T., et al., *Protein adsorption, lymphocyte adhesion and platelet adhesion/activation on polyurethane ureas is related to hard segment content and composition*. J Biomater Sci Polym Ed, 1994. **6**(6): p. 497-510.
47. Altankov, G., K. Richau, and T. Groth, *The role of surface zeta potential and substratum chemistry for regulation of dermal fibroblasts interaction*. Materialwissenschaft und Werkstofftechnik, 2003. **34**(12): p. 1120-1128.
48. Faucheux, N., et al., *Self-assembled monolayers with different terminating groups as model substrates for cell adhesion studies*. Biomaterials, 2004. **25**(14): p. 2721-2730.
49. Lundqvist, M., I. Sethson, and B.-H. Jonsson, *Protein Adsorption onto Silica Nanoparticles: Conformational Changes Depend on the Particles' Curvature and the Protein Stability*. Langmuir, 2004. **20**(24): p. 10639-10647.
50. Andrade, J.D. and V. Hlady, *Protein adsorption and materials biocompatibility: A tutorial review and suggested hypotheses*, in *Biopolymers/Non-Exclusion HPLC*. 1986, Springer Berlin Heidelberg. p. 1-63.
51. Czeslik, C., *Proteinadsorption an festen Grenzflächen. Erwünscht und unerwünscht*. Chemie in unserer Zeit, 2006. **40**(4): p. 238-245.
52. Norde, W. and J. Lyklema, *Why proteins prefer interfaces*. J Biomater Sci Polym Ed, 1991. **2**(3): p. 183-202.
53. Morra, M., *On the molecular basis of fouling resistance*. J Biomater Sci Polym Ed, 2000. **11**(6): p. 547-69.
54. Tsai, W.B., et al., *Platelet adhesion to polystyrene-based surfaces preadsorbed with plasmas selectively depleted in fibrinogen, fibronectin, vitronectin, or von Willebrand's factor*. Journal of Biomedical Materials Research, 2002. **60**(3): p. 348-359.
55. Groth, T., et al., *The hemocompatibility of biomaterials invitro - investigations on the mechanism of the whole-blood clot formation test*. Atla-Alternatives to Laboratory Animals, 1992. **20**(3): p. 390-395.

56. Grinnell, F. and M.K. Feld, *Fibronectin Adsorption on Hydrophilic and Hydrophobic Surfaces Detected by Antibody-Binding and Analyzed during Cell-Adhesion in Serum-Containing Medium*. Journal of Biological Chemistry, 1982. **257**(9): p. 4888-4893.
57. Tang, L.P. and J.W. Eaton, *Fibrin(Ogen) Mediates Acute Inflammatory Responses to Biomaterials*. Journal of Experimental Medicine, 1993. **178**(6): p. 2147-2156.
58. Ngankam, A.P., G.Z. Mao, and P.R. Van Tassel, *Fibronectin adsorption onto polyelectrolyte multilayer films*. Langmuir, 2004. **20**(8): p. 3362-3370.
59. Hu, W.J., J.W. Eaton, and L.P. Tang, *Molecular basis of biomaterial-mediated foreign body reactions*. Blood, 2001. **98**(4): p. 1231-1238.
60. Gray, J.J., *The interaction of proteins with solid surfaces*. Current Opinion in Structural Biology, 2004. **14**(1): p. 110-115.
61. Rabe, M., D. Verdes, and S. Seeger, *Understanding protein adsorption phenomena at solid surfaces*. Advances in Colloid and Interface Science, 2011. **162**(1-2): p. 87-106.
62. Altankov, G. and T. Groth, *Fibronectin matrix formation by human fibroblasts on surfaces varying in wettability*. J Biomater Sci Polym Ed, 1996. **8**(4): p. 299-310.
63. Hynes, R.O., *The Extracellular Matrix: Not Just Pretty Fibrils*. Science, 2009. **326**(5957): p. 1216-1219.
64. Hynes, R.O., *Integrins: bidirectional, allosteric signaling machines*. Cell, 2002. **110**(6): p. 673-87.
65. Frisch, S.M. and E. Ruoslahti, *Integrins and anoikis*. Current Opinion in Cell Biology, 1997. **9**(5): p. 701-706.
66. Geiger, B., et al., *Transmembrane crosstalk between the extracellular matrix and the cytoskeleton*. Nat Rev Mol Cell Biol, 2001. **2**(11): p. 793-805.
67. Faucheux, N., et al., *The dependence of fibrillar adhesions in human fibroblasts on substratum chemistry*. Biomaterials, 2006. **27**(2): p. 234-245.
68. Danen, E.H.J. and A. Sonnenberg, *Integrins in regulation of tissue development and function*. Journal of Pathology, 2003. **200**(4): p. 471-480.
69. Giancotti, F.G. and E. Ruoslahti, *Transduction - Integrin signaling*. Science, 1999. **285**(5430): p. 1028-1032.

70. Anselme, K., *Osteoblast adhesion on biomaterials*. Biomaterials, 2000. **21**(7): p. 667-681.
71. Puleo, D.A. and R. Bizios, *Formation of focal contacts by osteoblasts cultured on orthopedic biomaterials*. Journal of Biomedical Materials Research, 1992. **26**(3): p. 291-301.
72. Geiger, B. and K.M. Yamada, *Molecular architecture and function of matrix adhesions*. Cold Spring Harb Perspect Biol, 2011. **3**(5).
73. Groth, T. and G. Altankov, *Studies on cell-biomaterial interaction role of tyrosine phosphorylation during fibroblast spreading on surfaces varying in wettability*. Biomaterials, 1996. **17**(12): p. 1227-1234.
74. Sahni, A., L.A. Sporn, and C.W. Francis, *Potential of endothelial cell proliferation by fibrin(ogen)-bound fibroblast growth factor-2*. J Biol Chem, 1999. **274**(21): p. 14936-41.
75. Wells, A., *EGF receptor*. The International Journal of Biochemistry & Cell Biology, 1999. **31**(6): p. 637-643.
76. Fan, V.H., et al., *Tethered Epidermal Growth Factor Provides a Survival Advantage to Mesenchymal Stem Cells*. STEM CELLS, 2007. **25**(5): p. 1241-1251.
77. Roux, P.P. and J. Blenis, *ERK and p38 MAPK-Activated Protein Kinases: a Family of Protein Kinases with Diverse Biological Functions*. Microbiology and Molecular Biology Reviews, 2004. **68**(2): p. 320-344.
78. Kennedy, S.G., et al., *The PI 3-kinase/Akt signaling pathway delivers an anti-apoptotic signal*. Genes Dev, 1997. **11**(6): p. 701-13.
79. Lembach, K.J., *Induction of human fibroblast proliferation by epidermal growth factor (EGF): enhancement by an EGF-binding arginine esterase and by ascorbate*. Proc Natl Acad Sci U S A, 1976. **73**(1): p. 183-7.
80. Cai, K., et al., *Polysaccharide-protein surface modification of titanium via a layer-by-layer technique: Characterization and cell behaviour aspects*. Biomaterials, 2005. **26**(30): p. 5960-5971.
81. Mao, J.S., et al., *A preliminary study on chitosan and gelatin polyelectrolyte complex cytocompatibility by cell cycle and apoptosis analysis*. Biomaterials, 2004. **25**(18): p. 3973-3981.

82. Kurella, A. and N.B. Dahotre, *Review paper: Surface Modification for Bioimplants: The Role of Laser Surface Engineering*. Journal of Biomaterials Applications, 2005. **20**(1): p. 5-50.
83. Bacakova, L., et al., *Adhesion and proliferation of rat vascular smooth muscle cells (VSMC) on polyethylene implanted with O+ and C+ ions*. Journal of Biomaterials Science-Polymer Edition, 2001. **12**(7): p. 817-834.
84. Vonarbourg, A., et al., *Parameters influencing the stealthiness of colloidal drug delivery systems*. Biomaterials, 2006. **27**(24): p. 4356-4373.
85. Klee, D., et al., *Surface modification of poly(vinylidene fluoride) to improve the osteoblast adhesion*. Biomaterials, 2003. **24**(21): p. 3663-3670.
86. Croll, T.I., et al., *A blank slate? Layer-by-layer deposition of hyaluronic acid and chitosan onto various surfaces*. Biomacromolecules, 2006. **7**(5): p. 1610-1622.
87. Tang, Z., et al., *Biomedical Applications of Layer-by-Layer Assembly: From Biomimetics to Tissue Engineering*. Advanced Materials, 2006. **18**(24): p. 3203-3224.
88. Sargent, R.B. and N.A. O'Brien, *Dielectric materials for thin-film-based optical communications filters*. Mrs Bulletin, 2003. **28**(5): p. 372-376.
89. *Langmuir-Blodgett Films*, G. Roberts, Editor 1990, Kluwer Academic: Norwell, MA.
90. Mrksich, M. and G.M. Whitesides, *Using self-assembled monolayers to understand the interactions of man-made surfaces with proteins and cells*. Annu Rev Biophys Biomol Struct, 1996. **25**: p. 55-78.
91. Mrksich, M., *A surface chemistry approach to studying cell adhesion*. Chemical Society Reviews, 2000. **29**(4): p. 267-273.
92. Erokhin, V., *Handbook of Thin Film Materials*, H.S. Nalwa, Editor 2002, Academic: San Diego, CA.
93. Senaratne, W., L. Andruzzi, and C.K. Ober, *Self-Assembled Monolayers and Polymer Brushes in Biotechnology: Current Applications and Future Perspectives*. Biomacromolecules, 2005. **6**(5): p. 2427-2448.
94. Decher, G., J.D. Hong, and J. Schmitt, *Buildup of ultrathin multilayer films by a self-assembly process: III. Consecutively alternating adsorption of anionic and cationic*

- polyelectrolytes on charged surfaces*. Thin Solid Films, 1992. **210–211**, Part 2(0): p. 831-835.
95. Iler, R.K., *Multilayers of Colloidal Particles*. Journal of Colloid and Interface Science, 1966. **21**(6): p. 569-&.
96. Decher, G., *Fuzzy Nanoassemblies: Toward Layered Polymeric Multicomposites*. Science, 1997. **277**(5330): p. 1232-1237.
97. Hammond, P.T., *Form and Function in Multilayer Assembly: New Applications at the Nanoscale*. Advanced Materials, 2004. **16**(15): p. 1271-1293.
98. Schlenoff, J.B., H. Ly, and M. Li, *Charge and mass balance in polyelectrolyte multilayers*. Journal of the American Chemical Society, 1998. **120**(30): p. 7626-7634.
99. Clark, S.L. and P.T. Hammond, *The Role of Secondary Interactions in Selective Electrostatic Multilayer Deposition*. Langmuir, 2000. **16**(26): p. 10206-10214.
100. Kotov, N.A., *Layer-by-layer self-assembly: The contribution of hydrophobic interactions*. Nanostructured Materials, 1999. **12**(5–8): p. 789-796.
101. Quinn, J.F., et al., *Next generation, sequentially assembled ultrathin films: beyond electrostatics*. Chemical Society Reviews, 2007. **36**(5): p. 707-718.
102. Schlenoff, J.B. and S.T. Dubas, *Mechanism of polyelectrolyte multilayer growth: Charge overcompensation and distribution*. Macromolecules, 2001. **34**(3): p. 592-598.
103. v. Klitzing, R., *Internal structure of polyelectrolyte multilayer assemblies*. Physical Chemistry Chemical Physics, 2006. **8**(43): p. 5012-5033.
104. Lyklema, J. and L. Deschênes, *The first step in layer-by-layer deposition: Electrostatics and/or non-electrostatics?* Advances in Colloid and Interface Science, 2011. **168**(1–2): p. 135-148.
105. Gribova, V., R. Auzely-Velty, and C. Picart, *Polyelectrolyte Multilayer Assemblies on Materials Surfaces: From Cell Adhesion to Tissue Engineering*. Chemistry of Materials, 2011. **24**(5): p. 854-869.
106. Mamedov, A.A. and N.A. Kotov, *Free-standing layer-by-layer assembled films of magnetite nanoparticles*. Langmuir, 2000. **16**(13): p. 5530-5533.
107. Srivastava, S. and N.A. Kotov, *Composite Layer-by-Layer (LBL) Assembly with Inorganic Nanoparticles and Nanowires*. Accounts of Chemical Research, 2008. **41**(12): p. 1831-1841.

108. Komatsu, T., *Protein-based nanotubes for biomedical applications*. *Nanoscale*, 2012. **4**(6): p. 1910-1918.
109. Mamedov, A.A., et al., *Molecular design of strong single-wall carbon nanotube/polyelectrolyte multilayer composites*. *Nature Materials*, 2002. **1**(3): p. 190-194.
110. Shiratori, S.S. and M.F. Rubner, *pH-dependent thickness behavior of sequentially adsorbed layers of weak polyelectrolytes*. *Macromolecules*, 2000. **33**(11): p. 4213-4219.
111. Kirchhof, K., *Nanostrukturierte Biomaterialbeschichtungen zur Steuerung von Zelladhäsion und –proliferation: pH-Wert-abhängige Multischichten aus Heparin und Chitosan in diskreter und Gradientenform*, 2009, Martin-Luther-University, Halle-Wittenberg, Germany: Halle (Saale), Germany.
112. Niepel, M.S., et al., *pH-dependent modulation of fibroblast adhesion on multilayers composed of poly(ethylene imine) and heparin*. *Biomaterials*, 2009. **30**(28): p. 4939-4947.
113. Halthur, T.J., P.M. Claesson, and U.M. Elofsson, *Stability of polypeptide multilayers as studied by in situ ellipsometry: Effects of drying and post-buildup changes in temperature and pH*. *Journal of the American Chemical Society*, 2004. **126**(51): p. 17009-17015.
114. Haynie, D.T., et al., *Polypeptide multilayer films: Role of molecular structure and charge*. *Langmuir*, 2004. **20**(11): p. 4540-4547.
115. He, Q., et al., *Layer-by-layer assembly of magnetic polypeptide nanotubes as a DNA carrier*. *Journal of Materials Chemistry*, 2008. **18**(7): p. 748-754.
116. He, P.G. and M. Bayachou, *Layer-by-layer fabrication and characterization of DNA-wrapped single-walled carbon nanotube particles*. *Langmuir*, 2005. **21**(13): p. 6086-6092.
117. Shi, X.Y., R.J. SaneDrin, and F.M. Zhou, *Structural characterization of multilayered DNA and polylysine composite films: Influence of ionic strength of DNA solutions on the extent of DNA incorporation*. *Journal of Physical Chemistry B*, 2002. **106**(6): p. 1173-1180.

118. Liu, A.H., G. Abbineni, and C.B. Mao, *Nanocomposite Films Assembled from Genetically Engineered Filamentous Viruses and Gold Nanoparticles: Nanoarchitecture- and Humidity-Tunable Surface Plasmon Resonance Spectra*. *Advanced Materials*, 2009. **21**(9): p. 1001-+.
119. Suci, P.A., et al., *Assembly of multilayer films incorporating a viral protein cage architecture*. *Langmuir*, 2006. **22**(21): p. 8891-8896.
120. Picart, C., et al., *Measurement of film thickness up to several hundreds of nanometers using optical waveguide lightmode spectroscopy*. *Biosensors & Bioelectronics*, 2004. **20**(3): p. 553-561.
121. Boura, C., et al., *Endothelial cells grown on thin polyelectrolyte multilayered films: an evaluation of a new versatile surface modification*. *Biomaterials*, 2003. **24**(20): p. 3521-3530.
122. Mhamdi, L., et al., *Study of the polyelectrolyte multilayer thin films' properties and correlation with the behavior of the human gingival fibroblasts*. *Materials Science & Engineering C-Biomimetic and Supramolecular Systems*, 2006. **26**(2-3): p. 273-281.
123. Tryoen-Toth, P., et al., *Viability, adhesion, and bone phenotype of osteoblast-like cells on polyelectrolyte multilayer films*. *Journal of Biomedical Materials Research*, 2002. **60**(4): p. 657-667.
124. Wittmer, C.R., et al., *Multilayer nanofilms as substrates for hepatocellular applications*. *Biomaterials*, 2008. **29**(30): p. 4082-4090.
125. Guillaume-Gentil, O., et al., *pH-controlled recovery of placenta-derived mesenchymal stem cell sheets*. *Biomaterials*, 2011. **32**(19): p. 4376-4384.
126. Mendelsohn, J.D., et al., *Fabrication of microporous thin films from polyelectrolyte multilayers*. *Langmuir*, 2000. **16**(11): p. 5017-5023.
127. Hajicharalambous, C.S., et al., *Nano- and sub-micron porous polyelectrolyte multilayer assemblies: Biomimetic surfaces for human corneal epithelial cells*. *Biomaterials*, 2009. **30**(23-24): p. 4029-4036.
128. Monika, S., *Layered polyelectrolyte complexes: physics of formation and molecular properties*. *Journal of Physics: Condensed Matter*, 2003. **15**(49): p. R1781.
129. Crouzier, T. and C. Picart, *Ion Pairing and Hydration in Polyelectrolyte Multilayer Films Containing Polysaccharides*. *Biomacromolecules*, 2009. **10**(2): p. 433-442.

130. Groth, T. and A. Lendlein, *Layer-by-Layer Deposition of Polyelectrolytes—A Versatile Tool for the In Vivo Repair of Blood Vessels*. *Angewandte Chemie International Edition*, 2004. **43**(8): p. 926-928.
131. Kirchhof, K., et al., *Multilayer coatings on biomaterials for control of MG-63 osteoblast adhesion and growth*. *Journal of Materials Science: Materials in Medicine*, 2009. **20**(4): p. 897-907.
132. Johansson, J.A., et al., *Build-up of collagen and hyaluronic acid polyelectrolyte multilayers*. *Biomacromolecules*, 2005. **6**(3): p. 1353-1359.
133. Zhang, J., et al., *Natural polyelectrolyte films based on layer-by layer deposition of collagen and hyaluronic acid*. *Biomaterials*, 2005. **26**(16): p. 3353-3361.
134. Vella, F., *Molecular biology of the cell (third edition): By B Alberts, D Bray, J Lewis, M Raff, K Roberts and J D Watson. pp 1361. Garland Publishing, New York and London. 1994*. *Biochemical Education*, 1994. **22**(3): p. 164-164.
135. Servaty, R., et al., *Hydration of polymeric components of cartilage - an infrared spectroscopic study on hyaluronic acid and chondroitin sulfate*. *International Journal of Biological Macromolecules*, 2001. **28**(2): p. 121-127.
136. Evanko, S.P., et al., *Hyaluronan-dependent pericellular matrix*. *Advanced Drug Delivery Reviews*, 2007. **59**(13): p. 1351-1365.
137. Opal, S.M., et al., *Antithrombin, heparin, and heparan sulfate*. *Critical Care Medicine*, 2002. **30**(5): p. S325-S331.
138. Seifert, B., P. Romaniuk, and T. Groth, *Bioresorbable, heparinized polymers for stent coating: in vitro studies on heparinization efficiency, maintenance of anticoagulant properties and improvement of stent haemocompatibility*. *Journal of Materials Science: Materials in Medicine*, 1996. **7**(8): p. 465-469.
139. Pankov, R. and K.M. Yamada, *Fibronectin at a glance*. *Journal of Cell Science*, 2002. **115**(20): p. 3861-3863.
140. G., D. and S.J. B., *Multilayer Thin Films*. 2nd ed. 2003: Wiley-VCH, Weinheim.
141. Decher, G., *Polyelectrolyte Multilayers, an Overview*, in *Multilayer Thin Films*. 2003, Wiley-VCH Verlag GmbH & Co. KGaA. p. 1-46.

142. Boddohi, S., C.E. Killingsworth, and M.J. Kipper, *Polyelectrolyte Multilayer Assembly as a Function of pH and Ionic Strength Using the Polysaccharides Chitosan and Heparin*. *Biomacromolecules*, 2008. **9**(7): p. 2021-2028.
143. Lundin, M., et al., *Layer-by-Layer Assemblies of Chitosan and Heparin: Effect of Solution Ionic Strength and pH*. *Langmuir*, 2011. **27**(12): p. 7537-7548.
144. Yoo, D., S.S. Shiratori, and M.F. Rubner, *Controlling bilayer composition and surface wettability of sequentially adsorbed multilayers of weak polyelectrolytes*. *Macromolecules*, 1998. **31**(13): p. 4309-4318.
145. Dubas, S.T. and J.B. Schlenoff, *Polyelectrolyte multilayers containing a weak polyacid: Construction and deconstruction*. *Macromolecules*, 2001. **34**(11): p. 3736-3740.
146. Richert, L., et al., *pH dependent growth of poly(L-lysine)/poly(L-glutamic) acid multilayer films and their cell adhesion properties*. *Surface Science*, 2004. **570**(1-2): p. 13-29.
147. Gopinadhan, M., et al., *The Influence of Secondary Interactions during the Formation of Polyelectrolyte Multilayers: Layer Thickness, Bound Water and Layer Interpenetration*†. *The Journal of Physical Chemistry B*, 2007. **111**(29): p. 8426-8434.
148. Quinn, J.F. and F. Caruso, *Facile tailoring of film morphology and release properties using layer-by-layer assembly of thermoresponsive materials*. *Langmuir*, 2004. **20**(1): p. 20-22.
149. Picart, C., *Polyelectrolyte multilayer films: From physico-chemical properties to the control of cellular processes*. *Current Medicinal Chemistry*, 2008. **15**(7): p. 685-697.
150. Lavalle, P., et al., *Comparison of the structure of polyelectrolyte multilayer films exhibiting a linear and an exponential growth regime: An in situ atomic force microscopy study*. *Macromolecules*, 2002. **35**(11): p. 4458-4465.
151. Elbert, D.L., C.B. Herbert, and J.A. Hubbell, *Thin polymer layers formed by polyelectrolyte multilayer techniques on biological surfaces*. *Langmuir*, 1999. **15**(16): p. 5355-5362.
152. Richert, L., et al., *Layer by layer buildup of polysaccharide films: Physical chemistry and cellular adhesion aspects*. *Langmuir*, 2004. **20**(2): p. 448-458.

153. Picart, C., et al., *Molecular basis for the explanation of the exponential growth of polyelectrolyte multilayers*. Proceedings of the National Academy of Sciences, 2002. **99**(20): p. 12531-12535.
154. Jomaa, H.W. and J.B. Schlenoff, *Salt-induced polyelectrolyte interdiffusion in multilayered films: A neutron reflectivity study*. Macromolecules, 2005. **38**(20): p. 8473-8480.
155. Mullaney, M., et al., *Investigation of Plasma Protein Adsorption on Functionalized Nanoparticles for Application in Apheresis*. Artificial Organs, 1999. **23**(1): p. 87-97.
156. Pilbat, A.M., et al., *Partial poly(glutamic acid) <-> poly(aspartic acid) exchange in layer-by-layer polyelectrolyte films. Structural alterations in the three-component architectures*. Langmuir, 2006. **22**(13): p. 5753-5759.
157. Gong, X., et al., *Multilayer polymer light-emitting diodes: White-light emission with high efficiency*. Advanced Materials, 2005. **17**(17): p. 2053-+.
158. Debreczeny, M., et al., *Multilayers built from two component polyanions and single component polycation solutions: A way to engineer films with desired secondary structure*. Journal of Physical Chemistry B, 2003. **107**(46): p. 12734-12739.
159. Quinn, A., et al., *Polyelectrolyte blend multilayer films: Surface morphology, wettability, and protein adsorption characteristics*. Langmuir, 2007. **23**(9): p. 4944-4949.
160. Quinn, A., et al., *Polyelectrolyte Blend Multilayers: A Versatile Route to Engineering Interfaces and Films*. Advanced Functional Materials, 2008. **18**(1): p. 17-26.
161. Crouzier, T., et al., *Polysaccharide-Blend Multilayers Containing Hyaluronan and Heparin as a Delivery System for rhBMP-2*. Small, 2010. **6**(5): p. 651-662.
162. Francius, G., et al., *Anomalous thickness evolution of multilayer films made from poly-L-lysine and mixtures of hyaluronic acid and polystyrene sulfonate*. Langmuir, 2007. **23**(5): p. 2602-2607.
163. Ariga, K., et al., *Alternate layer-by-layer assembly of organic dyes and proteins is facilitated by pre-mixing with linear polyions*. Chemistry Letters, 1997(1): p. 25-26.
164. Salloum, D.S. and J.B. Schlenoff, *Protein adsorption modalities on polyelectrolyte multilayers*. Biomacromolecules, 2004. **5**(3): p. 1089-1096.

165. Hamada, K., et al., *Adsorption of bovine serum albumin onto poly(methyl methacrylate) stereocomplex films with a molecularly regulated nanostructure*. Journal of Polymer Science Part a-Polymer Chemistry, 2003. **41**(12): p. 1807-1812.
166. Gergely, C., et al., *Human serum albumin self-assembly on weak polyelectrolyte multilayer films structurally modified by pH changes*. Langmuir, 2004. **20**(13): p. 5575-5582.
167. Ladam, G., et al., *Protein adsorption onto auto-assembled polyelectrolyte films*. Langmuir, 2001. **17**(3): p. 878-882.
168. Ladam, G., et al., *Protein adsorption onto auto-assembled polyelectrolyte films*. Biomolecular Engineering, 2002. **19**(2-6): p. 273-280.
169. Muller, M., et al., *Selective interaction between proteins and the outermost surface of polyelectrolyte multilayers: Influence of the polyanion type, pH and salt*. Macromolecular Rapid Communications, 2001. **22**(6): p. 390-395.
170. Wittmer, C.R., et al., *Fibronectin terminated multilayer films: Protein adsorption and cell attachment studies*. Biomaterials, 2007. **28**(5): p. 851-860.
171. Discher, D.E., P. Janmey, and Y.-l. Wang, *Tissue Cells Feel and Respond to the Stiffness of Their Substrate*. Science, 2005. **310**(5751): p. 1139-1143.
172. Richert, L., et al., *Elasticity of native and cross-linked polyelectrolyte multilayer films*. Biomacromolecules, 2004. **5**(5): p. 1908-1916.
173. Richert, L., et al., *Improvement of stability and cell adhesion properties of polyelectrolyte multilayer films by chemical cross-linking*. Biomacromolecules, 2004. **5**(2): p. 284-294.
174. Schneider, A., et al., *Elasticity, biodegradability and cell adhesive properties of chitosan/hyaluronan multilayer films*. Biomedical Materials, 2007. **2**(1): p. S45-S51.
175. Picart, C., et al., *Primary cell adhesion on RGD-functionalized and covalently crosslinked thin polyelectrolyte multilayer films*. Advanced Functional Materials, 2005. **15**(1): p. 83-94.
176. Wu, Z.R., et al., *Layer-by-layer assembly of polyelectrolyte films improving cytocompatibility to neural cells*. Journal of Biomedical Materials Research Part A, 2007. **81A**(2): p. 355-362.

177. Berg, M.C., et al., *Controlling mammalian cell interactions on patterned polyelectrolyte multilayer surfaces*. Langmuir, 2004. **20**(4): p. 1362-1368.
178. Fischer, D., et al., *In vitro cytotoxicity testing of polycations: influence of polymer structure on cell viability and hemolysis*. Biomaterials, 2003. **24**(7): p. 1121-1131.
179. Trimpert, C., et al., *Poly(ether imide) Membranes Modified with Poly(ethylene imine) as Potential Carriers for Epidermal Substitutes*. Macromolecular Bioscience, 2006. **6**(4): p. 274-284.
180. Godbey, W.T., et al., *Poly(ethylenimine)-mediated transfection: A new paradigm for gene delivery*. Journal of Biomedical Materials Research, 2000. **51**(3): p. 321-328.
181. Funhoff, A.M., et al., *Endosomal Escape of Polymeric Gene Delivery Complexes Is Not Always Enhanced by Polymers Buffering at Low pH*. Biomacromolecules, 2003. **5**(1): p. 32-39.
182. Brunot, C., et al., *Cytotoxicity of polyethyleneimine (PEI), precursor base layer of polyelectrolyte multilayer films*. Biomaterials, 2007. **28**(4): p. 632-640.
183. Suh, J., H.J. Paik, and B.K. Hwang, *Ionization of Poly(Ethylenimine) and Poly(Allylamine) at Various Phs*. Bioorganic Chemistry, 1994. **22**(3): p. 318-327.
184. Kichler, A., *Gene transfer with modified polyethylenimines*. Journal of Gene Medicine, 2004. **6**: p. S3-S10.
185. Kolasińska, M., R. Krastev, and P. Warszyński, *Characteristics of polyelectrolyte multilayers: Effect of PEI anchoring layer and posttreatment after deposition*. Journal of Colloid and Interface Science, 2007. **305**(1): p. 46-56.
186. Castelnovo, M. and J.F. Joanny, *Formation of polyelectrolyte multilayers*. Langmuir, 2000. **16**(19): p. 7524-7532.
187. Choosakoonkriang, S., et al., *Biophysical characterization of PEI/DNA complexes*. Journal of Pharmaceutical Sciences, 2003. **92**(8): p. 1710-1722.
188. Mazeau, K., S. Perez, and M. Rinaudo, *Predicted influence of N-acetyl group content on the conformational extension of chitin and chitosan chains*. Journal of Carbohydrate Chemistry, 2000. **19**(9): p. 1269-1284.
189. Rinaudo, M., M. Milas, and P. Ledung, *Characterization of Chitosan - Influence of Ionic-Strength and Degree of Acetylation on Chain Expansion*. International Journal of Biological Macromolecules, 1993. **15**(5): p. 281-285.

190. Domard, A. and M. Domard, *Chitosan: Structure-Properties Relationship and Biomedical Applications*, in *Polymeric Biomaterials*, S. Dumitriu, Editor 2002, Marcel Dekker, Inc.: USA. p. 187-211.
191. Dash, M., et al., *Chitosan-A versatile semi-synthetic polymer in biomedical applications*. *Progress in Polymer Science*, 2011. **36**(8): p. 981-1014.
192. Sorlier, P., et al., *Relation between the degree of acetylation and the electrostatic properties of chitin and chitosan*. *Biomacromolecules*, 2001. **2**(3): p. 765-772.
193. Schatz, C., et al., *Typical physicochemical behaviors of chitosan in aqueous solution*. *Biomacromolecules*, 2003. **4**(3): p. 641-648.
194. Kasaai, M.R., *Calculation of Mark-Houwink-Sakurada (MHS) equation viscometric constants for chitosan in any solvent-temperature system using experimental reported viscometric constants data*. *Carbohydrate Polymers*, 2007. **68**(3): p. 477-488.
195. Muzzarelli, R.A.A., *Chitins and chitosans for the repair of wounded skin, nerve, cartilage and bone*. *Carbohydrate Polymers*, 2009. **76**(2): p. 167-182.
196. Senel, S. and S.J. McClure, *Potential applications of chitosan in veterinary medicine*. *Advanced Drug Delivery Reviews*, 2004. **56**(10): p. 1467-1480.
197. Fu, J., et al., *Construction of anti-adhesive and antibacterial multilayer films via layer-by-layer assembly of heparin and chitosan*. *Biomaterials*, 2005. **26**(33): p. 6684-6692.
198. Wang, H.M., D. Loganathan, and R.J. Linhardt, *Determination of the Pka of Glucuronic-Acid and the Carboxy Groups of Heparin by C-13-Nuclear-Magnetic-Resonance Spectroscopy*. *Biochemical Journal*, 1991. **278**: p. 689-695.
199. Salmivirta, M., K. Lidholt, and U. Lindahl, *Heparan sulfate: a piece of information*. *The FASEB Journal*, 1996. **10**(11): p. 1270-9.
200. Capila, I. and R.J. Linhardt, *Heparin - Protein interactions*. *Angewandte Chemie-International Edition*, 2002. **41**(3): p. 391-412.
201. Roden, in *Heparin: chemical and biological properties clinical applications*, D.A. Lane and U. Lindahl, Editors. 1989, Edward Arnold: LIVERPOOL, MERS, United Kingdom. p. 1-23.

202. Barlow, G.H., M.M. Mozen, and L.J. Coen, *Biological Chemical + Physical Comparison of Heparin from Different Mammalian Species*. *Biochimica Et Biophysica Acta*, 1964. **83**(3): p. 272-&.
203. Powell, A.K., et al., *Interactions of heparin/heparan sulfate with proteins: Appraisal of structural factors and experimental approaches*. *Glycobiology*, 2004. **14**(4): p. 17r-30r.
204. Pike, D.B., et al., *Heparin-regulated release of growth factors in vitro and angiogenic response in vivo to implanted hyaluronan hydrogels containing VEGF and bFGF*. *Biomaterials*, 2006. **27**(30): p. 5242-5251.
205. Groth, T. and W. Wagenknecht, *Anticoagulant potential of regioselective derivatized cellulose*. *Biomaterials*, 2001. **22**(20): p. 2719-2729.
206. Gericke, M., et al., *Semi-Synthetic Polysaccharide Sulfates as Anticoagulant Coatings for PET, 1-Cellulose Sulfate*. *Macromolecular Bioscience*, 2011. **11**(4): p. 549-556.
207. Zhang, K., et al., *Synthesis of carboxyl cellulose sulfate with various contents of regioselectively introduced sulfate and carboxyl groups*. *Carbohydrate Polymers*, 2010. **82**(1): p. 92-99.
208. Bourin, M.C. and U. Lindahl, *Glycosaminoglycans and the Regulation of Blood-Coagulation*. *Biochemical Journal*, 1993. **289**: p. 313-330.
209. Mulloy, B., P.A.S. Mourão, and E. Gray, *Structure/function studies of anticoagulant sulphated polysaccharides using NMR*. *Journal of Biotechnology*, 2000. **77**(1): p. 123-135.
210. Rabenstein, D.L., *Heparin and heparan sulfate: structure and function*. *Natural Product Reports*, 2002. **19**(3): p. 312-331.
211. Heinze, T. and A. Koschella, *Carboxymethyl Ethers of Cellulose and Starch – A Review*. *Macromolecular Symposia*, 2005. **223**(1): p. 13-40.
212. Fischer, S., et al., *Properties and Applications of Cellulose Acetate*. *Macromolecular Symposia*, 2008. **262**(1): p. 89-96.
213. Hettrich, K., et al., *New Possibilities of the Acetosulfation of Cellulose*. *Macromolecular Symposia*, 2008. **262**(1): p. 162-169.

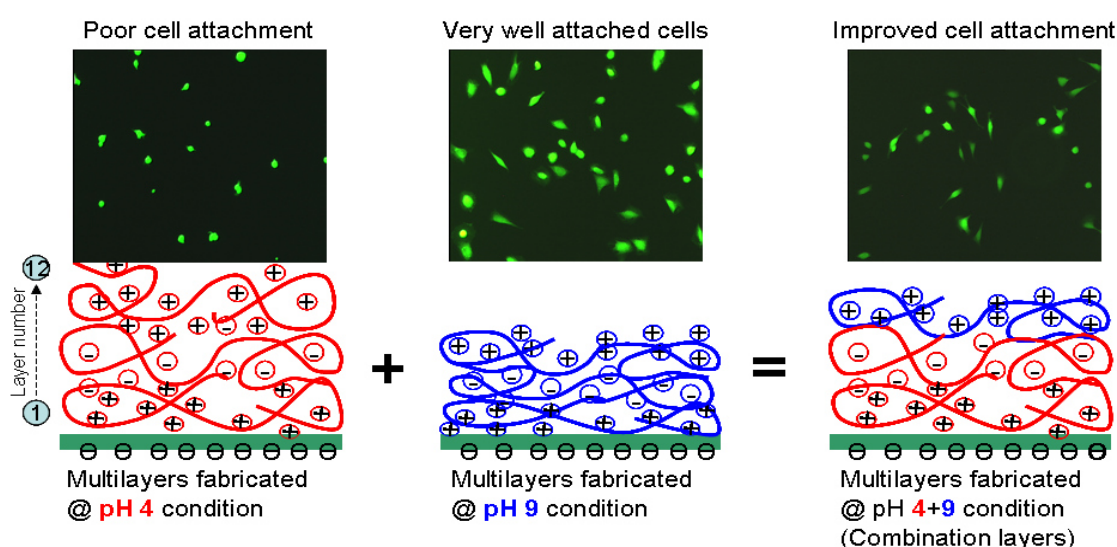
214. Philipp, B., et al., *¹³C-N.M.R. spectroscopic study of the homogeneous sulphation of cellulose and xylan in the N₂O₄-DMF system.* Carbohydrate Research, 1987. **164**(0): p. 107-116.
215. Saake, B., J. Puls, and W. Wagenknecht, *Endoglucanase fragmentation of cellulose sulfates derived from different synthesis concepts.* Carbohydrate Polymers, 2002. **48**(1): p. 7-14.
216. Vikartovská, A., et al., *Improvement of the stability of glucose oxidase via encapsulation in sodium alginate–cellulose sulfate–poly(methylene-co-guanidine) capsules.* Enzyme and Microbial Technology, 2007. **41**(6–7): p. 748-755.
217. Bučko, M., et al., *Immobilization of a whole-cell epoxide-hydrolyzing biocatalyst in sodium alginate–cellulose sulfate–poly(methylene-co-guanidine) capsules using a controlled encapsulation process.* Enzyme and Microbial Technology, 2005. **36**(1): p. 118-126.
218. Stadlbauer, V., et al., *Morphological and functional characterization of a pancreatic β -cell line microencapsulated in sodium cellulose sulfate/poly(diallyldimethylammonium chloride).* Xenotransplantation, 2006. **13**(4): p. 337-344.
219. Van Damme, L., et al., *Lack of Effectiveness of Cellulose Sulfate Gel for the Prevention of Vaginal HIV Transmission.* New England Journal of Medicine, 2008. **359**(5): p. 463-472.
220. Yamamoto, I., et al., *Synthesis, structure and antiviral activity of sulfates of cellulose and its branched derivatives.* Carbohydrate Polymers, 1990. **14**(1): p. 53-63.
221. Zhang, K., et al., *Synthesis and Bioactivity of Cellulose Derivatives.* Macromolecular Symposia, 2009. **280**(1): p. 28-35.
222. Peschel, D., et al., *Modulation of osteogenic activity of BMP-2 by cellulose and chitosan derivatives.* Acta Biomaterialia, 2012. **8**(1): p. 183-193.
223. Baumann, H., et al., *Concepts for preparation of novel regioselective modified cellulose derivatives sulfated, aminated, carboxylated and acetylated for hemocompatible ultrathin coatings on biomaterials.* Macromolecular Chemistry and Physics, 2000. **201**(15): p. 1950-1962.

224. Wang, Z.M., et al., *Preparation and anticoagulation activity of sodium cellulose sulfate*. International Journal of Biological Macromolecules, 2007. **41**(4): p. 376-382.
225. Gericke, M., T. Liebert, and T. Heinze, *Interaction of Ionic Liquids with Polysaccharides, 8 – Synthesis of Cellulose Sulfates Suitable for Polyelectrolyte Complex Formation*. Macromolecular Bioscience, 2009. **9**(4): p. 343-353.
226. Wang, Z.-M., et al., *Homogeneous sulfation of bagasse cellulose in an ionic liquid and anticoagulation activity*. Bioresource Technology, 2009. **100**(4): p. 1687-1690.
227. Zhang, K., et al., *Synthesis and spectroscopic analysis of cellulose sulfates with regulable total degrees of substitution and sulfation patterns via C-13 NMR and FT Raman spectroscopy*. Polymer, 2011. **52**(1): p. 26-32.
228. Dong, P., et al., *Comparison Study of Corrosion Behavior and Biocompatibility of Polyethyleneimine (PEI)/Heparin and Chitosan/Heparin Coatings on NiTi alloy*. Journal of Materials Science & Technology, 2010. **26**(11): p. 1027-1031.
229. Carroll, L.A. and R.J. Koch, *Heparin stimulates production of bFGF and TGF-beta 1 by human normal, keloid, and fetal dermal fibroblasts*. Med Sci Monit, 2003. **9**(3): p. BR97-108.
230. Weigert, C., et al., *Low-molecular-weight heparin prevents high glucose- and phorbol ester-induced TGF-beta 1 gene activation*. Kidney International, 2001. **60**(3): p. 935-943.
231. Pye, D.A., et al., *Heparan Sulfate Oligosaccharides Require 6-O-Sulfation for Promotion of Basic Fibroblast Growth Factor Mitogenic Activity*. Journal of Biological Chemistry, 1998. **273**(36): p. 22936-22942.
232. Weltrowski, A., et al., *Mitogenic Activity of Sulfated Chitosan and Cellulose Derivatives is Related to Protection of FGF-2 from Proteolytic Cleavage*. Macromolecular Bioscience, 2012. **12**(6): p. 740-750.

Chapter 2

Tuning cell adhesion and growth on biomimetic polyelectrolyte multilayers by variation of pH during layer-by-layer assembly

Neha Aggarwal, Noomi Altgärde, Sofia Svedhem, Georgios Michanetzis, Yannis Missirlis,
Thomas Groth



2.1. Abstract

Polyelectrolyte multilayers of chitosan and heparin were assembled on glass where heparin was applied at pH = 4, 9 and 4 during the formation of first layers followed by pH = 9 at the last steps (denoted pH 4+9). Measurements of wetting properties, layer mass and topography showed that multilayers formed at pH = 4 were thicker, contained more water and had a smoother surface compared to those prepared at pH = 9 while the pH = 4+9 multilayers expressed intermediate properties. pH = 9 multilayers were more cell adhesive and supported growth of C2C12 cells than pH = 4 ones. However, 4+9 pH condition improved the bioactivity to a similar level of pH = 9 layers. Multilayers prepared using pH 4+9 conditions form thick enough layers that may allow efficient loading of bioactive molecules as well as significantly bioactive surfaces.

2.2. Introduction

In the field of tissue engineering and implantable biomaterials, the design of materials at micrometer or nanometer scale to control their bulk and surface properties still presents a great challenge. Although the bulk properties of a functional material, like mechanical strength, play an important role for biomedical applications but also surface properties are of chief importance.^[1, 2] The material surface is the site where the biological events take place; from protein adsorption over the initial inflammatory response to the remodelling of tissue.^[3] Hence, various techniques have been developed for the functionalization of biomaterial surfaces to make them more biocompatible and bioactive. Out of these techniques, polyelectrolyte multilayer (PEM) coatings offer great potential as an easy, non-covalent modification of biomaterial surfaces. Such multilayer thin films are prepared by exploiting a facile, yet elegant technique called the layer-by-layer (LBL) method, which was introduced by Decher and co-workers in 1990s.^[4] Principally, this powerful technique is based on the alternating adsorption of oppositely charged polyelectrolytes onto a charged substrate. PEM characteristics like thickness, viscoelasticity, topography, surface charge and wettability are dependent on the adsorbed polyelectrolytes, i.e. intrinsic properties (molar mass, charge density, chain stiffness) as well as on the suspending solution properties (pH value, ionic strength, temperature) and also the type of substrate.^[5-7] The LBL technique which has abundant tunable possibilities, enables the design of a vast range of material coatings with controlled intrinsic and extrinsic properties. The above mentioned technique is advantageous in making PEM films as layers which can be deposited on materials of varying size and of complex geometries like scaffolds and implants. It also allows for incorporation of charged species from biological sources^[8, 9] to inorganic.^[10]

Precise control of cell adhesion and spreading on implant materials is crucial for desired cell growth and differentiation around these materials.^[11] Moreover, release of bioactive molecules from the bulk of the implant^[12] or from surface coatings^[13] is often suggested as an additional tool to control cell differentiation in a desired direction. Immobilization of charged bio-macromolecules like glycosaminoglycans (GAGs) or proteins can lead to desired bioactivity of PEM films depending on the affinity of the molecules and the conditions of their deposition (e.g. pH).^{[5, 6][14]} For example, the GAG heparin is a strong polyanion that possesses a high affinity towards adhesive proteins (e.g. fibronectin) and growth factors (e.g. bone morphogenic proteins) interacting via specific heparin-binding domains.^[15, 16] Thereby, heparin may act as a reservoir system protecting growth factors from proteolytic digestion but also presenting them to their corresponding receptors.^[17, 18] Hence heparin has been used as a

component of bioactive hydrogels in the field of tissue engineering ^[19] and recently also as a component of PEMs on biomaterials.^[20, 21] Furthermore, recent work has shown that heparin can be used as a system for controlled release of growth factors, although in this case, loading efficiency of the heparin/poly-L-lysine multilayers was limited due to condensation of the multilayers.^[22] Previous studies with heparin as a polyanion in multilayers showed that multilayers prepared at lower pH have a higher mass and are highly cell repulsive as compared to those prepared at higher pH.^[20, 21] On the other hand, thicker multilayers were found to be more useful for loading and sustained release of growth factors.^[23]

Hence, in the present study, biomimetic multilayer coatings from heparin and chitosan were prepared at different pH to allow control of layer mass and surface properties, as well as protein adsorption, cell adhesion and growth. In contrast to many other studies with chitosan and heparin we present a method to alternate between ion pairing and hydrogen bonding by varying the pH of the heparin solution from 4 to 9 leading to differences in both layer mass and adhesivity for C2C12 myoblast cells. A particular novelty of this study was the finding that a change of the pH from 4 to 9 during a 7-layer-assembly allows formation of thicker multilayers with a high adhesivity for cells. In the future, this could be used as a system for controlled release of growth factors in different tissue engineering applications.

2.3. Materials and Methods

2.3.1. Materials

Glass cover slips (Menzel, Germany) for PEM fabrication were cleaned for 2 hours with 0.5 M NaOH (Roth, Germany) dissolved in 96% ethanol (Roth, Germany) followed by excessive rinsing with micropure water (10 X 5 minutes). Gold-coated sensors for SPR measurements were obtained from IBIS Technologies (Hengelo, The Netherlands). Gold-coated AT-cut quartz crystals for QCM-D measurements were obtained from Q-sense (Göteborg, Sweden). All new sensors were cleaned using 99.8% ethanol (Merck, Germany) and rinsed thoroughly with micropure Milli-Q water. Sensors were immediately incubated overnight in an ethanol (p.a.) solution of 2 mM mercaptoundecanoic acid (MUDA, 95%, Sigma, Deisenhofen, Germany) to obtain a negatively charged surface by the formation of a self-assembled monolayer exposing carboxyl groups. Silicon wafers (Silicon materials, Kaufering, Germany) with a size of 10 x 10 mm were treated with a solution of NH₄OH (27%), H₂O₂ (30%) and water (1:1:5, v/v/v) at 70°C for 15 minutes and subsequently washed with Milli-Q water.

For the preparation of polyelectrolyte solutions, poly(ethylene imine) (PEI, P) (MW 750,000 g/mol, Sigma), heparin (min. 150 IU/mg, MW 8,000-15,000 g/mol, Applichem Darmstadt, Germany) and chitosan (medical grade) with a deacetylation degree of 85 % (MW 500,000 g/mol, 85/500/A1, Heppe, (Halle Saale, Germany) were dissolved in deionised water containing 0.14 M NaCl at a concentration of 2 mg/ml under stirring. Chitosan solution containing 0.05 M acetic acid was solubilised at 50°C for 3 h.

2.3.2. Polyelectrolyte Multilayer (PEM) Assembly

When appropriate, multilayer films were fabricated on cleaned glass and silicon (with its oxide layer on top) substrates (another version of the protocol was used in for the SPR and QCM-D experiments, see below).

PEI was used as a first anchoring layer for homogenous coating of the surface with a positive charge followed by adsorption of polyanion layers of heparin (HEP, H) and polycation of chitosan (CHI, C). Each layer was formed by immersing the substrates in polyelectrolyte solutions for 7 minutes followed by rinsing with deionised water containing 0.14 M NaCl (3 X 4 minutes). By alternating adsorption of HEP and CHI, multilayers were built up to 11 and 12 layers abbreviated as P(H-C)₅ (PEI plus 5 bilayers of HEP and CHI) and P(H-C)₅H (PEI plus 5 bilayers of HEP and CHI plus HEP), respectively. The pH of the PEI and polyanionic HEP solutions were adjusted to pH 4 or 9 with either HCl or NaOH, while the pH of the CHI solution was kept constant at pH 4 as it becomes insoluble at pH values higher than 6. Hence three sets of PEMs were prepared, where the pH of the HEP solution was applied either at acidic conditions, at basic conditions, or using a combination of both. In the later case, the PEI (for first layer) and HEP solution were applied at pH 4 up to the formation of 7th layer, and after the formation of 7th layer the pH of the HEP solution was adjusted to 9 which was maintained up to the 12th layer (named as 4+9).

2.3.3. Physical Characterization of Multilayers

Water contact angle (WCA) measurements were done by an OCA15+ device from Dataphysics (Filderstadt, Germany) to determine the wettability of multilayer surfaces. By applying the sessile drop method, 5 to 6 samples of each type of pH combination and terminal multilayer surfaces were measured by dispensing 3-4 drops of 3 µl pure water with a flow rate of 0.5 µl/s. For each droplet, at least 10 independent measurements were recorded by the

built-in software. The contact angle values presented here are the means of two independent measurements and each measurement was done in triplicates.

The multilayer formation process was monitored by surface plasmon resonance (SPR) and quartz crystal microbalance with dissipation (QCM-D). SPR is based on the detection of changes in the refractive index (RI) at the gold-liquid interface of the SPR gold sensor surface caused by the adsorption of molecules. The resulting change in the SPR angle shift (m°) is proportional to the mass (Γ_{SPR}) of adsorbed molecules on the surface i.e.,^[24]

$$122 m^\circ \approx 1 \text{ ng/mm}^2 \quad (1)$$

For QCM-D, the technique is described elsewhere.^[25] Briefly, when an alternating potential is applied, the QCM-D sensor (i.e. a quartz crystal disc) oscillates, and its resonance frequency, f , is subjected to change (Δf) by mass adsorption on the sensor surface. The dampening of the oscillatory motion as the driving potential is switched off is related to structural properties of the added layer on the sensor surface, and it is quantified as energy dissipation (ΔD).

For thin, rigid, and evenly distributed surface films, resonance frequency shifts (Δf) can be related to changes in adsorbed mass on the sensor surface (Δm_{QCM-D}) by using the Sauerbrey equation.^[26]

$$\Delta m_{QCM-D} = - C \Delta f_n / n \quad (2)$$

where n ($n = 1, 3, 5, \dots, 13$) is the overtone number and C is the mass sensitivity constant that depends on the quartz crystal. For the crystals applied here ($f_0 = 5 \text{ MHz}$), $C = 0.177 \text{ mg/m}^2\text{Hz}$. The water content of the adsorbed film can be determined by comparing the mass obtained by QCM-D and the mass obtained by SPR (assuming that the two masses were obtained under equivalent condition). Furthermore, the same data can be used to calculate the effective density of the layer using the following equation

$$\rho_{eff} = \rho_f (\Gamma_{SPR} / \Delta m_{QCM-D}) + \rho_0 (1 - \Gamma_{SPR} / \Delta m_{QCM-D}) \quad (3)$$

where Γ_{SPR} is adsorbed amount calculated from SPR measurements, ρ_f is the bulk density of polymer ($\rho_{CHI} = 1410 \text{ Kg m}^{-3}$), and ρ_0 is the density of the liquid (997 Kg m^{-3}).^[27]

Using the effective density, the layer thickness can be estimated by the following equation:

$$d = \Delta m_{QCM-D} / \rho_{eff} \quad (4)$$

The procedure followed for the SPR and the QCM-D experiments was as follows. The measurements were carried out in the flow cell of the device using gold sensors treated with

mercaptoundecanoic acid (see above), thus providing negatively charged surfaces to be comparable with the multilayer formation on glass. First, the positively charged polyelectrolyte PEI was introduced to the sensor surface for 7 minutes, followed by 12 min of rinsing with sodium chloride solution of the same pH value. After the formation of the first layer of PEI, alternating layers of HEP and CHI were adsorbed up to 12 layers, where the HEP solution was applied at either pH 4 or pH 9, or at a combination of both; pH 4+9. Each adsorption step was followed by the rinsing step described above to remove unbound polyelectrolyte.

Plasma fibronectin (pFN, Roche, Germany) was reconstituted and diluted to 20 µg/ml in phosphate buffered saline (PBS, 150 mM NaCl, pH 7.4). The fibronectin solution was introduced into the QCM-D flow cell after the formation of the 12th layer. The adsorption process was performed for 1 hour to measure the protein adsorption capacity of the terminal HEP layer. All measurements were done in duplicates and measured values are represented as averages.

Multilayers prepared on cleaned silicon wafers were dried using compressed nitrogen and studied with a multimode atomic force microscope (AFM, Digital Instruments, Veeco, Santa Barbara, CA). Images were taken in tapping mode using low conductivity Antimony (n) doped Si tips (TESPA, Veeco/Bruker, Santa Barbara, CA) at a frequency of 360 kHz. The samples were prepared in triplicates and images were taken under ambient laboratory conditions. Surface topography and roughness were monitored and roughness analysis was performed using the software Gwyddion 2.30.

2.3.4. Biological Investigations

Short-term cell adhesion and cell proliferation studies were conducted with different multilayer coatings on glass slides using the skeletal muscle cell line C2C12 (DSMZ, Braunschweig, Germany, Product Nr.: ACC 565). Cryo conserved cells were thawed and expanded by culturing them in Dulbecco's modified Eagle medium (DMEM, Biochrom AG, Berlin, Germany) supplemented with 10% fetal bovine serum (FBS, Biochrom AG), 2 mM L-Glutamine, 100 U/ml Penicillin und 100 µg/ml Streptomycin (Biochrom AG). C2C12 cells were harvested from the culture flask by using 0.25% Trypsin, 0.02% EDTA (Biochrom AG) prior to reaching confluence followed by subsequent washing with DMEM and resuspended in DMEM with 10% FBS at a concentration of 25,000 cells/ml.

Glass cover slips with CHI and HEP terminated multilayers were placed into 12-well tissue culture plates. Sterilization of each sample was done by using 70% ethanol for 10 min followed by excessive rinsing with sterile PBS. The re-suspended cells were seeded on the sterilized samples and incubated at 37°C in a humidified 5% CO₂/95% air atmosphere using a NUAIRE[®] DH Autoflow incubator (NuAire Corp., Plymouth, Minnesota, USA). For cell adhesion studies, cells were incubated for 4 hours while for cell proliferation, cell were cultured for 1 and 3 days. After the end of incubation periods, culture medium was aspirated and samples were washed with PBS to remove non-adherent cells. Cell fixation was done using 4% (w/v) phosphate buffered formaldehyde solution (Roti-Histofix, Roth, Germany) for 5 minutes at room temperature. Later on phase contrast images were taken for analyzing the cell morphology and quantification of cell attachment and spreading. Morphological parameters and surface coverage by cells were analyzed by using Image processing software “ImageJ, NIH”.

2.4. Results and Discussion

2.4.1. Measurements of Wetting Properties during Multilayer Formation

Static water contact angle (WCA) measurements have been applied frequently to characterize the change of terminal layer composition during assembly of multilayers and were used here to study wetting properties after the deposition of each layer prepared at specific pH value. Figure 2.1 shows the WCA values of clean glass and all subsequent PEI, CHI and HEP layers up to the 12th (HEP terminated) layer. The alternating contact angles between CHI and HEP layers correlate to the change in the composition of the terminating molecule layer. It is notable that the differences from one layer to the next layer were greater for layers prepared at pH 4 than pH 9. Since pure CHI films have been characterized as quite hydrophobic (WCA ~ 100°)^[28] while HEP films as hydrophilic (WCA ~ 25°),^[29] the large difference in WCA between the layers at pH 4 illustrates a dominance of either CHI or HEP in the outer layers after the corresponding coating step. As CHI is a weak polyelectrolyte with a pKa value of around 6.5, its charge is highly affected by changes in pH during the assembly. In analogy to previous studies, adsorption of CHI was carried out at pH 4, at which pH CHI is highly charged.^[30] Hence, for multilayers prepared at pH 4, when both HEP and CHI are charged, ion pairing should occur between the two polymers, leading to conditions under which a dominance of terminal composition by either the polycation CHI or polyanion HEP is achieved.^[31] By contrast, the use of pH 9 during adsorption of HEP resulted in smaller WCA

differences between CHI and HEP layers. While the WCA of CHI layers remained comparable to CHI layers at pH 4, the WCA of HEP layers were shifted to higher values pointing to a higher proportion of CHI in the outer layer under this condition. Since the previously adsorbed CHI is not charged at pH 9, other mechanisms than ion pairing must be responsible for the adsorption of HEP. Such mechanisms could be based on the formation of hydrogen bonds, which has been reported for HEP-CHI interaction with FTIR studies.^[32] Likewise, a distinct change in surface wettability can be seen in Figure 2.1 as the pH of the HEP solution is changed from 4 to 9 after the formation of 7th layer. The 8th layer (assembled at pH 9) became less hydrophilic than the ones assembled at pH 4. WCA became even higher than compared to layer exclusively formed at pH 9, which indicates a dominance of CHI in the outermost layers for systems formed with the HEP solution at pH 9 as well as by the pH 4+9 condition. Indeed, a dominance of CHI in CHI-HEP multilayers assembled at pH 4.2 has been detected by Lundin et al. recently.^[30]

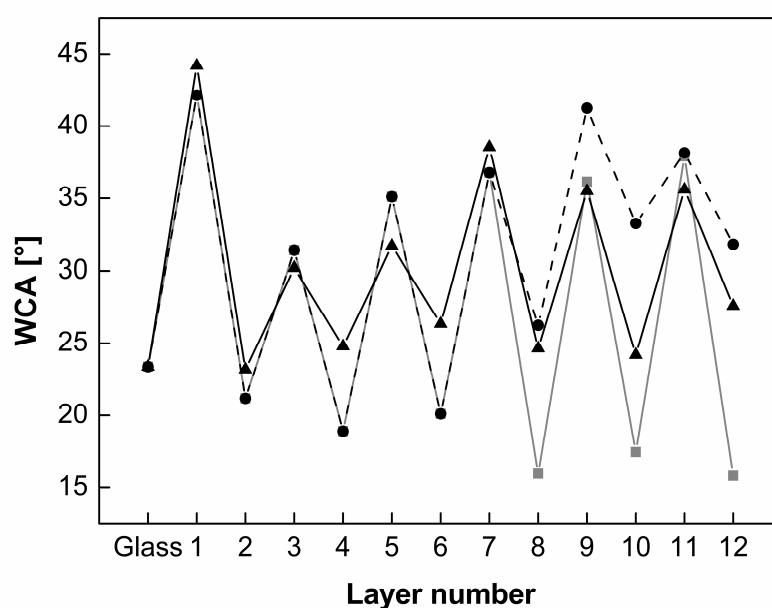


Figure 2.1: Static water contact angles (WCA) during multilayer formation up to 12 layers. WCA are plotted as a function of the pH of the heparin (HEP) solution (square) pH 4, (circle) pH 4+9 and (triangle) pH 9 during the multilayer formation process. pH value of chitosan (CHI) solution was kept constant at 4. (1-12; 1 = poly (ethylene imine), all odd numbers = CHI and even numbers = HEP).

2.4.2. Measurements of Multilayer Growth

The multilayer growth dependence on the pH conditions used was measured by SPR and QCM-D, which in combination allow both the measurement of adsorbed quantities of polyelectrolytes and also an estimation of the water content of the layers. Figure 2.2 shows the effect of the pH condition on the adsorbed quantities of polyelectrolytes measured by SPR. The assembly process was strongly dependent on the pH conditions used and the multilayer growth seemed to be exponential in all cases, in accordance with observations for other polysaccharide-based multilayer systems.^[33] Figure 2.2 shows that at pH 4, when ion pairing should dominate, more mass was adsorbed at each step.^[34] A significantly lower mass increase was observed when the pH of the HEP solution was changed to 9. Here, ion pairing should not occur and hydrogen bonding should become the dominating mechanism.^[32] Not surprisingly, the change in pH of the HEP solution after the 7th layer from 4 to 9 causes a decreased slope of the curve, similarly to formation at pH 9. However it should be underlined that no mass loss was observed under this condition, which would point to a decomposition of multilayers due to the change in complexation conditions.

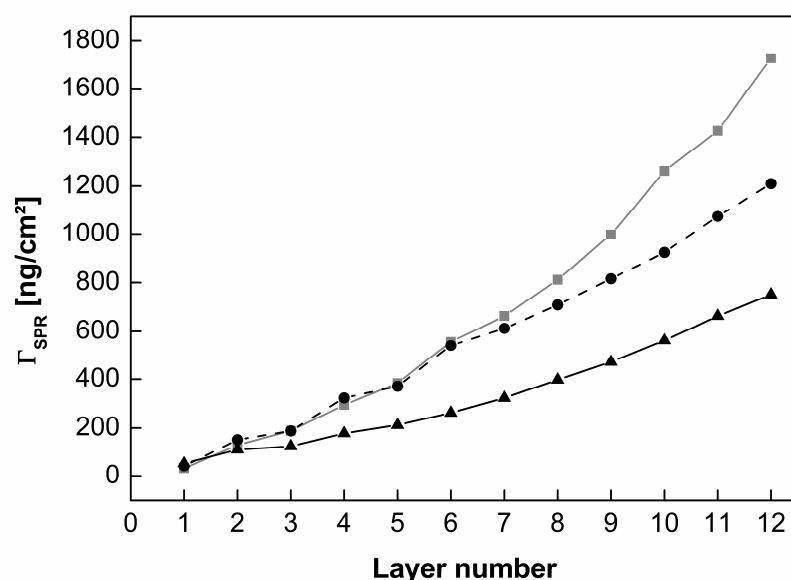
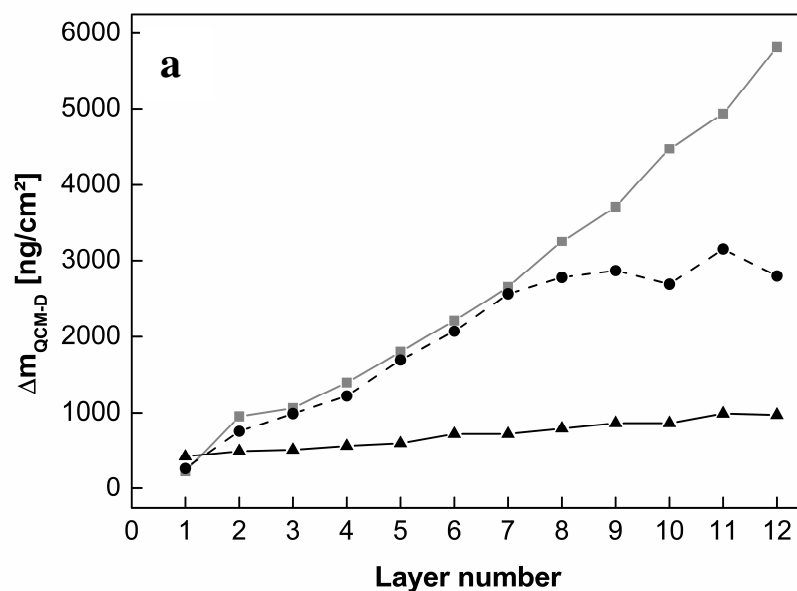


Figure 2.2: Accumulated mass during multilayer formation up to 12 layers calculated from SPR angle shifts. Layer mass Γ_{SPR} is plotted as a function of the layer number for the different pH conditions of the heparin (HEP) solution during the multilayer formation process; (square) pH 4, (circle) pH 4+9 and (triangle) pH 9. The pH value of the chitosan (CHI) solution was

kept constant at pH 4. (1-12; 1 = poly (ethylene imine), odd numbers = CHI, even numbers = HEP).

While SPR measures the mass of adsorbed polysaccharides based on changes in the refractive index near the sensor surface, QCM-D measures all mass which is acoustically coupled to the oscillatory motion of the QCM-D sensor, i.e. the polyelectrolyte mass and the solvent which is associated with it. The adsorbed mass in QCM-D was calculated from measured frequency shifts according to the Sauerbrey equation ^[26] and is shown in Figure 2.3 a. The Sauerbrey equation is only valid for rigid film and holds as a good approximation here since the dissipation response is less than 10% of the frequency response. Also, the separation between frequency overtones is negligible. Here, a similar trend of mass adsorption was obtained regarding the pH regimes as in the SPR measurements. Generally, the calculated QCM-D layer masses were much larger than those measured by SPR, particularly for the pH 4 and pH 4+9 regime. This indicates that a substantial amount of water was bound to these layers. By contrast, multilayers prepared at the pH 9 regime had a lower water content since only a small layer growth was observed with QCM-D. Table 2.1 compares layer masses obtained by SPR and QCM-D and the resulting water content along with the estimated thickness of terminal CHI (11th) and HEP (12th) layers. The layer masses and thicknesses obtained for the pH 4 regime are almost identical to those measured by others at pH 4.2 and 150 mM NaCl.^[30] Furthermore, similar water contents in polyelectrolyte multilayers have been observed in multilayer systems prepared from polysaccharides at comparable ionic strength with poly-L-lysine as polycation.^[33] For the pH 4+9 combination, it was also observed that the change of the pH value of the HEP solution from pH 4 to 9 from the 8th layer on resulted in a fluctuation of layer mass with an increase for CHI and a decrease for HEP. Since such behaviour was not seen during the SPR measurements, this indicates that there is a large change in water content after the change in pH, with higher water content after the adsorption of CHI and a decrease after the adsorption of HEP. The change in water content is also reflected by the decreased thickness of the multilayer to about 50% compared to the pH 4 system. This is also in accordance with a shift to higher WCA that indicates a high proportion of CHI in the terminal layers when HEP is applied at pH 9. By contrast, the multilayer growth when applying HEP at pH 9 was very low, and the incremental mass increase was independent of the terminal layer, both with respect to layer mass and thickness as shown in Table 2.1.

The water content of the multilayers is related to their viscoelastic properties, and also to the ability of proteins and cells to adhere.^[35] Dissipation values obtained from QCM-D measurements are shown in Figure 2.3 b. Under all conditions, the dissipation varies greatly between CHI and HEP layers and indicates a stiffening of the PEM after HEP adsorption. Such effect has been observed in previous studies and is likely related to diffusion of HEP into the underlying layers, leading to compaction and displacement of water molecules.^{[30][33]} Figure 2.3 b also shows that the mean dissipation values were higher for multilayers formed at pH 4, which is related to the higher water content (Table 2.1). It is also interesting to note that the addition of CHI during the 4+9 scheme causes a large increase in dissipation. This could indicate that previously bound HEP is leaving the multilayer system and being displaced by water molecules. An alternative interpretation of this result is that CHI inside the multilayer system exist in a more coiled and flexible conformation due to break of ionic bond within the multilayers that makes the whole systems more flexible. This is supported by the higher water content and layer thickness of the CHI terminated 11th multilayer compared to addition of HEP as the 12th layer.



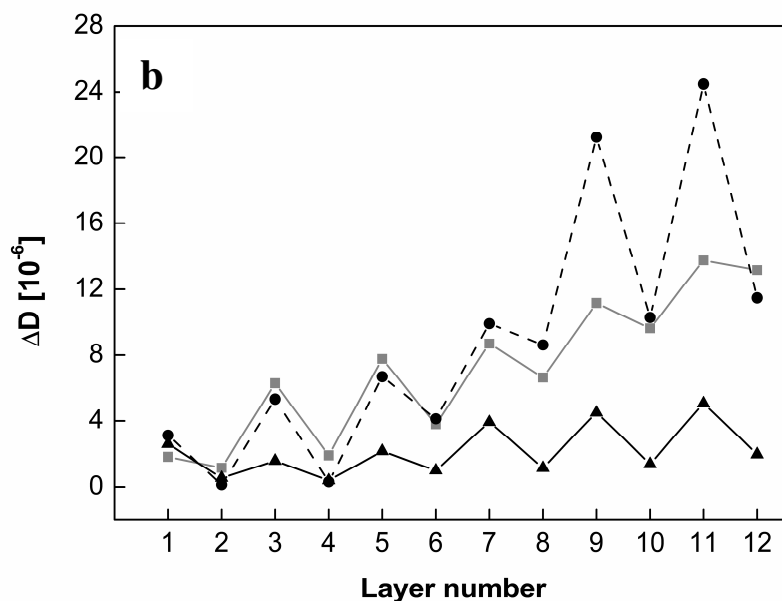


Figure 2.3: Multilayer assembled from chitosan (CHI) at pH 4 and Heparin (HEP) at (square) pH 4, (circle) pH 4+9 and (triangle) pH 9 measured with QCM-D. **(a)** QCM-D mass calculated from the Sauerbrey equation as a function of layer number. **(b)** Dissipation change ΔD as a function of layer number. (1-12; 1 = poly (ethylene imine), all odd numbers = CHI and even numbers = HEP). Results represent values at the 5th overtone.

Table 2.1: Multilayer mass, water content and layer thickness

| | pH regime | Γ_{SPR}^a (ng/cm ²) | Δm_{QCM-D}^b (ng/cm ²) | Water content ^c | Layer thickness ^d (nm) |
|---|-----------|---|---|----------------------------|--------------------------------------|
| Until 11 th (CHI layer) | pH 4 | 1426 | 4938 | 71% | 44.3 |
| | pH 4+9 | 1075 | 3151 | 66% | 28 |
| | pH 9 | 663 | 991 | 33% | 8 |
| Until the 12 th (HEP layer) | pH 4 | 1727 | 5823 | 70% | 52 |
| | pH 4+9 | 1210 | 2797 | 57% | 24 |
| | pH 9 | 751 | 974 | 23% | 7.4 |

^{a)}SPR masses were estimated using equation (1); ^{b)}QCM-D masses were estimated using the Sauerbrey equation and the frequency shift at the 5th overtone; ^{c)}apparent water content was approximated by $(m_{QCM-D} - m_{SPR})/m_{QCM-D} * 100$. ^{d)}Layer thickness was calculated as described above in section 2.3, equation (4) and (3).

QCM-D was also used to measure the adsorption of plasma fibronectin on the terminal HEP layer (12th layer). Despite the fact that fibronectin is contained in serum only in smaller quantities, it was chosen as a model protein to illustrate adsorption of proteins with heparin-binding domains in general that are important for cells to adhere and grow on material surfaces.^[3, 15] Moreover most tissue cells are able to secrete fibronectin.^[15] Fibronectin adsorbed on PEMs formed according to the pH 9 and pH 4+9 regime, indicated by a decrease in frequency (Table 2.2). The quantity of adsorbed protein was calculated from the Sauerbrey equation. In contrast, the pH 4 layers did not support adsorption on fibronectin. There is an increase in the frequency shift at pH 4 condition which indicate a decrease in the layer mass, but there was no protein adsorption as this has been also found previously by SPR measurements performed for fibronectin adsorption at pH 5 condition.^[36] Adsorption was carried out under physiological pH 7.4, which will also affect hydration of the multilayers. However, the adsorbed quantities of fibronectin shown here are similar to those bound to multilayer systems composed of poly-L-lysine and dextran shown in another study.^[37] The adsorption of fibronectin was measured on the terminal HEP layer only, but can also be used as an indicator for the ability of the previous CHI layer to bind this protein because of the intermingled composition of terminal layers at the pH 9 regime indicated by WCA measurements and results of previous studies that showed no significant differences in fibronectin adsorption either on heparin or chitosan terminal layers.^[36] Overall, these results show that multilayers prepared at pH 9 have a higher affinity to adhesive proteins like fibronectin that possess HEP-binding domains, which confirms results of previous studies.^[36]

Table 2.2: Fibronectin (FN) adsorption on terminal HEP layer measured by QCM-D

| pH value | <u>pH 4</u> | <u>pH 4+9</u> | <u>pH 9</u> |
|--|--------------------|----------------------|--------------------|
| Δf (Hz) | 66 | -25 | -31 |
| FN adsorption (ng/cm²) | 0 | 443 | 548 |

Resulting QCM-D frequency shifts (Δf) when adding fibronectin (FN), 20 μ g FN/ml dissolved in PBS at pH 7.4 to terminal (12th) heparin (HEP) layer. Note that because of the increase of frequency on pH 4 multilayer system no adsorption of FN could be calculated.

2.4.3. Studies of Multilayer Surface Topography by Atomic Force Microscopy (AFM)

The surface topography of clean Si wafers and multilayer surfaces prepared at different pH values was analyzed by AFM in dry state. Figure 2.4 shows that the topography of multilayers was highly dependent on the pH conditions during assembly and the terminal layer. All surfaces had a granular surface morphology with a roughness increasing from pH 4, pH 4+9 to pH 9 (see also Table 2.3). It is also visible that the addition of HEP to the previous CHI layer leads to an increase granularity of multilayers, which might be explained by a compaction of multilayer systems observed by decreased dissipation values seen with QCM-D. It should be noted that multilayers prepared at pH 9 showed rather island like structures more prominently as compared to the layers prepared at pH 4. Since, surface topography was visualized from dry samples, the structures visible may swell upon hydration. However the differences in morphology indicate a more island-like structure of multilayers at pH 9 compared to smoother layers at pH 4. Similar findings have been made by others.^[38] The coiled conformation of weak polyelectrolytes (PEI and indirectly CHI) at higher pH might contribute in the formation of more island like structures at pH 9 multilayer system.^[36] In general, AFM investigations also showed that process parameters like pH condition and type of polyelectrolytes greatly affect the multilayer surface structure.^[5]

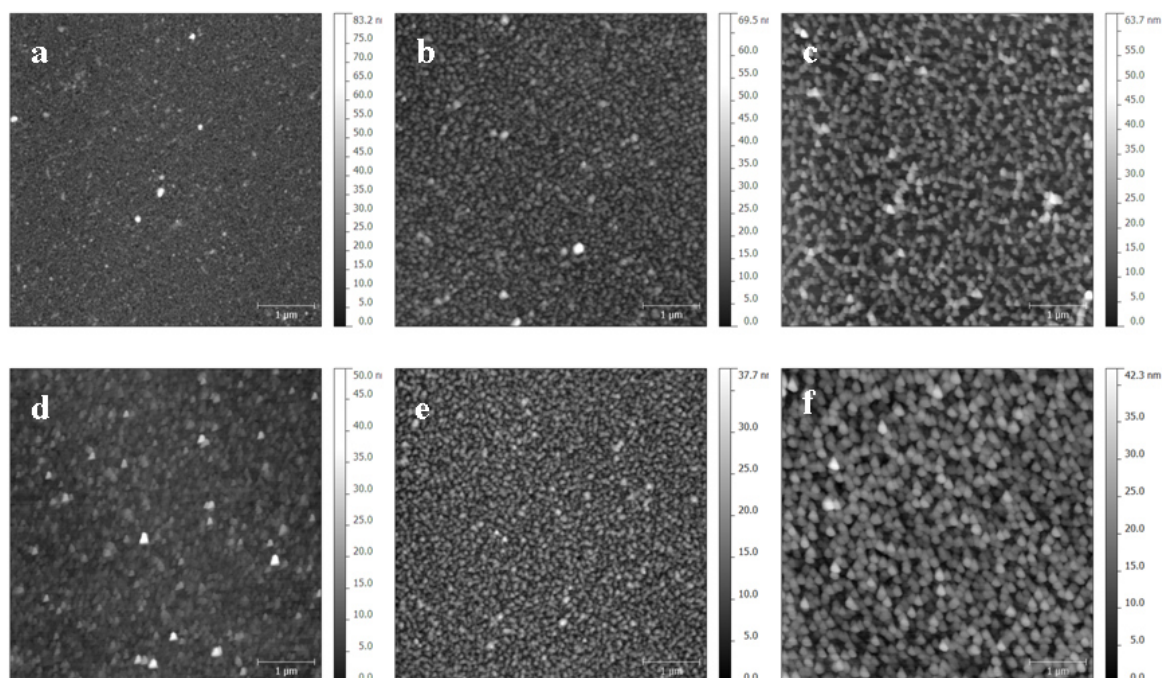


Figure 2.4: Atomic force microscopy images (AFM) images of chitosan (CHI) terminal layer (a-c) and heparin (HEP) terminal layer (d-f) prepared at pH 4 (a & d), pH 4+9 (b & e) and pH 9 (c & f). Scan size of all the images is 5x5 μm .

Table 2.3: PEM surface roughness evaluation by AFM in dry condition

| <u>Roughness average (R_a) (nm)</u> | <u>pH 4</u> | <u>pH 4+9</u> | <u>pH 9</u> |
|--|--------------------|----------------------|--------------------|
| 11 th (CHI layer) | 3.3 | 3.8 | 4.8 |
| 12 th (HEP layer) | 3.0 | 3.2 | 4.7 |

2.4.4. Adhesion and Growth of C2C12 Cells on Multilayers

PEM systems have been suggested for the coating of implant surfaces and tissue engineering scaffolds to improve cell attachment and growth.^[35] In addition, such multilayer systems have been shown to be applicable as release system for growth factors that promote differentiation of cells.^[13] Cell adhesion and spreading are prerequisites for growth and differentiation, since related signal transduction processes require ligation of integrins to extracellular matrix components.^[39] Hence cell adhesion studies were carried out on terminal CHI (11th) and HEP (12th) layers to learn how the pH value during the multilayer formation affects the interaction with cells. C2C12 cells were seeded on multilayers in the culture medium supplemented with 10% fetal bovine serum that contains so-called attachment factors particularly vitronectin and some fibronectin.^[40] Figure 2.5 shows the morphology of C2C12 cells 4 h after seeding on either terminal 11th CHI layer (upper row) or 12th HEP layer (lower row) by phase contrast microscopy. While the effect of terminal layer seems to be negligible, the pH during multilayer formation has obviously a great effect on cell adhesion and spreading. In the case of pH 4 multilayers (Figure 2.5 a & d), in general cells were round. There were no differences whether CHI or HEP was the terminal layer, which was surprising when the results of WCA measurements were considered. By contrast elongated and well spread C2C12 cells were found on multilayers prepared at pH 9 (Figure 2.6 c & f). pH 4+9 combination layers also shows more cells adhering with a more spread phenotype that was similar to pH 9 conditions (see Figure 2.5 b & e).

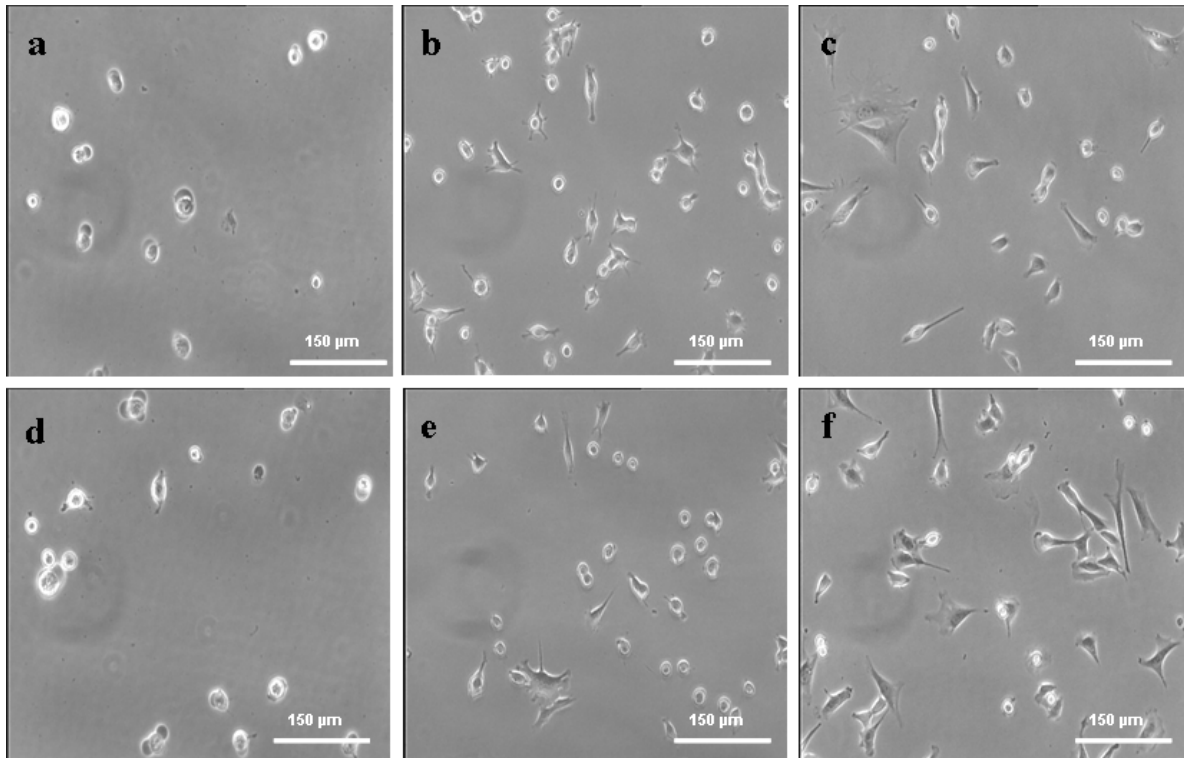
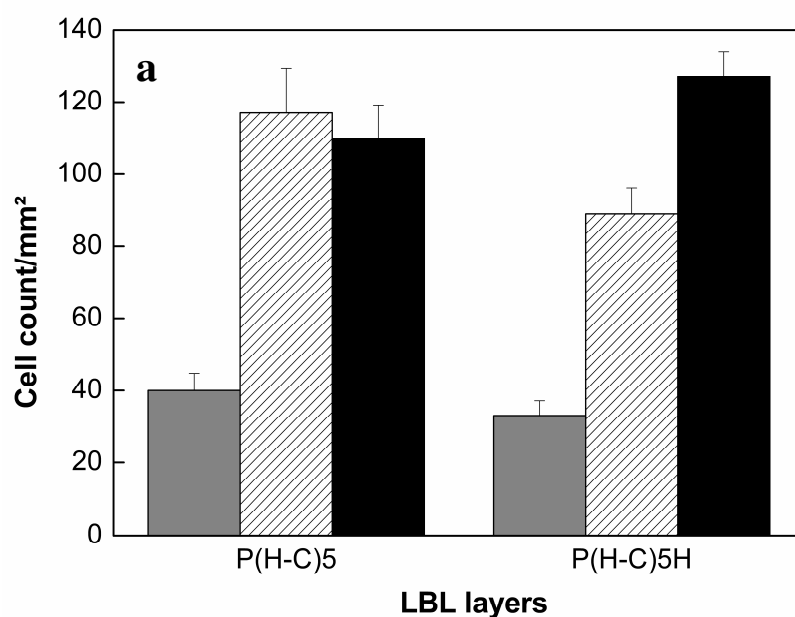


Figure 2.5: Phase contrast images of C2C12 cells cultured in DMEM and 10% FBS for 4 h on multilayers prepared at different pH conditions; chitosan (CHI) terminated, 11th layer (a-c) and heparin (HEP) terminated, 12th layer (d-f) on pH 4 (a & d), pH 4+9 (b & e) and pH 9 (c & f).

Quantitative data on cell adhesion and spreading were obtained from analysis of phase contrast images and are presented in Figure 2.6 a & b. They confirm the qualitative observations and show that in any of the pH setups the terminal layers does not affect largely the degree of cell spreading (Figure 2.6 b) and also with one exception the number of cells adhering (see Figure 2.6 a). These investigations showed that multilayers assembled at pH 9 were more adhesive for and promoted spreading of C2C12 cells in comparison to pH 4 layers, where fewer cells attached and spread only little. Similar observations were made with osteoblast previously.^[20] The multilayers prepared with pH variation from 4 to 9 (layers with pH 4+9 condition) have shown a noticeable improvement in cell attachment or cell count. Here it was also found that cell adhesion on CHI-terminated layers was higher than on HEP-terminated layers. The higher adhesion and spreading of cells on pH 9 and pH 4+9 multilayer systems is in accordance with the findings on fibronectin adsorption here and in recent work, that showed no measurable presence of fibronectin on multilayers prepared at low pH value while fibronectin adsorbed on multilayers prepared at higher pH values.^[36]

Since during cell culture serum was used, the results can be interpreted in terms of adsorption of adhesive proteins with HEP binding domains (i.e. fibronectin and vitronectin). This is supported by assumptions from Lundin et al. using the same polyelectrolytes stating that the surface of multilayers has a rather heterogeneous composition.^[30] Hence, the chemistry of surfaces exposed to serum and cells is obviously presenting both CHI and HEP in the case of pH 9 and pH 4+9 multilayer systems. The question remains, why multilayers prepared at pH 4 do not adsorb fibronectin and support cell adhesion although, HEP should be present there particularly when HEP forms the terminal layer (see results of WCA measurements). One of the reasons for suppressed cell adhesion could be the high water content and with the swollen state of this multilayer the low stiffness of the substratum. Soft substrata have been found to suppress cell adhesion and spreading due to the suppressed signalling via integrins regarding mechanotransduction.^[41] This has been also observed in several studies on polysaccharide-based multilayers where their flexibility was reduced by chemical cross-linking and subsequent increased cell adhesion.^[42] However, even then the lack of any measurable adsorption of fibronectin despite the presence of HEP indicates also that during ion-pairing HEP is engaged in interaction with CHI that jeopardizes its interaction with HEP-binding epitopes in proteins like fibronectin and vitronectin. Hence the reason for the low adhesivity of multilayers prepared here at low pH could be twofold, namely a soft nature of the substratum and the lack of protein adsorption.



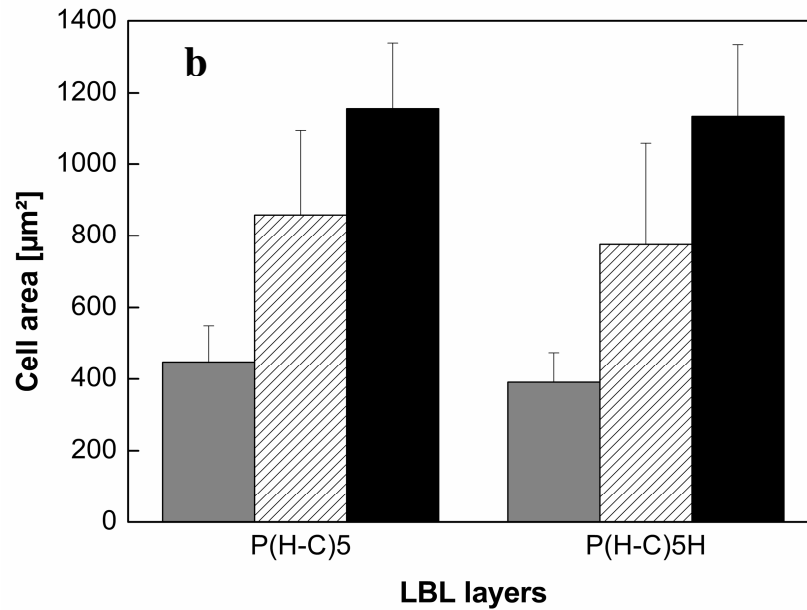


Figure 2.6: (a) Cell adhesion and (b) spreading of C2C12 cell (cell area) evaluation by C2C12 cells after 4 hours culture in DMEM with 10% FBS on chitosan (CHI) terminated and heparin (HEP) terminated multilayers prepared at different pH conditions (pH 4 – grey, pH 4+9 – hatched and pH 9 – black bars).

To see whether initial effect of multilayers on cell adhesion would also prevail during longer culture of cells, proliferation studies were done with C2C12 cells for 1 and 3 days. Figure 2.7 shows the morphology of cells during the culture period only on HEP-terminated multilayers since they were no noticeable differences in cell growth on either terminal layer.

As can be seen in Figure 2.7 cells were able to grow on all substrata and cell numbers increased from 1 (left lane) to 3 (right lane) days. It is also obvious that cell spreading was improved on multilayers prepared at pH 4 although cell number was considerably lower. The phase contrast micrographs show that the cell coverage after 1 and 3 days was lowest on pH 4 multilayers followed by pH 4+9 and pH 9 layers. On pH 9 layers C2C12 cells have almost reached confluence after 3 days of culturing and hence they are more proliferation supporting than pH 4 ones. pH 4+9 layer setup also shows more coverage of the surface by the cells if compared with pH 4 layers which is in good agreement with the cell adhesion results.

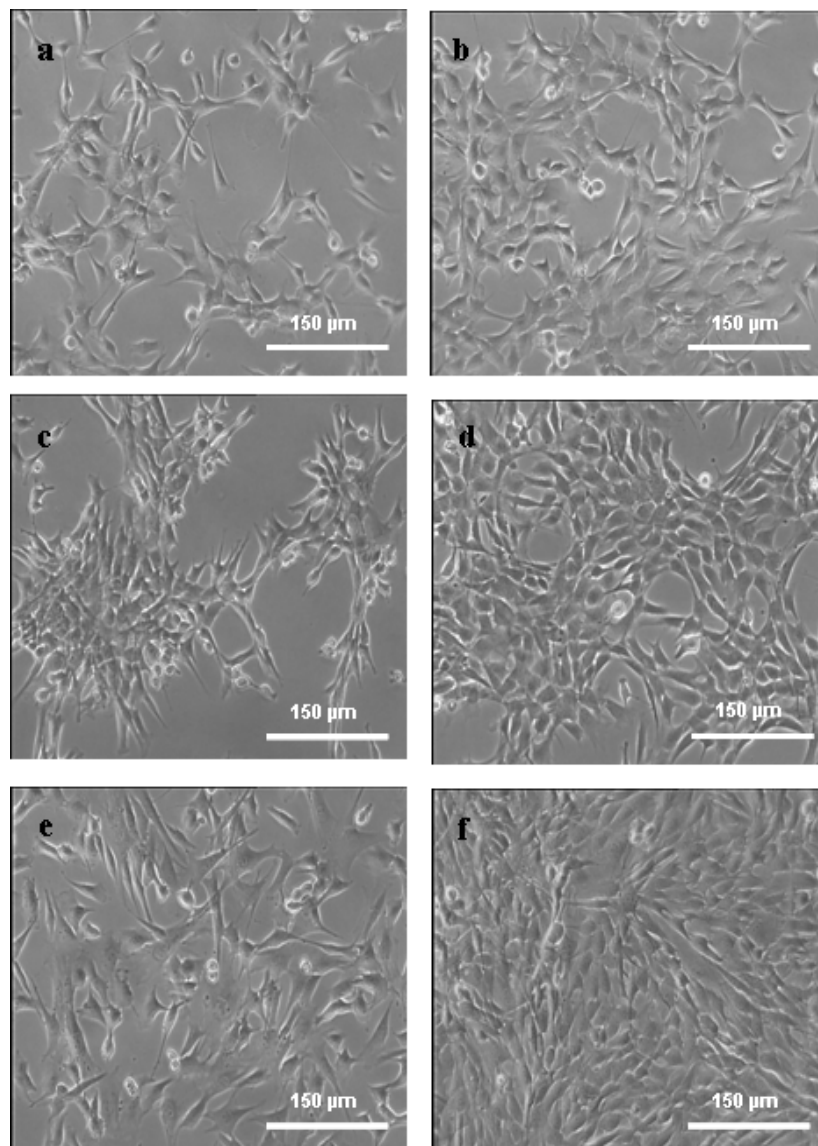


Figure 2.7: Phase contrast images of C2C12 cells cultured in DMEM and 10% FBS on heparin (HEP)-terminated multilayers prepared at different pH conditions; pH 4 (a & b), pH 4+9 (c & d) and pH 9 (e & f); for 1 day (a,c,e) and 3 days (b,d,f).

Quantitative data on cell proliferation were obtained by analysis of surface coverage from phase contrast images over the culture period of 3 days. Results in Figure 2.8 show a remarkable coincidence with that of adhesion studies and confirm the lower cytocompatibility of multilayers prepared at pH 4 vs. those prepared at pH 9 and pH 4+9 in a quantitative manner. Since cell adhesion and related signal transduction processed during ligation of integrins drive mitogenic responses of cells via mitogen-activated protein kinase (MAPK) pathway^[43], the reduced cell growth shows the important role of adhesivity of substrata. The application of distinct pH regimes during assembly of multilayer systems and choice of

biogenic polyelectrolytes particularly polysaccharides and glycosaminoglycans provides a tool to modulate cell adhesion to the desired extent as it has been shown in this and our previous work. [20, 21] [44, 45]

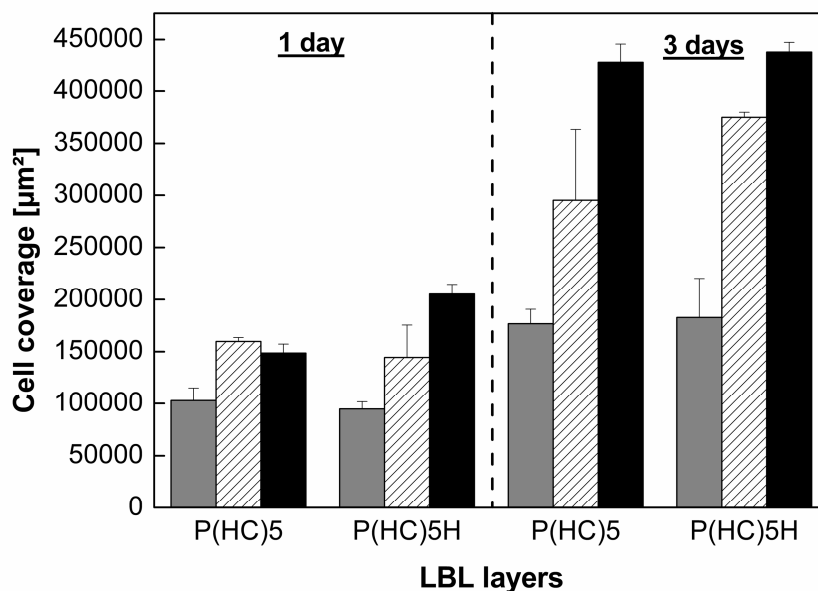


Figure 2.8: Surface coverage evaluation by C2C12 cells after culture in DMEM and 10% FBS on chitosan (CHI) terminated and heparin (HEP) terminated multilayers prepared at different pH conditions (pH 4 – grey bars, pH 4+9 – hatched bars and pH 9 – black bars) after 1 and 3 days of cultivation.

2.5. Conclusion

We could show in this work that polyelectrolyte multilayer (PEM) coatings made from heparin (HEP) (a strong polyelectrolyte) and chitosan (CHI) (a weak polyelectrolyte) can be used to affect adhesion and growth of C2C12 cells by simple adjustment of pH of HEP solution during multilayer assembly (the pH of the CHI solution was kept constant at pH 4 throughout the experiments). The conditions for the HEP adsorption had a great effect on the wetting properties of multilayers and particularly the layer mass, its water content and surface topography. The pH value of HEP solution was varied from pH 4 to pH 9. These differences are likely due to the charge and conformation of the previously adsorbed CHI layer that changes the adsorption of HEP from preferential ion pairing to hydrogen bonding (at pH 9). The idea of the current work was to optimize multilayer thickness vs. its adhesiveness for cells. Since cell adhesion is dependent on both the mechanical properties of the substrate and the ability to bind proteins that allow ligation of integrins, we have applied here a specific pH

regime with formation of layers of higher mass at low pH 4 (this can potentially be exploited in future studies to load growth factor in to the film), followed by a switch to pH 9 leading to a suspension of layer growth. Furthermore, the surface properties achieved under these circumstances allowed the subsequent adsorption of adhesive proteins like fibronectin and promoted adhesion and growth of cells to a similar extent like thin, rigid multilayers prepared at pH 9. Hence, such multilayer system prepared by variation of pH might be very useful to support initial cell attachment and growth while at the same time also providing multilayers with additional functions, such as reservoirs and delivery systems for growth factors and similar molecules.

2.6. Acknowledgements

The work was funded partly by German Academic Exchange Service and the Greek in the frame of bilateral cooperation between Germany and Greece and European Union Seventh Framework Program (FP7/2007-2013) under grant agreement n° NMP4-SL-2009-229292 (Find & Bind). The support of Dr. H. S. Leipner from Interdisciplinary Center for Materials Research at Martin Luther University in some of the AFM studies is greatly acknowledged.

2.7. References

1. B. D. Ratner, *Journal of Biomedical Materials Research*. **1993**, 27, 837.
2. D. G. Castner, B. D. Ratner, *Surface Science*. **2002**, 500, 28.
3. T. Groth, Z. M. Liu, M. Niepel, D. Peschel, K. Kirchhof, G. Altankov, N. Faucheux, *Advances in Regenerative Medicine: Role of Nanotechnology, and Engineering Principles*, 1st edition Springer, New York, 2010, p. 253.
4. G. Decher, J. D. Hong, J. Schmitt, *Thin Solid Films*. **1992**, 210, 183.
5. Z. Tang, Y. Wang, P. Podsiadlo, N. Kotov, *Adv. Mater.* **2006**, 18, 3203.
6. P. T. Hammond, *Adv. Mater.* **2004**, 16, 1271.
7. M. Schönhoff, *Rev. J. Phys. Condens. Mater.* **2003**, 15, 1781.
8. Y. Lvov, K. Ariga, I. Ichinose, T. Kunitake, *J. Am. Chem. Soc.* **1995**, 117, 6117.
9. Y. Lvov, H. Haas, G. Decher, H. Möhwald, *Langmuir*. **1994**, 10, 4232.

10. J. Schmitt, G. Decher, W. J. Dressick, S. L. Brandow, R. E. Geer, R. Shashidhar, J. M. Calvert, *Adv. Mater.* **1997**, *9*, 61.
11. H. Shin, S. Jo, A. G. Mikos, *Biomaterials.* **2003**, *24*, 4353.
12. M. D. Kofron, X. Li, C. T. Laurencin, *Curr. Opin. Biotechnol.* **2004**, *15*, 399.
13. T. Crouzier, K. Ren, C. Nicolas, C. Roy, C. Picart, *Small.* **2009**, *5*, 598.
14. G. Decher, J. B. Schlenoff, *Multilayer Thin Films* 1st edition Wiley-VCH, Weinheim **2003**.
15. R. Pankov, K. M. Yamada, *J. Cell. Sci.* **2002**, *115*, 3861.
16. W. H. Burgess, T. Maciag, *Annu. Rev. Biochem.* **1989**, *58*, 575.
17. S. E. Sakiyama-Elbert, J. A. Hubbell, *J. cont. rel.* **1999**, *65*, 389.
18. A. Weltrowski, M. S. Almeida, D. Peschel, K. Zhang, S. Fischer, T. Groth, *Macromolecular Bioscience.* 2012, *12*, **740**.
19. M. V. Tsurkan, K. Chwalek, K. R. Levental, U. Freudenberg, C. Werner, *Macromol. Rapid Commun.* **2010**, *31*, 1529.
20. K. Kirchhof, K. Hristova, N. Krasteva, G. Altankov, T. Groth, *J Mater Sci: Mater Med.* **2009**, *20*, 897.
21. M. S. Niepel, D. Peschel, X. Sisquella, J. A. Planell T. Groth, *Biomaterials.* **2009**, *30*, 4939.
22. T. Crouzier, A. Szarpak, T. Boudou, A. Rachel, C. Picart, *Small.* **2010**, *6*, 651.
23. T. Crouzier, L. Fourel, T. Boudou, C. Albigès-Rizo, C. Picart, *Adv. Mater.* **2011**, *23*, H111.
24. R. B. M. Schasfoort, A. J. Tudos, *Handbook of Surface Plasmon Resonance.* 1st edition RSC Publishing, Cambridge, **2008**.
25. M. Rodahl, F. Höök, A. Krozer, P. Brzezinski, B. Kasemo, *Rev. Sci. Instrum.* **1995**, *66*, 3924.
26. G. Z. Sauerbrey, *Z. Phys. A: Hadrons Nucl.* **1959**, *155*, 206.
27. F. Hook, B. Kasemo, T. Nylander, C. Fant, K. Sott, H. Elwing, *Anal. Chem.* **2001**, *73*, 5796.
28. I. Leceta, P. Guerro, K. de la Caba, *Carbohydrate polymers.* **2013**, *93*, 339.

29. R.P. Mota, I. A. Perrenoud, R. Y. Honda, M. A. Algatti, M.E. Kayama, K.G. Kostov, T. Sadahito China, N. C. Cruz, Biocompatible thin films obtained from heparin-methane plasma processes. *Proceedings 11th International Symposium on Process Engineering Singapore*. **2012**
30. M. Lundin, F. Solaqa, E. Thormann, L. Macakova, E. Blomberg, *Langmuir*. **2011**, 27, 7537.
31. J. P. Schlenoff, S.T. Dubas, *Macromolecules* **2001**, 34, 592.
32. P. Dong, W. Hao, Y. Xia, G. Da, T. Wang, *J. Mater. Sci. Technol.* **2010**, 26, 1027.
33. T. Crouzier C. Picart, *Biomacromolecules* **2009**, 10, 433.
34. S. Boddohi, C. E. Killingsworth, M. J. Kipper, *Biomacromolecules*. **2008**, 9, 2021.
35. L. Richert, Ph. Lavallo, D. Vautier, B. Senger, J.-F. Stoltz, P. Schaaf, J.-C. Voegel, C. Picart, *Biomacromolecules*. **2002**, 3, 1170.
36. K. Kirchhof, *Nanostrukturierte Biomaterialbeschichtungen zur Steuerung von Zelladhäsion und -proliferation: pH-Wert-abhängige Multischichten aus Heparin und Chitosan in diskreter und Gradientenform*, Ph.D. Thesis, **2009**.
37. C.R. Wittmer, J.A. Phelps, W.M. Saltzman, P.R. Van Tassel, *Biomaterials*. **2007**, 28, 851.
38. B.S. Kim, H. Gao, A. A. Argun, K. Matyjaszewski, P. T. Hammond, *Macromolecules* **2009**, 42, 368.
39. R.O. Hynes, *Cell*. **2002**, 110, 673.
40. J.G. Steele, G. Johnson, P.A. Underwood, *Journal of Biomedical materials Research* **1992**, 7, 861.
41. D. E. Discher, P. Janmey, Y. Wang, *Science*. **2005**, 310, 1139.
42. L. Richert, F. Boulmedias, P. Lavallo, J. Mutterer, E. Ferreux, G. Decher, P. Schaaf, J. C. Voegel, C. Picart, *Biomacromolecules*. **2004**, 5, 284.
43. E. A. Clark, R. O. Hynes, *J. Biol. Chem.* **1996**, 271, 14814.
44. K. Kirchhof, A. Andar, H. B. Yin, N. Gadegaard, M. O. Riehle, T. Groth, *Lab on a Chip*. **2011**, 11, 3326.
45. Z-M. Liu, G. Qinyi, Z-K. Xu, T. Groth, *Macromolecular Bioscience*. **2010**, 10, 1043.

Chapter 3

Synthesis of novel cellulose derivatives and investigation of their mitogenic activity in the presence and absence of FGF2

D. Peschel, K. Zhang, N. Aggarwal, E. Brendler, S. Fischer, T. Groth

3.1. Abstract

Novel cellulose sulfates (CS) with controlled degree of sulfation (DS_S) were synthesized through acetosulfation as well as direct sulfation. CS containing carboxyl (CO) or carboxymethyl (CM) groups were prepared by TEMPO oxidation or by carboxymethylation with chloroacetic acid. The derivatization was characterized by nuclear magnetic resonance and Raman spectroscopy. The derivatives were investigated regarding their cytotoxicity and mitogenic activity by modulation of 3T3 fibroblast proliferation with or without exogenous FGF2. All derivatives were non-toxic for 3T3 cells. CS strongly promoted FGF2-induced proliferation, which was positively related to overall DS_S . In the absence of FGF2, minute quantities of CS with intermediate degree of sulfation exerted stronger mitogenic effects than heparin. No significant promoting effects of CO and CM on cell proliferation were found though the structure of CO shows similarities to heparin.

3.2. Introduction

Glycosaminoglycans (GAG) like heparin or heparan sulfate cooperate with growth factors and play pivotal roles for the regulation of proliferation and differentiation of cells. The participation of GAG in the formation of growth factor receptor-ligand complexes to initiate signal transduction in cells is well described [1-3]. Studies with heparin oligosaccharides have shown that the increase in fibroblast growth factor (FGF2)-induced proliferation depends on the degree of sulfation, especially at 6-*O*-position [4]. X-ray analysis of the crystal structure of the ternary FGF-FGF receptor-heparin complex demonstrated that the binding of the amino groups of FGF to heparin is realised by hydrogen bonds to the 2-*O*, *N*, 6-*O* sulfate and 6-*COO* groups [5]. It should be noted that sulfated polysaccharides can also lead to suppression of the effects of growth factors by inhibiting the binding to its receptor as described for FGF2 [6,7].

It was shown in this context that polysulfated compounds, unlike heparin, have the feasibility to dock into the heparin-binding domain of FGF2, demonstrated by molecular modelling studies [8]. Therefore sulfated polysaccharides like maltohexaose sulfate have been used as suppressors of tumour growth, showing that the suppressing effect was critically dependent on the chain length and degree of sulfation [9]. It should be noted that several of these compounds also expressed cytotoxic effects, especially an increasing degree of sulfation [10,11].

Furthermore, GAG such as heparin and other sulfated polysaccharides also prolong the half life of growth factors owing to the formation of reservoirs and protection against proteolytic digestion or acidic conditions [12,14]. In this respect, it was observed that the sulfation pattern of GAG which prolong the half life can differ from that forming the receptor-ligand complex [3]. The “reservoir” function of heparin has been exploited in several tissue engineering applications, showing sustained release of growth factors from different scaffold materials [15,17]. However, GAG such as heparin not only prolong the half life of growth factors, but can also directly control the proliferation of cells by modulating the cellular production of growth factors such as FGF2 and transforming growth factor (TGF) β 1 [18,19]. Because of the multiple effects of GAG such as heparin on cells, several sulfated polysaccharides and other compounds have been synthesized in the past. An increase in FGF-induced mitogenic activity was found with dextran sulphate, (1-6)- α -D-mannopyranan sulphate and sulfonated polymers such as poly (vinylsulfonate) [20,10]. The potentiating effect increased with higher degree of sulfation, although the underlying mechanisms were not further investigated.

Naturally occurring heparins differ greatly regarding their molecular composition, and hence their biological activity depends on the source [1]. Therefore, synthetic routes to preparing substances with controlled heparinoid activity may be attractive for a variety of biomedical but also biotechnological applications. So far, many compounds with heparinoid activity have been synthesized [7-10], but relatively little attention has been paid to cellulose derivatives. Cellulose is one of the most abundant natural occurring polysaccharides, and thus it can be obtained in large quantities. Cellulose sulfates (CS) have been synthesized by variety of methods with heterogeneous or homogeneous sulfation in different solvents [21-25]. In contrast to cellulose, CS shows highly improved solubility in water and better enzymatic degradability [21,23]. Because of that, CS found a wide use in biotechnology and pharmaceuticals to encapsulate enzymes and cells [26-28], as inhibitors for HIV viruses and anticoagulant effectors [29-31]. Other derivatives of cellulose like carboxymethyl and carboxyl cellulose have high commercial importance in the paper, cosmetic and

pharmaceutical industries [32]. However, the derivatisation of cellulose with sulfate as well as carboxymethyl or carboxyl groups has rarely been done [33]. Moreover, the ability of cellulose derivatives to cooperate with growth factors and to modulate growth and differentiation of cells has never been investigated.

The present study introduced novel routes of cellulose derivatisation to obtain defined substitution patterns with sulfate, carboxylate and also carboxymethyl groups. Moreover, it showed that certain derivatives particularly CS have strong mitogenic activity not only in the presence of FGF2, but also without the addition of growth factor, on 3T3 mouse fibroblasts, which were used as a model system for other cells also responding to FGF2. These results indicate strongly that CS may deserve application in the field of tissue engineering as scaffold components which help to control cellular behaviour.

3.3. Experimental

3.3.1. Cellulose materials for chemical modification

Native cellulose (AC, with 97.0% alpha cellulose) with an average degree of polymerisation (DP) of 1180 was purchased from Buckeye Technologies Inc. (Memphis, USA). Microcrystalline cellulose (MCC) with a DP of 275-277 was obtained from J. Rettenmaier & Söhne GmbH (Rosenberg, Germany). Irradiated cellulose (IC) with an average DP of 113 was attained through treating cellulose (DP ~ 500) with electron-beam. Cellulose-2.5-acetate (C2.5A) with a degree of substitution by acetyl groups of 2.5 was obtained from M&G Group (Verbania-Pallanza, Italy). C2.5A and cellulose were used without further treatment. Dimethylformamide (DMF), dimethylacetamide (DMAc) and dimethyl sulfoxide (DMSO) were freshly distilled before use. Deionized water was used. Other chemicals were all of laboratory grade and used as received. The dialysis membrane used for purification of products was purchased from Spectrum Laboratories Inc. (Rancho Dominguez, USA) and had an approximate molecular weight cut-off of 500 Da.

3.3.2. Synthesis of cellulose sulfates (CS)

The synthesis of CS was carried out either as acetosulfation of cellulose or as direct sulfation of cellulose and C2.5A to obtain products with different degrees of substitution with sulfate (DS_s). For a typical acetosulfation, 10 g cellulose were swollen in 500 ml anhydrous DMF at room temperature (RT) for 14 h. The reaction agent – either chlorosulfuric acid or sulfuric acid and acetic anhydride in DMF or DMAc – was dropped into the cellulose suspension

under vigorous stirring within 15 min. Then the temperature was raised to 50°C, and the system was kept at 50°C for 5 h. After that the mixture was cooled down to RT and poured into a saturated solution of anhydrous sodium acetate in ethanol. Thereafter, the precipitate was washed with 4% sodium acetate solution in ethanol and deacetylated with 1 M ethanolic solution of sodium hydroxide for 15 h. The pH value was adjusted to 8.0 with acetic acid/ethanol (50/50, w/w). After washing with ethanol the product was collected through centrifugation, then dissolved in water, filtered, dialysed in deionized water and lyophilized.

For direct sulfation, the cellulose was suspended in DMF for 14 h, and C2.5A was dissolved in DMF. Chlorosulfuric acid was then dropped into the suspension or the solution within 15 min. After that, the mixture was kept at RT for a designated duration. After reaction, the mixture was poured into the saturated solution of anhydrous sodium acetate in ethanol and washed with 4% sodium acetate solution in ethanol. Then the product was dissolved in water and the pH was adjusted to 8.0 with acetic acid/ethanol (50/50, w/w). After being washed with ethanol the product was collected through centrifugation, then dissolved in water, filtered, dialysed in deionized water and lyophilized.

3.3.3. Oxidation of CS

CS from different starting materials (MCC, IC, AC) were used for carboxylation according to the oxidation method in Ref. 41 to obtain products with different DS_{COO} . First 1 g CS was dissolved in 60 ml water. The oxidation agent consisting of 2,2,6,6-tetramethylpiperidine-1-oxyl radical (TEMPO), NaBr and NaOCl was dissolved in water under stirring until complete dissolution. Then the oxidation agent was added slowly to the solution of CS. The remaining NaOCl was dropped into the solution to maintain the pH at 10.5. After addition of the remaining NaOCl, the pH was maintained constant for up to 4 h using 0.5 M NaOH solution. Thereafter 5 ml of methanol was added to stop oxidation, and the pH was then adjusted to 7.5 with 0.5 M HCl solution. The mixture was then poured into 300 ml ethanol and the product was obtained by centrifugation. The precipitate was washed with ethanol/water (80/20, v/v), dissolved in water, filtered, dialysed in deionized water and lyophilized.

3.3.4. Carboxymethylation of CS

CS from different starting materials (MCC, C2.5A) were used for carboxymethylation to obtain products with different DS_{CM} . First, 1.5 g CS suspended in 75 ml isopropyl alcohol (IPA) or dissolved in 175 ml DMSO was stirred for 0.5 h. Then 22 ml NaOH aqueous

solution (3.75 M) was dropped into the suspension. After stirring for another 3 h, 3.85 g chloroacetic acid was added in solid state. The temperature of the reaction mixture was raised to 55°C, and it was maintained for 5 h. After being cooled down to RT, the reaction mixture was precipitated in five vol. of ethanol under stirring for 0.5 h. The precipitate, isolated by centrifugation, was dissolved afterwards in water, and the pH value was adjusted to 7.5 with acetic acid/water (50/50, v/v). This solution was precipitated again in 5 vol. of ethanol, and the product was collected by centrifugation. After being washed three times with ethanol/water (80/20, v/v), the product was dissolved in water, filtered, dialysed in deionized water and lyophilized.

3.3.5. Characterization of reaction products

The ^{13}C NMR spectra were recorded at RT using a Bruker DFX 400 spectrometer with samples dissolved in D_2O , with a frequency of 100.13 MHz, 30° pulse length, 0.3 acq. time and a relaxation delay of 3 s. Scans between 5000 and 20000 were accumulated.

^1H NMR was carried out according to Refs. 37 and 38, and the spectra were obtained after the hydrolysis in 25% $\text{D}_2\text{SO}_4/\text{D}_2\text{O}$ using a Bruker Ultrashield 500 Plus spectrometer with a frequency of 500.13 MHz and accumulation number between 8 and 16.

Fourier Transform Raman spectra of the samples in small aluminium discs were recorded with a Bruker MultiRam spectrometer with a liquid-nitrogen-cooled Ge diode as detector. The spectra were recorded over a range of 3500-0 cm^{-1} with an operating spectral resolution of 3 cm^{-1} .

3.3.6. Preparation of solutions of heparin and cellulose derivatives for biological experiments

Porcine intestinal mucosa (PIM) heparin was obtained from Calbiochem (Gibbstown, USA). Cellulose derivatives used in the biological studies were named according to their substituent and overall degree of substitution, such as CS-X for cellulose sulfates, CO-X for carboxylated cellulose derivatives and CM-X for carboxymethylated cellulose derivatives. Heparin and cellulose derivatives were dissolved in cell culture media for the cytotoxicity assays and the investigation of mitogenic effects. After dissolving at RT over night, the polysaccharides were sterilised by filtering through a 0.2 μm filter and further diluted in cell culture media.

3.3.7. Cell culture

3T3-L1 fibroblast cells obtained from ATCC (Manassas, USA) were cultured in flasks (75cm², Greiner bio-one, Frickenhausen, Germany) in Dulbecco's modified Eagle medium (DMEM, Biochrom AG, Berlin, Germany) supplemented with 10% fetal bovine serum (FBS, Biochrom AG) and 1% penicillin-streptomycin-fungizone (PSF, Promocell, Heidelberg, Germany) in a 37°C humidified atmosphere of 5% CO₂ and 95% air. Cells were harvested by treatment with trypsin/EDTA (Biochrom AG). Trypsinization was stopped by addition of FBS and cells were washed twice with DMEM.

3.3.8. Cytotoxicity assay

The cellulose derivatives and heparin were dissolved in DMEM without FBS, but with 1% PSF (Promocell, Heidelberg, Germany) and 1% insulin-transferrin-selenium A (ITS, Gibco, New York, USA) at concentrations of 10 µg and 1000 µg ml⁻¹. 3T3-L1 fibroblast cells were seeded at a density of 40,000 cells/well in 96-well plates (Greiner bio-one) in DMEM supplemented with 10% FBS and 1% PSF, and cultured for 48 h to reach confluence. Then the plates were washed once with DMEM only and 200 µl of either DMEM with dissolved cellulose derivatives, heparin for comparison or DMEM (control) alone were added. Cells were incubated as described above for further 24 h. The viability of cells was measured with QBlue assay (BioChain, Hayward, USA). This assay is based on the utilization of the redox dye resazurin, which is converted into a highly fluorescent product (resorufin) by reductases of metabolically active cells. The fluorescent intensity was measured with an excitation wavelength of 544 nm and an emission wavelength of 590 nm by the plate reader Fluostar Optima (BMG Labtech, Offenburg, Germany). The viability was calculated as a ratio to the control. Measurements were carried out in quadruplicates and given as means ± standard deviation.

3.3.9. Investigation of mitogenic effects of cellulose derivatives on 3T3-L1 fibroblasts

3T3-L1 fibroblast cells were seeded at a density of 10,000 cells/well in black 96-well plates (Greiner bio-one) in DMEM supplemented with 10% FBS and 1% PSF and cultured for 24. After washing the plates with DMEM only, the cellulose derivatives or heparin were applied to the cells in DMEM without FBS at a concentration range of 1 - 1000 µg ml⁻¹ for 48 h in the presence or absence of 10 ng ml⁻¹ FGF2. Proliferation was measured on the basis of the DNA content using the Quant-iTTM PicoGreen dsDNA quantification assay (Invitrogen, Karlsruhe,

Germany). The fluorescent intensity was measured with excitation wavelength of 485 nm and an emission wavelength of 520 nm by the Fluostar Optima plate reader. The proliferation was expressed as a ratio of the control wells with 10 ng ml⁻¹ FGF2. All experiments were carried out with six wells per sample and dilution from which means and standard deviation were calculated.

3.4. Results and discussion

3.4.1. Synthesis of CS

The substitution of cellulose by sulfate groups and their distribution were analyzed by ¹³C NMR. Figure 3.1 shows the ¹³C NMR spectra of heparin (for comparison) and selected CS with different DS_S values. The spectrum of heparin shown in Figure 3.1a yielded expectable results regarding the distribution of substituents, but was carried out for comparison with biological effects of cellulose derivatives. The presence of sulfate groups on C₆ of heparin was observed based on a chemical shift from 60.5 to 67 ppm. Also the peak of C₁ of heparin was shifted from 102.5 ppm to 99.8 and 97.2 ppm, which indicates the presence of sulfate groups on C₂ in both repeating units of heparin [34-36]. Furthermore, a peak at 175 ppm was found, which indicates the presence of carboxyl groups on C₆ of heparin. Figure 3.1b also shows that the peaks of unsubstituted C₁-C₆ of anhydro glucose unit (AGU) of cellulose are located at 102.3, 74.7, 73.9, 78.3, 72.9 and 60 ppm. After sulfation at the 6-*O*-, 2-*O*- or 3-*O*-positions, the signals of the relevant carbons were shifted (see Figure 3.1 b-d). The signal of C₆ was shifted from 60 to around 66.4 ppm after sulfation and that of C₂ from 74.7 to 80.8 ppm. It is also visible that there was no shift of the signal of 3-*O*-position.

Figure 3.2 shows the Raman spectra of MCC and two CS with different DS_S values. Three peaks at 1096, 1121 and 1152 cm⁻¹ in the MCC spectrum disappeared and two new peaks at 1072 and 1123 cm⁻¹ in the Raman spectra of CS emerged. In addition, the intensity of the peak at 1040 cm⁻¹, which stands for OH vibration, became weaker in CS until it almost vanished if CS had a high DS_S value like CS-1.69. There were also other newly emerging peaks at 1272 and 829 cm⁻¹ because of the sulfation of cellulose. The former could be assigned to the asymmetric S-O stretching vibration and the latter should be caused by the asymmetric and symmetric S-O-C stretching vibrations [37, 38].

The DS_S values of the synthesized CS were calculated on the basis of the integrated peak areas of ¹³C NMR [35] and are summarized in Table 3.1. It has been reported that the analytical results of ¹³C NMR have only small variations of 1-2%, which makes this approach

feasible for calculating the degree of derivatisation [39]. As shown in Table 3.1, sulfation of cellulose could be successfully achieved through either acetosulfation or direct sulfation. Based on the DS_S values shown in Table 3.1 determined by ^{13}C NMR, it can be stated that the sulfation took place primarily at 6-*O*-position, especially when the DS_S values of CS were not very high. CS with higher DS_S values above 1.5 became more intensively substituted in the 2-*O*-position as well. When the DS was about 2, as in CS-1.94, the 2-*O*-position was sulfated almost completely (DS_{S2} value of 0.94). By contrast, only a weak substitution could be detected with ^{13}C NMR spectroscopy at the 3-*O*-position (as a peak at around 82.1 ppm). Therefore, the calculation of the DS_S value at 3-*O*-position was not possible here.

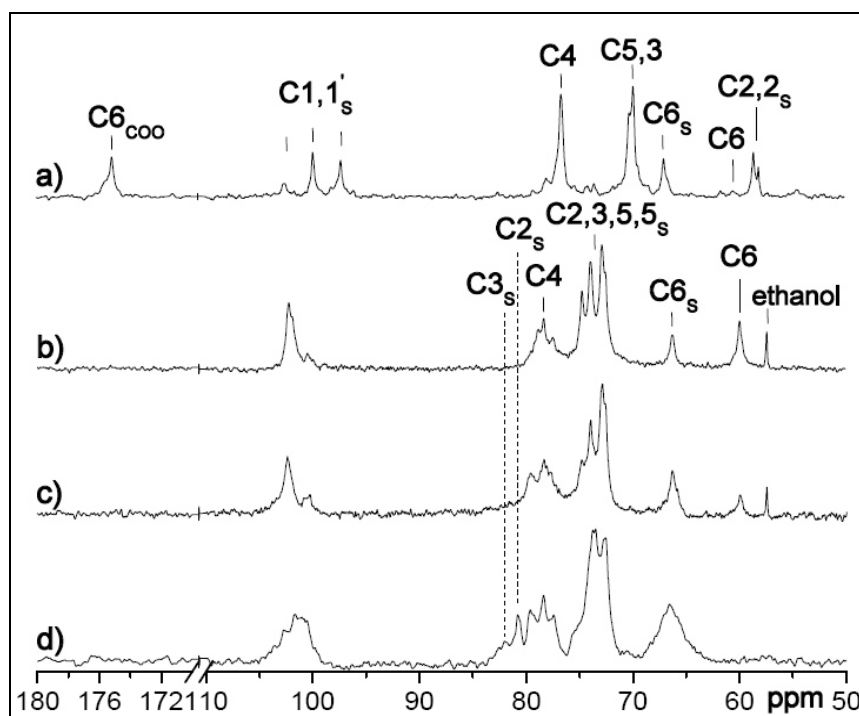


Figure 3.1: ^{13}C NMR spectra (180-50 ppm) of heparin and CS in D_2O at RT: (a) heparin; (b) CS-0.37; (c) CS-0.92 ; and (d) CS-1.80

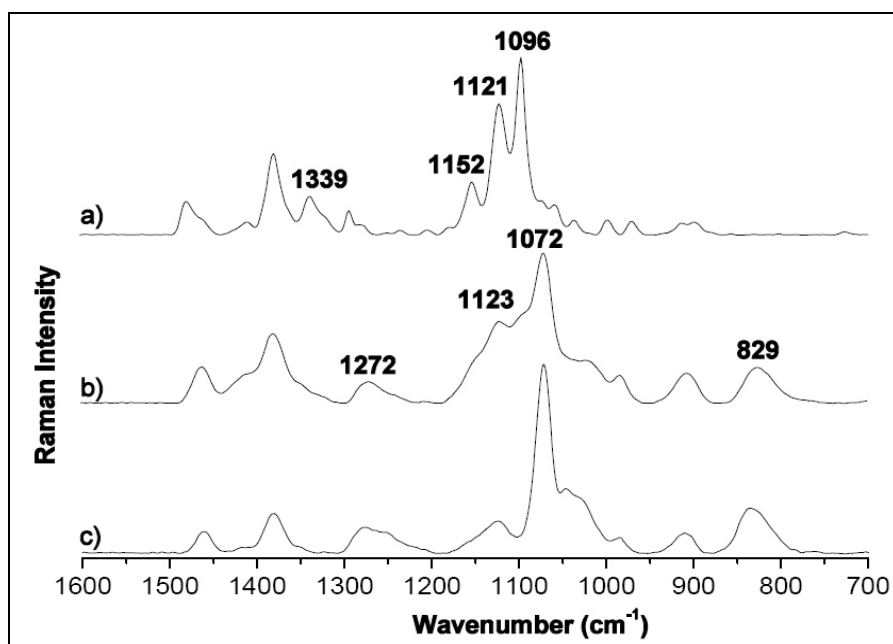


Figure 3.2: Raman spectra ($1600\text{-}700\text{ cm}^{-1}$) of (a) MCC; (b) CS-0.58; and (c) CS-1.69.

In earlier studies, CS were synthesized in a variety of ways mostly by heterogeneous reactions [21-23]. So far, only a few quasi-homogeneous sulfations have been performed, but the distribution of sulfate groups was not analyzed in contrast to the present study [24, 25]. CS with higher DS_S were obtained previously. However, the products with low DS_S were not water soluble as here. According to the data in Table 3.1, the acetosulfation resulted in a primary sulfation of 6-*O*-position. Higher reaction temperatures resulted here in a decrease of DS_S . It can also be seen from Table 3.1 that with an increasing amount of chlorosulfuric acid up to 3 mol mol^{-1} AGU, the DS_{S6} and DS_{S2} rose to 0.77 and 0.15 respectively. In contrast, the use of sulfuric acid as sulfating agent resulted in complete sulfation at 6-*O*-position and much higher DS_{S2} up to 0.69. The highest DS_S were achieved after direct sulfation, where the primary hydroxyl groups were completely sulfated. The hydroxyl groups at 2-*O*-position could be sulfated up to 94% under these conditions. It should also be emphasized that all CS obtained in this study were water soluble. Wang et al. [36] synthesized CS through direct sulfation of cellulose with chlorosulfuric acid. They observed that a concentration of the sulfating agent of 4.5 mol mol^{-1} AGU yielded a DS_S value of only 1.70 under RT [36]. It should be noted that a product with higher DS_S value was obtained here using the same sulfating agent and reaction temperature, presumably due to the different reaction time and starting material. Taken together, by choosing specific reaction parameters, it was possible obtain gradually increasing DS_S values in 2-*O*-position and 6-*O*-position whereas 3-*O*-

position was not modified.

3.4.2. Oxidation of CS

To follow the change in substitution pattern of CS, Figure 3.3 shows a comparison of ^{13}C NMR spectra of CS-0.37 (Figure 3.3a) with that of oxidized CS (CO-0.67, Figure 3.3b). It shows that a new signal emerges at 175.5 ppm representing the shifted signal of C_6 (see Figure 3.3b). However, also the signal of sulfated C_6 at 66.4 ppm was also still visible. These results indicate that cellulose derivatives contained both carboxyl and sulfate groups at 6-*O*-position after oxidation. The quantity of carboxyl groups at the 6-*O*-position was also determined by ^{13}C NMR, and is listed in Table 3.2. It is visible that an increased concentration of oxidation agents raised the DS_{COO} values of derivatives during oxidation of low sulfated cellulose. At the end, a DS_{COO} value as high as 0.67 could be obtained under the application of 0.1 mol TEMPO, 3 mol NaBr and 16 mol NaClO per mol of free primary hydroxyl groups. It is well known that native cellulose is resistant to TEMPO oxidation because of its crystallinity and limited accessibility of the primary hydroxyl groups [40, 41]. Apparently, the good solubility of CS in water and its lack of crystalline regions promoted the successful carboxylation of cellulose here. The results of carboxylation of CO-0.11 and CO-0.31, which used higher (CS-0.97) and lower (CS-0.39) sulfated cellulose also demonstrate a certain dilemma. A larger quantity of the oxidation agent in the case of CO-0.11 did not lead to a higher oxidation yield at the 6-*O*-position (see Table 3.2). This finding can be related to the quantity of non-sulfated 6-*O*-positions, which is lower in the case of CO-0.31 and implies that highly sulfated CS are less useful for carboxylation. Hence, products that are highly sulfated at 2-*O*-position and have a mixed functionalization at 6-*O*-position with carboxyl and sulfate groups are probably difficult to obtain. Table 3.2 also shows the similarities between CO-0.67 and heparin regarding the degree of derivatisation at 6-*O*-position. However, sulfation at 2-*O*-position in CO-0.67 was negligible in comparison with heparin.

3.4.3. Carboxymethylation of CS

To enhance the potential steric accessibility of the carboxyl groups for interaction with FGF2, cellulose derivatives containing carboxymethyl groups with the methyl group as spacer element were synthesized. The obtained products were all water soluble. Figure 3.3c also shows the ^{13}C NMR spectroscopy of one carboxymethylated product, namely CM-1.01. It can be seen in Figure 3.3c that new signals at 178.4, 178.5 and 179.3 ppm emerged in the

spectrum of CM-1.01 compared with CS-0.37 (Figure 3.3a), which represent the carbonyl groups of the carboxymethyl groups at 2-*O*-, 3-*O*- and 6-*O*-position. Moreover, new peaks in the spectrum of CM-1.01 at 71.8, 70.9 and 70.2 ppm were detected, which correspond to methylene groups at 2-*O*-, 3-*O*- and 6-*O*-position; peaks at 82.7 and 69.3 ppm as a result of the presence of carboxymethyl groups were also found. Based on these observations, it was concluded that CS was carboxymethylated at all three positions. The DS_{CM} values were also determined with ¹H NMR (spectra not shown here) according to Refs. [32, 42, 43] and can be found in Table 3.3. According to previous work [32], one-step reactions normally lead to a maximum DS_{CM} value of about 1.3–1.5. From the results presented here, it is apparent that a total DS_{CM} of 1.47 was obtained after a one-step reaction. The 6-*O*- and 2-*O*-positions seemed to be preferred during the substitution reaction in IPA. It can be concluded that the reactivity of all three positions follow the order 6-*O*>2-*O*>>3-*O*.

In the current study, the effects of different solvents such as IPA or in DMSO on carboxymethylation of CS were also studied as shown in Table 3.3. Both solvents led to similar DS_{CM} values. It is noteworthy that the application of larger volume of IPA resulted in higher DS_{CM}, which becomes apparent comparing CM-1.09 and CM-1.47 (see Table 3.3 also). Use of DMSO as solvent did not show any particular advantages over IPA concerning the overall degree of derivatisation. Even with increased concentrations of NaOH and ClCH₂COOH, a DS_{CM} of only 1.25 was obtained. However, it seems that with DMSO as solvent, the carboxymethyl groups are more evenly distributed in CM-1.25 than in other CM samples. These results are consistent with results of other studies showing that the use of IPA as solvent during the mercerisation increased carboxymethylation, particularly at 6-*O*-position [44]. Overall, products with a similar sulfation degree could be obtained, differing in degree of substitution and distribution of carboxymethyl groups in the 2-*O*-, 3-*O*- and 6-*O*-positions.

Table 3.1: Synthesis of CS using chlorosulfuric acid or sulfuric acid as sulfating agent under different conditions

| Samples | starting material | molar ratio ^a | T ^b (°C) | DS _S (¹³ C NMR) ^c | | | |
|---------|-------------------|--------------------------|---------------------|---|------------------|------------------|--------|
| | | | | DS _{S6} | DS _{S2} | DS _{S3} | Total |
| CS-0.31 | C2.5A | 2,35 | RT | 0.24 | 0.07 | 0 ^d | 0.31 |
| CS-0.37 | AC | 0.85 / 8 | 60 | 0.33 | 0.04 | 0 | 0.37 |
| CS-0.39 | IC | 0.85 / 8 | 70 | 0.36 | 0.03 | 0 | 0.39 |
| CS-0.40 | MCC | 0.85 / 8 | 70 | 0.38 | 0.02 | 0 | 0.40 |
| CS-0.43 | MCC | 0.55 / 8 | 50 | 0.38 | 0.05 | 0 | 0.43 |
| CS-0.58 | IC | 0.85 / 8 | 50 | 0.52 | 0.06 | 0 | 0.58 |
| CS-0.66 | AC | 0.85 / 8 | 40 | 0.60 | 0.06 | 0 | 0.66 |
| CS-0.92 | AC | 3 / 8 | 50 | 0.77 | 0.15 | 0 | 0.92 |
| CS-0.97 | MCC | 3 / 8 | 50 | 0.73 | 0.24 | 0 | 0.97 |
| CS-1.57 | MCC | 3 / 8 | 50 | 1 | 0.57 | 0 | 1.57 |
| CS-1.69 | MCC | 3 / 8 | 50 | 1 | 0.69 | 0 | 1.69 |
| CS-1.80 | MCC | 4.5 / 0 | RT | 1 | 0.80 | n. d. | > 1.80 |
| CS-1.94 | MCC | 13 / 0 | RT | 1 | 0.94 | n. d. | > 1.94 |

^a Molar ratio in mol sulfating agent/acetylating agent per mol AGU. Sulfating agent: sulfuric acid for CS-1.57 and CS-1.69 with DMAc and DMF as reaction medium, chlorosulfuric acid for other samples with DMF as reaction medium.

^b T: reaction temperature in °C. The reaction duration was 5 h. For CS-1.57, CS-1.80 and CS-1.94, they were 6, 6 and 3 h respectively.

^c DS_{SX}: DS values of sulfate groups on carbon C₆, C₃ or C₂, determined with ¹³C-NMR.

^d 0: no substitution at 3-*O*-position and DS_{S3} = 0; n. d.: substitution not determined.

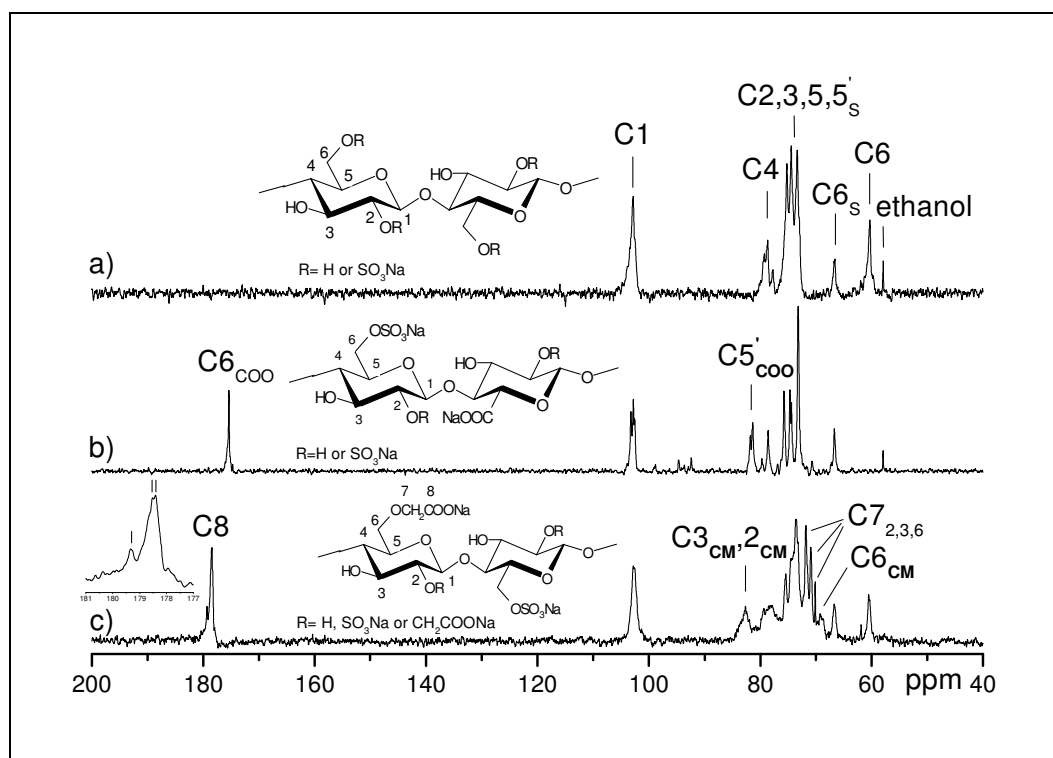


Figure 3.3: ^{13}C NMR spectra (200-40 ppm) of NaCS and NaCS containing carboxyl or carboxymethyl groups in D_2O at RT: (a) CS-0.37; (b) CO-0.67; and (c) CM-1.01.

Table 3.2: Oxidation of CS with TEMPO/NaBr/NaClO at RT and pH 10.5 in water.

| Samples | Starting material | Mol ratio (mol per mol primary OH-groups) | | | Duration of reaction (h) | DS (^{13}C NMR) | | |
|---------|-------------------|---|------|-------|--------------------------|-------------------------------|-------------------------------|--------------------------------|
| | | TEMPO | NaBr | NaClO | | DS _{S6} ^a | DS _{S2} ^a | DS _{COO} ^b |
| ----- | | | | | | | | |
| Heparin | | | | | 0.43 | 0.83 | 0.54 | |
| ----- | | | | | | | | |
| CO-0.11 | CS-0.97 | 0.05 | 1.5 | 8 | 1 | 0.73 | 0.24 | 0.11 |
| CO-0.31 | CS-0.39 | 0.0275 | 0.85 | 4 | 2 | 0.36 | 0.04 | 0.31 |
| CO-0.67 | CS-0.37 | 0.1 | 3 | 16 | 3 | 0.33 | 0.04 | 0.67 |

^a DS values of sulfate groups on carbon C₆ or C₂, determined with ^{13}C -NMR.

^b DS values of carboxyl groups on C₆, determined by ^{13}C -NMR.

Table 3.3: Carboxymethylation of CS with ClCH₂COOH and NaOH at 55°C for 5 h.

| Samples | Starting material | Mol ratio (mol per mol free OH-groups of NaCS) | | | DS _{CM} ^a | | | DS _s ^b |
|----------------------|-------------------|--|------------------------|-------------------|-------------------------------|-------------------|------|------------------------------|
| | | NaOH | ClCH ₂ COOH | DS _{CM2} | DS _{CM3} | DS _{CM6} | | |
| | | | | | | | | |
| CM-1.01 _c | CS-0.40 | 4 | 2 | 0.3 | 0.25 | 0.46 | 0.40 | |
| CM-1.09 _c | CS-0.31 | 4 | 2 | 0.36 | 0.20 | 0.53 | 0.31 | |
| CM-1.25 _c | CS-0.43 | 6 | 3 | 0.41 | 0.37 | 0.47 | 0.43 | |
| CM-1.47 ^c | CS-0.31 | 4 | 2 | 0.54 | 0.26 | 0.67 | 0.31 | |

^a DS values of carboxymethyl groups, determined with ¹H-NMR.

^b Overall DS values of sulfate groups with majority on C₆, determined with ¹³C NMR.

^c Intermediate NaCS for the carboxymethylation dispersed in 75 ml (CM-1.01 and CM-1.09) or 150 ml IPA (CM-1.47) or dissolved in 175 ml DMSO (CM-1.25).

3.4.4. Cytotoxicity measurements

Cytotoxicity measurements were performed with derivatives to be further investigated regarding their mitogenic activity. For comparison with the mitogenic effects (see next paragraph), only the higher sulfated celluloses are shown in Figure 3.4A. By contrast, all the carboxylated derivatives are presented in Fig. 3.4B. Obviously, for most derivatives little but no significant reduced viability was observed at concentrations of 10 µg and 1000 µg ml⁻¹. The carboxymethylated derivative CM-1.47 showed some cytotoxic effect at 1000 µg ml⁻¹, but this effect was not significant (Figure 3.4B). Other sulfated polysaccharides such as dextran sulfate bearing (1→6) glycosidic bonds and (1→6)-α-D-mannopyranan sulfate possess some cytotoxicity for the same cell type only at a high degree of sulfation and molecular weight. The overall sulfation degree of the toxic products was more than 1.56, and the molecular weight higher than 100 kDa [11]. Polysulfonated anions such as polystyrene sulfonate or poly vinyl sulfonate also lead to an impaired viability, even in the presence of FGF2 [10]. Sulfated hyaluronan with a DS_s of 1.0 and a molecular weight 200 kDa significantly decreased the viability of human astrocytes after one week with 100 µg ml⁻¹ [45]. Taken together, the cellulose derivatives synthesized in this study did not show any significant negative impact on the viability of 3T3-L1 fibroblasts after 24 h. Hence, it was concluded that they may be suitable for experiments investigating their mitogenic effect on cells.

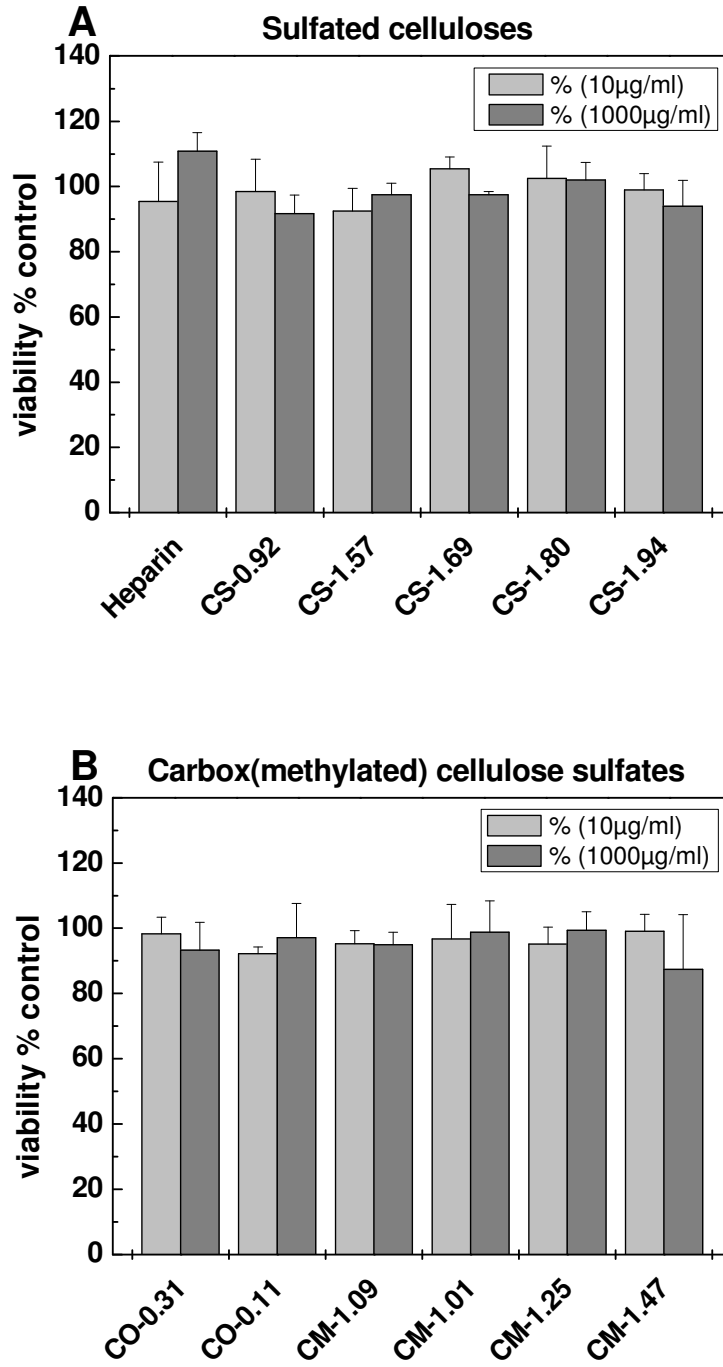


Figure 3.4: Measurement of cytotoxicity of the cellulose derivatives. Viability was measured by QBlue assay with 3T3-L1 fibroblast cells treated with cellulose derivatives or heparin at concentrations of 10 μg and 1000 $\mu\text{g ml}^{-1}$ for 24 h and compared to cells in DMEM only (control): (A) heparin and sulphated celluloses and (B) carboxylated and carboxymethylated CS.

3.4.5. Screening investigation on mitogenic effects of cellulose derivatives in the presence of FGF2

To obtain an overview on the mitogenic activity of the various cellulose derivatives synthesised in this study, their effect on the growth of 3T3 fibroblasts was tested at a concentration of 1 mg ml⁻¹ in combination with 10 ng ml⁻¹ FGF2 after 48 h incubation. To prevent any influence of other growth factors, neither FBS nor ITS (containing insulin) were added to the medium. It was observed that cellulose sulfates with a DS_S below 0.66 did not promote or even slightly inhibited the proliferation of 3T3-L1 fibroblast cells (data not shown here). Only the derivative CS-0.37 as one representative of them is shown in Figure 3.5A. With an increase in 6-*O* sulfation up to 1.0, the proliferation increased up to 120 % of the control (10 ng ml⁻¹ FGF2 only). Although the derivative CS-1.57 has a 2-*O* sulfation of 0.57, the increase in proliferation up to this derivative strongly depended on the degree of 6-*O*-sulfation. With a further increase of sulfation at 2-*O*-position, the proliferation continuously increased up to 160% of the control. Hence, it seems that the degree of sulfation in both positions plays an important role in the enhancement of the mitogenic activity of FGF2.

In contrast to the finding with CS, only some of the carboxylated and carboxymethylated derivatives possessed a small mitogenic activity as shown in Figure 3.5B. Moreover, the mitogenic activity was not related to the degree of carboxylation or carboxymethylation as was observed for the degree of sulfation. The highest mitogenic activity of carboxylated cellulose was found for the derivative CO-0.11(120%), although the difference from CO-0.31 was not significant. It should be noted here that CO-0.11 possessed the highest sulfation degree in the 2-*O*- and 6-*O*-positions, but only a small DS_{COO} of 0.11 at 6-*O*-position (see Table 3.2). Notably, the lowest mitogenic activity was found for CO-0.67 (77 %), which has a similar degree of sulfation to CO-0.31, but the highest DS_{COO} at 6-*O*. The results confirm that a higher degree of sulfation obviously provokes enhanced mitogenic activity. They also indicate that an increase in DS_{COO} leads to impaired proliferation, which was an unexpected finding if one considers that heparin possesses a similar DS_{COO} (see Table 3.2 for comparison) Figure 3.5B also demonstrates that the mitogenic activity correlated with neither the degree of carboxymethylation nor distribution of carboxymethyl groups (compare with Table 3.3). The lowest activity was observed for CM-1.01, which caused a slightly impaired proliferation of 82%. The strongest mitogenic activity was seen for CM-1.09 (110%). The higher carboxymethylated derivatives CM-1.25, CM-1.47 again led to a slight decline in proliferation. Compared with the sulfated derivatives, the maximum mitogenic activity corresponds to the lower sulfated derivative CS-0.66 (108%). This may be considered as a

first indicator that the concept to enhance the biological activity by increasing the accessibility of carboxylic groups by a methyl spacer does not work.

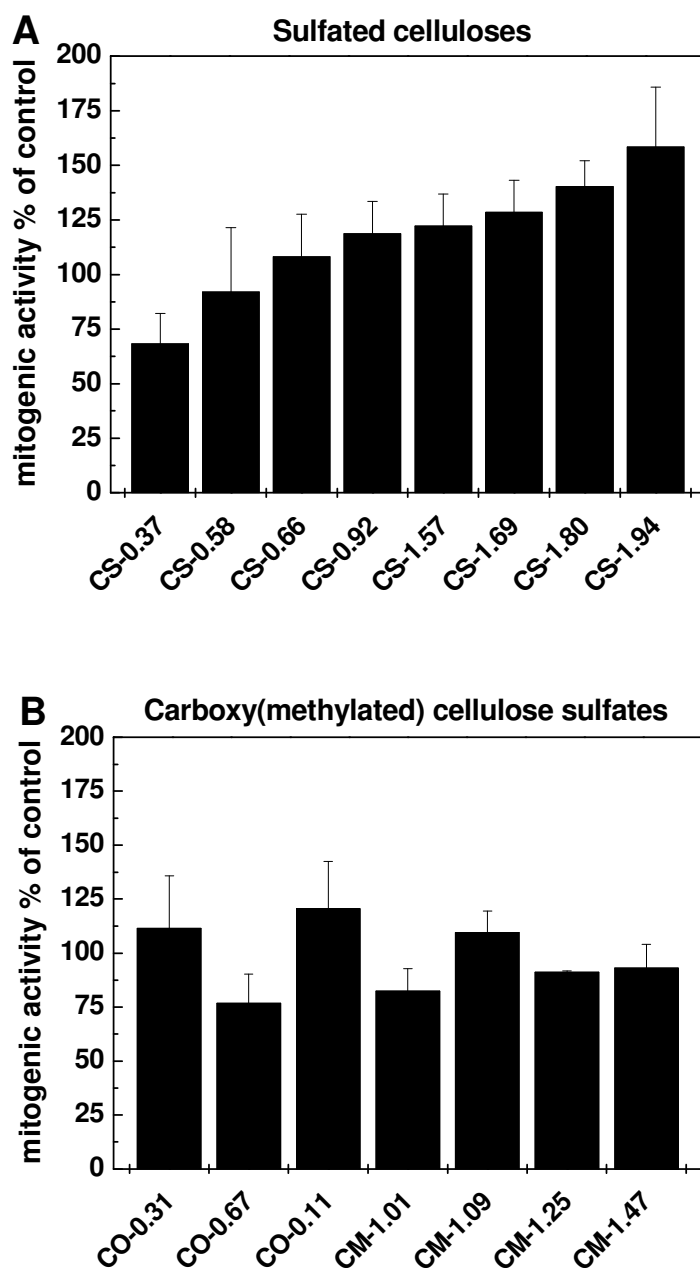


Figure 3.5: Mitogenic activity of 1 mg ml⁻¹ of sulfated celluloses and carboxylated/carboxymethylated CS in the presence of FGF2. Proliferation was measured by incubation of 3T3-L1 fibroblasts with 1 mg ml⁻¹ of cellulose derivatives and 10 ng ml⁻¹ FGF2 for 48 h and related to the control with 10 ng ml⁻¹ FGF2 only: (A) sulfated celluloses and (B) carboxylated and carboxymethylated cellulose sulfates.

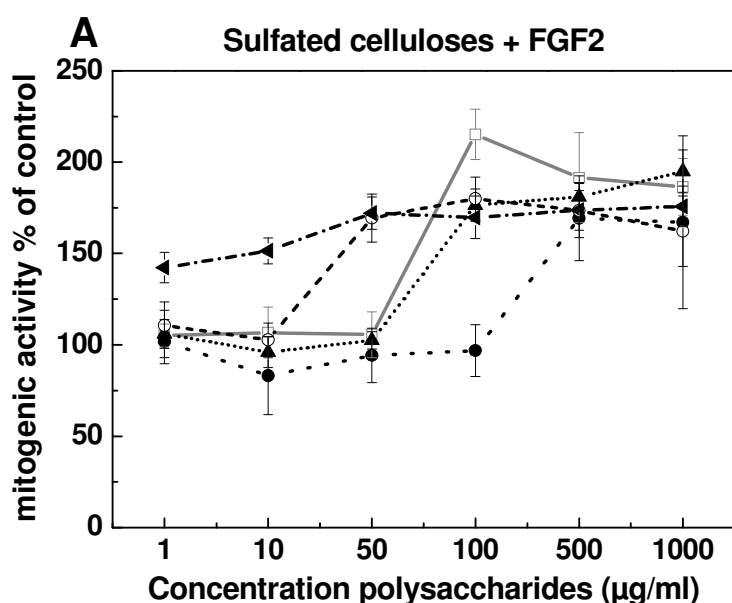
3.4.6. Concentration-dependent effects of cellulose derivatives on 3T3 cell proliferation in the presence of exogenous FGF2

To learn more about the concentration-dependent mitogenic effects of the cellulose derivatives, selected derivatives were investigated in a range from 1 μg to 1 mg in the presence of 10 ng ml^{-1} FGF2. Most of the CS, which have shown an increase in proliferation of >20% compared with the control during the previous experiment, starting from CS-0.92, were included in this study. All CS yielded results compared with heparin at a concentration of 1 mg ml^{-1} (Figure 3.6A) and increased the growth of 3T3 cells up to 195% compared with the control, which was DMEM with 10 ng ml^{-1} FGF2 alone. The cellulose derivative with comparatively low degree of sulfation, CS-0.92, increased the proliferation only at concentrations of 500 $\mu\text{g ml}^{-1}$ and 1 mg ml^{-1} up to 169%; at lower concentrations it led even to a slightly but not significantly impaired proliferation. With increasing DS_s, the concentration of CS necessary to elevate the proliferation became lower, down to 1 $\mu\text{g ml}^{-1}$ for CS-1.94. In general, a stepwise concentration related increase in proliferation from the lower to the higher sulfated derivatives was observed, which is also clearly visible from the effective dose (ED50) values in Table 3.4, which define the 50% value regarding the range of mitogenic activity of curves in Figure 3.6A. The highest mitogenic activity was found for heparin (215% compared with the control), but only at a concentration of 100 $\mu\text{g ml}^{-1}$. It is remarkable that derivative CS-1.94 showed a remarkable mitogenic activity over the whole concentration range, which was higher than that of heparin particularly at lower concentrations. This holds also for the other highly sulfated cellulose sulfate CS-1.80 at concentrations <100 $\mu\text{g ml}^{-1}$.

For the concentration-dependent investigations of the carboxylated and carboxymethylated cellulose derivatives, only those with an increased mitogenic activity in the first assay (1 mg ml^{-1}) were selected, except for the carboxymethylated derivative CM-1.25. Figure 3.6B demonstrates that all of them showed an increased mitogenic activity only at concentrations of 500 $\mu\text{g ml}^{-1}$ and 1 mg ml^{-1} with a maximum of 149% compared to FGF2 control for derivative CO-0.11. This derivative also possessed the highest mitogenic activity among the carboxylated/ carboxymethylated derivatives in the former assay (see Figure 3.4). Compared with the derivative CS-0.92, which possessed a similar degree of sulfation at 2-*O*- and 6-*O*-positions (see Table 3.1), CS-0.11 had a reduced mitogenic activity, especially at 500 $\mu\text{g ml}^{-1}$. The carboxyl groups at this higher degree of sulfation possibly impair the activity of the derivative. The carboxymethylated derivatives also show similar results to the first assay, with

an increase up to 137% at 1 mg ml⁻¹. At concentrations <500 µg ml⁻¹, a slight decrease in proliferation down to 72% compared to the control with FGF2 was evident for all derivatives.

The remarkable mitogenic activity of higher sulfated cellulose derivatives in comparison with heparin is certainly related to the difference in degree of derivatisation and site. Heparin from PIM used in this study possesses a 6-*O*-sulfation of only 0.43 (besides a 6-*O*-carboxylation of 0.54) and a 2-*O*-sulfation of 0.83 in comparison with 1.0 and 0.94 for CS-1.94 respectively (see Table 3.2 for comparison). Obviously, the higher degree of sulfation at these positions is related to the higher mitogenic activity of cellulose derivatives. Nevertheless, although the present investigation does not allow any firm conclusions about the mechanism of mitogenic activity of CS something can be learnt from previous work with other sulfated compounds. Several studies have shown the effects of polysulfated compounds on growth factor-induced cellular behaviour [7,8,10,20]. First, protection against proteolytic degradation of FGF2 prolonging its biological activity was shown not only for heparin, but also a (1→3)-β-galactan sulfate with a high DS_S of 2.0, and several other polysulfated compounds [13,46,8]. Thus a prolonged life time of FGF2 can be expected also in the current study as one reason for the mitogenic activity, particularly of higher sulfated cellulose derivatives. Another possible explanation for the mitogenic activity of CS is the increased binding of FGF2 to its receptor, which was also shown by Pye et al. for heparan sulfate oligosaccharides, where an increased sulfation was linked to elevated cell growth [4].



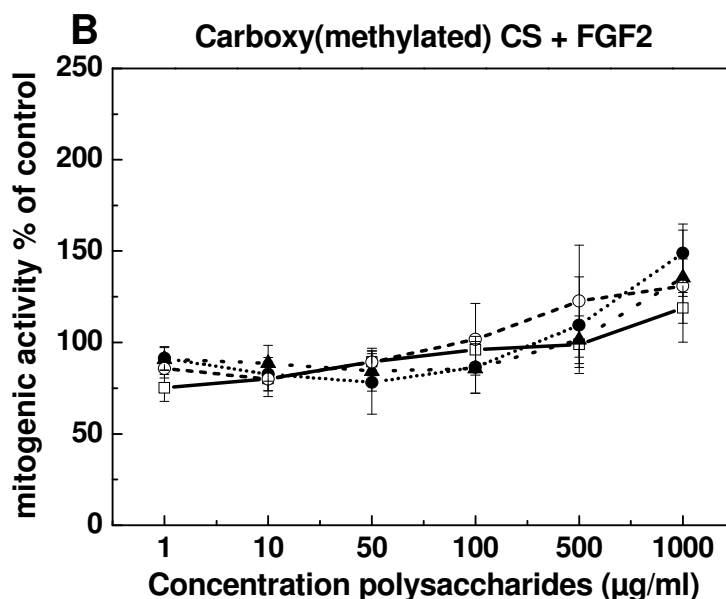


Figure 3.6: Mitogenic activity of the cellulose derivatives in the presence of FGF2. Proliferation was measured by incubation of the 3T3-L1 fibroblast cells with $1 \mu\text{g ml}^{-1}$ up to 1 mg ml^{-1} of selected cellulose derivatives or heparin and 10 ng ml^{-1} FGF2 for 48 h. Data are expressed as percentage of the control with 10 ng ml^{-1} FGF2, only: (A) heparin (\square), sulfated cellulose CS-0.92 (\bullet), CS-1.57 (\blacktriangle), CS-1.80 (\circ), CS-1.94 (\blacktriangleleft) and (B) carboxylated and carboxymethylated CS CO-0.31 (\square), CO-0.11 (\bullet), CM-1.09 (\blacktriangle), CM-1.25 (\circ).

In contrast to CS, only some of the other cellulose derivatives (CO and CM) expressed a low mitogenic activity, which seems to be related rather to the presence of sulfate than of carboxyl and carboxymethyl groups. Other studies have shown no mitogenic activity of carboxymethyl cellulose in the presence of FGF2 with the same cell type [10]. Although in this study the DS_{COO} was 1.5-2.4 per AGU, concentrations up to $60 \mu\text{g ml}^{-1}$ were not enough to induce any mitogenic activity [10]. Since, it is desirable to obtain mitogenic effects already at minimal concentrations, CS seems to have clear advantages over carboxylated and carboxymethylated derivatives.

Table 3.4: ED50 values of the mitogenic activity of sulfated celluloses in the presence of 10 ng ml⁻¹ FGF2

| Samples | ED50 ^a | % mitogenic activity ^b |
|---------|-------------------------|-----------------------------------|
| heparin | 73.73 | 157.59 |
| CS-0.92 | 303.10 | 134.61 |
| CS-1.57 | 80.39 | 147.45 |
| CS-1.80 | 32.40 | 139.99 |
| CS-1.94 | < 1 μg ml ⁻¹ | 137.85 |

^a effective doses for 50% activity in μg ml⁻¹

^b mitogenic activity (compared to the control with 10 ng ml⁻¹ FGF2) at the respective ED50 values

3.4.7. Concentration-dependent effects of cellulose derivatives on 3T3 cell proliferation in the absence of exogenous FGF2

The direct impact of the cellulose derivatives on the proliferation of 3T3-L1 fibroblasts was studied at the same concentrations as in the former experiments but without addition of FGF2. The data were related to 3T3 cells cultured in medium without FGF2, which was considered as control. The results were interesting, and differed strongly from that in the presence of FGF2. Most obviously, almost all CS investigated either decreased or increased the proliferation in a concentration-dependent manner (see Figure 3.7A), because of the diverse effects at different concentrations, ED50 values were not calculated here. The derivative CS-0.92 showed increased proliferation compared with the control only at a concentration of 1 mg ml⁻¹. The highest mitogenic activity at the lower concentration range was observed for the middle sulfated derivative CS-1.57 (222% at 50 μg ml⁻¹). It should be noted that its mitogenic activity at lower concentrations exceeded that of heparin by far. Higher concentrations of CS-1.57 caused only a slight reduction. CS-1.80 caused an increase only at concentrations > 100 μg ml⁻¹ (190% with 100 μg ml⁻¹), but lower concentrations suppressed the proliferation (55% with 50 μg ml⁻¹), these concentration-dependent effects strongly resembled that of heparin, although heparin was less effective at higher concentrations. Interestingly, the overall degree of derivatisation at 2-*O*- and 6-*O*-positions is similar in CS-1.80 and heparin (see Table 3.2 for comparison). Surprisingly, the highest sulfated product, CS-1.94, yielded a slight increase only at 1 mg ml⁻¹ (131% of the FGF2 control), but a suppression of proliferation was not obvious at any concentration. Comparable to the results with the addition of FGF2, CS-1.94 showed almost a constant mitogenic activity over the whole concentration range. But CS with

lower degree of derivatisation, especially at 2-*O*-position lead to higher mitogenic activity without FGF2, even at relatively low concentrations. Hence, it seems that a certain degree of 2-*O*-sulfation can foster the mitogenic activity of the cellulose derivatives. With the exception of CM-1.09, all of the carboxylated and carboxymethylated CS did not show any promoting effect on cell growth. By contrast, a slight decrease in comparison with the control without FGF2 was observed for some of them (see Figure 3.7B). The results above show that the effects of the cellulose derivatives in the absence of exogenous growth factors depend highly on derivatisation, especially the degree of sulfation. Indeed, the findings in this experiment were puzzling, since both promoting and inhibiting effects were observed.

There are a number of explanations for the mitogenic activity of CS in dependence on the DS_S and sulfation site. Other studies have shown a dramatic increase in the production of growth factor FGF2 after addition of heparin to fibroblasts, but accompanied by a reduction in population doubling time [18]. Similar studies with heparin also resulted in reduced cell growth, but increased expression of FGF2, FGF receptor 1 and cell-associated heparan sulfate proteoglycans [47]. These effects could not be elicited by other GAG such as chondroitin sulfate or hyaluronan, which are less or not sulfated [47]. Suppression of cell proliferation in the presence of heparin was found to be related to inhibition of the first cell cycle traverse [48], a blockade of the induction of histone H3 RNA and ATP/ADP carrier protein 2F1 [49]. For heparin, antagonism to the action of inositol 1,4,5-triphosphate-activated Ca²⁺ release [50] and suppression of the induction of c-fos, by inhibiting the activation of the MAPK [51] has been shown. Promoting effects, in contrast, have also been described and were related to protection of growth factors from proteolytic degradation [13,46] and presentation of growth factor to its receptor forming a ternary complex [4,5]. Since all these effects are dependent on degree and site of functionalization/derivatisation, molecular weight and concentration, it is quite difficult to compare effects of previous work with the findings of the current study. Indeed, it was to some extent surprising that none of the carboxylated CS expressed a remarkable mitogenic activity because their structure shows some similarities to heparin. Their DS_S was probably not high enough to become potent mitogenic inducers. In contrast, CS with intermediate and high DS_S possessed a mitogenic activity far exceeding that of heparin, which makes these materials alone, or more specifically, together with FGF2, highly interesting for applications to improve wound healing, smooth muscle growth, vascularization, haematopoiesis or differentiation of nerve cells [52-55]. The substances can be used as part of scaffolds to incorporate and release growth factors with defined kinetics. Further studies will

be devoted to the use of the cellulose derivatives in three-dimensional tissue culture applications.

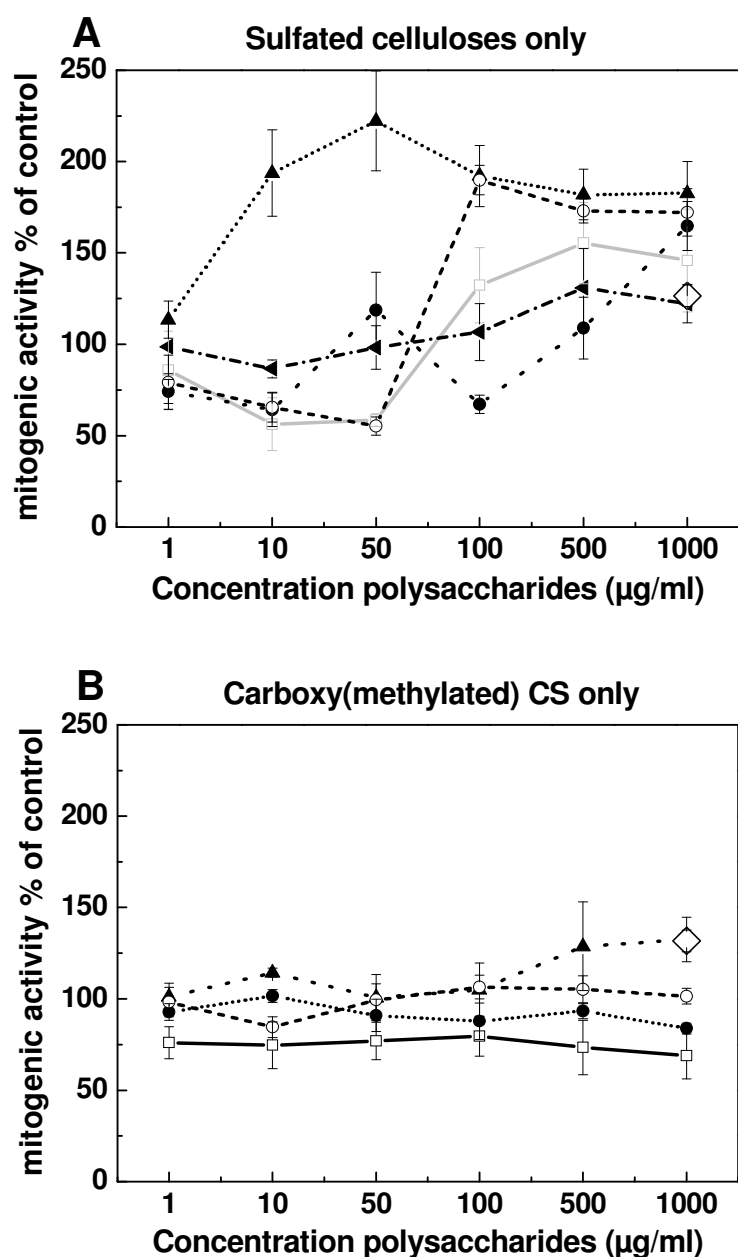


Figure 3.7: Mitogenic activity of cellulose derivatives in the absence of FGF2. Proliferation was measured by incubation of the 3T3-L1 fibroblast cells with $1 \mu\text{g ml}^{-1}$ up to 1mg ml^{-1} of selected cellulose derivatives or heparin without the addition of FGF2 for 48 h. Data are expressed as percentage of the control without FGF2. (A) heparin (□), sulphated cellulose CS-0.92 (●), CS-1.57 (▲), CS-1.80 (○), CS-1.94 (◄), 10 ng ml^{-1} FGF2 only (◇) and (B) carboxylated and carboxymethylated cellulose sulfates CO-0.31 (□), CO-0.11 (●), CM-1.09 (▲), CM-1.25 (○), 10 ng ml^{-1} FGF2 only (◇).

3.5. Summary and Conclusions

This study introduced a number of routes to obtain cellulose derivatives with different degrees and patterns of sulfation and carboxylation/carboxymethylation. It should be noted that, by the selection of starting material, means of derivatization and conditions, a gradual increase in 2-*O*- and 6-*O*-sulfation and differences in carboxylation/carboxymethylation degree and distribution could be obtained. Middle and highly sulfated celluloses far exceeded the mitogenic activity of heparin, notably at lower concentrations. Carboxylated and carboxymethylated CS were less competent to enhance the activity of FGF2, possibly due to a lower degree of sulfation in 2-*O*- and 6-*O*-position. Highly sulfated celluloses enhanced cell growth remarkably also without any additional growth factor at lower concentrations. The results obtained in this study indicate that CS represent a highly effective alternative to heparin in tissue culture applications as supplements to media, but more importantly as component of scaffolds, able to bind, protect and control the release of growth factors. Further studies are needed to understand the underlying mechanism of mitogenic activity of CS stimulating the proliferation of cells.

3.6. Acknowledgment

This work was supported by the Deutsche-Forschungsgemeinschaft (Gr 1290/7-1 & Fi 755 1/2)

3.7. References

- [1] Capill, Linhardt RJ. Heparin-Protein Wechselwirkungen. *Angew Chem* 2002;114:426-50.
- [2] Garcia-Garcia MJ, Anderson KV. Essential role of glycosaminoglycans in Fgf signaling during mouse gastrulation. *Cell* 2003;114:727-37.
- [3] Xingbin A, Do AT, Lozynska O, Gullberg MK, Lindahl U, Emerson Jr CP. QSulf1 remodels the 6-O sulfation of cell surface heparin sulphate proteoglycans to promote Wnt signalling. *J Cell Biol* 2003;162:341- 51.
- [4] Pye D A, Vives RR, Turnbull JE, Callagher JT. Heparan sulfate oligosaccharides require 6-O-sulfation for promotion of basic fibroblast growth factor mitogenic activity. *J Biol Chem* 1998;273:22936- 46.
- [5] Schlessinger J, Plotnikov A, Ibrahimi OA, Eliseenkova AV, Yeh BK, Yayon A, et al. Crystal structure of a ternary FGF-FGFR-heparin complex reveals a dual role for heparin in FGFR binding and dimerization. *Mol Cell* 2000;6:743-50.

- [6] Coltrini D, Rusnati M, Zoppetti G, Oreste P, Grazioli G, Naggi A, et al. Different effects of mucosal, bovine lung and chemically modified heparin on selected biological properties of basic fibroblast growth factor. *Biochem J* 1994;303:583-90.
- [7] Leali D, Belleri M, Urbinati C, Coltrini D, Oreste P, Zoppetti G, et al. Fibroblast growth factor-2 antagonist activity and angiostatic capacity of sulfated *Escherichia coli* K5 polysaccharide derivatives. *J Biol Chem* 2001;276:37900-8.
- [8] Liekens S, Leali D, Neyts J, Esnouf R, Rusnati M, Dell'Era P, et al. Modulation of fibroblast growth Factor-2 Receptor Binding, signaling, and mitogenic activity by heparin-mimicking polysulfonated compounds. *Mol Pharmacol* 1999;56:204-13.
- [9] Parish CR, Freemann CF, Brown KJ, Francis DJ, Cowden WB. Identification of sulfated oligosaccharide-based inhibitors of tumor growth and metastasis using novel in vitro assays for angiogenesis and heparanase activity. *Cancer Res* 1999;59:3433-41.
- [10] Hatanaka K, Ohtsuki T, Kunou M. Effects of synthetic polyanions on 3T3-L1 fibroblast proliferation stimulated by fibroblast growth factors. *Chem Lett* 1994;1407-10.
- [11] Kunou M, Hatanaka K. The effect of growth factors on the cytotoxicity of sulphated polysaccharides. *Carbohydr Polym* 1997;34:335-42.
- [12] Nimni ME. Polypeptide growth factors: targeted delivery systems. *Biomaterials* 1997;18:1201-25.
- [13] Bürgermeister J, Paper DH, Vogl H, Linhardt RJ, Franz G. LaPSvS1, a (1-3)- β -galactan sulfate and its effect on angiogenesis in vivo and in vitro. *Carbohydr Res* 2002;337:1459-65.
- [14] Gospodarovicz D, Cheng J. Heparin protects basic and acidic FGF from inactivation. *J Cell Physiol* 1986;128:475-84.
- [15] Jeon O, Kang SW, Lim HW, Chung JH, Kim BS. Long-term and zero-order release of basic fibroblast growth factor from heparin conjugated poly(L-lactide-co-glycolide) nanospheres and fibrin gels, *Biomaterials* 2006;27:1598-607.
- [16] Chung YI, Tae G, Yuk SH. A facile method to prepare heparin-functionalised nanoparticles for controlled release of growth factors. *Biomaterials* 2006;27:2621-6.
- [17] Jeon O, Song SJ, Kang SW, Putnam AJ, Kim BS. Enhancement of ectopic bone formation by bone morphogenic protein-2 released from heparin conjugated poly(L-lactide-co-glycolide) scaffold. *Biomaterials* 2007;28:2763-71.
- [18] Carroll LA, Koch RJ. Heparin stimulates production of bFGF and TGF-beta 1 by human normal, keloid, and fetal dermal fibroblasts. *Med Sci Monitor* 2003;9:BR97-108.

- [19] Weigert C, Brodbeck K, Häring HÜ, Gambaro G, Schleicher ED. Low-molecular-weight heparin prevents high-glucose and phorbol ester-induced TGF- β 1 gene activation. *Kidney Int* 2001;60:935-43.
- [20] Kunou M, Hatanaka K. Effects of heparin, dextran sulphate, and synthetic (16)- α -D-mannopyranan sulphate and acidic fibroblast growth factor on 3T3-L1 fibroblasts. *Carbohydr Polym* 1995;28:107-12.
- [21] Philipp B, Wagenknecht W. Cellulose sulphate half-ester. Synthesis, structure and properties. *Cell Chem Technol* 1983;17:443-59.
- [22] Hettrich K, Wagenknecht W, Volkert B, Fischer S. New possibilities of the acetosulfation of cellulose. *Macromol Symp* 2008;262:162-9.
- [23] Saake B, Puls J, Wagenknecht W. Endoglucanase fragmentation of cellulose sulfates derived from different synthesis concepts. *Carbohydr Polym* 2002;48:7-14.
- [24] Gericke M, Liebert T, Heinze T. Interaction of ionic liquids with polysaccharides, 8 – Synthesis of cellulose sulfates suitable for polyelectrolyte complex formation. *Macromol Biosci* 2009;9:343-53.
- [25] Wang ZM, Li L, Xiao KJ, Wu JY. Homogeneous sulfation of bagasse cellulose in an ionic liquid and anticoagulation activity. *Bioresour Technol* 2009;100:1687-90.
- [26] Vikartovská A, Bucko M, Mislovicová D, Pätoprsty V, Lacík I, Gemeiner P. Improvement of the stability of glucose oxidase *via* encapsulation in sodium alginate–cellulose sulfate–poly(methylene-*co*-guanidine) capsules. *Enzyme Microb. Technol.* 2007;41:748-55.
- [27] Bucko M, Brygin M. Immobilization of a whole-cell epoxide-hydrolyzing biocatalyst in sodium alginate–cellulose sulfate–poly(methylene-*co*-guanidine) capsules using a controlled encapsulation process. *Enzyme Microb Technol.* 2006;36:118-26.
- [28] Stadlbauer V, Stiegler PB, Schaffellner S, Hauser O, Halwachs G, Iberer F et al. Morphological and functional characterization of a pancreatic b-cell line microencapsulated in sodium cellulose sulfate/poly(diallyldimethylammonium chloride). *Xenotransplantation* 2006;13:337-43.
- [29] Van Damme L, Roshini Govinden MD, Mirembe FM, Taylor D. Lack of effectiveness of cellulose sulphate gel for the prevention of vaginal HIV transmission. *New Engl J Med* 2008;359:463-72.
- [30] Yamamoto I, Takayama K, Matsuzaki K, Hatanaka K, Uryu T, Yamamoto N, et al. Synthesis, structure and antiviral activity of sulfates of cellulose and its branched derivatives. *Carbohydr Polym* 1991;14:53-63.

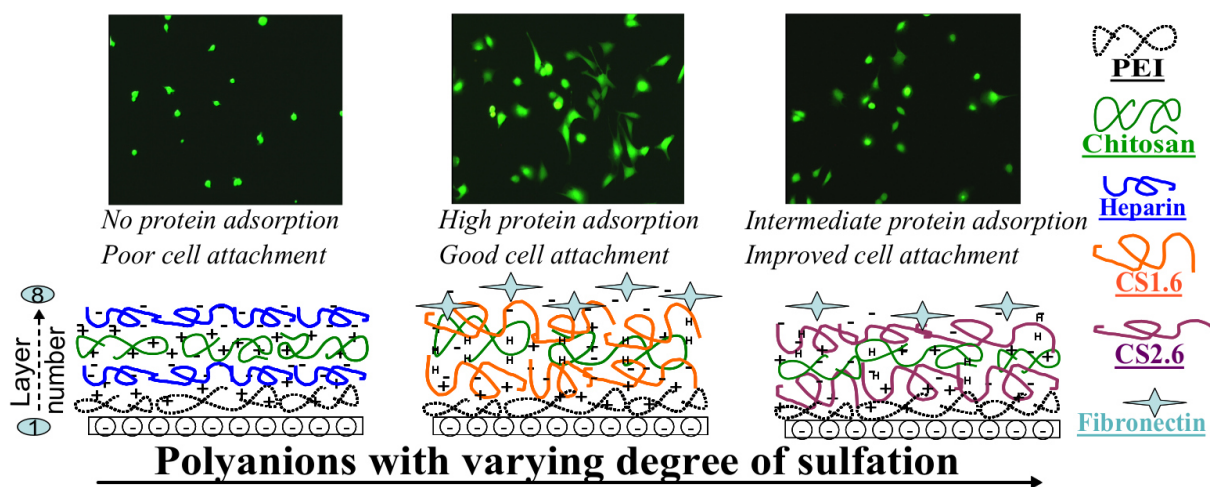
- [31] Groth T, Wagenknecht W. Anticoagulant potential of regioselective derivatized cellulose. *Biomaterials* 2001;22:2719-29.
- [32] Heinze T, Koschella A. Carboxymethyl ethers of cellulose and starch – A review. *Macromol Symp* 2005;223:13-29.
- [33] Schnaubelrauch M, Heinze T, Klemm D, Nehls I, Kötzt J. Investigation on synthesis and characterization of carboxy-groups containing cellulose sulfates. *Polym Bull* 1991;27:147-53.
- [34] Rabenstein DL. Heparin and heparan sulfate: structure and function. *Nat Prod Rep* 2002;19:312–31.
- [35] Nehls I, Wagenknecht W, Philipp B, Stscherbina D. Characterization of cellulose and cellulose derivatives in solution by high resolution ^{13}C -NMR spectroscopy. *Prog. Polym Sci* 1994;19:29-78.
- [36] Wang ZM, Li L, Zheng BS, Normakhamatov N, Guo SY. Preparation and anticoagulation activity of sodium cellulose sulfate. *Int J Biol Macromol* 2007;41:376-82.
- [37] Chaidedgumjorn A, Toyoda H, Woo ER, Lee KB, Kim YS, Toida T, et al. Effect of (1→3)- and (1→4)-linkages of fully sulfated polysaccharides on their anticoagulant activity. *Carbohydr Res* 2002;337:925-33.
- [38] Socrates G. Infrared and Raman characteristic group frequencies. 3rd ed. Chichester: John Wiley; 2001.
- [39] Baumann H, Faust V. Concepts for improved regioselective placement of *O*-sulfo, *N*-sulfo, *N*-acetyl, and *N*-carboxymethyl groups in chitosan derivatives. *Carbohydr Res* 2001;331:43-57.
- [40] Saito T, Isogai A. TEMPO-mediated oxidation of native cellulose. The effect of oxidation conditions on chemical and crystal structures of the water-insoluble fractions. *Biomacromolecules* 2004;5:1983-9.
- [41] Saito T, Isogai A. Ion-exchange behavior of carboxylate groups in fibrous cellulose oxidized by the TEMPO-mediated system. *Carbohydr Polym* 2005;61:183-90.
- [42] Ho FFL, Kloslewicz DW. Proton nuclear magnetic resonance spectrometry for determination of substituents and their distribution in carboxymethylcellulose. *Anal Chem* 1980;52:913-6.
- [43] Baar A, Kulicke WM, Szablikowski K, Kiesewetter R. Nuclear magnetic resonance spectroscopic characterization of carboxymethylcellulose. *Macromol Chem Phys* 1994;195:1483-92.

- [44] Stigsson V, Kloow G, Germgård U. The influence of the solvent system used during manufacturing of CMC. *Cellulose* 2006;13:705-12.
- [45] Yamada T, Sawada R, Tsuchiya T. The effect of sulfated hyaluronan on the morphological transformation and activity of cultured human astrocytes. *Biomaterials* 2008; 29:3503–13.
- [46] Sommer A, Rifkin DB. Interaction of heparin with human basic fibroblast growth factor: protection of the angiogenic protein from proteolytic degradation by a glycosaminoglycan. *J Cell Physiol* 1989; 138:215-20.
- [47] Skaletz-Rorowski A, Schmidt A, Breithardt G, Buddecke E. Heparin-induced overexpression of basic fibroblast growth factor, basic fibroblast growth factor receptor, and cell-associated proteoglycan sulfate in cultured coronary smooth muscle cells. *Arterioscler Throm Vasc* 1996; 16:1063-9.
- [48] Reilly CF, Fritze LMS, Rosenberg RD. Heparin inhibition of smooth muscle cell proliferation: a cellular site of action. *J Cell Physiol* 1986; 129:11-9.
- [49] Reilly CF, Kindyn MS, Brown KE, Rosenberg RD, Sonensheinn GE. Heparin prevents vascular smooth muscle cell progression through the G1 phase of the cell cycle. *J Biol Chem* 1989; 264:6990-5.
- [50] Ghosh TK, Eis PS, Mullaney JM, Ebert CL, Gill DL. Competitive, reversible, and potent antagonism of inositol 1,4,5- trisphosphate-activated calcium release by heparin. *J Biol Chem* 1988; 263:11075-9.
- [51] Miralem T, Wang A, Whiteside CI, Templeton DM. Heparin inhibits mitogen-activated protein kinase-dependent and -independent c-fos induction in mesangial cells. *J Biol Chem* 1996; 271:17100–6.
- [52] Rieck PW, Cholidis S, Hartmann C. Intracellular signaling pathway of FGF-2-modulated corneal endothelial cell migration during wound healing in vitro. *Exp Eye Res* 2001; 73:639-50.
- [53] Schwartz SM, Liaw L. Growth-control and morphogenesis in the development and pathology of arteries. *J Cardiovasc Pharm* 1993; 21:S31-49.
- [54] Bikfalvi A, Han ZC. Angiogenic factors are hematopoietic growth-factors and vice-versa. *Leukemia* 1994; 8:523-9
- [55] Baird A. Fibroblast growth factors: activities and significance of non-neurotrophin neurotrophic growth factors. *Curr Opin Neurobiol* 1994; 4:78-86

Chapter 4

Study on multilayer structures prepared from heparin and semi-synthetic cellulose sulfates as polyanions and their influence on cellular response

Neha Aggarwal, Noomi Altgärde, Sofia Svedhem, Kai Zhang, Steffen Fischer, Thomas Groth



4.1. Abstract

Multilayer coatings of polycationic chitosan paired with polyanionic semi-synthetic cellulose sulfates or heparin were prepared by the layer-by-layer method. Two different cellulose sulfates (CS) with high (CS2.6) and intermediate (CS1.6) sulfation degree were prepared by sulfation of cellulose. Multilayers were fabricated at pH 4 and the resulting films were characterized by several methods. The multilayer ‘optical’ mass, measured by surface plasmon resonance, showed little differences in the total mass adsorbed irrespective of which polyanion was used. In contrast, ‘acoustic’ mass, calculated from quartz crystal micro balance with dissipation monitoring, showed the lowest mass and dissipation values for CS2.6 (highest sulfation degree) multilayers indicating formation of stiffer layers compared to heparin and CS1.6 layers which led to higher mass and dissipation values. Water contact angle and zeta potential measurements indicated formation of more distinct layers with using heparin as polyanion, while use of CS1.6 and CS2.6 resulted into more fuzzy intermingled

multilayers. CS1.6 multilayers significantly supported adhesion and growth of C2C12 cells where as only few cells attached and started to spread initially on CS2.6 layers but favored long term cell growth. Contrastingly cells adhered and grew poorly on to the layers of heparin. This present study shows that cellulose sulfates are attractive candidates for multilayer formation as potential substratum for controlled cell adhesion. Since a peculiar interaction of cellulose sulfates with growth factors was found during previous studies, immobilization of cellulose sulfate in multilayer systems might be of great interest for tissue engineering applications.

4.2 Introduction

In the field of tissue engineering and implantable biomaterials, the appropriate design of biomaterials at micro and nanometer scale to control their bulk and surface properties to direct cell fate is a great challenge. Apart from bulk composition, which controls mechanical and other properties, the biomaterial surface features are of prime importance in dictating the interaction of the material with its environment.[1],[2] Hence, surface modification and functionalization of biomaterials have become very important for biomaterials research and a large number of techniques have been developed for this purpose.[3],[4] A physical surface modification technique called the layer-by-layer (LbL) technique, introduced by Decher and co-workers in 1990s [5], has been adopted for biomaterials surface modification to improve their biocompatibility during the last years.[6] The LbL technique is based on electrostatic attraction and ion-pairing of oppositely charged polyelectrolytes that are alternately adsorbed onto charged substrata.[7] It is important to note that the conditions during complexation of the polyelectrolytes, e.g., temperature, pH and ionic strength, control the multilayer properties, particularly when weak polyelectrolytes are involved.[8] The selection of appropriate polyelectrolytes and complexation conditions allows the design of material coatings with controlled intrinsic (bulk) and extrinsic (surface) properties.[9] While the majority of research with the layer-by-layer method is based on fully synthetic polyelectrolytes, multilayer films consisting of charged polysaccharides have gained an increasing attention during the last years.[10, 11]

Glycosaminoglycans (GAGs), a class of polysaccharides, are an important component of the extracellular matrix (ECM). The GAGs are built from sugar rings, which are linked by glycosidic bonds and possess various charged functional moieties, like amino, sulfate or carboxylic groups. Many GAGs like heparin and chondroitin sulfate are strong polyanions

due to the presence of sulfate groups. In addition, they have a bioactivity that is expressed by specific interactions with proteins and cells. For example, heparin possesses a multitude of binding partners such as adhesive proteins (e.g. fibronectin) and growth factors (e.g. bone morphogenic proteins), which regulate adhesion, movement, growth and differentiation of cells.[12] Therefore heparin has been used as a component of multilayer coatings on biomaterial surfaces.[13],[14] Despite the exceptional multifunctionality of heparin, it is associated with certain drawbacks like the isolation from animal sources, e.g., porcine mucosa or bovine lung, which limits availability in larger quantities and contributes also to chemical heterogeneity and variability of physiological activity.[12, 15]. Therefore a chemical modification of more abundantly occurring polysaccharides like cellulose to achieve heparinoid features has been suggested previously.[16] In this regard, regioselective sulfation of cellulose has been shown particularly effective to achieve a bioactivity comparable to that of heparin with respect to growth factors and cell interactions.[17],[18] Because of the inherent charge density depending on the degree of sulfation, cellulose sulfates are interesting candidates for the LbL technique, and such multilayers were used previously to generate blood compatible surfaces.[19] Also other studies have shown the usage of sulfated polysaccharides including cellulose sulfates in multilayers and investigated the influence of charge density on internal structure of multilayers and their biological interactions.[20, 21] On the other hand, many of the natural polycations are weak polyelectrolytes with amino groups as the charged moieties. Such weak polycations used in the LbL technique are often polypeptides like poly-L-lysine[14] or polysaccharides like chitosan.[22] Chitosan is a copolymer of N-acetylglucosamine and glucosamine linked via 1-4-beta glycosidic bonds produced by deacetylation of chitin, which is also available in huge quantities. However, the degree of deacetylation influences the various properties of chitosan like its solubility, biodegradability [23]. Chitosan possesses remarkable antimicrobial activity and promotes wound healing through a number of mechanisms.[24],[25] Hence, it is not surprising that chitosan has been applied in different studies as polycation during multilayer formation.[13],[22]

Polysaccharide-based multilayer formation has been studied recently showing that the charge of GAGs and the deposition conditions like pH and ionic strength allow to control the multilayer composition and thickness.[26],[27] It was shown that film thickness increases when the pH of the adsorbing polyelectrolyte is close to its pK_a value and the ionic strength increases within a narrow range [27],[28], which affects also the hydration and swelling properties of the films [29]. It is also important to note that during the construction of

multilayer films, the local interactions inside the multilayers are likely to depend on the nature of the polyelectrolytes that forms the outer layer. As shown by Xie et al., the ionization of weak polyelectrolytes inside multilayers, when interacting with strong polyelectrolytes, is dependent on the nature of the outermost layer of the film [30]. That means the ionization of weak polyelectrolytes changes during the subsequent addition of polyelectrolytes leading also to variations in corresponding film properties like thickness, hydration and mechanical properties [10], which in turn leads to differences in protein adsorption, controlled release of bioactive molecules like growth factors and cell responses [31]. Along with the presence of GAGs (e.g. heparin) in the outermost layers, adsorption of adhesive proteins like fibronectin or vitronectin may be affected [32],[33], that is crucial for interactions with cells, which require specific adhesive ligands for communication with integrin cell receptors [34],[35]. Hence, the use of natural or semi-synthetic GAGs bears great advantages for multilayer formation because of the change of multilayer properties due to the different charge density of molecules and dependence of charge and conformation on pH value and ionic strength [14],[10]. In addition, the intrinsic bioactivity and biodegradability of these polyelectrolytes allows for highly biocompatible and bioresponsive surface coatings that are useful for a large variety of biomedical applications like blood compatible surface [36] or new approaches for making scaffolds and systems for different tissue engineering applications [37],[38].

The current study investigates the construction of polyelectrolyte multilayers (PEM) assembled from semi-synthetic cellulose sulfates and heparin as polyanions in a comparative manner. Chitosan was used as polycation to pair with the polyanions. Additionally, poly(ethylene imine) (PEI) was applied to make the first polycation layer as a uniform anchoring layer to provide a better bonding to the underlying model glass or gold surfaces [39]. Two different cellulose sulfates (CS), CS2.6 and CS1.6 (where 2.6 and 1.6 shows the number of sulfate groups per repeating unit) with high and intermediate sulfation degree were used to study the multilayer formation process as well as their biological responses in comparison to heparin, that has only one sulfate group per repeating unit. The results of the study show significant differences in the multilayer properties from cellulose sulfates and heparin in relation to layer mass, amount of coupled water during layer growth, and other surface properties for the different polyanions, which in turn affected the adsorption of fibronectin and adhesion and growth of C2C12 myoblast cells.

4.3. Experimental Section

4.3.1. Materials

Microcrystalline cellulose (MCC) with an average DP of 276 was received from J. Rettenmaier & Söhne GmbH (Germany). Chlorosulfonic acid was purchased from Merck Schuchardt OHG (Germany) and sulfuric acid (98%) from Carl Roth GmbH (Germany). *N,N*-dimethylformamide (DMF) was freshly distilled before synthesis. Deionized water was used in all experiments. Dialysis membrane with a molecular weight cut off of 500 Daltons was obtained from Spectrum Laboratories Inc (Rancho Dominguez, USA). Other chemicals were all of analysis grade and used as received.

Multilayers were fabricated on microscopy glass cover slips (Menzel, Germany). Prior to layer formation cover slips were cleaned for 2 hours with 0.5 M NaOH (Roth, Germany) dissolved in 96% ethanol (Roth, Germany) followed by excessive rinsing with micropure water (10 x 5 min). New gold coated sensors for SPR (IBIS Technologies, Hengelo, The Netherlands) and AT-cut gold-coated quartz crystals for QCM-D (Q-sense, Gothenburg, Sweden) measurements were cleaned with 99.8% ethanol (Merck, Germany) and rinsed thoroughly with micropure water. After rinsing sensors were dried with nitrogen (1 bar) and placed immediately overnight in an ethanol (p.a.) solution of 2 mM mercaptoundecanoic acid (MUDA, 95%, Sigma, Germany) to obtain a negatively charged surface by the formation of a self-assembled monolayer exposing carboxyl groups [40].

For preparing polyelectrolyte solutions, poly (ethylene imine) (PEI) (MW 750,000 g/mol, Sigma, Germany), heparin (min 150 IU/mg, MW 8000-15,000 g/mol, Applichem, Germany), and two different cellulose sulfates synthesized (see below) CS1.6 and CS2.6 were dissolved under stirring at a concentration of 2 mg/ml in water containing 0.14 M NaCl. Chitosan solution was prepared from medical grade chitosan with a deacetylation degree of 85 % (MW 500,000 g/ mol, 85/ 500/ A1, Heppe, Germany) in 0.14 M NaCl and 0.05 M acetic acid at 50°C for 3 h.

4.3.2 Synthesis of cellulose sulfates (CS)

Cellulose sulfates (CS) were prepared via direct sulfation or acetosulfation of cellulose as described before [41]. Briefly, 0.5 g MCC was suspended in 25 ml DMF for overnight. The sulfating reagent, chlorosulfonic acid in DMF or the mixture of sulfuric acid and acetic anhydride in DMF was added slowly to the cellulose suspension. After the incubation at room

temperature (RT) or 50°C for the desired time, the solution was cooled down to RT and poured into a saturated ethanolic solution of anhydrous sodium acetate. The precipitate was collected for further treatment. During the acetosulfation of cellulose, a deacetylation of the product using 1 M ethanolic solution of sodium hydroxide was carried out at RT for 15 h and the deacetylated product was collected via centrifugation. After washing with 4% sodium acetate solution in ethanol, final products were dissolved in water. The pH value of the solution was adjusted to 8.0 with acetic acid/ethanol (50/50, w/w) and the solution was filtered, dialyzed against deionized water and lyophilized.

4.3.3. Characterization of cellulose sulfate (CS) and heparin

The contents of carbon, hydrogen and nitrogen were determined with Elemental Analyser vario EL from Elementar (Hanau, Germany). The content of sulfur was measured with Elemental Analyser Eltra CS 500 (Neuss, Germany). Total degree of sulfation DS_S was calculated according to the equation: $total\ DS_S = (S\%/32)/(C\%/12)$. Molecular weights of CS are measured using size exclusion chromatography (SEC) with PSS Suprema 3000 and 100 Å columns (Polymer Standards Service GmbH, Mainz, Germany). The detection was carried out with a Waters 410 reflective index (RI) detector (Waters Corporation, Milford, MA, USA) and 0.1 mol/l NaCl aqueous buffer was used as mobile phase. The columns were calibrated with pullulan standards (Sigma-Aldrich, Switzerland). Empower Pro software (Waters Corporation) was used for the analysis. The ^{13}C NMR spectra were recorded at RT on Bruker DFX 400 spectrometer (Bruker) with a frequency of 100.13 MHz, 30° pulse length, 0.35 acq. time and a relaxation delay of 3 s. The scans of 20000 were accumulated and D_2O was used. FT Raman spectra were recorded on a Bruker MultiRam spectrometer (Bruker, Ettlingen, Germany) Ge diode as detector that is cooled with liquid-nitrogen. A cw-Nd:YAG-laser with an exciting line of 1064 nm was applied as light source for the excitation of Raman scattering. The spectra were recorded over a range of 3500-150 cm^{-1} using an operating spectral resolution of 3 cm^{-1} and a laser power output of 100 mW.

4.3.4. Polyelectrolyte Multilayer Formation

Polyelectrolyte multilayers were assembled on cleaned glass cover slips or on gold coated sensor substrates (see above) using the following steps (the protocol was adapted for SPR and QCM-D measurements as described below). The gold sensors were functionalized by mercaptoundecanoic acid (MUDA) to achieve the negative charge on the sensor surfaces

comparable to glass which was used as a substrate to make multilayers. A first anchoring layer of PEI was formed on the glass to obtain a surface with a positive charge. This was followed by adsorption of polyanion layers of heparin (HEP) or CS1.6 or CS2.6 and then polycation layer of chitosan (CHI). Each of the layers was prepared by incubation of glass surfaces in polyelectrolyte solutions for 7 min followed by rinsing with an aqueous solution containing 0.14 M NaCl (3 x 4 min). Multilayers were built up to the 7th and 8th layer by alternating deposition of polyanion and polycation. The pH value of each polyelectrolyte solution and rinsing solution was adjusted to pH 4 by using either HCl or NaOH.

4.3.5. Characterization of Multilayer

4.3.5.1. *Measurement of mass adsorption and multilayer growth:*

The multilayer build-up and measurement of adsorbed mass was studied by surface plasmon resonance (SPR) (IBIS-iSPR equipment IBIS Technologies B.V., Hengelo, Netherlands) and quartz crystal microbalance with dissipation monitoring (QCM-D) (E4 instrument Q-Sense, Gothenburg, Sweden) techniques. The ‘optical’ mass of the adsorbed molecules during the formation of each layer was calculated by Eq. (1) as the change in SPR angle shift (m°) is proportional to the mass (Γ_{SPR}) of adsorbed molecules on the surface [42].

$$122 \text{ m}^\circ \approx 1 \text{ ng/mm}^2 \quad (1)$$

QCM-D measurements were performed to quantify adsorbed ‘acoustic’ mass on the sensor. For rigid and evenly distributed films, the resonance frequency shifts (Δf) can be related to changes in mass that is acoustically coupled to the sensor surface (Δm_{QCM-D}) by using the Sauerbrey equation Eq. (2) [43].

$$\Delta m = - C \Delta f / n \quad (2)$$

where n ($n = 1, 3, 5, \dots, 13$) is the overtone number and C is the mass sensitivity constant specific for the quartz crystal, here $C = 0.177 \text{ mg/m}^2\text{Hz}$ for ($f_0 = 5 \text{ MHz}$). The dissipation factor (D) is a measure of the dampening of the oscillatory motion when the driving voltage of the quartz crystal is shut off. It can be related to structural properties of the added layer on the sensor surface.

The calculations for the measurements of coupled/trapped water in the multilayer systems were determined by comparing the masses obtained by QCM-D and SPR, under the assumption that the two masses were obtained for equivalent multilayer structures.

The SPR and the QCM-D measurements were made in the flow cell of each of the device using cleaned gold sensors previously treated with MUDA (see above). The treatment with MUDA was done to acquire a negative charge on sensor surfaces that provides similar conditions like a negatively charged glass substrate used for the WCA, zeta potential and biological studies. After fixation of sensors in the flow chamber, firstly, the polycation PEI solution was introduced to the chamber exposing the sensor surface for 7 min, followed by rinsing of 12 min with water containing 0.14 M NaCl. Formation of the primary PEI layer was followed by alternate introduction of the polyanion HEP/CS1.6/CS2.6 and the polycation CHI to form the subsequent layers of CHI-HEP and CHI-CS systems. The layers were adsorbed up to 8 layers and all the polyelectrolyte and rinsing solutions were applied at pH 4. The rinsing steps were done after each layer deposition to remove unbound polyelectrolyte.

The protein binding ability of these different multilayer surfaces were studied by QCM-D. Plasma fibronectin (pFN, Roche, Germany) was used as the model protein. 20 $\mu\text{g/ml}$ fibronectin was reconstituted in phosphate buffered saline (PBS, 150 mM NaCl, pH 7.4) and introduced into the QCM-D flow cell after the formation of final (polyanion) layer. The adsorption process was performed for 1 hour. All the measurements were done in duplicates and represented as average.

4.3.5.2. *Water contact angle and zeta potential measurements*

The surface wettability of the multilayers was determined by water contact angle (WCA) measurements using an OCA15+ device from Dataphysics (Filderstadt, Germany). By applying the sessile drop method, 3-4 cover slips from each type of multilayer system and terminal layer surface were studied by dispensing 3-4 drops of 3 μl of water at a flow rate of 0.5 $\mu\text{l/s}$. At least 10 independent measurements were recorded for each droplet by the built-in software and the contact angle values presented here are the means of two independent measurements.

Zeta (ζ) potentials of the multilayer surfaces were measured by SurPASS device (Anton Paar, Graz, Austria). Specially designed glass cover slips for the measuring chamber were used for multilayer deposition followed by streaming potential measurements. Two cover slips, modified identically with multilayer fabrication procedure were fixed on the stamps and placed oppositely in the flow chamber. A flow rate of 100-150 ml/min was achieved at a maximum pressure of 300 mbar by adjusting the width of the flow chamber. 1 mM potassium

chloride was used as electrolyte and 0.1 N HCl for pH titration. The measurements from pH 10.5 to 2.25 were performed by an automated titration program.

4.3.6. Biological Investigations

4.3.6.1. Cell culture

In all of the cell studies, the skeletal muscle cell line C2C12 (DSMZ, Germany, Product Nr.: ACC 565) was used. Cryo conserved C2C12 cells were thawed and cultured in Dulbecco's modified Eagle medium (DMEM, Biochrom AG, Germany) supplemented with 10% fetal bovine serum (FBS, Biochrom AG), 2 mM L-Glutamine, 100 U/ml Penicillin and 100 µg/ml Streptomycin (Biochrom AG) at 37°C in humidified 5% CO₂/95% air atmosphere using a NUAIRE® DH Autoflow incubator (NuAire corp., Plymouth, Minnesota, USA). Cells were harvested from pre-confluent cultures by trypsinization using 0.25% Trypsin, 0.02% EDTA followed by subsequent washing with DMEM and resuspended in DMEM with 10% FBS at a concentration of 25,000 cells/ml.

4.3.6.2. Cell adhesion and spreading

Short-term cell adhesion studies were conducted on different multilayer coatings of CHI and polyanion (HEP or both CS) terminated on glass slides. These multilayer coated glass substrates were placed in 12-well tissue culture plates followed by sterilization with 70% ethanol for 10 min and excessive washing with sterile PBS. C2C12 cells in DMEM with a concentration of 25,000 cells/ml were seeded on the sterilized multilayer surfaces and incubated for 4 h at 37°C in a humidified 5% CO₂/95% air atmosphere. After 4 h, culture medium was aspirated and exchanged with fresh medium twice so that non-adherent cells could be removed. The attached cells were stained by adding 5 µl FDA (fluorescein diacetate) solution (0.01% vol/vol) to each well containing 1 ml of cell culture medium (over the multilayer samples) and incubated for 3-5 min. Images were made after the staining with a fluorescence microscope Axiovert 100 (Carl Zeiss Microimaging, Jena, Germany) fitted with a CCD camera for analyzing the cell morphology and quantification of cell attachment and spreading. Image processing software "ImageJ, NIH" was used for analyzing all the required parameters.

4.3.6.3. *Cell morphology*

Immunofluorescence staining was performed on the polyanion terminal layers (HEP or both CS) after 4 h of cell culture at 37°C in DMEM supplemented with 10% FBS (Biochrom AG) by immunofluorescence microscopy. Adherent cells were fixed with Roti[®] – Histofix (Roth, Karlsruhe, Germany) for 15 min and rinsed with PBS. After fixing, permeabilization of cells was done by 0.1% (v/v) Triton X-100 in PBS for 10 min followed by three times rinsing with PBS. Non-specific binding sites were blocked by incubation with 1% bovine serum albumin (BSA, Sigma, Germany) in PBS at RT for 30 min. Adherent cells were triple stained by subsequent staining of focal adhesion complexes with mouse monoclonal antibody against vinculin (Sigma, Germany) and Cy2[®]conjugated AffiniPure Goat Anti-Mouse IgG-conjugated anti-mouse immunoglobulin (Dianova, Germany). Actin filaments and nuclei were stained with BODIPY[®] phalloidin (5 μ M, Molecular Probes, Germany) and TO-PRO3 (1 μ M, Molecular Probes, Germany), respectively. Each incubation step was performed for 30 min followed by extensive washing with PBS. Finally all samples were mounted on objective slides with Mowiol[®] 4-88 (Merck, Germany) and investigated with a confocal laser scanning microscope (LSM 710, Carl Zeiss MicroImaging GmbH, Jena, Germany) using a 63x immersion oil objective. The acquired images were processed with ZEN software.

4.3.6.4. *Cell growth measurements*

Cell proliferation measurements were conducted on multilayers terminated by the polyanions (HEP or both CS) on coated glass slides placed in 12-well plates. Similar to cell adhesion studies, the samples were sterilized and seeded with the cell density of 25,000 cells/ml in DMEM with 10% FBS. Cells were seeded on the polyanion (HEP or both CS) terminal layers and cultured for 1 and 3 days. Phase contrast images were taken with Axiovert 100 microscope equipped with a CCD camera at the different days of culture followed by quantification of viable cells. QBlue fluorescence assay (BioChain, USA), which quantifies the metabolic activity of cells was employed here to measure the quantity of viable cells at the end of culture period. The slides with cells were transferred to the new 12-well plates (to avoid the inclusion of cells grown on well plate surface) and were washed with DMEM. This was followed by addition of 500 μ l fresh DMEM and 50 μ l of Qblue assay reagent. After 3 h of incubation at 37°C, 100 μ l of the supernatant was transferred from each well to a 96-well black plate and fluorescence intensity (excitation wavelength 544 nm,

emission wavelength 590 nm) was measured with a fluorescence plate reader (BMG LABTECH, Fluostar OPTIMA, Offenburg, Germany). All biological data were statistically analyzed by one-way ANOVA (analysis of variance) and the means were compared by Tukey test at a significance level of 0.05.

4.4. Results and Discussion

4.4.1. Cellulose sulfates and heparin

Two different CS variants with intermediate and high degree of sulfation (DS_S) were synthesized. CS1.6 with a DS_S of 1.57 was prepared via acetosulfation using sulfuric acid as sulfating agent, while CS2.6 with a DS_S of 2.59 was obtained after direct sulfation using chlorosulfonic acid as sulfating agent. FT Raman spectroscopic analysis of these CS variants (Figure 4.1A) showed characteristic bands at 1075, 847 and 589 cm^{-1} ascribed to the following vibrational modes of the sulfate groups $\nu_s(O=S=O)$, $\nu(C-O-S)$ and $\delta(O=S=O)$, respectively [44]. After the normalization of the spectra with respect to the band at 1380 cm^{-1} , attributed to vibrations of cellulose backbone [41], it is visible that the intensities of the three bands ascribed to vibrations of sulfate groups increase with higher total DS_S of CS. In addition, it is visible that the intensities of the bands at 2896 and 2966 cm^{-1} representing the stretching vibrations of CH and CH_2 change their relationship after the sulfation.

In addition to FT Raman spectroscopy, ^{13}C NMR spectra of CS and HEP showed the typical chemical shifts of carbons due to the sulfation of hydroxyl groups of their repeating units (Figure 4.1B). With the sulfation at C6 position in anhydroglucose unit (AGU) of cellulose, the signal of C6 shifted from 60 ppm to 66.5 ppm, while new signals were detectable between 80 and 85 ppm due to the sulfation at C2 and C3 positions. Moreover, the signal of C1 shifted from 102 ppm to 100 ppm when the C2 position is sulfated. Based on the integrals of the signals attributed to original as well as substituted C6 and C1 of AGU, the ratio of sulfated C6 and C2 positions can be calculated, which are corresponding to the partial DS_S at these positions [41]. Accordingly, CS2.6 has a complete sulfation of hydroxyl groups at C6 and C2 position due to the complete shift of the signals derived from C6 and C1. CS1.6 has a complete sulfation of primary hydroxyl groups (C6) and partial sulfation of hydroxyl groups at C2 position. In comparison, HEP has an intermediate to high degree of sulfation depending on the source, but it contains also carboxyl groups at C6 position of the uronic acid monomer, which is visible by the large peak around 175 ppm in Figure 4.1B-iii [45]. Moreover, it is also notable that HEP has a higher DS at C2 position compared to C6 position.

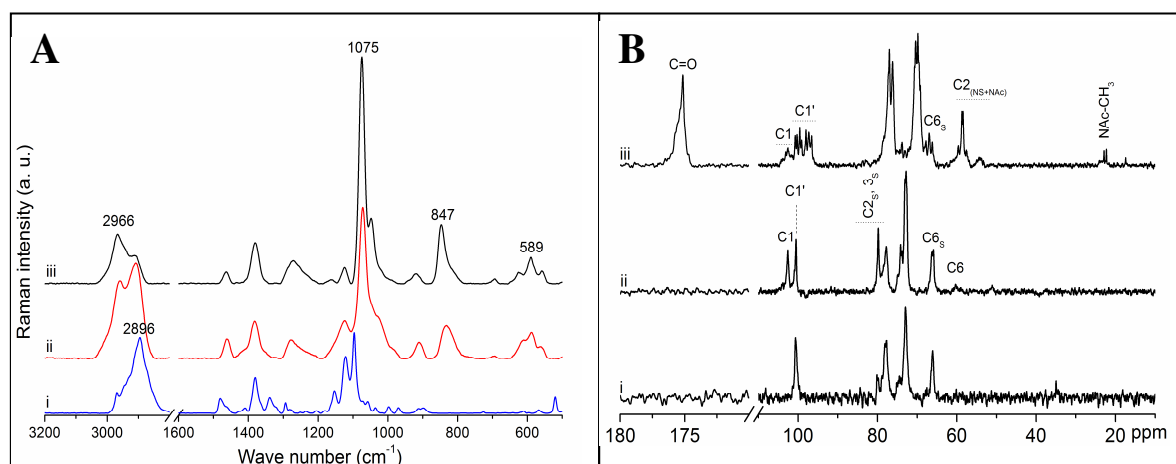


Figure 4.1: (A) FT Raman spectra ($3100\text{-}500\text{ cm}^{-1}$) of (i) microcrystalline cellulose, (ii) CS1.6 and (iii) CS2.6. and (B) ^{13}C NMR spectra ($180\text{-}10\text{ ppm}$) of (i) CS2.6, (ii) CS1.6 and (iii) heparin in D_2O .

The total DS_s of CS and HEP was assessed by elemental analysis. The total DS_s of 2.6 for CS2.6 is much higher than the sum of partial DS_{S2} and DS_{S6} , which were estimated using ^{13}C NMR spectroscopy. This fact indicates a substantial sulfation at C3 position for CS2.6. This discrepancy is due to the fact that the partial DS_{S3} cannot be exactly calculated using ^{13}C NMR spectroscopy due to the broad signals of $\text{C}2_s/\text{C}3_s$, which are also partly overlapped by C4-signal. It is also interesting to note that the DS_s of HEP is lower than that of both CS. Molecular weights of cellulose sulfates (M_n and M_w) were assessed by gel permeation chromatography (Table 4.1). Due to the high amount of chlorosulfonic acid (13 mol/mol AGU) used for the direct sulfation, the resulting total DS_s of CS2.6 is much higher than of CS1.6. However, the average molecular weight of CS2.6 is smaller than of CS1.6 (Table 4.1), although the sulfation temperature for CS2.6 (RT) was lower than that for CS1.6 (50°C). Thus, a higher total DS_s of CS may often be accompanied by a lower molecular weight [46]. Possibly, there is a balance between the acidic hydrolysis of cellulose during the sulfation and the DS of the final products.

Table 4.1: Synthesis and characterization of CS and heparin

| Samples | Molar ratio ^a | Reaction temperature (°C) /duration (h) | DS _S ^b | | | DO ^b | MW _w | MW _n | MW _w /MW _n |
|---------------|--------------------------|---|------------------------------|------------------|-------|-----------------|-----------------|-----------------|----------------------------------|
| | | | DS _{S6} | DS _{S2} | total | | | | |
| | | | DS _S | | | | | | |
| CS1.6 | 3/8 | 50 / 6 | 0.91 | 0.55 | 1.57 | 0 | 77748 | 37549 | 2.07 |
| CS2.6 | 13 | RT / 2.5 | 1 | 1 | 2.59 | 0 | 64961 | 36197 | 1.79 |
| Heparin (HEP) | n.a. | n.a. | 0.27 | 0.8 | 1.01 | 0.26 | *8000-25000 | | |

^a molar ratios in mol sulfuric acid and mol acetic anhydride per mol AGU for CS1.6 and mol chlorosulfonic acid per mol AGU for CS2.6, respectively. ^b DS_{S6}, DS_{S2} and DO (degree of oxidation) were analysed with ¹³C NMR spectroscopy. The total DS_S was determined by elemental analysis. *MW_w of heparin: provided by the data sheet from the supplier.

In summary, the degree of sulfation of the polyanions rises from HEP to CS1.6 and CS2.6. Additionally, HEP possesses also carboxyl groups at C6 position not present in CS. Because of the varying degree of derivatisation, different effects of polyanions on multilayer properties were expected.

4.4.2. Characterization of multilayer formation

Studies on the multilayer formation were performed by the surface sensitive analytical techniques SPR and QCM-D. SPR is an optical technique that allows for the determination of adsorbed mass of macromolecules ('optical' mass), while QCM-D is an acoustic technique and provides complementary information about adsorbed mass of macromolecules including their hydration state as total absorbed mass ('acoustic' mass). In addition, the dissipation measurements by QCM-D provide information about the viscoelastic properties of the adsorbed layers.

Figures 4.2 and 4.3 shows the SPR and the QCM-D results, respectively, obtained during adsorption of CHI-HEP, CHI-CS1.6 and CHI-CS2.6 using similar experimental conditions. The layer masses calculated from SPR data (angle shifts) by using Eq. (1) are displayed in Figure 4.2. The results obtained show clear differences in the mass adsorption pattern caused by the use of different polyanions (HEP/CS1.6/CS2.6) paired with CHI. In the case of the CHI-HEP multilayer system, the layer growth was exponential, which was also shown previously for other polysaccharide-based multilayers systems [14]. Besides the growth behaviour, the multilayer mass was also in accordance with previous studies obtained under comparable conditions for CHI-HEP multilayers [22]. Multilayer mass of systems with CS (CHI-CS1.6 & CHI-CS2.6) was slightly larger, but showed also a different increment behavior compared to the CHI-HEP system. For both CHI-CS systems, the mass evolution by SPR for each layer appeared staircase-like indicating more mass adsorption during the CS1.6 and CS2.6 deposition of the polyanion (even layer numbers) as compared to the CHI deposition steps (odd layer number except the first).

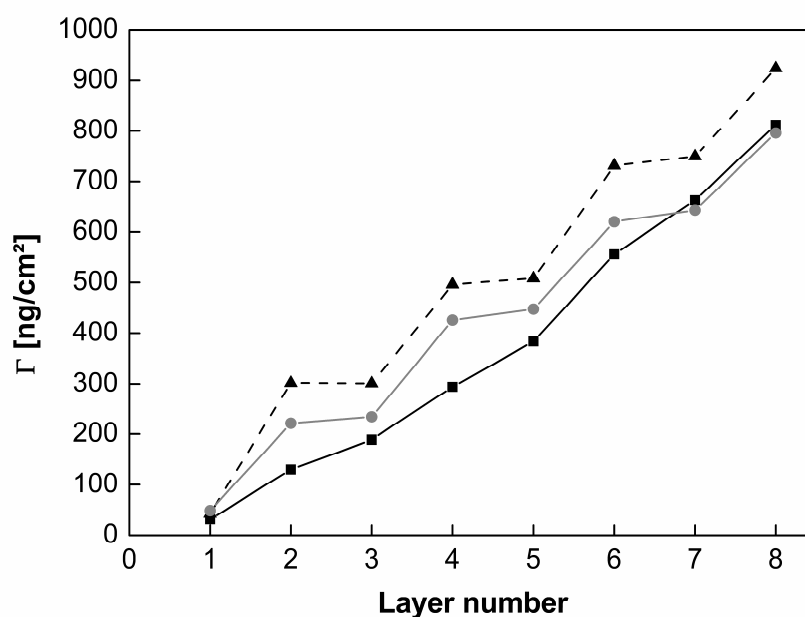


Figure 4.2: Multilayer mass Γ_{SPR} calculated from SPR angle shifts. Layer 1 is always PEI. Even layers: polyanions, odd layers: polycation CHI Solid lines (■): CHI-HEP system, dashed lines (▲): CHI-CS1.6 system and grey solid lines (●): CHI-CS2.6 system

Figure 4.3A shows result of QCM-D measurements where the change in adsorbed mass calculated by the Sauerbrey equation (2) is plotted against the layer number. The Sauerbrey equation is only valid for rigid films and here it holds as a good approximation since the

dissipation response shown in Figure 4.3B are relatively small compared to the frequency response. QCM-D measurements showed in Figure 4.3A also depicted exponential multilayer growth for the CHI-HEP system. The layer masses obtained from the QCM-D data were much larger than the corresponding masses measured by SPR, which points to a substantial amount of water entrapped in the CHI-HEP multilayers. Similar to the SPR results during CHI-CS1.6 multilayer formation, although less striking, the adsorbed mass increase measured by QCM-D also showed a staircase shaped curve. A similar trend was reported in a previous study during multilayer formation from poly-L-lysine and hyaluronan [14]. In contrast, a very low mass increase was measured by QCM-D during CHI-CS2.6 multilayer formation. The dissipation values for the CHI-HEP system showed alternately increased values upon addition of CHI followed by strongly decreased values upon addition of HEP. The decrease of dissipation values after addition of HEP indicates a stiffening of the multilayer system. Such alternating changes were absent in the dissipation values measured for the CHI-CS1.6 and CHI-CS2.6 systems. For the CHI-CS1.6 system, an almost linear increase was observed with addition of either CHI or CS1.6. The monotonic increase in the dissipation values for the CHI-CS1.6 system suggests that the nature of the film is more homogeneous[22]. On contrary the CHI-CS2.6 layer system seemed to be very condensed as the dissipation values remained almost constant by the addition of either polyelectrolytes.

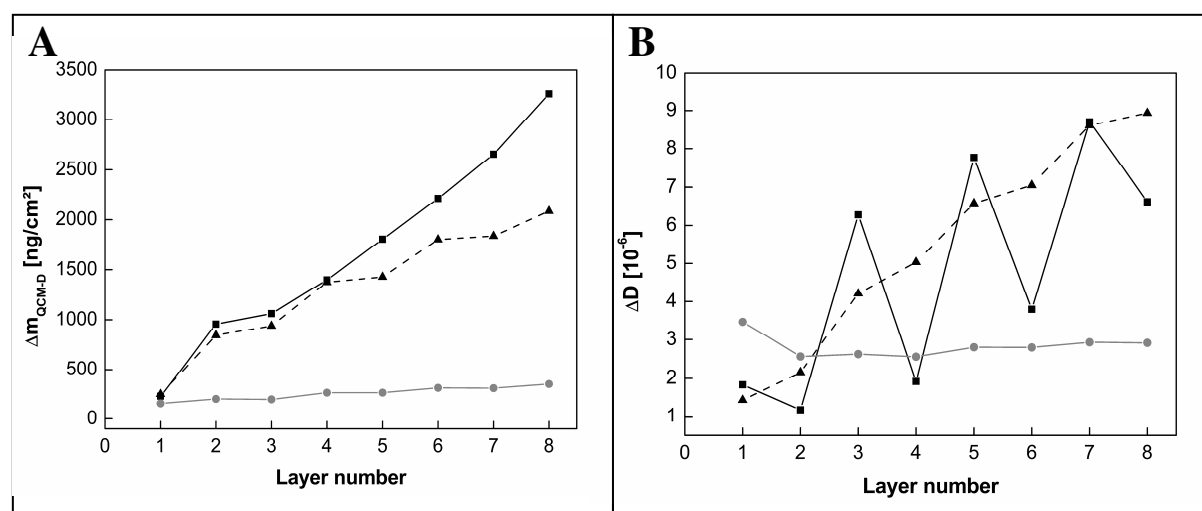


Figure 4.3: (A) The mass for increasing numbers of layers in the multilayer structures obtained by QCM-D and modelling using the Sauerbrey equation and (B) the corresponding QCM-D dissipation change (ΔD). Layer 1 is always PEI. Even layers: polyanions, odd layers: polycation chitosan. Solid lines (\blacksquare): CHI-HEP system, dashed lines (\blacktriangle): CHI-CS1.6 system and grey solid lines (\bullet): CHI-CS2.6 system.

Comparison of layer masses obtained by SPR and QCM-D and the resulting water content of the terminal CHI (7th) and polyanion (8th) layers are summarized in Table 4.2. The CHI-HEP layer system seemed to be more hydrated than the CHI-CS systems. It is also important to note that the addition of HEP did not change the relatively high water content of multilayers (75%). Also the CHI-CS1.6 multilayer had a relatively high water content of about 60%. By contrast, the total adsorbed (“acoustic”) mass measured by QCM-D was lower for CHI-CS2.6 multilayer system and also lower than the optical mass estimated by SPR. This points to an overestimation of layer mass by SPR due to a strong condensation of the multilayer system. These layers might also have a very different refractive index because of the high degree of sulfation. Using the Sauerbrey equation to estimate the mass from QCM-D measurements always leads to an underestimation. More extensive modelling was done, taking viscoelasticity into account (Voigt model), but this did not solve the SPR/QCM-D discrepancy for CS 2.6 (modelling data is added in supplementary information). This indicates that the water content of CHI-CS2.6 multilayers was very low.

CHI-HEP system assembled at pH 4 showed an exponential growth behaviour, which was also observed in other studies for these polyelectrolytes [22]. Ion pairing is most likely the prevailing mechanism of multilayer formation due to the protonation of amino groups of CHI that interact with carboxylic and sulfate groups of HEP [27]. The SPR curve for CHI-HEP system depicts nearly an equal contribution of both polyelectrolytes to the multilayer mass. Moreover, the comparison of layer mass calculated from SPR and QCM-D measurements reveals a relatively high water content of these multilayers. It is also interesting to note from dissipation measurements that addition of HEP leads always to a stiffening of multilayers while addition of CHI reverses this. This implies diffusion of HEP in and out of multilayers contributing to exponential film growth and electrostatic cross-linking that changes mechanical properties of films described previously for other polysaccharide-based multilayers [14, 22]. SPR measurements showed also higher layer masses adsorbed for CS-based systems and indicated also a dominance of the polyanion with less contribution of CHI to layer mass. Such dominating presence of CS in the CHI-CS1.6/CS2.6 layer systems (unlike CHI-HEP system) draws the attention towards the fact that they contain only sulfate groups and no carboxylic groups like HEP. Dominance of sulfate groups over carboxylic groups in ion-pairing has been observed before by others during the multilayer formation with poly-L-lysine and different GAGs [14]. However, additional contribution of cellulose sulfate adsorption during the multilayer formation may originate from hydrogen

bonding to CHI by remaining hydroxyl groups of cellulose. Adsorption of CHI under acidic and basic conditions on cellulose has also been reported previously and was explained by the structural similarity of both polymer backbones and hydrogen bonding [47]. This could also explain why more cellulose sulfates adsorb than simple ion pairing would allow and could lead to the observed dominance of polyanions. On the other hand, QCM-D measurements revealed that water content of multilayers CHI-HEP and CHI-CS1.6 was quite similar. Dissipation values increased with each adsorption step of the CHI-CS1.6 films. This points to the inability of CS to diffuse into the films and also to the fact that particularly films from CHI-CS1.6 may bind substantial quantities of water, probably again due to the larger number of unmodified hydroxyl groups. The obvious lack of reversibility of CS1.6 adsorption further supports the idea that not only ion pairing but also hydrogen bonding contributes to multilayer formation. By contrast, multilayer mass of CHI-CS2.6 measured by QCM-D was lower than SPR calculated mass. Since calculation of layer mass from SPR angle shift was approximated by Eq. (1), changes in refractive index during layer growth were not considered. Hence, changes of refractive index could be responsible for higher layer mass measured by SPR compared to QCM-D for the CHI-CS2.6 system.

4.2.2.1. Measurement of fibronectin adsorption by QCM-D

Fibronectin adsorption on the terminal polyanion layers measured by QCM-D is displayed in Table 4.2. No decrease in frequency was observed on CHI-HEP multilayer which indicates that fibronectin adsorption was very low and not detectable there, which is in agreement with previous studies [48],[49]. The CHI-CS1.6 and CHI-CS2.6 multilayers systems showed a decrease in frequency that indicates adsorption of fibronectin. The quantity of fibronectin adsorbed on CHI-CS1.6 was higher compared to CHI-CS2.6 multilayers. The ability of both CS to adsorb fibronectin goes along with previous reports of our group about capacity of cellulose sulfates to bind growth factors that possess HEP-binding domains [17],[18]. It indicates also that in contrast to HEP, both CS are contained in multilayers in a conformation that allows interaction with proteins. Furthermore, the effects of sulfation patterns of CS (CS1.6 & CS2.6) might play an additional role in interaction with proteins as also shown in some previous work [50] and influence the protein binding abilities of different multilayers. However, this could not be further explored in the present study due to the low number of derivatives.

Table 4.2: Multilayer mass, water content and fibronectin adsorption

| Multilayer systems | | Γ_{SPR}^a (ng/cm ²) | Δm_{QCM-D}^b (ng/cm ²) | Water content ^c | Fibronectin adsorption ^d (ng/cm ²) |
|--------------------|-----------------------------------|---|---|----------------------------|--|
| CHI-HEP | 7 th layer (HEP-CHI) | 663 | 2655 | 75% | |
| | 8 th layer (CHI-HEP) | 812 | 3257 | 75% | ._** |
| CHI-CS1.6 | 7 th layer (CS1.6-CHI) | 749 | 1837 | 59% | |
| | 8 th layer (CHI-CS1.6) | 924 | 2085 | 56% | 832 |
| CHI-CS2.6 | 7 th layer (CS2.6-CHI) | 643 | 312 | - | |
| | 8 th layer (CHI-CS2.6) | 796 | 354 | - | 301 |

^a)SPR masses were estimated using Eq. (1); ^b)QCM-D masses were estimated using the Sauerbrey equation and the frequency shift at the 5th overtone by Eq. (2); ^c)apparent water content was approximated by $(m_{QCM-D} - m_{SPR})/m_{QCM-D} * 100$. Water content was not calculated for CS2.6. ^d)QCM-D frequency shifts (Δf) were used for calculation of fibronectin adsorption by Sauerbrey equation (2).**Fibronectin adsorption was not detectable in case of CHI-HEP multilayers.

4.4.3. Water contact angle (WCA) and zeta potential measurements

Figure 4.4A shows the results of static water contact angle (WCA) measurements (clean glass, PEI -1, polyanions -even numbers and CHI -odd numbers), which were executed after the deposition of each layer for all multilayer systems. CHI-HEP multilayers showed alternating values with lower WCA for HEP and higher for CHI. These differences in WCA values point to the formation of more separated layers constituted by either CHI or HEP dominating the wetting properties of the surface. While immobilized CHI as polysaccharide with primary amino groups represents a less wettable material, binding of HEP with carboxylic and sulfate groups makes a highly wettable surface. Such oscillating behaviour of water contact angles during multilayer formation from CHI and HEP at acidic pH values and the same ionic strength was also reported in previous studies [22]. By contrast no such alternating WCA values were observed for CHI-CS1.6 or very low differences were seen for CHI-CS2.6 system. Figure 4.4A illustrates that WCA of CHI-CS1.6 did only increase slightly after adsorption of PEI and subsequent addition of CS1.6 and CHI. No alternating WCA were observed here. The average WCA were also highest from all multilayer systems. This suggests a dominance of one polyelectrolyte in the system, which is probably CS1.6 when results of SPR measurements are taken into account. Also CHI-CS2.6 showed only small changes with each

layer adsorption step, which points towards the formation of more intermingled multilayers, composed of both CHI and CS2.6.

Figure 4.4B shows the zeta potential of multilayers terminated either by CHI or the polyanions (HEP/CS1.6/CS2.6) in dependence on pH value of electrolyte solution (1 mM KCl). It should be noted that zeta potential measurements of polyelectrolyte multilayer systems are not only sensitive to outermost layer composition, but represent rather the potential of a permeable swollen surface layer [51]. Therefore it was observed that for each type of multilayer system and regardless of terminal layer type (either CHI or polyanion) zeta potentials were positive at acidic pH when CHI is the potential-determining polyelectrolyte and became negative at basic pH when polyanion charges become dominant.

This indicates that besides electrostatic attraction of polyelectrolytes also changes in the chemical potential of molecules between multilayers and surrounding liquid phases could drive diffusion of polyelectrolytes to the interface and inside multilayers as also discussed previously by Picart and Boudou et al.[52], [53]. When comparing the three different systems at pH 3 and CHI was the terminal layer, the potentials of CHI-CS1.6 and CHI-CS2.6 multilayers were about 20 mV lower than CHI-HEP. This is in agreement with conclusion deduced by the SPR studies that CHI is a minor component in CHI-CS multilayers. On the other hand, zeta potentials of the multilayer made of CHI-HEP and CHI-CS2.6 that bind probably pre-dominantly by ion pairing were also higher at basic pH values, which indicates more adsorption of chitosan than on CS1.6. The point of zero charge (when zeta potential is zero) was about one pH unit lower for CHI-CS1.6 systems in comparison to CHI-HEP independent on terminal layer which further supports the above idea of lesser contribution by CHI. Besides that when CHI was the terminal layer the zeta potentials for the CHI-CS1.6 and CHI-CS2.6 systems shows equal or lower potentials and that may be due to the higher content in sulfate groups of CS compared to HEP. On the other hand zeta potentials of the HEP terminating layers in the basic range (above pH 7, Figure 4.4B) show lower zeta potentials for the CHI-HEP system which indicates a different way of HEP adsorption compared to CS. It has been suggested that HEP diffuses in and out of multilayers, which is probably also easier due to its lower molecular weight. Interpenetration of HEP in the CHI layers has also been reported before [54]. Such interpenetration by HEP would also disturb the expected interaction with HEP-binding domains of proteins like fibronectin as observed also in the present study. By contrast, both cellulose sulfates are larger with CS1.6 being largest and able to integrate not only by ion pairing but also hydrogen bonding, which could hamper diffusion of both. This was also supported by dissipation measurements showing only striking changes

after HEP addition. Hence, possibly more HEP may protrude into the multilayer system, which makes the zeta potential of these multilayers more negative than that of the CS. Such differences and domination of either of the polyelectrolyte were absent in the CHI-CS1.6 and CHI-CS2.6 multilayers which indicates the formation of intermingled terminal layers.

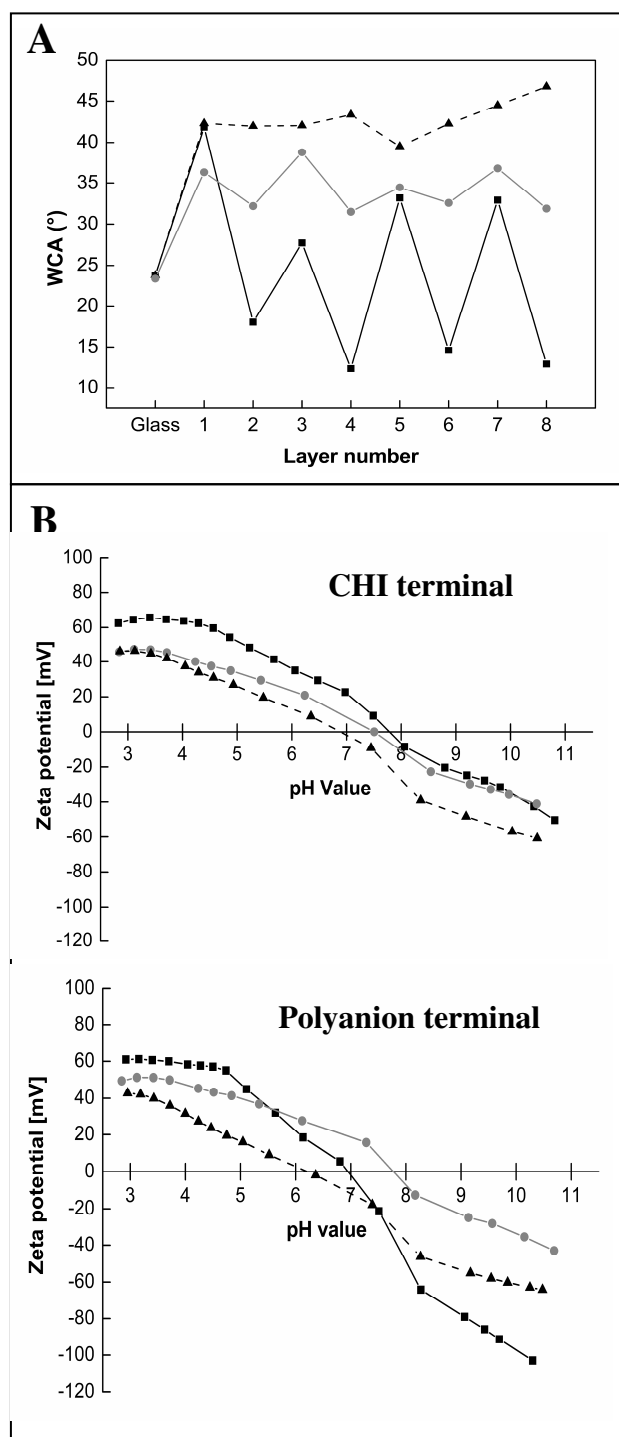


Figure 4.4: (A) Static water contact angles (WCA) plotted as function of layer number and layer 1 is always PEI, even layers: polyanion, odd layers: polycation (CHI). (B) Zeta (ζ)

potential measurements of the outermost CHI (7th) and polyanion (8th) layers. ζ potentials are plotted as function of pH value. Solid lines (■): CHI-HEP system, dashed lines (▲): CHI-CS1.6 system and grey solid lines (●): CHI-CS2.6 system.

4.4.4. Adhesion and growth of C2C12 cells on multilayers

Polyelectrolyte multilayers coatings on implants and tissue engineering scaffolds have been suggested for the improvement of cell attachment [55]. As cell adhesion and spreading are the prerequisites for growth and differentiation [56], such studies were carried out here with C2C12 cells on terminal CHI (7th) and polyanion (HEP/CS1.6/CS2.6) (8th) layers to learn about the effect of multilayer composition on adhesion and growth of cells. C2C12 cells were chosen because of their ability to differentiate into osteoblast-like cells or myotubes depending on the presence of growth factor like BMP-2 as well as on the mechanical properties of the substratum [31],[57],[18]. C2C12 cells were seeded on multilayer surfaces in the culture medium supplemented with 10% fetal bovine serum that contains attachment factors like vitronectin and fibronectin [58]. After 4 h incubation, fluorescein diacetate (FDA) and immunofluorescence staining was performed on cells, and analysis of cell count and size was done using the micrographs. Figure 4.5A shows the cell counts while the figure for cell size is provided in the supplementary document as Figure S4.2. Indeed, a close correlation of fibronectin adsorption results with cell adhesion and spreading was observed. The cell count as well as the cell spreading (cell size) was significantly lower on the CHI-HEP multilayer system ($p \leq 0.05$) compared to both CS terminated multilayers, which is also in agreement with the lack of fibronectin adsorption on CHI-HEP. It is important to note that fibronectin was used as a model protein that possess HEP-binding domains (to study the interaction of multilayer surfaces with adhesive proteins) like other proteins in serum that are related to adhesion (e.g. vitronectin) and growth of cells (e.g. FGFs). As mentioned above fibronectin is present in serum and is also secreted by many cell types including C2C12 cells.[59],[60] According to previous studies, HEP should support the binding of fibronectin[12], which is not seen here and points to an unfavorable conformation of HEP in the multilayer system. Others also found low binding of BMP-2 growth factor to HEP in ternary multilayer systems with HEP and hyaluronan as polyanions [61]. On the other hand, even the higher water content and dissipation of CHI-CS1.6 multilayers did not inhibit cell adhesion as these layers showed the highest cell count and spreading along with highest adsorption of fibronectin. This indicates that the amount of water which was coupled in these multilayers was not blocking

cell adhesion and spreading, also implying that the primary reason for low cell attachment on CHI-HEP multilayers was the lack of interaction of HEP with adhesive proteins.

Figure 4.5B shows the morphology of C2C12 cells seeded in the presence of 10% FBS that supports the results of quantitative measurements. In general cells were round and loosely attached on CHI-HEP multilayers (Figure 4.5B-i). Therefore, they were detached during washing steps included in the immunofluorescence staining procedure and no cells were found on HEP-terminated multilayers in the microscopic survey (Figure 4.5B-ii). Oppositely elongated and well spread C2C12 cells were found on CHI-CS1.6 multilayer surfaces (Figure 4.5B-iii and iv). CHI-CS2.6 multilayers (Figure 4.5B-v and vi) provoked more spreading of cells in comparison to CHI-HEP layers, but less than CHI-CS1.6. There were very minor differences in the appearance and size of cells on CHI and polyanion (HEP/CS1.6/CS2.6) terminal layers. Hence quantitative data and images achieved on polyanion terminal layers are shown here only. Figure 4.5B-iv and vi shows the staining of actin cytoskeleton by BODIPY-phalloidin (red), focal adhesions with vinculin by a monoclonal antibody (green) and nuclei by TO-PRO-3 (blue). Cells seeded on CHI-CS1.6 layers expressed longitudinal stress fibres with many focal adhesion plaques (Figure 4.5B-iv), whereas cells on terminal CS2.6 layers showed poorly developed or under expressed actin fibres and lack of focal adhesions. The well developed focal adhesions on CHI-CS1.6 layers (Figure 4.5B-iv) indicate the adsorption of adhesive proteins like fibronectin and vitronectin present in serum [58], which is also in agreement with the fibronectin adsorption data achieved through QCM-D measurements. It is worthy to note here that presence of serum proteins is probably also a contributing factor in cell adhesion on CHI-CS2.6 layers, which had a lower affinity to fibronectin compared to CHI-CS1.6 layers lead to lower cell count and spreading. The initial cellular events like adhesion and spreading are dependent on the ligation of integrin molecules to extracellular matrix proteins like fibronectin [62]. Adhesion of cells is a prerequisite for further cell growth, during ligation of integrins to extracellular matrix components leads to prevention of apoptosis and promote signalling through mitogen-activated protein (MAP) kinase pathways [63],[64]. Therefore, initial adhesion responses can be used for predication of cell proliferation and also differentiation.

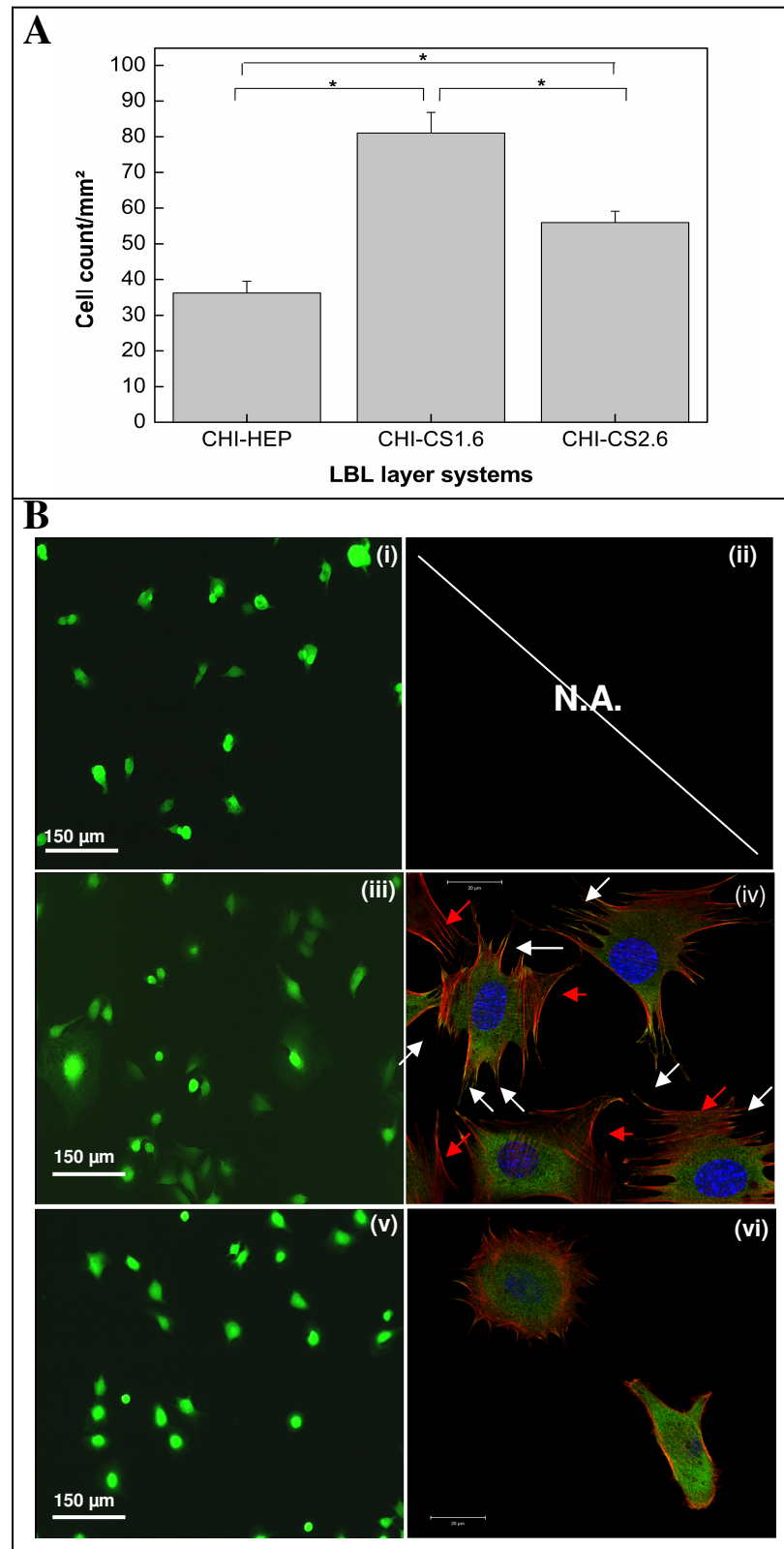


Figure 4.5: (A) Adhesion of C2C12 cells on polyanion (HEP/CS1.6/CS2.6) terminated multilayers. Data represent means, standard deviations and ANOVA. Significance level of $p \leq 0.05$ is indicated by the asterisks. (B) Fluorescence images of C2C12 cells plated on terminal HEP (i and ii), CS1.6 (iii and iv) and CS2.6 (v and vi). The left column of images show cells

stained with FDA while right one immuno-fluorescence staining. The red staining shows actin, green vinculin and blue nuclei of cells. White arrows show focal adhesions positive for vinculin. Red arrows show actin stress fibres.

The proliferation of C2C12 cells on different multilayer systems was studied after incubation periods of 24 and 72 h. The quantification of cell growth or viable cells was measured by performing QBlue assay after the different incubation periods (see Figure 4.6A). QBlue assay measures metabolic activity of cells and can be therefore taken as a measure for quantity of living cells on substrata [65]. The data obtained via QBlue assay suggested that cell growth was lower on CHI-HEP layers compared to CHI-CS1.6 and CHI-CS2.6 layers after 24 and 72 h which is in line with the findings of adhesion studies. On both CHI-HEP and CHI-CS1.6 layers (Figure 4.6B-i – HEP, Figure 4.6B-iii - CS1.6), cells showed a reduced degree of spreading and a tendency to form bulky aggregates in contrast to cells seeded on CHI-CS2.6 layers (more spread phenotype). The CHI-CS2.6 multilayers showed increased cell growth in span of 72 h. Besides the quantitative findings, cell morphology studied during cell growth with phase contrast microscopy also indicated most surface coverage on CHI-CS2.6 layers by C2C12 cells. Improved growth of cells on CHI-CS2.6 multilayers was already visible after 24 h of incubation as shown in Figure 4.6B-v. These differences in cell growth between different polyanion multilayers were also maintained after 72 h with an increase in cell numbers from 24 to 72 h most strikingly for CHI-CS2.6 multilayers. We assume that such improved cell behaviour on CHI-CS2.6 multilayers might be due to more secretion of proteins as C2C12 cells are able to activate FN synthesis under certain circumstances [60]. In addition, moderate changes in multilayer structure of CHI-CS2.6 during the long term culture could also improve interaction with proteins and support growth of cells. CHI-CS1.6 multilayers supported continuous cell growth in aggregates (Figure 4.6B-iv) while CHI-HEP layers led to more evenly distributed cells on the substratum like CHI-CS2.6 after 72 h. However in general coverage of surface by cells depicted in the micrographs Figure 4.6B coincided well with the quantitative data presented in Figure 4.6A. Although cell adhesion experiments suggested that cell growth should be highest on CHI-CS1.6 multilayer, this was not the case. This suggests that water content of multilayers could be an additional parameter that controls long-term cell responses. The higher amount of coupled water in CHI-HEP multilayers could be the reason for the weaker cell growth on these layers similar to observations of Discher et al. on hydrogels [66]. Water content was also quite high in CHI-CS1.6 multilayers and this seems to become more important when cells start to grow. The observation that C2C12 cells

form larger cluster and aggregates, which was peculiar, indicates also a different nature of substratum that promotes migration of cells. CHI-CS2.6 multilayers had much lower water content and dissipation values, which obviously seems to be a promoter of cell growth [67]. Hence the selection of either HEP, CS1.6 or CS2.6 for formation of multilayers may provide a tool to adjust cell adhesion and growth to the desired extent.

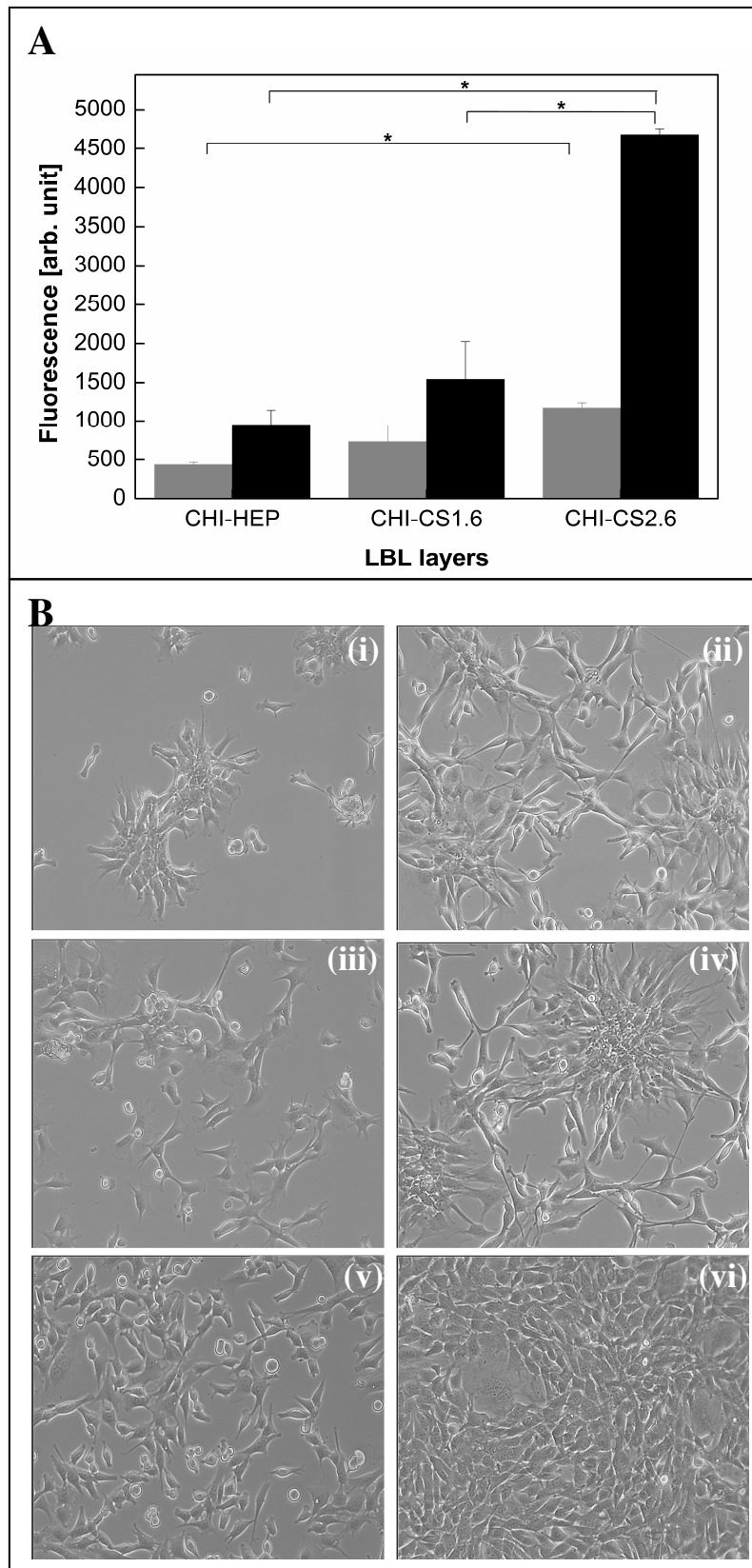


Figure 4.6: (A) Cell proliferation measurements done after 1 (grey bars) and 3 (black bars) days of C2C12 cell culture on polyanion (HEP/CS1.6/CS2.6) terminated. Data represent means, standard deviations and ANOVA Significance level of $p \leq 0.05$ is indicated by the asterisks. (B) Phase contrast images on polyanion CHI-HEP (i and ii), CHI-CS1.6 (iii and iv)

and CHI-CS2.6 (v and vi) terminated layers after incubation times of 1 day (i, iii, and v) & 3 days (ii, iv and vi).

4.5. Conclusion

This current work shows that polyelectrolyte multilayer (PEM) coatings prepared from three different polyanions (HEP/CS1.6/CS2.6) paired with CHI assembled at pH 4 can be used to attain multilayer systems with varying bulk and surface properties along with specific effects on cell behaviour. Since HEP is a natural GAG with limited abundance, cellulose sulfates might be potential alternative materials to prepare bioactive surface coatings. Therefore, immobilization of these cellulose sulfates was done on a model biomaterial as multilayer coatings and characterized physico-chemically and biologically to acquire a deeper knowledge about their construction and bioactivity as surface coatings. The results achieved from the various characterization techniques depicted that CHI-HEP and CHI-CS1.6 multilayers have higher layer mass and are more hydrated as compared to CHI-CS2.6 which possessed lower mass adsorption with little or neglectable water content. Nearly both polyelectrolytes (CHI and HEP) contributed similarly in CHI-HEP multilayer fabrication following the formation of distinct layers, while dominance of polyanions and formation of more intermingled layers was realized for CS-based films. Due to the presence of sulfate groups along with carboxylic groups in HEP and solely sulfate groups in CS, different type of chemical interactions with amino groups of CHI appeared, which led to a multilayer formation process with specific growth patterns, hydration, mechanical properties as well as fibronectin adsorption and cellular response. CHI-HEP multilayers showed almost no fibronectin adsorption and significantly lower cell count and spreading, pointing to an unfavorable conformation of HEP in the multilayer system depriving the interaction of HEP molecules with adhesive proteins where as CHI-CS1.6 and CHI-CS2.6 multilayer systems favoured fibronectin adsorption as well as cell response. The multilayers prepared from cellulose sulfates have shown the ability of making an advantageous position as surface coatings that very well promotes the adhesion and growth of cells. Moreover such multilayers could also be used as potential reservoirs for loading small bioactive molecules like growth factors as these cellulose sulfates were also found to be capable of binding with growth factors like FGF-2 and BMP-2. The above mentioned multilayer layer systems might be very useful for making bioactive coatings of tissue engineering and implants for regeneration of bone and other tissues.

4.6. Acknowledgements

This work was funded partly by Deutsche Forschungsgemeinschaft under grant agreements GR1290/7-1 & GR1290/7-2, FI755/4-1 & FI755/4-2 and by the European Union Seventh Framework Program (FP7/2007-2013) under grant agreement n° NMP4-SL-2009-229292 (Find&Bind).

4.7. References

- [1] B.D. Ratner, New ideas in biomaterials science—a path to engineered biomaterials, *Journal of Biomedical Materials Research*, 27 (1993) 837-850.
- [2] D.G. Castner and B.D. Ratner, Biomedical surface science: Foundations to frontiers, *Surface Science*, 500 (2002) 28-60.
- [3] T. Groth, Z.-M. Liu, M. Niepel, D. Peschel, K. Kirchhof, G. Altankov and N. Fauchaux, Chemical and Physical Modifications of Biomaterial Surfaces to Control Adhesion of Cells, in: V.P. Shastri, G. Altankov, A. Lendlein (Eds.) *Advances in Regenerative Medicine: Role of Nanotechnology, and Engineering Principles*, Springer Netherlands, 2010, pp. 253-284.
- [4] Z. Ma, Z. Mao and C. Gao, Surface modification and property analysis of biomedical polymers used for tissue engineering, *Colloids and Surfaces B: Biointerfaces*, 60 (2007) 137-157.
- [5] G. Decher, J.D. Hong and J. Schmitt, Buildup of ultrathin multilayer films by a self-assembly process: III. Consecutively alternating adsorption of anionic and cationic polyelectrolytes on charged surfaces, *Thin Solid Films*, 210–211, Part 2 (1992) 831-835.
- [6] Z. Tang, Y. Wang, P. Podsiadlo and N.A. Kotov, Biomedical Applications of Layer-by-Layer Assembly: From Biomimetics to Tissue Engineering, *Advanced Materials*, 18 (2006) 3203-3224.
- [7] J.B. Schlenoff and S.T. Dubas, Mechanism of Polyelectrolyte Multilayer Growth: Charge Overcompensation and Distribution, *Macromolecules*, 34 (2001) 592-598.
- [8] M. Schönhoff, Self-assembled polyelectrolyte multilayers, *Current Opinion in Colloid & Interface Science*, 8 (2003) 86-95.
- [9] P.T. Hammond, Form and Function in Multilayer Assembly: New Applications at the Nanoscale, *Advanced Materials*, 16 (2004) 1271-1293.
- [10] T. Crouzier, T. Boudou and C. Picart, Polysaccharide-based polyelectrolyte multilayers, *Current Opinion in Colloid & Interface Science*, 15 (2010) 417-426.

- [11] J.M.R. Grech, J.F. Mano and R.L. Reis, Chitosan Beads as Templates for Layer-by-Layer Assembly and their Application in the Sustained Release of Bioactive Agents, *Journal of Bioactive and Compatible Polymers*, 23 (2008) 367-380.
- [12] I. Capila and R.J. Linhardt, Heparin - Protein interactions, *Angew Chem Int Edit*, 41 (2002) 391-412.
- [13] J. Fu, J. Ji, W. Yuan and J. Shen, Construction of anti-adhesive and antibacterial multilayer films via layer-by-layer assembly of heparin and chitosan, *Biomaterials*, 26 (2005) 6684-6692.
- [14] T. Crouzier and C. Picart, Ion Pairing and Hydration in Polyelectrolyte Multilayer Films Containing Polysaccharides, *Biomacromolecules*, 10 (2009) 433-442.
- [15] G. Franz and S. Alban, Structure-activity relationship of antithrombotic polysaccharide derivatives, *International Journal of Biological Macromolecules*, 17 (1995) 311-314.
- [16] T. Groth and W. Wagenknecht, Anticoagulant potential of regioselective derivatized cellulose, *Biomaterials*, 22 (2001) 2719-2729.
- [17] D. Peschel, K. Zhang, N. Aggarwal, E. Brendler, S. Fischer and T. Groth, Synthesis of novel celluloses derivatives and investigation of their mitogenic activity in the presence and absence of FGF2, *Acta Biomaterialia*, 6 (2010) 2116-2125.
- [18] D. Peschel, K. Zhang, S. Fischer and T. Groth, Modulation of osteogenic activity of BMP-2 by cellulose and chitosan derivatives, *Acta Biomaterialia*, 8 (2012) 183-193.
- [19] M. Gericke, A. Doliska, J. Stana, T. Liebert, T. Heinze and K. Stana-Kleinschek, Semi-Synthetic Polysaccharide Sulfates as Anticoagulant Coatings for PET, 1-Cellulose Sulfate, *Macromolecular Bioscience*, 11 (2011) 549-556.
- [20] M. Koetse, A. Laschewsky, A.M. Jonas and W. Wagenknecht, Influence of Charge Density and Distribution on the Internal Structure of Electrostatically Self-assembled Polyelectrolyte Films, *Langmuir*, 18 (2002) 1655-1660.
- [21] S.M. Oliveira, T.H. Silva, R.L. Reis and J.F. Mano, Nanocoatings containing sulfated polysaccharides prepared by layer-by-layer assembly as models to study cell-material interactions, *Journal of Materials Chemistry B*, 1 (2013) 4406-4418.
- [22] M. Lundin, F. Solaqa, E. Thormann, L. Macakova and E. Blomberg, Layer-by-Layer Assemblies of Chitosan and Heparin: Effect of Solution Ionic Strength and pH, *Langmuir*, 27 (2011) 7537-7548.
- [23] M. Dash, F. Chiellini, R.M. Ottenbrite and E. Chiellini, Chitosan—A versatile semi-synthetic polymer in biomedical applications, *Progress in Polymer Science*, 36 (2011) 981-1014.

- [24] R.A.A. Muzzarelli, Chitins and chitosans for the repair of wounded skin, nerve, cartilage and bone, *Carbohydrate Polymers*, 76 (2009) 167-182.
- [25] S. Şenel and S.J. McClure, Potential applications of chitosan in veterinary medicine, *Advanced Drug Delivery Reviews*, 56 (2004) 1467-1480.
- [26] P. Lavalle, C. Picart, J. Mutterer, C. Gergely, H. Reiss, J.-C. Voegel, B. Senger and P. Schaaf, Modeling the Buildup of Polyelectrolyte Multilayer Films Having Exponential Growth χ , *The Journal of Physical Chemistry B*, 108 (2003) 635-648.
- [27] S. Boddohi, C.E. Killingsworth and M.J. Kipper, Polyelectrolyte multilayer assembly as a function of pH and ionic strength using the polysaccharides chitosan and heparin, *Biomacromolecules*, 9 (2008) 2021-2028.
- [28] L. Richert, P. Lavalle, E. Payan, X.Z. Shu, G.D. Prestwich, J.F. Stoltz, P. Schaaf, J.C. Voegel and C. Picart, Layer by layer buildup of polysaccharide films: Physical chemistry and cellular adhesion aspects, *Langmuir*, 20 (2004) 448-458.
- [29] S.E. Burke and C.J. Barrett, pH-responsive properties of multilayered poly(L-lysine)/hyaluronic acid surfaces, *Biomacromolecules*, 4 (2003) 1773-1783.
- [30] A.F. Xie and S. Granick, Weak versus Strong: A Weak Polyacid Embedded within a Multilayer of Strong Polyelectrolytes, *Journal of the American Chemical Society*, 123 (2001) 3175-3176.
- [31] T. Boudou, T. Crouzier, C. Nicolas, K. Ren and C. Picart, Polyelectrolyte Multilayer Nanofilms Used as Thin Materials for Cell Mechano-Sensitivity Studies, *Macromolecular Bioscience*, 11 (2011) 77-89.
- [32] K. Kirchhof, K. Hristova, N. Krasteva, G. Altankov and T. Groth, Multilayer coatings on biomaterials for control of MG-63 osteoblast adhesion and growth, *J Mater Sci: Mater Med*, 20 (2009) 897-907.
- [33] M.R. Kreke, A.S. Badami, J.B. Brady, R. Michael Akers and A.S. Goldstein, Modulation of protein adsorption and cell adhesion by poly(allylamine hydrochloride) heparin films, *Biomaterials*, 26 (2005) 2975-2981.
- [34] R.O. Hynes, Integrins: Bidirectional, Allosteric Signaling Machines, *Cell*, 110 (2002) 673-687.
- [35] T. Groth, G. Altankov, A. Kostadinova, N. Krasteva, W. Albrecht and D. Paul, Altered vitronectin receptor (αv integrin) function in fibroblasts adhering on hydrophobic glass, *Journal of Biomedical Materials Research*, 44 (1999) 341-351.

- [36] J.L. Chen, Q.L. Li, J.Y. Chen, C. Chen and N. Huang, Improving blood-compatibility of titanium by coating collagen–heparin multilayers, *Applied Surface Science*, 255 (2009) 6894-6900.
- [37] S.S. Silva, J.M. Oliveira, J. Benesch, S.G. Caridade, J.F. Mano and R.R. Reis, Hybrid biodegradable membranes of silane-treated chitosan/soy protein for biomedical applications, *Journal of Bioactive and Compatible Polymers*, 28 (2013) 385-397.
- [38] J.F. Mano, G.A. Silva, H.S. Azevedo, P.B. Malafaya, R.A. Sousa, S.S. Silva, L.F. Boesel, J.M. Oliveira, T.C. Santos, A.P. Marques, N.M. Neves and R.L. Reis, Natural origin biodegradable systems in tissue engineering and regenerative medicine: present status and some moving trends, *Journal of The Royal Society Interface*, 4 (2007) 999-1030.
- [39] M. Kolasińska, R. Krastev and P. Warszyński, Characteristics of polyelectrolyte multilayers: Effect of PEI anchoring layer and posttreatment after deposition, *Journal of Colloid and Interface Science*, 305 (2007) 46-56.
- [40] N. Patel, M.C. Davies, M. Hartshorne, R.J. Heaton, C.J. Roberts, S.J.B. Tendler and P.M. Williams, Immobilization of Protein Molecules onto Homogeneous and Mixed Carboxylate-Terminated Self-Assembled Monolayers, *Langmuir*, 13 (1997) 6485-6490.
- [41] K. Zhang, E. Brendler, A. Geissler and S. Fischer, Synthesis and spectroscopic analysis of cellulose sulfates with regulable total degrees of substitution and sulfation patterns via C-13 NMR and FT Raman spectroscopy, *Polymer*, 52 (2011) 26-32.
- [42] R.B.M. Schasfoort, Tudos, A. J. , *Handbook of Surface Plasmon Resonance*, in, RSC Publishing, Cambridge, 2008, pp. 128.
- [43] G. Sauerbrey, Verwendung von Schwingquarzen zur Wägung dünner Schichten und zur Mikrowägung, *Z. Physik*, 155 (1959) 206-222.
- [44] G. Socrates, *Infrared and Raman characteristic group frequencies*, 3. ed., John Wiley & Sons, 2004.
- [45] F. Zhang, B. Yang, M. Ly, K. Solakyildirim, Z. Xiao, Z. Wang, J. Beudet, A. Torelli, J. Dordick and R. Linhardt, Structural characterization of heparins from different commercial sources, *Anal Bioanal Chem*, 401 (2011) 2793-2803.
- [46] K. Zhang, D. Peschel, E. Bäucker, T. Groth and S. Fischer, Synthesis and characterisation of cellulose sulfates regarding the degrees of substitution, degrees of polymerisation and morphology, *Carbohydrate Polymers*, 83 (2011) 1659-1664.
- [47] H. Orelma, I. Filpponen, L.-S. Johansson, J. Laine and O.J. Rojas, Modification of Cellulose Films by Adsorption of CMC and Chitosan for Controlled Attachment of Biomolecules, *Biomacromolecules*, 12 (2011) 4311-4318.

- [48] K. Kirchhof, Nanostrukturierte Biomaterialbeschichtungen zur Steuerung von Zelladhäsion und -proliferation: pH-Wert-abhängige Multischichten aus Heparin und Chitosan in diskreter und Gradientenform, in, Vol Ph.D., Martin-Luther-University, Halle-Wittenberg, Germany, Halle (Saale), Germany, 2009.
- [49] N. Aggarwal, N. Altgärde, S. Svedhem, G. Michanetzis, Y. Missirlis and T. Groth, Tuning Cell Adhesion and Growth on Biomimetic Polyelectrolyte Multilayers by Variation of pH During Layer-by-Layer Assembly, *Macromolecular Bioscience*, 13 (2013) 1327-1338.
- [50] L. Yuan, Z. Yue, H. Chen, H. Huang and T. Zhao, Biomacromolecular affinity: Interactions between lysozyme and regioselectively sulfated chitosan, *Colloids and Surfaces B: Biointerfaces*, 73 (2009) 346-350.
- [51] J.F.L. Duval, D. Kuettner, C. Werner and R. Zimmermann, Electrohydrodynamics of Soft Polyelectrolyte Multilayers: Point of Zero-Streaming Current, *Langmuir*, 27 (2011) 10739-10752.
- [52] C. Picart, J. Mutterer, L. Richert, Y. Luo, G.D. Prestwich, P. Schaaf, J.-C. Voegel and P. Lavalley, Molecular basis for the explanation of the exponential growth of polyelectrolyte multilayers, *Proceedings of the National Academy of Sciences*, 99 (2002) 12531-12535.
- [53] T. Boudou, T. Crouzier, K. Ren, G. Blin and C. Picart, Multiple Functionalities of Polyelectrolyte Multilayer Films: New Biomedical Applications, *Advanced Materials*, 22 (2010) 441-467.
- [54] T. Serizawa, M. Yamaguchi and M. Akashi, Alternating bioactivity of polymeric layer-by-layer assemblies: Anticoagulation vs procoagulation of human blood, *Biomacromolecules*, 3 (2002) 724-731.
- [55] L. Richert, P. Lavalley, D. Vautier, B. Senger, J.F. Stoltz, P. Schaaf, J.C. Voegel and C. Picart, Cell Interactions with Polyelectrolyte Multilayer Films, *Biomacromolecules*, 3 (2002) 1170-1178.
- [56] H. Shin, S. Jo and A.G. Mikos, Biomimetic materials for tissue engineering, *Biomaterials*, 24 (2003) 4353-4364.
- [57] J. Ballester-Beltrán, M. Cantini, M. Lebourg, P. Rico, D. Moratal, A. García and M. Salmerón-Sánchez, Effect of topological cues on material-driven fibronectin fibrillogenesis and cell differentiation, *J Mater Sci: Mater Med*, 23 (2012) 195-204.
- [58] J.G. Steele, G. Johnson and P.A. Underwood, Role of serum vitronectin and fibronectin in adhesion of fibroblasts following seeding onto tissue culture polystyrene, *Journal of Biomedical Materials Research*, 26 (1992) 861-884.

- [59] J.C. Adams, J.D. Clelland, G.D.M. Collett, F. Matsumura, S. Yamashiro and L. Zhang, Cell-Matrix Adhesions Differentially Regulate Fascin Phosphorylation, *Molecular Biology of the Cell*, 10 (1999) 4177-4190.
- [60] E.B. Izevbigie and W.G. Bergen, β -Adrenergic Agonist Hyperplastic Effect Is Associated with Increased Fibronectin Gene Expression and Not Mitogen-Activated Protein Kinase Modulation in C2C12 Cells, *Proceedings of the Society for Experimental Biology and Medicine*, 223 (2000) 302-309.
- [61] T. Crouzier, A. Szarpak, T. Boudou, R. Auzély-Velty and C. Picart, Polysaccharide-Blend Multilayers Containing Hyaluronan and Heparin as a Delivery System for rhBMP-2, *Small*, 6 (2010) 651-662.
- [62] O. Guillame-Gentil, O. Semenov, A.S. Roca, T. Groth, R. Zahn, J. Vörös and M. Zenobi-Wong, Engineering the Extracellular Environment: Strategies for Building 2D and 3D Cellular Structures, *Advanced Materials*, 22 (2010) 5443-5462.
- [63] E.A. Clark and R.O. Hynes, Ras activation is necessary for integrin-mediated activation of extracellular signal-regulated kinase 2 and cytosolic phospholipase A(2) but not for cytoskeletal organization, *J Biol Chem*, 271 (1996) 14814-14818.
- [64] T. Groth and G. Altankov, Studies on cell-biomaterial interaction: role of tyrosine phosphorylation during fibroblast spreading on surfaces varying in wettability, *Biomaterials*, 17 (1996) 1227-1234.
- [65] S. Gil, S. Sarun, A. Biete, Y. Prezado and M. Sabés, Survival Analysis of F98 Glioma Rat Cells Following Minibeam or Broad-Beam Synchrotron Radiation Therapy, *Radiat Oncol*, 6 (2011) 1-9.
- [66] D.E. Discher, P. Janmey and Y.-l. Wang, Tissue Cells Feel and Respond to the Stiffness of Their Substrate, *Science*, 310 (2005) 1139-1143.
- [67] L. Richert, F. Boulmedais, P. Lavalle, J. Mutterer, E. Ferreux, G. Decher, P. Schaaf, J.-C. Voegel and C. Picart, Improvement of Stability and Cell Adhesion Properties of Polyelectrolyte Multilayer Films by Chemical Cross-Linking, *Biomacromolecules*, 5 (2003) 284-294.

4.8. Supporting Information

Results

Characterization of multilayer formation

Table S4.1: Multilayer mass measured through SPR and QCM-D.

| Multilayer systems | | Γ_{SPR}^a (ng/cm ²) | Δm_{QCM-D}^b (ng/cm ²) | Voigt (ng/cm ²) ^c | |
|--------------------|-----------------------------------|---|---|--|----------|
| | | | | mean | χ^2 |
| CHI-HEP | 7 th layer (HEP-CHI) | 663 | 2655 | 3960 ± 340 | 3E5 |
| | 8 th layer (CHI-HEP) | 812 | 3257 | 4410 ± 290 | 2E5 |
| CHI-CS1.6 | 7 th layer (CS1.6-CHI) | 749 | 1837 | 2910 ± 90 | 3E3 |
| | 8 th layer (CHI-CS1.6) | 924 | 2085 | 2992 ± 92 | 3E3 |
| CHI-CS2.6 | 7 th layer (CS2.6-CHI) | 643 | 312 | 640 ± 100 | 9E3 |
| | 8 th layer (CHI-CS2.6) | 796 | 354 | 680 ± 120 | 1E4 |

- a) SPR masses were estimated using equation (1) (see main text); b) QCM-D masses were estimated using the Sauerbrey equation and the frequency shift at the 5th overtone and c) QCM-D masses evaluated through Voigt modelling.

To estimate the mass of a multilayer build-up in QCM-D, the Sauerbrey equation can be used if the layers are assumed to be rigidly attached to the surface and the energy dissipating from the system is disregarded. In order to take the dissipation into account, another model based on continuum mechanics using a Voigt element can be used to describe viscoelastic properties of the adsorbed layer.[1]

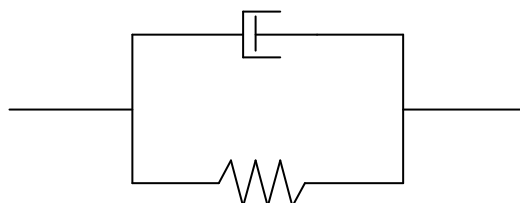


Figure S4.1: Schematic illustration of a viscoelastic Voigt element with a dash pot (viscous) and spring (elastic) in parallel.

A one-layer frequency independent model in the modeling software QTools (Biolin Scientific) was used. A density of 1100 kg/m^3 was assumed and the 5th to 9th overtone was used.

Adhesion and growth of C2C12 cells on multilayers

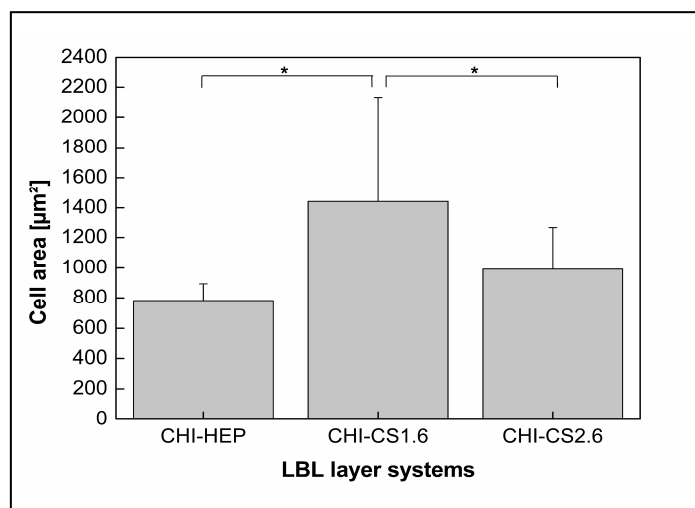


Figure S4.2: Size of C2C12 cells plated 4 hours in DMEM with 10 % FBS on polyanion (HEP/CS1.6/CS2.6) terminated multilayers prepared with either of the polyanion paired with CHI. Data represent means, standard deviations and ANOVA. Significance level of $p \leq 0.05$ is indicated by the asterisks.

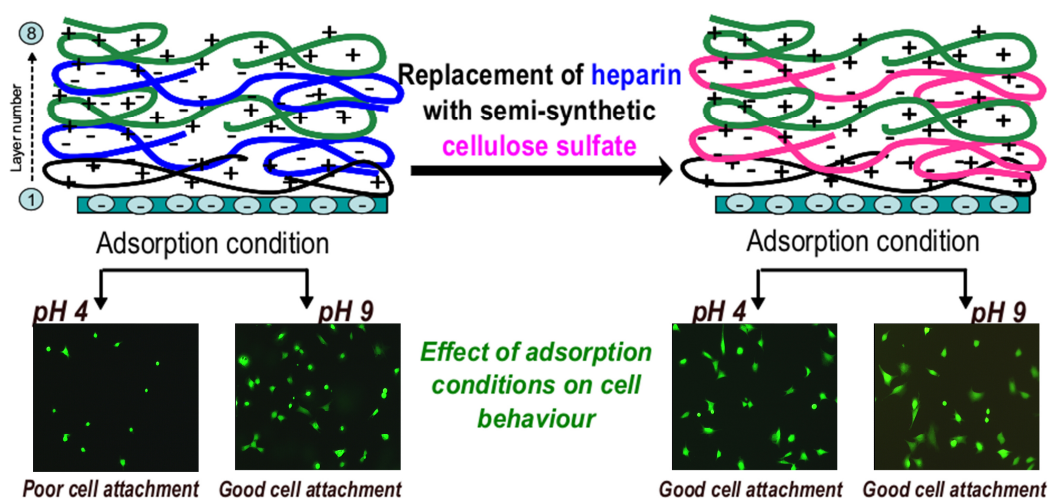
Reference

[1] M.V. Voinova, M. Rodahl, M. Jonson and B. Kasemo, Viscoelastic acoustic response of layered polymer films at fluid-solid interfaces: Continuum mechanics approach, *Phys Scripta*, 59 (1999) 391-396.

Chapter 5

Effect of molecular composition of heparin and cellulose sulfate on multilayer formation and cell response

Neha Aggarwal, Noomi Altgårde, Sofia Svedhem, Kai Zhang, Steffen Fischer, Thomas Groth



5.1. Abstract

Here, Layer by layer method was applied to assemble films from chitosan paired with either heparin or a semi-synthetic cellulose sulfate (CS) that possessed a higher sulfation degree than heparin. Ion pairing was exploited during multilayer formation at pH 4 while hydrogen bonding is likely to occur at pH 9. Effects of polyanions and pH value during layer formation on multilayers properties were studied by surface plasmon resonance (“dry layer mass”), quartz crystal microbalance with dissipation monitoring (“wet layer mass”), water contact angle and zeta potential measurements. Bioactivity of multilayers was studied regarding fibronectin adsorption and adhesion/proliferation of C2C12 myoblast cells. Layer growth and dry mass were higher for both polyanions at pH 4 when ion pairing occurred, while it decreased significantly with heparin at pH 9. By contrast CS as polyanion resulted also in high layer growth and mass at pH 9, indicating a much stronger effect of hydrogen bonding

between chitosan and CS. Water contact angle and zeta potential measurements indicated a more separated structure of multilayers from chitosan and heparin at pH 4, while CS led to a more fuzzy intermingled structure at both pH values. Cell behaviour was highly dependent on pH during multilayer formation with heparin as polyanion and was closely related to fibronectin adsorption. By contrast, CS and chitosan did not show such dependency on pH value, where adhesion and growth of cells was high. Results of this study show that CS is an attractive candidate for multilayer formation that does not depend so strongly on pH during multilayer formation. In addition, such multilayer system also represents a good substrate for cell interactions despite the rather soft structure. As previous studies have shown specific interaction of CS with growth factors, multilayers from chitosan and CS may be of great interest for different biomedical applications.

5.2. Introduction

Chemical and physical surface modifications are frequently employed to adjust biomaterials to specific medical applications.¹ Passivated coatings are used to make blood-compatible devices², bioactive surfaces which are desirable in many tissue engineering applications.³ Bioactive surfaces can be prepared by chemical binding of biogenic molecules like peptides, proteins or carbohydrates to establish covalent bonds, while adsorption exploits physical forces between surfaces and molecules.⁴ The latter techniques are not only easier but also more useful to maintain the bioactivity of rather labile species like proteins that may be damaged during chemical reactions. The layer-by-layer (LBL) method introduced by Gero Decher et al. represents such a technique based on electrostatic attraction and ion pairing by alternating adsorption of oppositely charged polyelectrolytes onto charged substrate.⁵ A large variety of biomolecules like proteins, DNA and also many carbohydrates represent polyelectrolytes and can be used to form multilayers by the LbL technique.⁶ Since the LbL technique is solution-based, complex material geometries and inner surfaces can be modified, which is advantageous for modification of implants and tissue engineering scaffolds.⁷ Another great advantage of the LbL technique is that the characteristics of multilayer films like charge, wetting properties, thickness and viscoelasticity can be tuned by the choice of polyelectrolytes (molar mass, charge density, chain stiffness) as well as the suspending solution properties (pH value, ionic strength, temperature).^{7,8} Many recent studies have looked at the interaction of cells with multilayers made of synthetic polyelectrolytes like poly (styrene sulfonate) (PSS) and poly (allyl amine) (PAA).⁹ In general, cell adhesion was lower

on polyanion-terminated multilayers and higher on polycation-terminated multilayers even after exposure to proteins like collagen and fibronectin.^{10,11} Since, cells require in general specific adhesive ligands for the interaction with integrins,¹² the adsorption of specific adhesive proteins like fibronectin or vitronectin is crucial for the bioactivity of surfaces.¹³ While much can be learnt from multilayer systems with such synthetic polyelectrolytes, medical applications of multilayers require the use of degradable and biocompatible polyelectrolytes.

Glycosaminoglycans (GAGs) have attracted increased interest recently due to their biocompatibility, degradability and intrinsic bioactivity.¹⁴ For example, heparin represents a strong polyanion that contains specific disaccharide units composed of either β -D-glucuronic acid or α -D-iduronic acid and 2-N-sulfo-glucosamine connected by a 1-4-glycosidic linkage. Heparin interacts with a large variety of proteins that regulate adhesion, movement, growth and differentiation of cells.¹⁵ Heparin has been used as component of hydrogels¹⁶ but also in forming multilayers on material surfaces¹¹ in the field of tissue engineering. However, an obvious disadvantage of heparin is the isolation from animal sources like porcine mucosa or bovine lung. This is not only limiting its availability in larger quantities but also related to significant differences regarding molecular composition, which varies between species and from batch to batch.¹⁵ Therefore, synthetic routes to modify natural occurring polysaccharides to achieve controlled heparinoid features might be of great use for many biomedical applications. For example, cellulose a naturally occurring polymer of anhydroglucose units linked by β -(1-4)-glycosidic bonds is one of the most abundant polysaccharides on earth. Chemical modifications of cellulose by regioselective carboxylation and sulfation have been carried out to achieve molecular similarity and bioactivity to heparin.¹⁷ Recent studies showed that cellulose sulfates (not the ones which were having carboxylic groups) had a higher bioactivity towards growth factors in comparison to heparin.^{18,19} Cellulose sulfates also demonstrated a high anticoagulant activity, like heparin in cooperation with anti-thrombin III.²⁰ Hence cellulose sulfates may represent an interesting material for production of hydrogels or bioactive surface coatings in different biomedical applications. Heparin has been successfully used in many studies with success as a bioactive surface coating.¹¹ By contrast only a few studies applied cellulose sulfates (CS) in multilayer coatings, i.e. to generate blood compatible surfaces²¹ or in preparation of microcapsules.²² So far, no studies about the effect of cellulose sulfate multilayers on adhesion and growth of cells exists. Therefore, it would be interesting to learn whether a cellulose sulfate with somewhat higher degree of sulfation and molecular weight would behave similarly to heparin regarding

film formation, surface properties and bioactivity towards protein adsorption, cell adhesion and proliferation.

In this study, polyelectrolyte multilayers (PEMs) were assembled either using heparin or cellulose sulfate as the polyanion and chitosan as a polycation that possesses good biocompatibility.²³ The cellulose sulfate selected here has demonstrated a moderate mitogenic and a high osteogenic activity in cooperation with growth factors FGF-2 and BMP-2 in previous studies.^{18,19} Since changes in the pH value of solutions affect charge and conformation of weak polyelectrolytes i.e. chitosan, variation in pH value were applied to affect formation of multilayers and resulting intrinsic and surface properties.^{11, 24} The bioactivity of these multilayers was studied regarding the adsorption of fibronectin and adhesion and growth of C2C12 myoblast cells. The result of this study show that multilayers from cellulose sulfate and chitosan possess certain advantages compared to those made of heparin and chitosan regarding their bioactivity and lower dependency on pH value during layer formation.

5.3. Materials and Methods

5.3.1. Materials.

Microcrystalline cellulose (MCC) with an average *DP* of 276 was received from J. Rettenmaier & Söhne GmbH (Rosenberg, Germany). *N,N*-dimethylformamide (DMF) was freshly distilled and deionized water was used in all experiments. Dialysis membrane from Spectrum Laboratories Inc (Rancho Dominguez, USA) has an approximate molecular weight cut off of up to 500 Daltons. Other chemicals were all of analysis grade and used as received.

Multilayer fabrication was done on glass cover slips of size 15 x 15 mm (Menzel, Germany), which were cleaned for 2 hours with 0.5 M NaOH (Roth, Germany) dissolved in 96% ethanol (Roth, Germany) followed by excessive rinsing with micropure water (10 X 5 minutes). New gold-coated sensors for SPR (IBIS Technologies, Hengelo, The Netherlands) and gold-coated AT-cut quartz crystals for QCM-D (Q-sense, Göteborg, Sweden) measurements were cleaned using 99.8% ethanol (Merck, Germany) and rinsed thoroughly with micropure water. After cleaning, sensors were immediately incubated over night in solution of 2 mM mercaptoundecanoic acid (95%, MUDA, SIGMA) in ethanol (p.a.) to obtain a negatively charged surface by the formation of a self-assembled monolayer exposing carboxyl groups.

Polyelectrolyte solutions of poly (ethylene imine) (PEI) (MW 750.000 g/mol, SIGMA, Germany), heparin (min 150 IU/mg, MW 8.000-15.000 g/mol, Applichem, Germany), cellulose sulfate and chitosan (medical grade) with a deacetylation degree of 85 % (MW 500.000 g/ mol, 85/ 500/A1, Heppe, Germany) were dissolved in deionized water containing 0.14 M NaCl at a concentration of 2 mg/ml under stirring. 0.05 M acetic acid was also added to the chitosan solution and it was solubilised at 50°C for 3 hours.

5.3.2. Synthesis of cellulose sulfate (CS)

The acetosulfation of cellulose was carried out as described before.²⁵ Briefly, 0.5 g cellulose was suspended over night in 25 ml DMF. The acetosulfating reagent, consisting of sulphuric acid and acetic anhydride in DMF was dropped into the cellulose suspension. After being kept at 50°C for 6 hours, the solution was cooled down to RT and poured into a saturated ethanolic solution of anhydrous sodium acetate. The precipitate was collected and deacetylated using 1 M ethanolic solution of sodium hydroxide at RT. Then, the deacetylated product was collected through centrifugation. After washing with 4% sodium acetate solution in ethanol, final products were dissolved in water. The pH value of the solution was adjusted to 8.0 with acetic acid/ethanol (50/50, w/w) and the solution was filtered, dialyzed against deionized water and lyophilized.

5.3.3. Characterization of cellulose sulfate (CS) and heparin

The contents of carbon, hydrogen and nitrogen were determined with Elemental Analyser vario EL from Elementar (Hanau, Germany). The content of sulphur was measured with Elemental Analyser Eltra CS 500 (Neuss, Germany). Total DS_S was calculated according to the equation:

$$\text{total DS}_S = (S\%/32)/(C\%/12) \quad (1)$$

The ¹³C NMR spectra were recorded at RT on Bruker DFX 400 spectrometer (Bruker) with a frequency of 100.13 MHz, 30° pulse length, 0.35 acq. time and a relaxation delay of 3 seconds. The scans of 20000 were accumulated and D₂O was used.

Molecular weights of CS in the form of mass and number-average molecular weights (MW_w and MW_n) are measured by size exclusion chromatography (SEC) with PSS Suprema 3000 and 100 Å columns (Polymer Standards Service GmbH, Mainz, Germany). The detection was carried out with a Waters 410 reflective index (RI) detector (Waters Corporation, Milford,

MA, USA) and 0.1 mol/l NaCl aqueous buffer was used as mobile phase. The columns were calibrated with pullulan standards (Sigma-Aldrich, Switzerland). Empower Pro software (Waters Corporation) was used for the analysis.

5.3.4. Polyelectrolyte multilayer assembly

Cleaned glass cover slips or gold-coated sensors were used as substrate for the multilayer deposition. A PEI layer was prepared as an anchoring layer for a homogenous coating and to obtain a surface with positive charge, followed by adsorption of heparin (HEP) or cellulose sulfate (CS) as the anionic layer and then chitosan (CHI) as the cationic layer. The multilayer films were fabricated by immersing the glass cover slips in polyelectrolyte solutions for 7 minutes followed by rinsing with deionized water containing 0.14 M NaCl (3x4 minutes). By alternating adsorption of CHI and HEP or CS, multilayers were build up to 7th and 8th layer with CHI and HEP/CS terminal layers, respectively. The pH value of the PEI and polyanionic (HEP/CS) solutions were adjusted to pH 4 and 9 with either HCl or NaOH, while the pH value of chitosan solution was kept constant at pH 4 as it becomes insoluble at pH values higher than 6. The two different systems prepared from polyanions HEP and CS paired with CHI at pH 4 and 9 conditions are abbreviated as CHI-HEP (4-4), CHI-HEP (4-9), CHI-CS (4-4) and CHI-CS (4-9).

5.3.5. Characterization of multilayer properties

5.3.5.1. Measurement of multilayer growth and mass

Surface plasmon resonance (SPR) using IBIS-iSPR equipment (IBIS Technologies B.V., Hengelo, Netherlands) and quartz crystal microbalance with dissipation monitoring (QCM-D) measurements using an E4 instrument (Q-Sense, Göteborg, Sweden) were performed to follow the multilayer formation process. Principally, SPR is based on the change in refractive index (RI) at the gold-liquid interface of the SPR gold sensor surface, caused by the adsorption of molecules. This is measured as a shift in the angle of the incident light (m°) and is proportional to the mass (Γ_{SPR}) of molecules adsorbed on the surface. For the instrument used here, this was estimated as²⁶:

$$122 m^\circ \approx 1 \text{ ng/ mm}^2 \quad (2)$$

Hence the “dry” mass of adsorbed polyelectrolytes was approximated by equation (2) disregarding small changes in refractive index of surface coatings due to adsorption of either chitosan or the different polyanions and salt ions as observed by others²⁷

The QCM-D technique is described in detail elsewhere.²⁸ Shortly, the QCM-D sensor (a quartz crystal disc) oscillates at its resonance frequency f when an alternating potential is applied. Mass adsorption on the sensor surface leads to a shift in this frequency (Δf). The Δf is related to the change in adsorbed mass (Δm_{QCM-D}) and can be estimated for thin, rigid, and evenly distributed surface films using the Sauerbrey equation.²⁹

$$\Delta m_{QCM-D} = -C\Delta f_n/n \quad (3)$$

where n ($n = 1, 3, 5, \dots, 13$) is the overtone number and C is the mass sensitivity constant that depends on the quartz crystal. For the crystal applied here, $f_0 = 5$ MHz and $C = 0.177$ mg/ m²Hz. The coupled water into the adsorbed film was estimated by comparing the mass obtained by QCM-D and SPR (assuming that the two masses were obtained under equivalent condition).

The same data can be exploited to determine the effective film density (ρ_{eff}) using the following equation

$$\rho_{eff} = \rho_f (\Gamma_{SPR} / \Delta m_{QCM-D}) + \rho_0 (1 - \Gamma_{SPR} / \Delta m_{QCM-D}) \quad (4)$$

where Γ_{SPR} is adsorbed amount calculated from SPR measurements, ρ_f is the bulk density of polymer ($\rho_{CHI} = 1410$ Kg m⁻³), and ρ_0 is the density of the liquid (997 Kg m⁻³).³⁰

The adsorbed mass is here calculated using the fifth overtone ($n = 5$) and is referred to as the Sauerbrey sensed mass, Δm_{QCM-D} and the total thickness (d) of the layers was calculated using the effective density as

$$d = \Delta m / \rho_{eff} \quad (5)$$

The dampening of the oscillatory motion as the driving potential is switched off is related to structural properties of the added layer on the sensor surface, and it is quantified as energy dissipation (ΔD).

In both SPR and QCM-D measurements, the polyelectrolytes were introduced into the flow cell of the device onto gold sensors treated with mercaptoundecanoic acid presenting carboxylic groups. This makes the gold surface negatively charged and the condition comparable with the glass for the multilayer formation process. First, the positively charged polyelectrolyte PEI was introduced to adsorb on the sensor surface for 7 minutes followed by

rinsing with NaCl solution for 12 minutes. After the formation of PEI, alternately HEP or CS and CHI layers were adsorbed up to 8 layers at pH 4 and 9. Each adsorption step was followed by the rinsing step described above to remove unbound polyelectrolyte.

The adsorption of plasma fibronectin (Roche, Germany) on the polyanion terminal layer was measured by QCM-D. Fibronectin was reconstituted and diluted to 20 $\mu\text{g/ml}$ in phosphate buffered saline (PBS, 150 mM NaCl, pH 7.4) and was introduced into the flow cell of QCM-D after the formation of last polyanion layer (valid for both type of pH conditions of both systems). The protein adsorption process was monitored for 1 hour to estimate the protein adsorption capacity of the terminal polyanion layer. All measurements were done twice and values obtained with both techniques are represented as averages.

5.3.5.2. *Water contact angle and surface zeta potential measurements*

Static contact angles were measured with ultrapure MilliQ water using an OCA15+ device (Dataphysics, Filderstadt, Germany) to determine the wettability of multilayer surfaces. Minimum three samples per pH combination and terminal multilayer surface were measured using the sessile drop method. 3-4 drops of 3 μl water with a flow rate of 0.5 $\mu\text{l/s}$ were applied and for each droplet, at least 10 independent measurements were recorded by the software of OCA15+ device. Each measurement was done twice, in triplicates and values obtained are represented as averages.

Streaming potential measurements were carried out to obtain zeta (ζ) potentials of multilayer surfaces by using a SurPASS device (Anton Paar, Graz, Austria). Glass cover slips with specific dimensions for the measuring chamber were used for sample preparation and zeta potential measurements. Two identical multilayer modified cover slips were fixed on stamps, which were placed oppositely in the SurPASS flow cell. The width of the flow cell was adjusted to a distance that a flow rate of 100 to 150 ml/min was achieved at a maximum pressure of 300 mbar. 1 mM potassium chloride was used as electrolyte. 0.1 N hydrochloric acid was used for pH titration. First, the pH value of the electrolyte was adjusted to pH 10.5 using 1 N sodium hydroxide before starting the measurement. The measurements repeated twice from pH 10.5 to 2.25 were performed by an automated titration program by using titration steps of 0.03 μl from pH 10.5 to 5.0 and 0.25 μl from pH 5.0 to 2.25.

5.3.6. Biological studies

5.3.6.1. Cell culture

Cryoconserved C2C12 cells (skeletal muscle cell line) (DSMZ, Germany, Product Nr.: ACC 565) were thawed and grown in Dulbeccos modified Eagle medium (DMEM, Biochrom, Germany) at 37°C in humidified 5% CO₂/95% air atmosphere using a NUAIRE® DH Autoflow incubator (NuAire USA). DMEM was supplemented with 10% fetal bovine serum (FBS, Biochrom), 2 mM L-Glutamine, 100 U/ml Penicillin and 100 µg/ml of Streptomycin (Biochrom, Germany). Cells were harvested from the almost confluent culture flask by using 0.25% Trypsin, 0.02% EDTA (Biochrom, Germany) followed by subsequent washing with DMEM and resuspended in DMEM with 10% FBS at a concentration of 25,000 cells/ml.

5.3.6.2. Measurement of cell adhesion and spreading

Adhesion of C2C12 cells was studied on glass cover slips coated with multilayer coatings of CHI and polyanion (HEP and CS) terminated. PEM modified glass cover slips were placed into 12-well tissue culture and sterilized with 70% ethanol for 10 min followed by excessive rinsing with sterile PBS. The resuspended cells were seeded on the sterilized samples in DMEM supplemented with 10% FBS (FBS, Biochrom) and incubated for 4 hours at 37°C in a humidified 5% CO₂/95% air atmosphere. After incubation, the culture medium was replaced with fresh medium twice to remove non-adherent cells. 5 µl fluorescein diacetate (FDA, SIGMA) solution (0.01% vol/vol) was added per well containing 1 ml of cell culture medium and incubated for 2-3 minutes before taking the images with a fluorescence microscope Axiovert 100 (Carl Zeiss Microimaging, Jena, Germany) equipped with a CCD camera. Image processing software “ImageJ, NIH” was used to quantify the data for cell adhesion and area calculation of duplicate experiments with at least five images per sample.

5.3.6.3. Cell morphology

The morphology of C2C12 cells was studied after 4 hours incubation at 37°C on terminal polyanion layers (either CS or heparin) in DMEM supplemented with 10% FBS (FBS, Biochrom) by phase contrast and immunofluorescence microscopy. Adherent cells were fixed with a 4% Paraformaldehyde solution (RotiHistofix[®], Roth GmbH) and rinsed with PBS. The cells were then permeabilized with 0.5% vol. Triton X-100 in PBS for 5 minutes. After

extensive rinsing with PBS, non-specific binding sites were blocked with 1% wt. bovine serum albumin (BSA, Merck) in PBS at RT for 30 minutes. C2C12 cells were stained by subsequent incubation with BODIPY[®] phalloidin (Invitrogen, Germany) to visualize actin, and mouse monoclonal antibody against vinculin (SIGMA) and Cy2[®]conjugated AffiniPure Goat Anti-Mouse IgG-conjugated anti-mouse immunoglobulin (Dianova, Germany) to show focal adhesions. Cell nuclei were stained with TO-PRO[®]3 Iodide (Invitrogen, Germany). All incubations were performed for 30 minutes followed by extensive washing with PBS. The samples were finally mounted with Mowiol (Roth, Germany) and examined with confocal laser scanning microscopy (LSM 710, Carl Zeiss MicroImaging GmbH, Jena, Germany) using a 63X oil immersion objective.

5.3.6.4. *Growth of C2C12 cells*

CHI-HEP and CHI-CS multilayers prepared on glass cover slips were placed in 12-well plates. 1 ml (25,000 cells/ml) C2C12 cells suspended in DMEM with 10% FBS were seeded either on terminal CHI or polyanion terminated multilayers and cultured for 1 and 3 days. Growth of cells was monitored by a phase contrast microscopy with Axiovert 100 equipped with a CCD camera and pictures were taken at the different days of culture. The quantity of viable cells was measured the same day with QBlue fluorescence assay (BioChain, USA), which quantifies the metabolic activity of cells. On the measuring day, medium with FBS was removed, samples were transferred into the new 12-well plates (to avoid the inclusion of cells grown on well plate surface as the cover slips were square shaped) and were washed with DMEM only, once. Then 500 μ l fresh DMEM were added to each well followed by 50 μ l Qblue assay reagent. After 3 hours of incubation at 37°C, 100 μ l of the supernatant was transferred from each well to a 96-well black plate. Fluorescence intensity (excitation wavelength 544 nm, emission wavelength 590 nm) was measured with a fluorescence plate reader (BMG LABTECH, Fluostar OPTIMA, Offenburg, Germany).

5.4 Results and Discussion

5.4.1. Synthesis of cellulose sulfate and analysis of chemical compositions

Cellulose sulfate (CS) was prepared through acetosulfation of cellulose using sulfuric acid as sulfating agent (Table 5.1). The compositions of synthesized CS and commercial heparin (HEP) were studied by ¹³C NMR spectroscopy according to previous studies^{17,19,25,31}

(Figure 5.1) and elemental analysis. The distribution of substituents within the repeating units are summarised in Table 5.1.

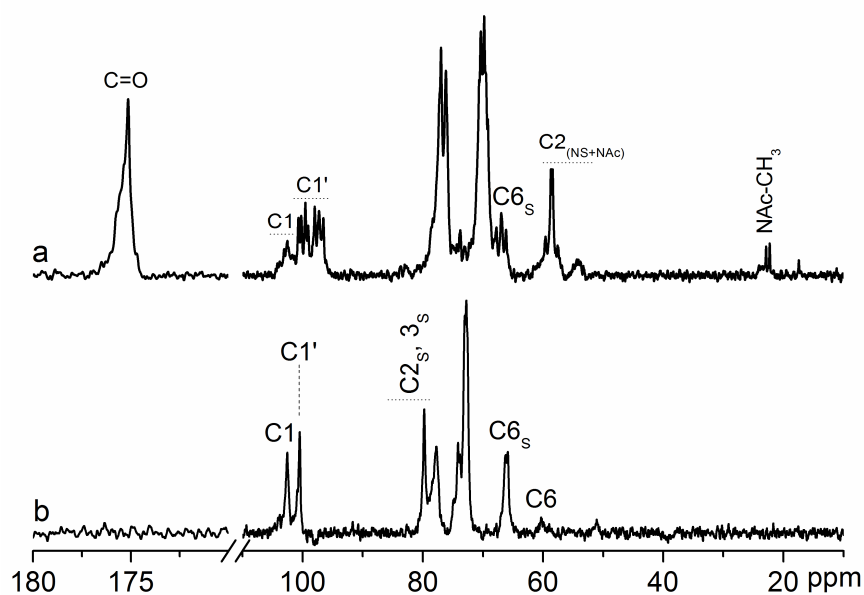


Figure 5.1: ^{13}C NMR spectra (120-10 ppm) of (a) heparin and (b) cellulose sulfate in D_2O at room temperature.

After the sulfation of primary hydroxyl groups at C6 position of anhydroglucose unit (AGU) of cellulose, the signal of C6 shifted from 60 ppm to 66 ppm (Figure 5.1b)^{17, 25}. Thus, the ratio of integrals of signals ascribed to C6' and (C6'+C6), $I_{\text{C6}'}$ and $I_{(\text{C6}'+\text{C6})}$, is equal to the partial sulfation degree at C6 position (DS_{S6}). Subsequently, the partial DS_{S6} was estimated based on $I_{\text{C6}'}/(I_{\text{C6}'}+I_{(\text{C6}'+\text{C6})})$ according to a previous studies.^{25,31} After the sulfation of hydroxyl groups at C2 position of cellulose, the signal of C1 shifted from 102.5 to 100.5 ppm (Figure 5.1b). Similar to DS_{S6} , the partial DS_{S2} was estimated using the integrals of signals derived from C1 and C1' according to $I_{\text{C1}'}/(I_{\text{C1}'}+I_{(\text{C1}'+\text{C1})})$ (see Table 5.1).²⁵ At the same time, signals between 80 and 82 ppm are attributed to C2 and C3 with sulfate groups at these positions.^{25,31} The sum of DSs of all functional groups determined by ^{13}C NMR is close to that determined by elemental analysis shown as DSs in Table 5.1. The slightly lower sum determined by ^{13}C NMR might be due to some sulfation at C3 position, which was below detection limit.

Within the ^{13}C NMR spectrum of HEP shown in Figure 5.1a, the signal around 102.5 ppm is attributed to C1, while the shifted signals of C1' between 96 and 101 ppm are due to the sulfation at C2 positions, which can be hydroxyl groups of the acidic repeating units or the amino groups of glucosamine units.^{25,32} Thus, the partial DS_{S2} was calculated to be 0.8, based on the ratio between the signal's integrals of C1' and (C1'+C1) (see Table 5.1). The signals between 65 and 68 ppm are attributed to sulfated C6 position.^{25,33} Using the integrals of the

signals ascribed to C_{6s} and the signals of (C1'+C1), the partial DS_{S6} can be estimated as 0.27 (see Table 5.1). The sum of partial DS_{S6} and DS_{S2} is altogether 1.07, which is close to the total DS_S determined by elemental analysis (see Table 5.1). Moreover, the glucosamine units within HEP backbone are generally sulfated or acetylated at amino groups.^{32,33} The carbons of CH₃-groups in acetyl groups showed signals around 22 ppm (Figure 5.1a). The signals between 50-60 ppm are derived from C2 with sulfated or acetylated amino groups.^{25,33} Based on the ratio of the integrals of signals ascribed to C_{2(Ns+NAc)} and (C1'+C1), the content of glucosamine units within the backbone of HEP was estimated to be 74%. Thus, the content of acidic repeat units as β-D-glucuronic acid and α-D-iduronic acid is 26%, i.e. the degree of oxidation (DO) is approximately 0.26 for the heparin backbone. Moreover, C₆ in carboxyl groups represents a signal at 175 ppm within the ¹³C NMR spectrum of HEP (Figure 5.1a). These carbons can be found in both β-D-glucuronic acid and α-D-iduronic acid as repeating units of HEP.³³ In comparison, no carboxyl groups are expected and found within the repeating units of CS (Figure 5.1b).

The molecular weight of CS was determined via SEC (chromatogram not shown here). It is obvious that the length of cellulose chains was reduced during the sulfation process, comparing the MW_n of 37549 for CS and MW_n of 44712 for starting cellulose (Table 5.1). However, the degree of sulfation of monomeric units of CS was significantly higher (DS_S ~ 1.6) with no carboxylic groups compared to HEP (DS_S ~ 1.0). The relatively low degree of sulfation of HEP compared to values reported by others sheds also a light on the variability of molecular composition of HEP depending on species and sources.¹⁵

Table 5.1: Preparation and characterization of CS and heparin

| samples | molar ratio ^a | reaction temperature (°C) /time (h) | DS _S ^b | | | DO | MW _w | MW _n | MW _w /MW _n |
|---------|--------------------------|-------------------------------------|------------------------------|------------------|-----------------------|------|-----------------|-----------------|----------------------------------|
| | | | DS _{S6} | DS _{S2} | total DS _S | | | | |
| CS | 3 / 8 | 50 / 6 | 0.91 | 0.55 | 1.57 | 0 | 77748 | 37549 | 2.07 |
| Heparin | n.a. | n.a. | 0.27 | 0.8 | 1.01 | 0.26 | 8000-25000 | | |

^a Molar ratios in mol sulphuric acid and mol acetic anhydride per mol AGU; ^b DS_{S6}, DS_{S2} and DO were analysed with ¹³C NMR spectroscopy. The total DS_S were determined via elemental

analysis. The integration values are generally accurate within 5% fault range. (n.a. - not applicable), MW_w of heparin: provided by the data sheet from the supplier.

5.4.2. Characterization of multilayer formation

The surface sensitive analytical techniques, SPR and QCM-D were used here to study the multilayer growth of CHI-HEP and CHI-CS systems in dependence on the pH regime. These investigations were used to deduce the amount of adsorbed polysaccharides (SPR) as well as the total layer mass including solvent (QCM-D). The SPR angle shifts were used to calculate the layer mass according to equation (2). Figure 5.2a & b show the effect of pH on adsorbed mass during multilayer formation with HEP and CS as polyanions and CHI as polycation. The obtained multilayer mass calculated with equation (2) represents a reasonable approximation for CHI-HEP multilayers at pH 4.2 and 150 mM NaCl since it is comparable with the results obtained by other groups.²⁷ The multilayer growth for the CHI-HEP (4-4) system was exponential as also shown for others polysaccharide-based multilayers systems.¹⁴ Recent studies suggested that diffusion of CHI is responsible for exponential film growth in HEP-CHI multilayers.³⁴ However, QCM-D dissipation measurements in the present study indicate that HEP and not CHI is the diffusible species (see Figure 5.3c & d). This may be due to the fact that CHI in the present study has a higher molecular weight than in the previous work.³⁴ Layer mass increase was significantly higher at pH 4 compared to pH 9 (Figure 5.2a & b). Here, ion pairing dominates, and protonation of CHI amino groups leads to the adsorption of more material.³⁵ Indeed, only a low increment of layer mass was observed during assembly of CHI-HEP (4-9) system. Ion pairing cannot occur here since the amino groups of the previously adsorbed CHI are not protonated. Hence, hydrogen bonding should become the prevailing mechanism, which was shown recently for HEP-CHI interaction in other studies.³⁶ Notably both HEP and CHI contributed almost equally to the layer mass increase at both pH values as evident by SPR measurements. By contrast, a different behaviour was observed for CHI-CS multilayer system. The SPR curves for the CHI-CS system (Figure 5.2a & b) show a much higher increase of the adsorbed mass during CS deposition (even layer number) as opposed to CHI deposition steps (odd layer number) under both pH conditions, representing a staircase-shape. Previous studies on multilayer formation with polysaccharides provides evidence for a dominating role of sulfate groups over carboxylic groups using poly-L-lysine.¹⁴ However, this does not explain why more material was adsorbed because in these studies, increasing charge density of molecules lead to lower

layer mass.¹⁴ The staircase pattern, which was observed during the formation of CHI-CS multilayers, might be due to charge compensation by addition of chitosan and formation of a quasi-soluble complex with CS thereby stripping it off from the surface. This could explain why there was almost no increase in the mass adsorption when CHI was deposited. Previous studies have also shown such phenomenon of formation of a quasi-soluble complex with the negative polymer, stripping it off from the surface and resulting in a lower film thickness.³⁷ It is also interesting to note that the difference in mass adsorption for CHI-CS multilayer between pH 4 and 9 was not so great in comparison to CHI-HEP system. Since ion pairing cannot occur during adsorption at pH 9, hydrogen bonding might be the prevailing mechanism for CS adsorption also here. It might be speculated here that the hydrogen bonding capacity of CS is an essential component during adsorption at both pH values because of the intermediate degree of sulfation, remaining hydroxyl groups can undergo hydrogen bonding to CHI. In this context it is also noteworthy that others observed adsorption of CHI under acidic and basic conditions on cellulose, which was explained by the structural similarity of both polymer backbones.³⁸ Hence, the higher sulfate content and ability to form hydrogen bonds may add to the higher contribution of CS to multilayer mass compared to HEP.

Findings of QCM-D measurements are shown in Figure 5.3. For the CHI-HEP (4-4) system, the multilayer growth was also exponential while the mass increase was very low and showed a rather linear behaviour for CHI-HEP (4-9) system. The low layer thickness displayed in Table 5.2 calculated by comparison of “dry” layer mass measured with SPR and “wet” by QCM-D according to equation (4) & (5), shows that at pH 9 only very thin surface coatings were generated, indicating adsorption and desorption of material with each steps. This might be due to the fact that the HEP was adsorbed at pH 9 followed by CHI adsorption at pH 4, which may lead to stripping of adsorbed HEP and complexation in solution.³⁷ On the other hand, the layer thickness increase after deposition of the 8th HEP layer at pH 4 was about 5 nm, which is on the length scale of the hydrodynamic radius of HEP according to a previous study.³⁵ It is also important to note that addition of HEP did not change the relatively high water content of multilayers at pH 4 (75 %), while a slight decrease of multilayer hydration was observed at pH 9 (Table 5.2). Again layer mass increase for the CHI-CS system showed a staircase-shaped curve with lower mass increase by CHI but higher by CS at pH 4, although the effect was not so pronounced as observed during SPR measurements. A similar behaviour was observed during multilayer formation from poly-L-lysine and hyaluronan in another study.¹⁴ This was particularly obvious at pH 9 when a rather linear mass increase was

observed during the last deposition steps (see Figure 5.3b). In strong contrast to the CHI-HEP system, the layer mass at pH 9 regime was higher than at pH 4. Particularly the observed linearity of mass increase at pH 9 at later deposition steps indicates that also CHI adsorption contributes to layer mass increase and uptake of water.

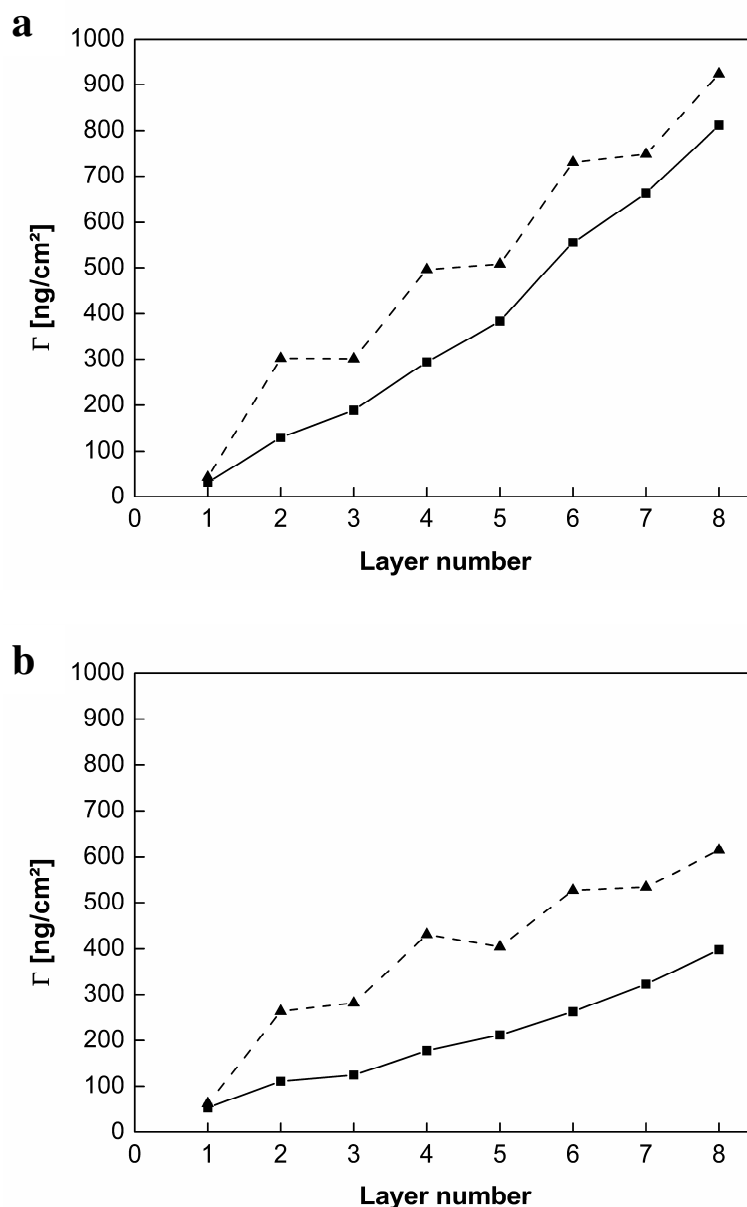


Figure 5.2: Multilayer mass Γ_{SPR} calculated from SPR angle shifts at (a) pH 4 and (b) pH 9 (CHI was always kept at pH 4). Solid lines (■): CHI-HEP system, dashed lines (▲): CHI-CS system. Layer 1 is always PEI, even layers: polyanion, odd layers: polycation.

The obvious inverse relationship between “dry” layer mass measured by SPR and “wet” mass by QCM-D for both pH regimes shown in Table 5.2 points to the fact that the CHI-CS (4-4)

multilayers must be more condensed due to electrostatic cross-linking than CHI-CS (4-9), where hydrogen bonding is anticipated and sulfate groups from CS and amino groups from CHI counter ions and couple water, respectively. This supports further the idea that hydrogen bonding in the CHI-CS system is an important parameter during multilayer formation at both pH values that leaves part of charges unpaired that contribute to attraction of counter ions and water molecules inside the layer. Additional evidence for a different way of layer built-up comes from calculation of layer thickness shown in Table 5.2. Here, the increase in layer thickness at the addition of the 8th layer CS is lower than for HEP at pH 4 despite the higher molecular weight of CS, which indicates either a different conformation of molecules or by the formation of a highly intermingled layer with integration of CS molecules inside CHI. Such intermingling of polyanions with CHI was suggested recently for HEP by Boddhi et al.³⁵ and seems to be more dominant for CS in the current study.

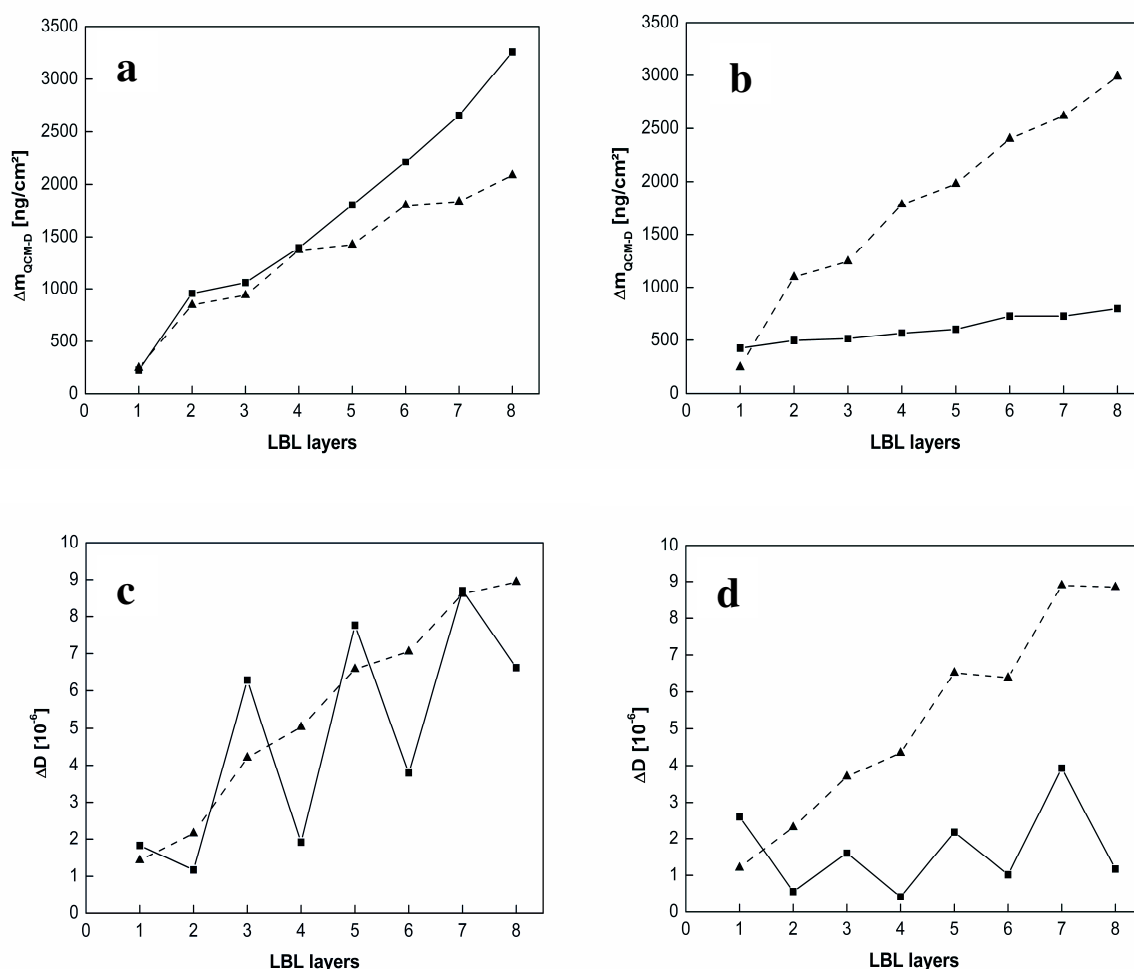


Figure 5.3: (a & b) shows QCM-D sensed mass calculated by the Sauerbrey equation while (c & d) measurement of dissipation change ΔD by QCM-D at (a, c) pH 4 and (b, d) pH 9

(CHI was always kept at pH 4). Solid lines (■): CHI-HEP system, dashed lines (▲): CHI-CS system. Layer 1 is always PEI, even layers: polyanion, odd layers: polycation

The dissipation measurements by QCM-D also revealed striking differences between both multilayer systems (Figure 5.3c & d). For the CHI-HEP system fluctuation of dissipation were observed with increase of dissipation after addition of CHI and a strong decrease after addition of HEP. These effects were also dependent on the pH value during multilayer formation with larger changes seen at pH 4. The increase in stiffness after addition of HEP is a strong hint that HEP and not CHI is the diffusible species in this system that leads to additional cross-linking of multilayers. This may be due to the higher molecular weight of CHI used in the current work compared to previous studies where CHI was suggested to be diffusible species.³⁴ Moreover, previous studies have shown diffusion of HEP in multilayer systems with similar effects on film elasticity that was explained by increased electrostatic cross-linking inside films after addition of HEP.²⁷ No such differences were observed for CHI-CS system. Here an almost linear increase with addition of either CHI or CS was observed with little difference between pH values during layer formation except the final steps at pH 9. Indeed the increasing dissipation values suggest a softer nature of films formed from CHI and CS particularly at pH 9. The higher water uptake under these conditions indicates that unpaired charges of CS as well as polar amino and hydroxyl groups take up essential quantities of water.

QCM-D studies were also used to measure the adsorption of fibronectin on the terminal polyanion layer. Fibronectin was used as a representative to measure the protein adsorption abilities of these multilayer surfaces for later cell adhesion and growth studies which were carried out in the presence of serum proteins (which also contains fibronectin). Table 5.2 shows fibronectin adsorption on both types of multilayer systems at both pH set-ups. Fibronectin addition on CHI-HEP (4-9) multilayers showed a decrease in frequency, which indicates adsorption of fibronectin, while for CHI-HEP (4-4) multilayers the frequency increased, which might be due to loss of material from the multilayer. This is in line with previous studies showing that there is no adsorption of fibronectin on terminal HEP layers at pH 4.^{39,24} On the other hand, fibronectin adsorption was seen for both of the CHI-CS systems, but was higher for CHI-CS (4-4) system.

Table 5.2: Multilayer mass, water content, layer thickness and apparent fibronectin adsorption on terminal HEP and CS layer

| | pH regime | Γ_{SPR}^a (ng/cm ²) | Δm_{QCM-D}^b (ng/cm ²) | Water content ^c | Layer thickness ^d (nm) | Fibronectin adsorption ^e (ng/cm ²) |
|-----------------------|-----------|---|---|----------------------------|--------------------------------------|--|
| (HEP-CHI) | pH 4 | 663 | 2655 | 75% | 24.1 | - |
| 7 th layer | pH 9 | 323 | 726 | 56% | 6.2 | - |
| (CHI-HEP) | pH 4 | 812 | 3257 | 75% | 29.6 | 0 |
| 8 th layer | pH 9 | 398 | 797 | 50% | 6.6 | 549 |
| (CS-CHI) | pH 4 | 749 | 1837 | 59% | 15.8 | - |
| 7 th layer | pH 9 | 535 | 2614 | 80% | 24.2 | - |
| (CHI-CS) | pH 4 | 924 | 2085 | 56% | 17.7 | 832 |
| 8 th layer | pH 9 | 615 | 2988 | 79% | 27.6 | 248 |

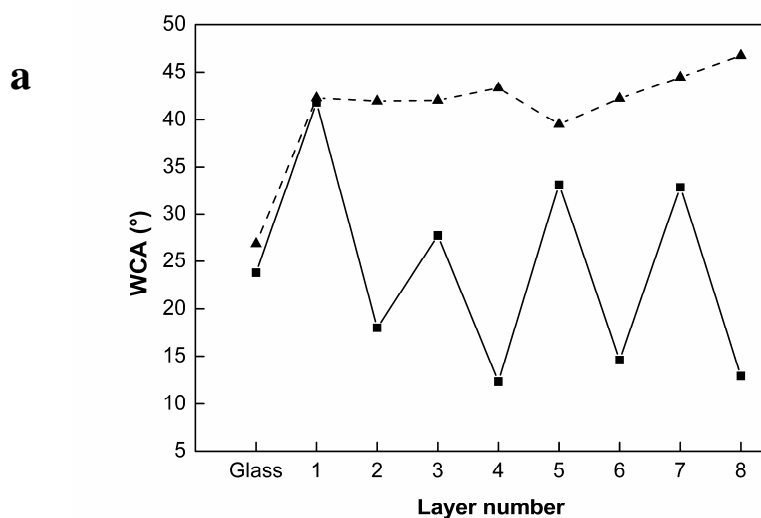
^a) SPR masses were estimated using equation (2); ^b) QCM-D masses were estimated using the Sauerbrey equation and the frequency shift at the 5th overtone; ^c) apparent water content was approximated by $(m_{QCM-D} - m_{SPR})/m_{QCM-D} * 100$. ^d) Layer thickness was calculated as described above in section 2.5.1 by equations (4) and (5). ^e) QCM-D frequency shifts (Δf) were used for calculation of fibronectin adsorption by Sauerbrey equation (3).

5.4.3. Measurements of wetting properties

Static water contact angle (WCA) measurements were done after the deposition of each layer for both types of multilayer systems prepared at pH 4 and 9. Figure 5.4a & b show the WCA values of clean glass, PEI (1st layer), polyanions (even number layers) and CHI (odd number layers). CHI-HEP multilayers showed alternating values with lower WCA for HEP and higher for CHI at both pH regimes. Contact angles measured for CHI-HEP (4-4) system showed greater differences as compared to CHI-HEP (4-9). This is a strong support of the idea that both electrolytes were more separated forming ad-layers constituted by either CHI or HEP. These differences in contact angles between the CHI and HEP layers solely represent the

characteristics of terminal layer and indicate the formation of more distinct layers without or less intermingling of polyelectrolytes during the fabrication of such multilayer systems. HEP is by far more hydrophilic because of the charged carboxylic and sulfate groups at pH 4. Hence lower contact angles are found when HEP is added. Similar findings were made by other groups showing also an oscillation of water contact angles during multilayer formation from CHI and HEP at acidic pH values and the same ionic strength.²⁷

By contrast lower differences were observed with CHI-HEP (4-9) layers, which indicate a more intermingled nature of multilayers. On the other hand, no such alternating WCA values were observed in CHI-CS multilayer systems formed at both pH 4 and 9. After the WCA increase due to the adsorption of PEI there was a small increase of WCA for both pH 4 and pH 9 regime. However, WCA values for final layers were higher in case of pH 4 compared to pH 9. The fact that no changes of wetting properties were observed strongly supports the idea that CS is rather integrating into CHI layers than forming well separated ad-layers. In addition the finding that mean WCA values at pH 9 were lower than at pH 4 is in line with the higher water content of this system as shown in Table 5.2 and allows the conclusion that more CS is adsorbed.



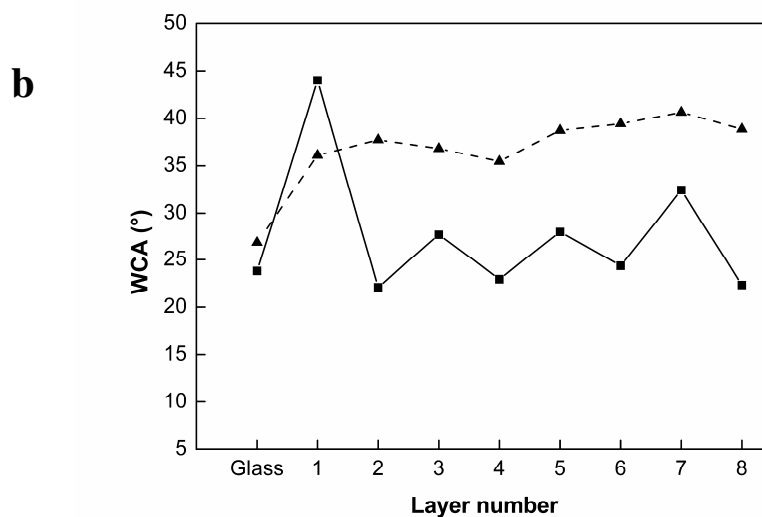


Figure 5.4: Water contact angle (WCA) measurements during multilayer formation at (a) pH 4 and (b) pH 9 (CHI was always kept at pH 4). Solid lines (■): CHI-HEP system, dashed lines (▲): CHI-CS system. Layer 1 is always PEI, even layers: polyanion, odd layers: polycation.

5.4.4. Measurement of zeta potentials

Figure 5.5 shows zeta potentials of the terminal CHI and polyanion (HEP or CS) layers prepared at pH 4 and pH 9 in dependence of pH value of electrolyte solution (1 mM KCl). The results show that whatever the pH was during layer preparation and independent of the terminal layer (either CHI or polyanion), zeta potential was positive at acidic pH values and became negative at basic pH values during the automatic titration process. Zeta potential measurements of polyelectrolyte multilayer systems which are in contrast to WCA measurements are not only sensitive to terminal layer composition, but also represent a potential permeable swollen surface layer.⁴⁰ Accordingly in multilayer systems polycations dominate the potential at acidic pH values while the negative charges of polyanions are displayed at basic pH values. When comparing the positive zeta potentials at pH 3 it is obvious that zeta potentials of CHI-CS multilayer were about 20 mV lower than CHI-HEP, except when CHI was terminal layer for systems formed at pH 9. This is well in line with the conclusions drawn from SPR and QCM-D studies that CHI is a minor component in the CHI-CS system. Such model is also supported by the observation that the point of zero charge (when zeta potential is zero) was about one pH unit lower for CHI-CS systems independent on terminal layer and pH during formation (see Figure 5.5a-d). A comparison of zeta potentials when CHI was the terminal layer (see Figure 5.5a and c) shows equal or lower

potentials for the CHI-CS system that may be due to the higher content in sulfate groups of CS compared to HEP. On the other hand zeta potentials in the acidic range (above pH 7, Figure 5.5b) shows lower zeta potentials for the CHI-HEP system, while no such difference was detected in multilayer formed at pH 9. This supports further the idea of more separated multilayers in CHI-HEP (4-4) system with a domination of the polyanion HEP as terminal layer on surface charge and more intermingled, fuzzy multilayers formed by CHI-CS at both pH conditions and CHI-HEP (4-9) system.

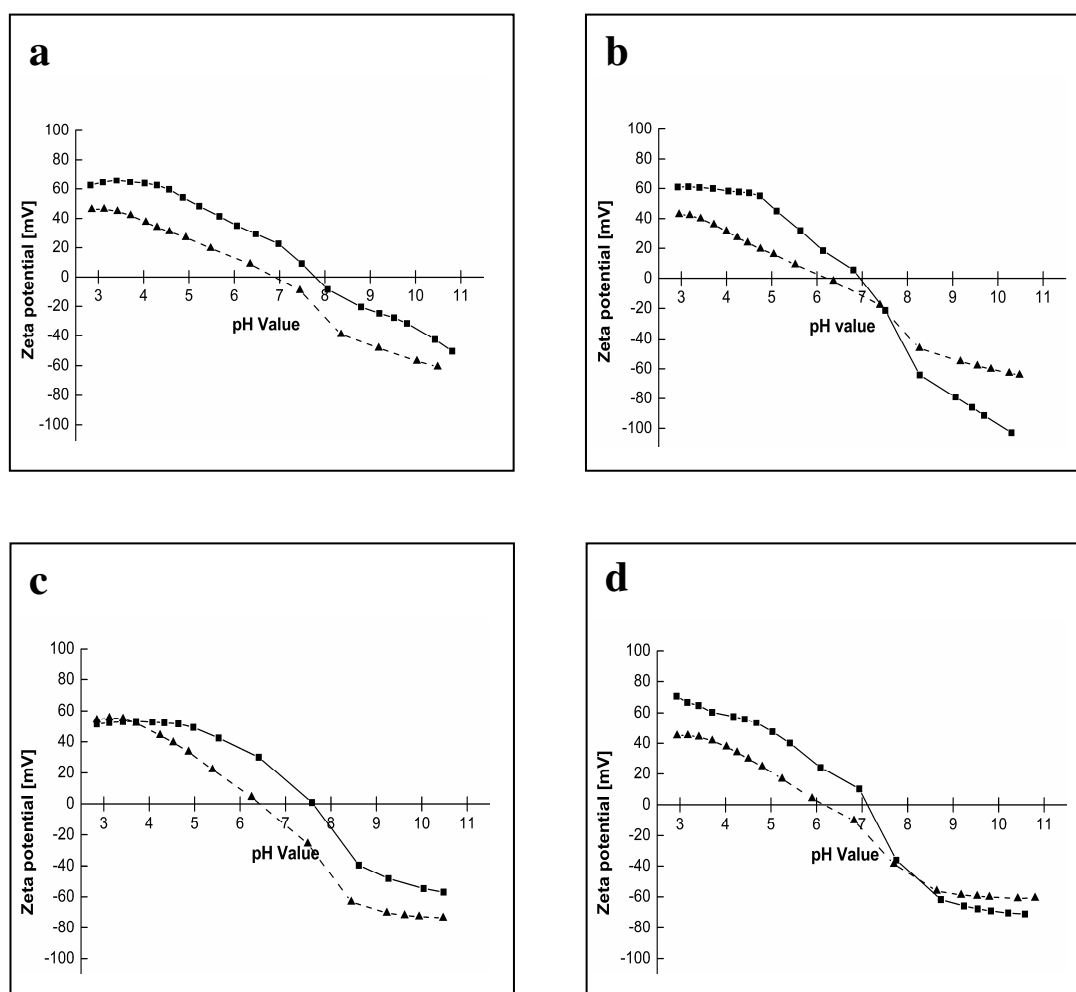


Figure 5.5: Zeta potential measurements of outermost CHI (7th) and polyanion (8th) terminal layers for both multilayer systems (HEP and CS) prepared at (a, b) pH 4 and (c, d) pH 9. (a, c) show CHI terminal layers, (b, d) polyanion terminal layers. Solid lines (■): CHI-HEP system, dashed lines (▲): CHI-CS system

5.4.5. Adhesion and growth of C2C12 cells on multilayers

Cell adhesion studies were performed to study the effect of multilayer composition and pH during their formation on adhesion and growth of cells. Here C2C12 cells were selected as a useful model because of their ability to differentiate into myotubes or osteoblast-like cells depending on mechanical properties of substrata, but also presence of osteogenic growth factor BMP-2.^{41,42,19} Multilayer surfaces (without any pre-adsorption of proteins) were seeded with C2C12 cells in medium containing 10% fetal bovine serum, which contains also adhesive proteins with HEP-binding domains like vitronectin and fibronectin.⁴³ Cells were stained with fluorescein diacetate (FDA) and micrographs were used for analysis of cell numbers and size. Results of quantitative evaluation are shown in Figure 5.6.

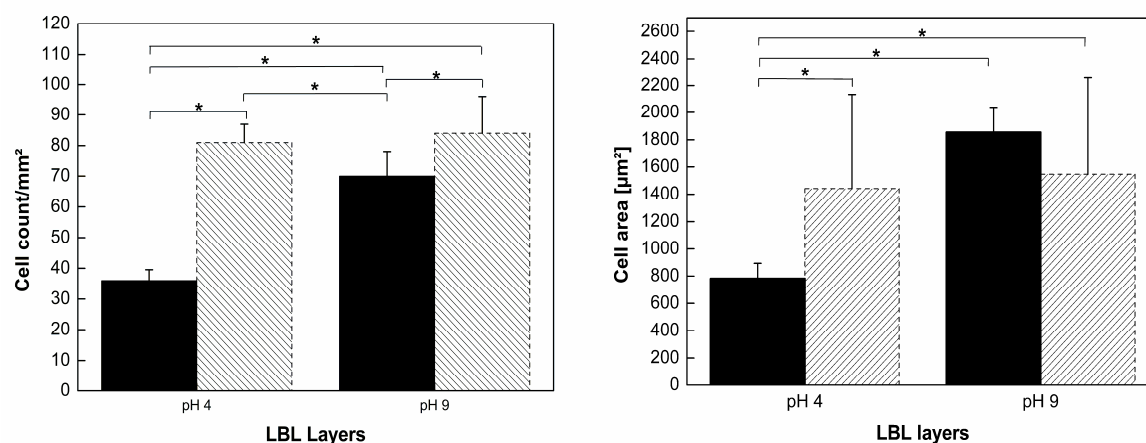


Figure 5.6: Adhesion (left) and size (right) of C2C12 cells plated 4 hours in DMEM with 10 % FBS on polyanion (HEP or CS) terminated multilayers prepared at either pH 4 or pH 9. (HEP - black bars, CS - hatched bars). Data represent means, standard deviations and ANOVA Significance level of $p \leq 0.05$ is indicated by the asterisks.

The quantitative analysis of cell adhesion after 4 hours showed a strong effect of pH value during assembly of multilayers for the CHI-HEP system. Here the number of adhering cells but also their size, i.e. their spreading was significantly lower on CHI-HEP (4-4) system as compared to CHI-HEP (4-9). The low number of adhering cells and their low degree of spreading are in agreement with the lack of fibronectin adsorption shown here and in previous studies.^{39, 24} Such finding is somewhat surprising because the presence of HEP should enable significant binding of fibronectin due to its HEP-binding domain.¹⁵ However, provided HEP adsorbs on chitosan at pH 4, when both molecules are highly charged, side-on with little loops

then the required steric interaction of HEP with fibronectin HEP-binding domains might be impaired. Similar findings on low binding of the growth factor BMP-2 to HEP that possesses a HEP-binding domain, were also made in ternary multilayer systems with hyaluronan and HEP as polyanions.⁴⁴ In addition also the higher water content of multilayers formed at pH 4 could be a reason for the lower cell adhesion as it is observed on hydrogels in general.⁴⁵ On the other hand, the similar or even higher water content and also dissipation values of CHI-CS multilayers formed either at pH 4 or pH 9 do not show such low cell adhesion (see below), which supports the idea that the lack of interaction of HEP with adhesive proteins is a major reason for the observation. By contrast, cell adhesion and spreading of C2C12 cells was high on CHI-HEP (4-9) multilayers, which is also in line with fibronectin adsorption, lower layer thickness and water content of these surface coatings. However, such a straight forward interpretation of cell adhesion on multilayers formed at both pH values from CHI-CS was not possible. There was no dependency of cell adhesion and spreading on pH value during formation of CHI-CS multilayers. The number of adhering cells were even exceeding those on terminal HEP layers of CHI-HEP (4-9) system, while cell spreading remained comparable. The possible reason behind such cell behaviour on both types of CHI-CS multilayers (pH 4 and 9) can be attributed to their protein (fibronectin/vitronectin) binding ability. The adsorption of proteins might have played a more important role for cell adhesion and spreading than the differences in water content and other multilayer properties. Hence it is important to notice that the critical fibronectin concentration to promote adhesion and spreading might have been already achieved in accordance to studies of Garcia et al. and K. Kirchof.^{46, 39} Also along with fibronectin, vitronectin possesses also a heparin-binding domain that promoted cellular interactions and leading to the formation of focal adhesion addressing alpha v beta 3 integrins⁴⁷ and is also the major attachment factor in serum. It is also interesting to note that cell spreading on CHI-HEP (4-4) multilayers corresponds well to data from another study about C2C12 cell spreading on soft multilayers formed from poly-L-lysine and hyaluronan while spreading on CHI-CS multilayers that have apparently similar mass and viscoelastic properties like CHI-HEP (4-4), is similar to cell behaviour on cross-linked PLL-HA multilayers in the study of Ren et al.⁴⁸

Additionally immune fluorescence studies were carried out with C2C12 cells adhering for 4 hours under the same conditions as described above. The images of C2C12 cells show in Figure 5.7 the staining of actin cytoskeleton by BODIPY-phalloidin (red), focal adhesions with vinculin by a monoclonal antibody (green) and nuclei by TO-PRO-3 (blue). Also here a strong effect of pH during multilayer formation was evident for CHI-HEP system, because

C2C12 cells were round and loosely attached on CHI-HEP (4-4) multilayers and were not retained during immunofluorescence staining. Hence, no images could be made for cells on these surfaces. On the other hand appearance and size of C2C12 cells on terminal HEP layers (pH 9 regime) and CS layers (pH 4 regime) were not very different, which corresponds also well to the quantitative data from adhesion studies shown in Figure 5.6. Hence Figure 5.7a shows here only C2C12 cells on terminal HEP layers prepared at pH 9 conditions. The cells are elongated with long actin stress fibres (red structures), while there were only poorly developed focal adhesions positive for vinculin at the cell periphery (green staining). Cells plated on terminal CS layers of CHI-CS (4-9) shown in Figure 5.7b expressed more longitudinal actin stress fibres and also numerous longer focal adhesions, positive for vinculin. Since cells were seeded in the presence of serum, adsorption of adhesive proteins from serum may precede the adhesion process of cells. The well developed focal adhesions of cells in Figure 5.7b indicate integrin ligation to adhesive proteins as major process of adhesion that is related to integrin clustering in focal adhesions.⁴⁹

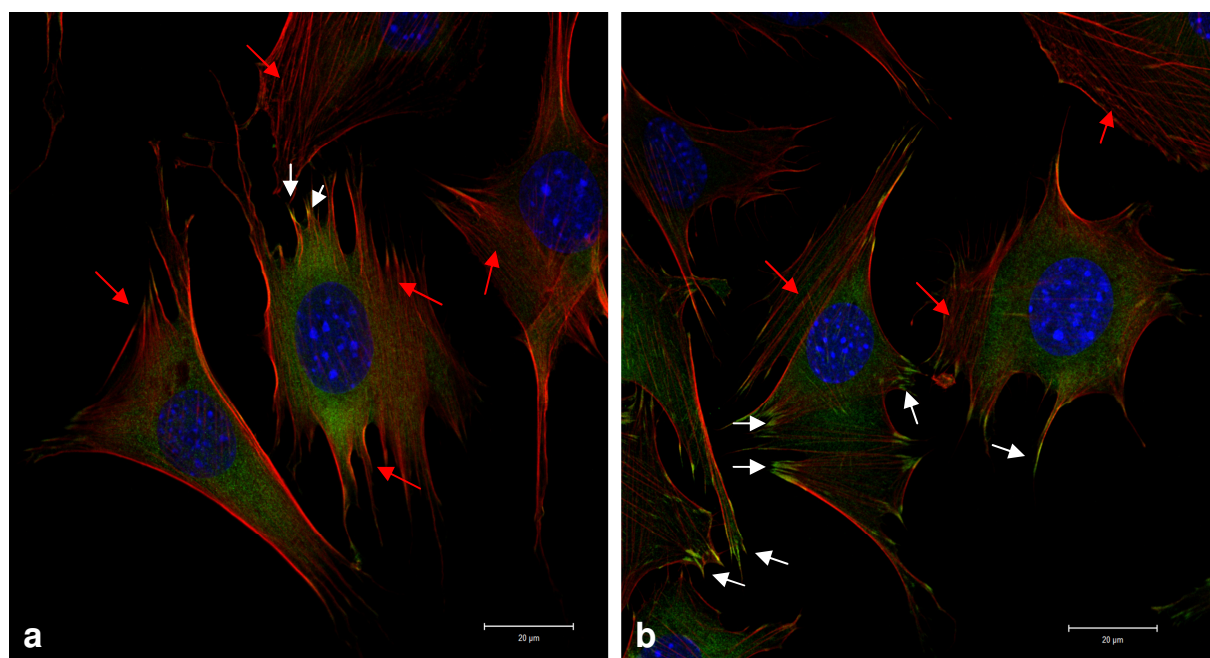


Figure 5.7: Fluorescence images of C2C12 cells plated on terminal HEP (a) and CS layer (b) in DMEM and 10% FBS for 4 hours. Both multilayers systems were prepared at pH 9. The red staining shows actin, the green vinculin and the blue nuclei of cells. White arrows show focal adhesions positive for vinculin. Red arrows show actin stress fibres.

Cell growth requires adhesion of cells with ligation of integrins to extracellular matrix components to prevent apoptosis and promote signal transduction via the mitogen-activated protein (MAP) kinase pathways.^{50 51} Hence adhesion measurements may be used for predication of later cell responses in terms of cell proliferation and also differentiation. Growth of C2C12 cells was studied on terminal polyanion layers for 24 and 72 hours. Data on quantity of viable cells after the different incubation periods were obtained by QBlue test and are shown in Figure 5.8. The cell growth was lower on terminal HEP layers compared to CS terminal layers after 24 and 72 hours, which is in accordance with the lack or lower fibronectin adsorption on HEP terminal layers and also closely related to the findings of adhesion studies. It was also detected that cell growth on multilayers prepared at pH 4 was lower than on multilayers prepared at pH 9. The fact that C2C12 cell growth was also dependent on pH during formation of CHI-CS multilayers is related to the observation of focal adhesion formation in Figure 5.7b although quantitative adhesion data showed only slightly higher count for cells on CHI-CS (4-9). It underlines also the need for more detailed studies on the adhesion process including expression of focal adhesions and involvement of receptor components. Beside the quantitative estimate of growth also cell morphology was studied with phase contrast microscopy. The corresponding micrographs are shown in Figure 5.9. The delayed growth of C2C12 cells on multilayers prepared at pH 4 is also visible in the appearance of cells after 24 hours incubation shown in Figure 5.9a (terminal layer HEP) and 5.9c (terminal layer CS). Cells on both polyanion layers had a reduced degree of spreading and tended to form bulky aggregates. By contrast, cells seeded on multilayers prepared at pH 9 (Figure 5.9e – HEP, Figure 5.9g - CS) had a more spread phenotype although also here cells tended to develop cell-cell contacts. These differences in cell growth between pH 4 and 9 during multilayer formation were also maintained after 72 hours and are visible by lower coverage of substrata (compare Figure 5.9b & d with 5.9f & h). It is also interesting to note that CS as terminal layer in systems prepared at pH 4 (Figure 5.9d) still promoted the growth of cells in huge aggregates while HEP as terminal layer provoked already more distribution of cells on the substratum (Figure 5.9b). However in general coverage of substrata and appearance of cells corresponded quite well to the quantitative data presented in Figure 5.8. Hence, variation of pH during multilayer formation from CHI-HEP is a useful tool to control cell adhesion on biomaterials while multilayers based on CHI-CS are less sensitive vs. change of pH during formation.

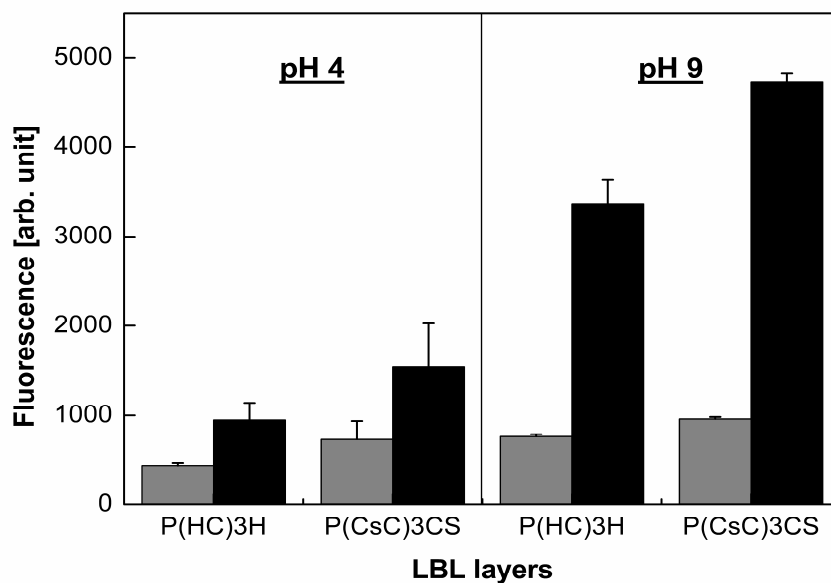


Figure 5.8: Cell proliferation measurements done after 1 (grey bars) and 3 (black bars) days of C2C12 cell culture in DMEM with 10% FBS on polyanion (HEP or CS) terminated multilayers prepared at different pH conditions. Graph consists of two parts, one with the measurements done on layers prepared at pH 4 while the other part for the layers prepared at pH 9.

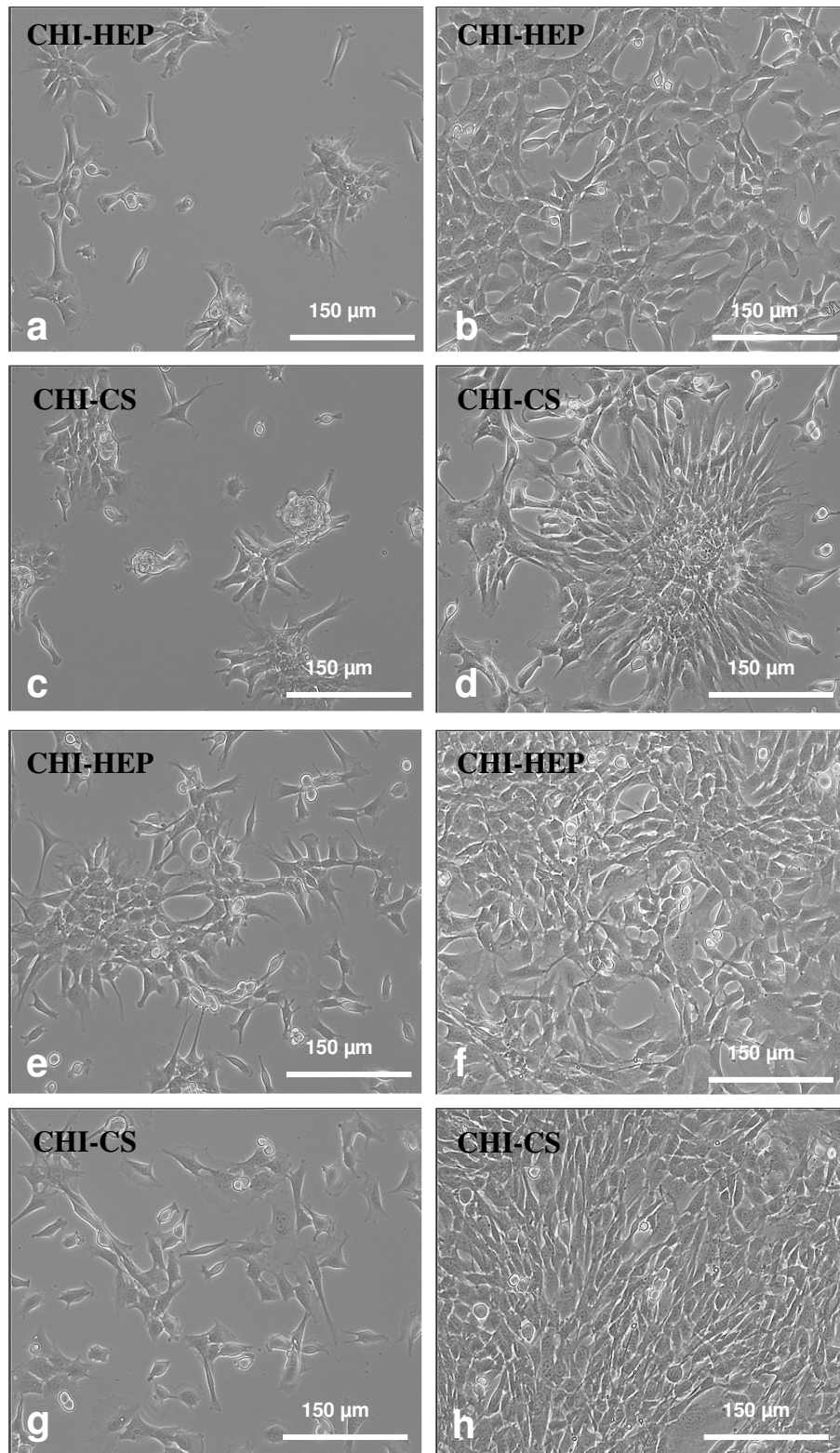


Figure 5.9: Phase contrast images of long term C2C12 cells cultured in DMEM and 10% FBS on polyanion terminated multilayer prepared at different pH regimes, pH 4 (a-d) & pH 9 (e-h) for 1 day (a, c, e, g) & 3 days (b, d, f, h).

5.5. Conclusions

The aim of this work was to compare the effect of chemical composition of two different polyanions adsorbed at two different pH conditions on multilayer bulk and surface properties and how this affects the behaviour of cells. Since HEP represents a natural glycosaminoglycan, CS a semi-synthetic one was selected as an alternative potential candidate for surface coatings. The adsorption process at pH 4 was most likely dominated by ion pairing⁵², while hydrogen bonding was leading when polyanions were adsorbed pH 9.³⁶ During these studies it was found that pH has a great effect on multilayer mass, water content, surface properties and cell responses in multilayer systems composed of HEP and CHI. The cell response, also pH driven, was predominantly due to the conformation of HEP in the multilayers that either allows binding of adhesive proteins or not and less related to the water content and mechanical properties of CHI-HEP multilayer systems. On the other hand multilayers prepared from CHI-CS showed little differences in properties with changing pH value, which indicated that hydrogen bonding has made an important contribution to the bonding of CHI in this system. Hence, CS despite of having relatively high sulfation degree, the remaining hydroxyl groups provided such systems which are less dependent on environment conditions like pH value, represented also an advantage during multilayer formation. More importantly, CS possessed a high bioactivity to promote adhesion and growth of cells on multilayers in addition to their ability to bind growth factors with HEP-binding domains like FGF-2 and BMP-2 provides them with huge advantages for making bioactive coating of tissue engineering and implants for regeneration of bone and other tissues.

5.6. Acknowledgements

This work was funded partly by Deutsche Forschungsgemeinschaft under grant agreements GR1290/7-1 & GR1290/7-2, FI755/4-1 & FI755/4-2 and by the European Union Seventh Framework Program (FP7/2007-2013) under grant agreement n° NMP4-SL-2009-229292 (Find&Bind).

5.7. References

1. Bauer, S.; Schmuki, P.; von der Mark, K.; Park, J., Engineering biocompatible implant surfaces: Part I: Materials and surfaces. *Progress in Materials Science* **2013**, 58, (3), 261-326.

2. Qi, P.; Maitz, M. F.; Huang, N., Surface modification of cardiovascular materials and implants. *Surface and Coatings Technology*, (0).
3. Aydin, H. M.; Turk, M.; Calimli, A.; Piskin, E., Attachment and growth of fibroblasts on poly(L-lactide/epsilon-caprolactone) scaffolds prepared in supercritical CO₂ and modified by polyethylene imine grafting with ethylene diamine-plasma in a glow-discharge apparatus. *International Journal of Artificial Organs* **2006**, 29, (9), 873-880.
4. Groth, T.; Liu, Z.-M.; Niepel, M.; Peschel, D.; Kirchof, K.; Altankov, G.; Faucheux, N., Chemical and Physical Modifications of Biomaterial Surfaces to Control Adhesion of Cells. In *Advances in Regenerative Medicine: Role of Nanotechnology, and Engineering Principles*, Shastri, V. P.; Altankov, G.; Lendlein, A., Eds. Springer Netherlands: 2010; pp 253-284.
5. Decher, G.; Hong, J. D.; Schmitt, J., Buildup of ultrathin multilayer films by a self-assembly process: III. Consecutively alternating adsorption of anionic and cationic polyelectrolytes on charged surfaces. *Thin Solid Films* **1992**, 210–211, Part 2, (0), 831-835.
6. Gribova, V.; Auzely-Velty, R.; Picart, C., Polyelectrolyte Multilayer Assemblies on Materials Surfaces: From Cell Adhesion to Tissue Engineering. *Chemistry of Materials* **2011**, 24, (5), 854-869.
7. Hammond, P. T., Form and Function in Multilayer Assembly: New Applications at the Nanoscale. *Advanced Materials* **2004**, 16, (15), 1271-1293.
8. Schonhoff, M., Layered polyelectrolyte complexes: physics of formation and molecular properties. *Journal of Physics-Condensed Matter* **2003**, 15, (49), R1781-R1808.
9. Moby, V.; Boura, C.; Kerdjoudj, H.; Voegel, J. C.; Marchal, L.; Dumas, D.; Schaaf, P.; Stoltz, J. F.; Menu, P., Poly(styrenesulfonate)/Poly(allylamine) multilayers: A route to favor endothelial cell growth on expanded poly(tetrafluoroethylene) vascular grafts. *Biomacromolecules* **2007**, 8, (7), 2156-2160.
10. Zanina, N.; Haddad, S.; Othmane, A.; Jouenne, T.; Vaudry, D.; Souiri, M.; Mora, L., Endothelial cell adhesion on polyelectrolyte multilayer films functionalised with fibronectin and collagen. *Chemical Papers* **2012**, 66, (5), 532-542.
11. Kirchof, K.; Hristova, K.; Krasteva, N.; Altankov, G.; Groth, T., Multilayer coatings on biomaterials for control of MG-63 osteoblast adhesion and growth. *Journal of Materials Science: Materials in Medicine* **2009**, 20, (4), 897-907.

12. Hynes, R. O., Integrins: Bidirectional, Allosteric Signaling Machines. *Cell* **2002**, 110, (6), 673-687.
13. Anselme, K., Osteoblast adhesion on biomaterials. *Biomaterials* **2000**, 21, (7), 667-681.
14. Crouzier, T.; Picart, C., Ion Pairing and Hydration in Polyelectrolyte Multilayer Films Containing Polysaccharides. *Biomacromolecules* **2009**, 10, (2), 433-442.
15. Capila, I.; Linhardt, R. J., Heparin - Protein interactions. *Angewandte Chemie-International Edition* **2002**, 41, (3), 391-412.
16. Zieris, A.; Prokoph, S.; Levental, K. R.; Welzel, P. B.; Grimmer, M.; Freudenberg, U.; Werner, C., FGF-2 and VEGF functionalization of starPEG-heparin hydrogels to modulate biomolecular and physical cues of angiogenesis. *Biomaterials* **2010**, 31, (31), 7985-7994.
17. Zhang, K.; Peschel, D.; Klinger, T.; Gebauer, K.; Groth, T.; Fischer, S., Synthesis of carboxyl cellulose sulfate with various contents of regioselectively introduced sulfate and carboxyl groups. *Carbohydrate Polymers* **2010**, 82, (1), 92-99.
18. Peschel, D.; Zhang, K.; Aggarwal, N.; Brendler, E.; Fischer, S.; Groth, T., Synthesis of novel celluloses derivatives and investigation of their mitogenic activity in the presence and absence of FGF2. *Acta Biomaterialia* **2010**, 6, (6), 2116-2125.
19. Peschel, D.; Zhang, K.; Fischer, S.; Groth, T., Modulation of osteogenic activity of BMP-2 by cellulose and chitosan derivatives. *Acta Biomaterialia* **2012**, 8, (1), 183-193.
20. Groth, T.; Wagenknecht, W., Anticoagulant potential of regioselective derivatized cellulose. *Biomaterials* **2001**, 22, (20), 2719-2729.
21. Gericke, M.; Doliska, A.; Stana, J.; Liebert, T.; Heinze, T.; Stana-Kleinschek, K., Semi-Synthetic Polysaccharide Sulfates as Anticoagulant Coatings for PET, 1-Cellulose Sulfate. *Macromolecular Bioscience* **2011**, 11, (4), 549-556.
22. Xie, Y.-L.; Wang, M.-J.; Yao, S.-J., Preparation and Characterization of Biocompatible Microcapsules of Sodium Cellulose Sulfate/Chitosan by Means of Layer-by-Layer Self-Assembly. *Langmuir* **2009**, 25, (16), 8999-9005.
23. Ravi Kumar, M. N. V., A review of chitin and chitosan applications. *Reactive and Functional Polymers* **2000**, 46, (1), 1-27.
24. Aggarwal, N.; Altgärde, N.; Svedhem, S.; Michanetzis, G.; Missirlis, Y.; Groth, T., Tuning Cell Adhesion and Growth on Biomimetic Polyelectrolyte Multilayers by Variation of

pH During Layer-by-Layer Assembly. *Macromolecular Bioscience* **2013**, DOI:10.1002/mabi.201300153

25. Zhang, K.; Brendler, E.; Geissler, A.; Fischer, S., Synthesis and spectroscopic analysis of cellulose sulfates with regulable total degrees of substitution and sulfation patterns via C-13 NMR and FT Raman spectroscopy. *Polymer* **2011**, 52, (1), 26-32.
26. Schasfoort, R. B. M., Tudos, A. J. , *Handbook of Surface Plasmon Resonance*. 1st ed.; RSC Publishing: Cambridge, 2008; p 128.
27. Lundin, M.; Solaqa, F.; Thormann, E.; Macakova, L.; Blomberg, E., Layer-by-Layer Assemblies of Chitosan and Heparin: Effect of Solution Ionic Strength and pH. *Langmuir* **2011**, 27, (12), 7537-7548.
28. Rodahl, M.; Hook, F.; Krozer, A.; Brzezinski, P.; Kasemo, B., Quartz crystal microbalance setup for frequency and Q-factor measurements in gaseous and liquid environments. *Review of Scientific Instruments* **1995**, 66, (7), 3924-3930.
29. Sauerbrey, G., Verwendung von Schwingquarzen zur Wägung dünner Schichten und zur Mikrowägung. *Zeitschrift für Physik* **1959**, 155, (2), 206-222.
30. Höök, F.; Kasemo, B.; Nylander, T.; Fant, C.; Sott, K.; Elwing, H., Variations in Coupled Water, Viscoelastic Properties, and Film Thickness of a Mefp-1 Protein Film during Adsorption and Cross-Linking: A Quartz Crystal Microbalance with Dissipation Monitoring, Ellipsometry, and Surface Plasmon Resonance Study. *Analytical Chemistry* **2001**, 73, (24), 5796-5804.
31. Zhang, K.; Peschel, D.; Bäucker, E.; Groth, T.; Fischer, S., Synthesis and characterisation of cellulose sulfates regarding the degrees of substitution, degrees of polymerisation and morphology. *Carbohydrate Polymers* **2011**, 83, (4), 1659-1664.
32. Rabenstein, D. L., Heparin and heparan sulfate: structure and function. *Natural Product Reports* **2002**, 19, (3), 312-331.
33. Xiao, Z.; Tappen, B. R.; Ly, M.; Zhao, W.; Canova, L. P.; Guan, H.; Linhardt, R. J., Heparin Mapping Using Heparin Lyases and the Generation of a Novel Low Molecular Weight Heparin. *Journal of Medicinal Chemistry* **2010**, 54, (2), 603-610.
34. Richert, L.; Lavallo, P.; Payan, E.; Shu, X. Z.; Prestwich, G. D.; Stoltz, J. F.; Schaaf, P.; Voegel, J. C.; Picart, C., Layer by layer buildup of polysaccharide films: Physical chemistry and cellular adhesion aspects. *Langmuir* **2004**, 20, (2), 448-458.

35. Boddohi, S.; Killingsworth, C. E.; Kipper, M. J., Polyelectrolyte Multilayer Assembly as a Function of pH and Ionic Strength Using the Polysaccharides Chitosan and Heparin. *Biomacromolecules* **2008**, 9, (7), 2021-2028.
36. Dong, P.; Hao, W.; Xia, Y.; Da, G.; Wang, T., Comparison Study of Corrosion Behavior and Biocompatibility of Polyethyleneimine (PEI)/Heparin and Chitosan/Heparin Coatings on NiTi alloy. *Journal of Materials Science & Technology* **2010**, 26, (11), 1027-1031.
37. Sui, Z.; Salloum, D.; Schlenoff, J. B., Effect of Molecular Weight on the Construction of Polyelectrolyte Multilayers: Stripping versus Sticking. *Langmuir* **2003**, 19, (6), 2491-2495.
38. Orelma, H.; Filpponen, I.; Johansson, L.-S.; Laine, J.; Rojas, O. J., Modification of Cellulose Films by Adsorption of CMC and Chitosan for Controlled Attachment of Biomolecules. *Biomacromolecules* **2011**, 12, (12), 4311-4318.
39. Kirchhof, K. Nanostrukturierte Biomaterialbeschichtungen zur Steuerung von Zelladhäsion und -proliferation: pH-Wert-abhängige Multischichten aus Heparin und Chitosan in diskreter und Gradientenform. Martin-Luther-University, Halle-Wittenberg, Germany, Halle (Saale), Germany, 2009.
40. Duval, J. F. L.; Kuettner, D.; Werner, C.; Zimmermann, R., Electrohydrodynamics of Soft Polyelectrolyte Multilayers: Point of Zero-Streaming Current. *Langmuir* **2011**, 27, (17), 10739-10752.
41. Boudou, T.; Crouzier, T.; Nicolas, C.; Ren, K.; Picart, C., Polyelectrolyte Multilayer Nanofilms Used as Thin Materials for Cell Mechano-Sensitivity Studies. *Macromolecular Bioscience* **2011**, 11, (1), 77-89.
42. Ballester-Beltrán, J.; Cantini, M.; Lebourg, M.; Rico, P.; Moratal, D.; García, A.; Salmerón-Sánchez, M., Effect of topological cues on material-driven fibronectin fibrillogenesis and cell differentiation. *Journal of Materials Science: Materials in Medicine* **2012**, 23, (1), 195-204.
43. Steele, J. G.; Johnson, G.; Underwood, P. A., Role of serum vitronectin and fibronectin in adhesion of fibroblasts following seeding onto tissue culture polystyrene. *Journal of Biomedical Materials Research* **1992**, 26, (7), 861-884.
44. Crouzier, T.; Szarpak, A.; Boudou, T.; Auzély-Velty, R.; Picart, C., Polysaccharide-Blend Multilayers Containing Hyaluronan and Heparin as a Delivery System for rhBMP-2. *Small* **2010**, 6, (5), 651-662.

45. Discher, D. E.; Janmey, P.; Wang, Y.-l., Tissue Cells Feel and Respond to the Stiffness of Their Substrate. *Science* **2005**, 310, (5751), 1139-1143.
46. García, A. J.; Boettiger, D., Integrin–fibronectin interactions at the cell-material interface: initial integrin binding and signaling. *Biomaterials* **1999**, 20, (23–24), 2427-2433.
47. Groth, T.; Altankov, G.; Kostadinova, A.; Krasteva, N.; Albrecht, W.; Paul, D., Altered vitronectin receptor (α v integrin) function in fibroblasts adhering on hydrophobic glass. *Journal of Biomedical Materials Research* **1999**, 44, (3), 341-351.
48. Ren, K.; Fourel, L.; Rouvière, C. G.; Albiges-Rizo, C.; Picart, C., Manipulation of the adhesive behaviour of skeletal muscle cells on soft and stiff polyelectrolyte multilayers. *Acta Biomaterialia* **2010**, 6, (11), 4238-4248.
49. Guillame-Gentil, O.; Semenov, O.; Roca, A. S.; Groth, T.; Zahn, R.; Vörös, J.; Zenobi-Wong, M., Engineering the Extracellular Environment: Strategies for Building 2D and 3D Cellular Structures. *Advanced Materials* **2010**, 22, (48), 5443-5462.
50. Schwartz, M. A.; Assoian, R. K., Integrins and cell proliferation: regulation of cyclin-dependent kinases via cytoplasmic signaling pathways. *Journal of Cell Science* **2001**, 114, (14), 2553-2560.
51. Stupack, D. G.; Cheresch, D. A., Get a ligand, get a life: integrins, signaling and cell survival. *Journal of Cell Science* **2002**, 115, (19), 3729-3738.
52. Schlenoff, J. B.; Dubas, S. T., Mechanism of Polyelectrolyte Multilayer Growth: Charge Overcompensation and Distribution. *Macromolecules* **2001**, 34, (3), 592-598.

Chapter 6

Multilayer films by blending heparin with semi-synthetic cellulose sulfates: Physico-chemical characterisation and cell responses

Neha Aggarwal, Thomas Groth

6.1. Abstract

Here, we report fabrication of polyelectrolyte multilayers by blending a natural glycosaminoglycan (heparin) with semi-synthetic cellulose sulfates as polyanions paired with polycation chitosan. Two types of polyanionic blends were prepared by mixing heparin with either cellulose sulfates (CS) of high (CS2.6) or intermediate (CS1.6) sulfation degree in equal mass ratios. Multilayer growth was monitored by surface plasmon resonance (SPR) and quartz crystal micro balance with dissipation monitoring (QCM-D) where as surface wettability was measured by water contact angle measurements (WCA). Both SPR and QCM-D showed differences in biomolecular mass adsorption and dissipation values for different multilayers and also helped in estimating the hydration levels of layers. WCA indicated arrangement of polyanion and polycation layers within the multilayer systems, whether distinct layers or more intermingled multilayers were established. Overall physico-chemical characterization data suggested a dominating incorporation of heparin over CS in blend multilayer systems. Biological interactions of these blend multilayers investigated with C2C12 cells also indicated a leading contribution of heparin in the blend systems. This current study suggested that heparin was preferentially incorporated over cellulose sulfates that are highly sulfated and points towards the dominance of carboxylic groups over sulfate groups in interacting with amino groups of chitosan.

6.2. Introduction

The appropriate design of material surfaces with nanoscale precision is a rapidly developing field with applications in biosensing and biomedical materials. Layer-by-layer (LBL) technique, introduced by Gero Decher and co-workers in 1990s,¹ is a widely utilized

technique to reliably engineer the surfaces and tailor various properties (surface and bulk) of multilayer films. This versatile technique is based on the alternate assembly of oppositely charged polyelectrolytes (i.e., a polyanion paired with a polycation) to form polyelectrolyte multilayer assemblies. A large array of polymeric materials or polyelectrolyte can be integrated to form such multilayer films and hence a diverse range of functionalities can be achieved for the biomaterial coatings.²⁻³ During the formation of multilayers the alternate adsorption of polyelectrolyte is typically driven by electrostatic interactions and subsequent ion pairing on to a charged substrate.⁴ While, ion pairing is probably the most abundant driving force applied during the multilayer assemblies, other forces like hydrogen bonding, hydrophobic interactions and covalent bonding has also come into picture.⁵ The use of such alternate driving forces with a flexible range of polyelectrolytes facilitates the inclusion of a wide variety of functionalities in the multilayer assemblies thereby increasing the spectrum of their potential applications as biomaterial coatings.²

Biomolecules, especially originating from the extracellular matrix of mammals are being widely exploited for designing of biocompatible and bioactive materials.⁶ Heparin, the most sulfated glycosaminoglycan, is commonly known for its anti-thrombogenic activity, but interacts also with a large variety of proteins that regulate adhesion, growth and differentiation of cells.⁷ Heparin represents a strong polyanion, composed of either β -D-glucuronic acid or α -D-iduronic acid and 2-N-sulfo-glucosamine connected by a 1-4-glycosidic linkage. Due to the high affinity of heparin towards several growth factors,⁸ it is often incorporated into the hydrogels⁹ and also recently used in making multilayer coatings on biomaterial surfaces.¹⁰⁻¹¹ However, the use of heparin has certain draw-backs. The isolation of heparin from animal sources, e.g., porcine mucosa or bovine lung limits its availability in larger quantities and also leads to substantial chemical heterogeneity and variability of physiological activity.^{12,7} Therefore, previous studies were conducted to replace heparin by modification of more abundantly occurring polysaccharides like cellulose to achieve heparinoid features.¹³⁻¹⁴ Regioselective sulfation of cellulose has been carried out to achieve molecular similarity and bioactivity to heparin,¹⁵ particularly with respect to interaction with growth factors and cells, when added as soluble substance to culture media.¹⁶⁻¹⁷ However, cellulose sulfates (CS) are also interesting candidates for LbL technique as they inherit high charge density depending on the degree of sulfation, which led to their application to make blood compatible multilayers.¹⁴ Recently, we also showed that multilayers composed of CS may be used to modulate adhesion and growth of cells.¹⁸

An innovative enhancement in LBL technique for tuning of film properties by blending of either polyanions or polycations has been introduced recently.¹⁹⁻²⁰ A number of studies have been reported that highlights the inherent simplicity of the blending technique and ability to enhance the functionality of the LBL films.²¹⁻²² Most of the work done in this direction was focused on the control of film's chemical composition, stability, growth regime, thickness and their response to protein adsorption²³⁻²⁴ by applying an appropriate blend ratio of the used PE. For example, the study on blends of HA-PSS built with PLL had shown the preferential adsorption of PSS over HA and also anomalous evolution of film thickness.²⁵ Stability of films prepared from several low molecular weight species was also improved by blending them with PSS.²⁶ Additionally, Crouzier et al. showed that blending can enhance the bioactivity of multilayer films by demonstrating the ability of HA-HEP blend films as potential growth factor reservoir and also probed the bioactivity of these films by measuring the alkaline phosphatase activity of C2C12 myoblast cells cultured on the films.²²

As discussed above, heparin is a biomolecule with wide application potential but due to its natural origin, varying bioactivity and relative scarcity, replacement by semi-synthetic molecules with heparinoid activity is desirable. In addition, some previous studies showed that ability of heparin to interact with proteins having heparin-binding domains is dependent on its way of incorporation.^{10,27-28} Relatively homogenous composed terminal heparin layers displayed negligible adsorption of fibronectin – a protein that possesses heparin binding domains^{10,28} and were cytophobic. It was hypothesized that a side-on arrangement of heparin inhibits interaction of heparin with fibronectin. By contrast, mixed (intermingled) composition of terminal layers promoted adsorption of fibronectin and adhesion and spreading of cells, which might be related due to a more loopy conformation.^{10,29} Since previous studies have shown that sulfation degree of glycosaminoglycans is an important parameter for multilayer composition and properties.²² We were interested to see how physical multilayer properties and cell behaviour changes with blending of either an intermediate sulfated cellulose (CS1.6) or a highly sulfated cellulose (CS2.6) with heparin as polyanions paired with chitosan as the polycation. Our studies show that heparin tends to displace the sulfated cellulose (CS1.6/CS2.6) yielding multilayer properties more comparable to heparin-chitosan multilayer systems but with different effects on the cell response.

6.3. Materials and Methods

Polyelectrolyte solutions, poly (ethylene imine) (PEI) (MW 750,000 g/mol, Sigma, Germany), heparin (HEP) (min 150 IU/mg, MW 8,000-15,000 g/mol, Applichem, Germany), and two different cellulose sulfates synthesized (see below) CS1.6 and Cs2.6 were prepared by dissolution under stirring at a concentration of 2 mg/ml in water containing 0.14 M NaCl. To prepare the blends, heparin and cellulose sulfate (CS1.6/Cs2.6) were dissolved in equal mass ratios (1 mg/ml each) in water containing 0.14 M NaCl. The two types of blends were abbreviated as HEP+CS1.6 and HEP+CS2.6. Chitosan (CHI) solution was prepared from medical grade chitosan with a deacetylation degree of 85 % (MW 500,000 g/mol, 85/ 500/ A1, Heppe, Germany) in 0.14 M NaCl and 0.05 M acetic acid at 50°C for 3 h. Cellulose sulfates (CS) were a kind gift from Dr. Steffen Fischer. Their synthesis and characterization has been described in much detail elsewhere.³⁰ The sulfation degree and molecular weight of CS and heparin are outlined in Table 6.1

Table 6.1: Characterization of CS and heparin

| Samples | DS _S ^b | | | DO ^b | MW _w | MW _n | MW _w / MW _n |
|--------------|------------------------------|------------------|--------------------------|-----------------|-----------------|-----------------|--------------------------------------|
| | DS _{S6} | DS _{S2} | total DS _S | | | | |
| Heparin(HEP) | 0.27 | 0.8 | 1.01 | 0.26 | | *8000- 25000 | |
| CS1.6 | 0.91 | 0.55 | 1.57 | 0 | 77748 | 37549 | 2.07 |
| CS2.6 | 1 | 1 | 2.59 | 0 | 64961 | 36197 | 1.79 |

^a molar ratios in mol sulfuric acid and mol acetic anhydride per mol AGU for CS1.6 and mol chlorosulfonic acid per mol AGU for CS2.6, respectively. ^b DS_{S6}, DS_{S2} and DO (degree of oxidation) were analysed with ¹³C NMR spectroscopy. The total DS_S was determined by elemental analysis. *MW_w of heparin: provided by the data sheet from the supplier.

Polyelectrolyte blend multilayers were deposited on microscopy glass cover slips (Menzel, Germany). Cover slips were cleaned for 2 h with 0.5 M NaOH (Roth, Germany) dissolved in 96% ethanol (Roth, Germany) and rinsed repetitively with micropure water (10 x 5 min).

99.8% ethanol (Merck, Germany) was used to clean new gold coated sensors for SPR (IBIS Technologies, The Netherlands) and AT-cut gold-coated quartz crystals for QCM-D (Q-sense, Sweden) measurements. After thorough rinsing with micropure water sensors were dried with nitrogen (1 bar) and were kept overnight in an ethanol (p.a.) solution of 2 mM mercaptoundecanoic acid (MUDA, 95%, Sigma, Germany) to generate a negatively charged self-assembled monolayer exposing carboxyl groups on sensors surface.³¹

Polyelectrolyte multilayer assembly: Polyelectrolyte multilayer films were fabricated on glass cover slips or on gold coated sensors. A first layer of PEI was formed on the substrates to obtain an anchoring layer with a positive charge. This was followed by adsorption of a polyanion layer of HEP or CS1.6 or CS2.6 or the blends (HEP+CS1.6 / HEP+CS2.6). Then a polycation layer of CHI was deposited. Each layer was assembled by incubating glass surfaces in polyelectrolyte solutions for 7 min followed by rinsing with an aqueous solution containing 0.14 M NaCl (3 x 4 min). Up to 8 multilayers with polyanion as terminal layer were built by alternating deposition of polyanions and polycation. The pH value of each polyelectrolyte solution and rinsing solution was adjusted to pH 4 by using either HCl or NaOH. The different systems prepared from polyanions paired with CHI are abbreviated as CHI-HEP, CHI-CS1.6, CHI-(HEP+CS1.6), CHI-CS2.6 and CHI-(HEP+CS2.6).

6.3.1. Characterization of multilayer properties

Multilayer growth measurement: Surface plasmon resonance (SPR) and quartz crystal microbalance with dissipation monitoring (QCM-D) measurements using IBIS-iSPR (IBIS Technologies B.V., Netherlands) and E4 instrument (Q-Sense, Sweden) were executed to follow the multilayer build-up process. SPR is based on the change in refractive index (RI) at the gold-liquid interface of the gold sensor surface which is caused by the adsorption of molecules. This is measured as a shift in the angle of the incident light (m°) and it is proportional to the mass (Γ_{SPR}) of molecules adsorbed on the surface. The ‘optical’ mass of the adsorbed molecules during the formation of each layer was calculated by equation (1)³²

$$122 m^\circ \approx 1 \text{ ng} / \text{mm}^2 \quad (1)$$

While the optical’ mass was quantified by SPR, the ‘acoustic’ mass of the adsorbed molecules was quantified by QCM-D measurements. Shortly, the QCM-D sensor (a quartz crystal disc) oscillates at its resonance frequency f when an alternating potential is applied. Mass adsorption on the sensor surface leads to a shift in this frequency (Δf) which is related to the

change in adsorbed mass (Δm_{QCM-D}) and can be estimated for thin, rigid, and evenly distributed surface films using the Sauerbrey equation (equation 2) ³³.

$$\Delta m = - C \Delta f / n \quad (2)$$

where n ($n = 1, 3, 5, \dots, 13$) is the overtone number and C is the mass sensitivity constant specific for the quartz crystal, here $C = 0.177 \text{ mg/m}^2\text{Hz}$ for ($f_0 = 5 \text{ MHz}$). The coupled water into the adsorbed film was estimated by comparing the mass obtained by QCM-D and SPR (assuming that the two masses were obtained under equivalent condition).

The dampening of the oscillatory motion when the driving voltage of the quartz crystal is shut off is related to structural properties of the added layer on the sensor surface, and it is quantified as energy dissipation (ΔD).

Both SPR and QCM-D investigations were made in the flow cell of each device onto gold sensors pre-treated with MUDA. PEI was introduced to adsorb on the sensor surface for 7 min followed by rinsing with NaCl solution for 12 min. After the formation of PEI layer, similarly successive layers were built by alternate adsorption of polyanions and CHI layers up to 8 layers.

Water contact angle (WCA): Static contact angle measurements were done by an OCA15+ device from Dataphysics (Germany) to determine the wettability of multilayer surfaces. By applying the sessile drop method, 3 to 4 samples of each type of multilayer system and terminal multilayer surfaces were measured by dispensing 3-4 drops of water. For each droplet, at least 10 independent measurements were recorded by the built-in software.

6.3.2. Biological Investigations

Short-term cell adhesion studies were conducted on different multilayer film surfaces using the skeletal muscle cell line C2C12 (DSMZ, Germany, Product Nr.: ACC 565). Cryo conserved cells were thawed and expanded by culturing them in Dulbecco's modified Eagle medium (DMEM, Biochrom AG, Berlin, Germany) supplemented with 10% fetal bovine serum (FBS, Biochrom AG), 2 mM L-Glutamine, 100 U/ml Penicillin and 100 $\mu\text{g/ml}$ Streptomycin (Biochrom AG) in humidified 5% CO₂/95% air atmosphere using a NUAIRE® DH Autoflow incubator (NuAire corp., Plymouth, Minnesota, USA). C2C12 cells were harvested from pre-confluent cultures by trypsinization using 0.25% Trypsin, 0.02% EDTA (Biochrom AG) followed by subsequent washing with DMEM and resuspended in DMEM with 10% FBS at a concentration of 25'000 cells/ml.

For the cell adhesion studies, multilayer coated glass substrates were placed in 12-well tissue culture plates followed by sterilization with 70% ethanol for 10 min and excessive rinsing with sterile PBS. C2C12 cells with a concentration of 25'000 cells/ml or 6000 cells/ cm² were seeded using DMEM supplemented with 10% FBS, 2 mM L-Glutamine, 100 U/ml Penicillin and 100 µg/ml Streptomycin on the sterilized multilayer surfaces and incubated for 4 h at 37°C in a humidified 5% CO₂/95% air atmosphere. After incubation, culture medium was aspirated and exchanged with fresh medium twice to remove the non-adherent cells. The attached cells were stained by adding 5 µl FDA (fluorescein diacetate) solution (0.01% vol/vol) to each well containing 1 ml of cell culture medium (over the multilayer samples) and incubated for 3-5 min. Images were made after the staining with a fluorescence microscope Axiovert 100 (Carl Zeiss Microimaging, Jena, Germany) for analyzing the cell morphology and quantification of cell attachment and spreading which was done by Image processing software "ImageJ, NIH".

Immunofluorescence staining was performed for the detailed study of cell morphology on each multilayer surface after 4 h of cell culture at 37°C by fluorescence microscopy. Attached cells were fixed with Roti[®] – Histofix (Roth, Germany) for 15 min and rinsed with PBS. Cell permeabilization was done by 0.1% (v/v) Triton X-100 in PBS for 10 min after cell fixation, followed by three times rinsing with PBS. 1% bovine serum albumin (BSA, Sigma, Germany) in PBS was applied for blocking the non-specific binding sites. Adherent cells were double stained by subsequent staining of focal adhesion complexes with mouse monoclonal antibody against vinculin (Sigma, Germany) and Cy2[®]conjugated AffiniPure Goat Anti-Mouse IgG-conjugated anti-mouse immunoglobulin (Dianova, Germany). Actin filaments were stained with BODIPY[®] phalloidin (5µM, Molecular Probes, Germany) and each incubation step was performed for 30 min followed by extensive washing with PBS. Each sample was mounted on objective holders with Mowiol[®] 4-88 (Merck, Germany) and investigated with Confocal Laser scanning microscope (LSM 710, Carl Zeiss MicroImaging GmbH, Jena, Germany) using 63x immersion oil objective. ZEN software was used to process the acquired images.

6.4 Results and Discussion

6.4.1. Multilayer growth measurement

The multilayer build-up process was examined by applying surface sensitive SPR and QCM-D analytical techniques. SPR, which is an optical technique allowed the determination

of adsorbed mass of macromolecules (optical/ dry mass), where as QCM-D (an acoustic technique) helped in deducing the information about adsorbed mass of macromolecules along with their hydration state as total absorbed mass (acoustic/ wet mass). Additionally, the information about the viscoelastic properties was also achieved by the QCM-D dissipation measurements. Figure 6.1a shows the multilayers mass calculated with equation (1) for the CHI-HEP, CHI-CS1.6 and CHI-(HEP+CS1.6) systems while Figure 6.1b for the CHI-HEP, CHI-CS2.6 and CHI-(HEP+CS2.6) systems. CHI-HEP system is included in both graphs for better comparison between the single and blend systems. The results show clear differences in the multilayer growth patterns of the different polyanion systems. An exponential layer growth was visible for the CHI-HEP multilayer system as also shown before for other polysaccharide-based multilayers systems.¹¹ The obtained multilayer mass was also consistent with previous studies by Lundin et al.³⁴ Here, it is indicated that ion pairing dominates, and protonation of CHI amino groups led to the adsorption of more HEP to accomplish complete charge reversal.³⁵

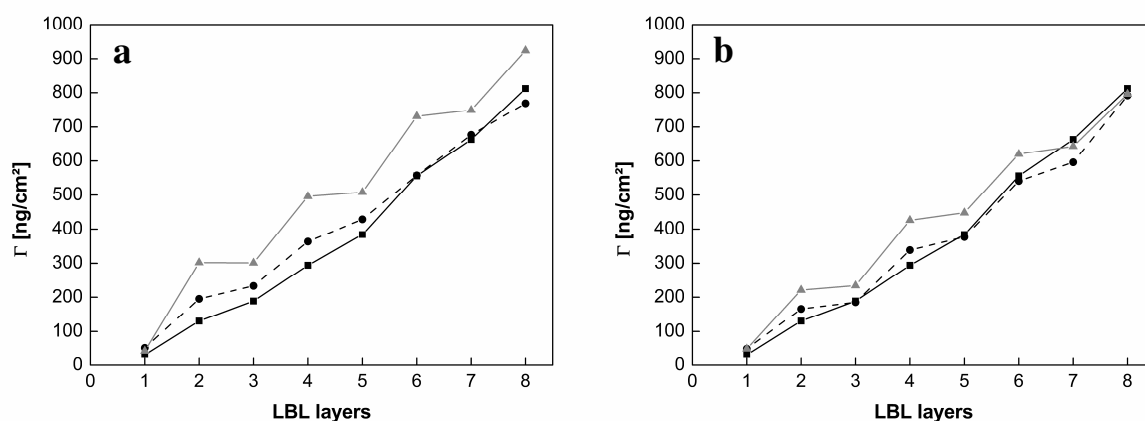


Figure 6.1: Multilayer mass Γ_{SPR} calculated from SPR angle shifts. Layer 1 is always PEI. Even layers: polyanions, odd layers: polycation CHI. **[a]** Γ_{SPR} for the CHI-HEP (Solid lines, ■), CHI-CS1.6 (gray solid lines, ▲) and CHI-(HEP+CS1.6) (dashed lines, ●) systems. **[b]** Γ_{SPR} for the CHI-HEP (Solid lines, ■), CHI-CS2.6 (gray solid lines, ▲) and CHI-(HEP+CS2.6) (dashed lines, ●) systems.

On the other hand, both multilayer systems of CS (CHI-CS1.6 & CHI-CS2.6), showed slightly larger adsorbed mass as well as different increment behavior compared to CHI-HEP system. The growth patterns of CS systems (Figure 6.1a,b) appeared staircase-like with an

indication of more mass adsorption during the adsorption of CS (even layer numbers) in comparison to the CHI deposition steps (odd layer number except PEI, the very first layer), as also shown in our recent studies for the CHI-CS1.6 layers.¹⁸ When the blends of either of these semi-synthetic cellulose sulfates with HEP were applied as polyanions, also distinct multilayer growth regimes were achieved during SPR studies (Figure 6.1a,b). The CHI-(HEP+CS1.6) multilayer system has shown somewhat an exponential growth similar to CHI-HEP system where as a staircase-like pattern was achieved with the CHI-(HEP+CS2.6) (in similarity with the pure CS systems as have also such staircase-like growth patterns).

The results of QCM-D measurements were done along with SPR measurements for the calculation of adsorbed multilayer mass (see Figure 6.2). The adsorbed mass was calculated by Sauerbrey equation (2). Sauerbrey equation is valid for rigid films, which represents a good approximation here as the dissipation responses shown in Figure 6.3 are relatively small compared to the frequency response and the films thickness is still relatively low. The overall adsorbed mass increment measured by QCM-D for each type of multilayer system (except for CHI-CS2.6 system) was much larger than the corresponding mass measured by SPR, which indicates that a substantial amount of water was coupled within these multilayer systems. Comparison of layer masses obtained by SPR and QCM-D and the resulting water content of the terminal polyanion (8th) layer are summarized in Table 6.2. Each multilayer system seems to be highly hydrated, which was also observed by others for polysaccharide-based multilayer systems.^{34,11} An exception was CHI-CS2.6 multilayer system that seems to be highly condensed. QCM-D studies also deduced the exponential multilayer growth for the CHI-HEP system. Similar to SPR results, the QCM-D curve for the CHI-CS1.6 layers also depicted the staircase like pattern. However, the CHI-CS2.6 system expressed a very low growth regime (Figure 6.2b). The reason for such staircase pattern might be due to the charge compensation by addition of CHI and also forming a quasi-soluble complex with CS thereby stripping it off from the surface as also shown in a previous study.³⁶ Hence there was almost no increase in the mass adsorption when CHI was deposited. Additionally the CHI-CS1.6 layers contains a noticeable amount of water (Table 6.2) and that might be because of the presence of hydrogen bonds between CHI and the remaining hydroxyl groups of intermediate sulfated CS.¹⁸ In case of CHI-CS2.6 multilayer system, the total adsorbed mass observed by QCM-D was lower than the optical mass estimated by SPR and which might be due to an overestimation of layer mass by SPR due to the strong condensation of the multilayer system. CHI-CS2.6 multilayers had the lowest mass adsorption possibly due to the very high charge density of CS2.6, which requires less CS to compensate the charges of CHI. Koetse et al. have

also shown that the cellulose sulfates with higher charge density produce thinner layers during multilayer assembly.³⁷ The multilayer growth of blend systems as studied by QCM-D had also shown exponential growth like CHI-HEP system (Figure 6.2). For the CHI-(HEP+CS1.6) system, the SPR and QCM-D data correlates as for both measurements the layer growth was found to be exponential. Contrastingly, the layer growth of CHI-(HEP+CS2.6) system depicted by SPR was step-wise staircase-like and by QCM-D exponential (except for the third layer). These differences between the SPR and QCM-D multilayer growth observation can be attributed to the measurement of entrapped water by QCM-D at each adsorption step (Table 6.2).

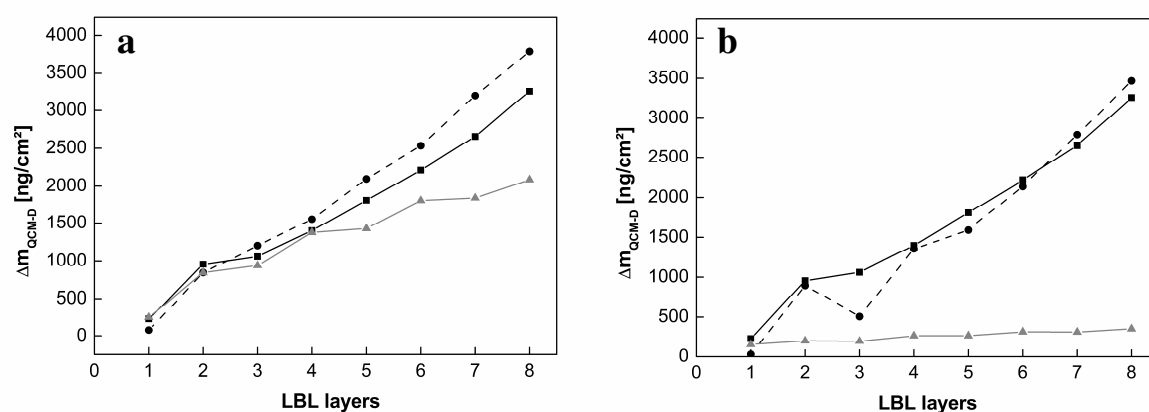


Figure 6.2: The mass for increasing numbers of layers in the multilayer structures obtained by QCM-D using the Sauerbrey equation. Layer 1 is always PEI. Even layers: polyanions, odd layers: polycation CHI. **[a]** $\Delta m_{\text{QCM-D}}$ for the CHI-HEP (Solid lines, ■), CHI-CS1.6 (gray solid lines, ▲) and CHI-(HEP+CS1.6) (dashed lines, ●) systems. **[b]** $\Delta m_{\text{QCM-D}}$ for the CHI-HEP (Solid lines, ■), CHI-CS2.6 (gray solid lines, ▲) and CHI-(HEP+CS2.6) (dashed lines, ●) systems.

The dissipation results showed oscillating increasing and decreasing ΔD values upon adsorption of CHI and HEP, respectively which points towards a swelling or stiffening of multilayers. On the other side, the CHI-CS1.6 system showed an almost linear increase with addition of either CHI or CS1.6 indicating a more homogeneous nature of the films³⁴ while the CHI-CS2.6 system seemed to be a condensed system as the dissipation values were very low and remained almost constant. The dissipation curves for the blend systems also showed alternating trends like CHI-HEP system. For both CHI-(HEP+CS1.6) and CHI-(HEP+CS2.6)

systems, the dissipation values decreased with adsorption of polyanions (HEP+CS1.6 / HEP+CS2.6) and increased with CHI adsorption with an exception of third layer adsorption in case of CHI-(HEP+CS2.6) system. Here, the CHI adsorption as third layer showed no increase in the dissipation value. The results of both SPR and QCM-D provides a strong indication towards the preferential adsorption of HEP over CS in the blend multilayers. In case of CHI-(HEP+CS1.6) multilayer system, HEP seems to be preferentially incorporated within the layers. This is suggested from the multilayer growth curves obtained from SPR and QCM-D (Figure 6.1a & 6.2a), which are similar to the CHI-HEP multilayer growth curves (exponential). Interestingly for CHI-(HEP+CS2.6) blend system, the multilayer growth trend achieved through SPR shows a striking similarity with pure CHI-CS2.6 system (also staircase-like), but not during the QCM-D measurements when also the coupled water comes into play. Then, the adsorbed mass pattern (Figure 6.2b) and dissipation curves (Figure 6.3b) of CHI-(HEP+CS2.6) followed the trend of CHI-HEP system. The higher mass adsorption with high amount of entrapped water (Table 6.2) and the alternating dissipation values give a clear indication of HEP dominance. In both type of blend multilayers of HEP and CS, HEP seems to be the preferentially incorporated polyanion, when they were paired with CHI. This indicates that carboxylic groups play certainly a major role here, as HEP that contains also carboxylic groups along with sulfate has shown his striking dominance over CS which have only sulfate groups. Also to add up, carboxylic groups have a great affinity towards the surrounding water (considered as a kosmotrope),³⁸ which is in line with the higher water content of the blend multilayer systems (Table 6.2). Interestingly, previous studies by Crouzier et al. showed a preferential interaction between sulfate groups and amino groups compared to carboxylic groups during multilayer formation of glycosaminoglycans and poly-L-lysine.²² Although, no direct evidence for a preferential interaction of carboxylic

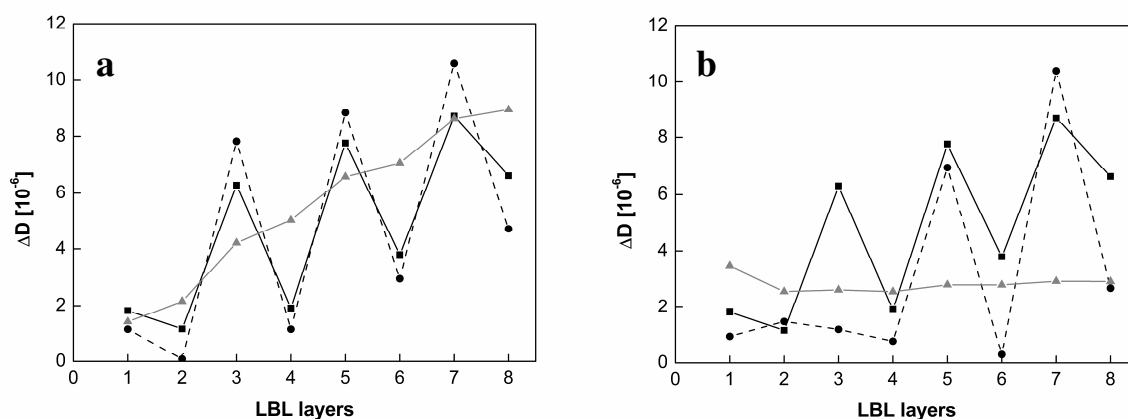


Figure 6.3: The corresponding QCM-D dissipation change (ΔD) in the multilayer structures observed by QCM-D. Layer 1 is always PEI. Even layers: polyanions, odd layers: polycation CHI. **[a]** ΔD for the CHI-HEP (Solid lines, ■), CHI-CS1.6 (gray solid lines, ▲) and CHI-(HEP+CS1.6) (dashed lines, ●) systems. **[b]** ΔD for the CHI-HEP (Solid lines, ■), CHI-CS2.6 (gray solid lines, ▲) and CHI-(HEP+CS2.6) (dashed lines, ●) systems.

Table 6.2: Illustration of Multilayer mass and water content

| Multilayer systems | Γ_{SPR}^a (ng/cm ²) | Δm_{QCM-D}^b (ng/cm ²) | Water content ^c |
|---|---|---|-------------------------------|
| 8 th layer [CHI-HEP] | 812 | 3257 | 75% |
| 8 th layer [CHI-CS1.6] | 924 | 2085 | 56% |
| 8 th layer [CHI-(HEP+CS1.6)] | 769 | 3793 | 80% |
| 8 th layer [CHI-CS2.6] | 796 | 354 | - |
| 8 th layer [CHI-(HEP+CS2.6)] | 792 | 3467 | 77% |

^{a)} SPR masses were estimated using equation (1); ^{b)} QCM-D masses were estimated using the Sauerbrey equation and the frequency shift at the 5th overtone; ^{c)} apparent water content was approximated by $(m_{QCM-D} - m_{SPR})/m_{QCM-D} * 100$.

6.4.2. Measurements of wetting properties

Static water contact angle (WCA) measurements are frequently used for the characterization of the terminal layer composition during multilayer deposition.^{10,34} Here, they were also used to study the wetting properties of the multilayer systems after the deposition of each layer as shown in Figure 6.4. An alternating trend of WCA values was obtained with CHI-HEP multilayers where WCA were lower when HEP was adsorbed while it was higher with CHI adsorption. Such alternating WCA differences with progression of each layer reflect the varying molecular composition of the terminating layer and points toward the formation of more separated layers constituted either from HEP or CHI observed also in other studies.^{34,10} On the contrary, CHI-CS1.6 multilayer system did not show such alternating WCA values as demonstrated in Figure 6.4a. The average WCA were also quite high for the CHI-CS1.6 layers and only slight changes in WCA were observed after the subsequent addition of CS1.6 and CHI. This suggests that the layers formed here were not sharply separated but rather intermingled. In addition, the WCA measurements suggest that terminal layers are dominated by one polyelectrolyte that is probably CS1.6 as also suggested by SPR data. However the WCA of CHI-(HEP+CS1.6) blends displayed alternating values like CHI-HEP system, which indicates again a dominating incorporation of HEP over CS1.6, when their blend was adsorbed as a polyanion. Although it is also noteworthy that the average WCA were higher for the blend system in comparison to pure CHI-HEP system, which points to a subdued presence of CS1.6 forming a ternary system with the other polyelectrolytes. Figure 6.4b illustrates that the changes in the WCA of CHI-CS2.6 multilayers were only small with adsorption of each layer which also points towards the formation of less separated multilayers of both CHI and CS2.6. While when CS2.6 was replaced by its blend with HEP during multilayer formation, an oscillating trend of WCA similar to CHI-HEP system was found. Though the WCA differences for CHI-(HEP+CS2.6) system from one to next layer were smaller than those of the CHI-HEP system. The achieved oscillating WCA suggested a changing composition of the terminal layers through blending of CS2.6 with HEP and indicated that HEP is an important partner of CHI in formation of ternary systems. The results again points towards the dominating presence of HEP in CHI-(HEP+CS2.6) multilayers which is also consistent with multilayer growth data as shown above.

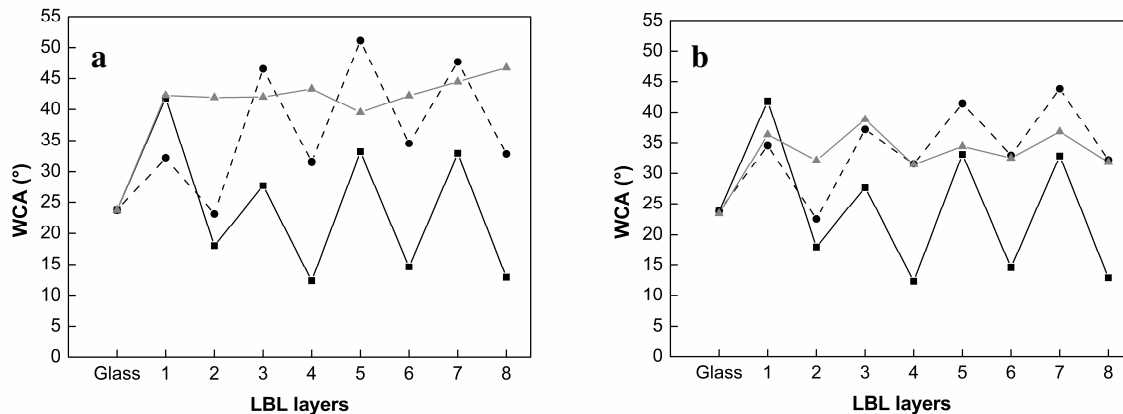


Figure 6.4 Static water contact angles (WCA) during multilayer formation up to 8 layers. Layer 1 is always PEI. Even layers: polyanions, odd layers: polycation CHI. [a] WCA for the CHI-HEP (Solid lines, ■), CHI-CS1.6 (gray solid lines, ▲) and CHI-(HEP+CS1.6) (dashed lines, ●) systems. [b] WCA for the CHI-HEP (Solid lines, ■), CHI-CS2.6 (gray solid lines, ▲) and CHI-(HEP+CS2.6) (dashed lines, ●) systems.

6.4.3. Adhesion measurements and morphological studies of C2C12 cells on multilayers

Cell adhesion and spreading are prerequisites for growth and differentiation.⁶ Polyelectrolyte multilayer coatings on implants and tissue engineering scaffolds have been also suggested before for the improvement of cell behaviour.³⁹ Therefore C2C12 cells were seeded on the different multilayer surfaces (terminal polyanion, 8th layer) for 4 h to learn about the effect of multilayer molecular composition on the cell attachment and their morphological features. C2C12 cells were seeded in the culture medium supplemented with 10% fetal bovine serum that contains adhesion proteins.⁴⁰ C2C12 were chosen as a model as they can differentiate into myotubes or osteoblast-like cells based on their environmental conditions like properties of substrata and presence of osteogenic growth factors.^{41-42,17} After seeding and incubating for 4 h, cells were stained with fluorescein diacetate (FDA) and the micrographs which were taken from the microscope were used for analysis of cell count and size. Figure 6.5 depicts the results of quantitative evaluation of both cell count (Figure 6.5a) and their average size (Figure 6.5b). The cell count as well as the cell spreading (cell size) were found to be significantly lower on both CHI-HEP and CHI-(HEP+CS1.6) multilayer systems in comparison to the other three CHI-CS1.6, CHI-CS2.6 and CHI-(HEP+CS2.6) systems. This lower number of adhering cells and their low degree of spreading on CHI-HEP multilayers is related to their inability to bind adhesive proteins like fibronectin, as already observed in previous studies.^{43,28} Although HEP should bind fibronectin,⁷ results of cell adhesion studies

indicate that this is not the case. Obviously, the conformation of HEP in the multilayer systems created by ion-pairing is unfavourable to interact with HEP-binding domains of proteins, which was also found by others with low binding of BMP-2 growth factor to HEP.²² On the other hand, we found previously that CHI-CS1.6 multilayers are capable of fibronectin adsorption and support of cell adhesion and growth.¹⁸ Although, fibronectin represents a minor compound in serum as attachment factor, also the other vitronectin, which is majorly present in the serum possesses also a HEP-binding domain and promotes cell adhesion and focal adhesion formation⁴⁴. Similar to the CHI-CS1.6, CHI-CS2.6 multilayer systems promoted also significant cell adhesion and spreading, which indicates likewise to CS1.6 that CS2.6 have also supported the adsorption of adhesive serum proteins. In case of blend multilayers, the CHI-(HEP+CS1.6) multilayer system had shown low cell count and spreading, very much similar to CHI-HEP multilayers. This again indicates along with the data from QCM-D and WCA studies a dominating presence of HEP in CHI-(HEP+CS1.6) blend system. HEP as dominating polyanion blocks obviously the cellular interactions on these blend layer surfaces like in CHI-HEP system. By contrast, the CHI-(HEP+CS2.6) multilayers provided the best surface for cell attachment and spreading. The cell count and spreading was much higher than on CHI-HEP layers and also they had shown improved cell count in comparison to CHI-CS2.6 multilayers. Here, it might be speculated that conformation of HEP in these ternary system of CHI-(HEP+CS2.6) is quite different than the other systems [CHI-HEP and CHI-(HEP+CS1.6)]. The improved bioactivity of such blend system also points towards the importance highly sulfated CS2.6 which was when mixed with HEP has positively affected its interactions with the surrounding adhesion proteins in turn with the cells.

The morphology of C2C12 cells supports finding of the quantitative studies and are shown in Figure 6.5c & 6.6. The morphology of cells shown in Figure 6.5c depicts that cells were round and on CHI-HEP and CHI-(HEP+CS1.6) multilayers (Figure 6.5c -i and iii). Oppositely elongated and well spread C2C12 cells were found on CHI-CS1.6 and CHI-(HEP+CS2.6) multilayer surfaces (Figure 6.5c -ii and v). CHI-CS2.6 multilayers (Figure 6.5c -iv) provoked more cell spreading and better attachment of cells in comparison to CHI-HEP and CHI-(HEP+CS1.6) multilayers but weakly in comparison of CHI-CS1.6 and CHI-(HEP+CS1.6) multilayers. Immune fluorescence studies show the staining of actin cytoskeleton by BODIPY-phalloidin (red) and focal adhesions with vinculin by a monoclonal antibody (green). On CHI-HEP multilayers, cells were poorly attached, got detached during the washing steps included in the immunofluorescence staining procedure.

Hence no cells were detected on these multilayers during the microscopic survey (no image of cells on CHI-HEP multilayers in Figure 6.6). Along with it, CHI-(HEP+CS1.6) systems also did not provoked a noticeable cell count and cell spreading on their surface (Figure 6.6b). Contrastingly well attached and spread cells were observed on CHI-CS1.6 multilayer surfaces (Figure 6.6a) with longitudinal stress fibres and well developed focal adhesions which indicate the integrin ligation to adhesive proteins from serum since cells were seeded in the presence of serum. Adhesion and spreading are dependent on the ligation of integrin molecules that are expressed in focal adhesions by integrin clustering.⁴⁵ The cells on terminal CS2.6 layers (Figure 6.6c) showed longitudinal actin fibres but less focal adhesions where as the CHI-(HEP+CS2.6) multilayers had expressed well developed focal adhesion plugs with actin fibres (Figure 6.6d). For better visualization of actin cytoskeleton and focal adhesions, we provide separate images of actin and vinculin staining in “supplementary information” (Figure S6.1). It is well known that cell adhesion is a prerequisite for further cell growth and during adhesion, ligation of integrins to extracellular matrix leads to prevention of apoptosis and promote signalling.⁴⁶ Hence, the initial cell responses observed here can be taken as indications of further growth and differentiation of cells.

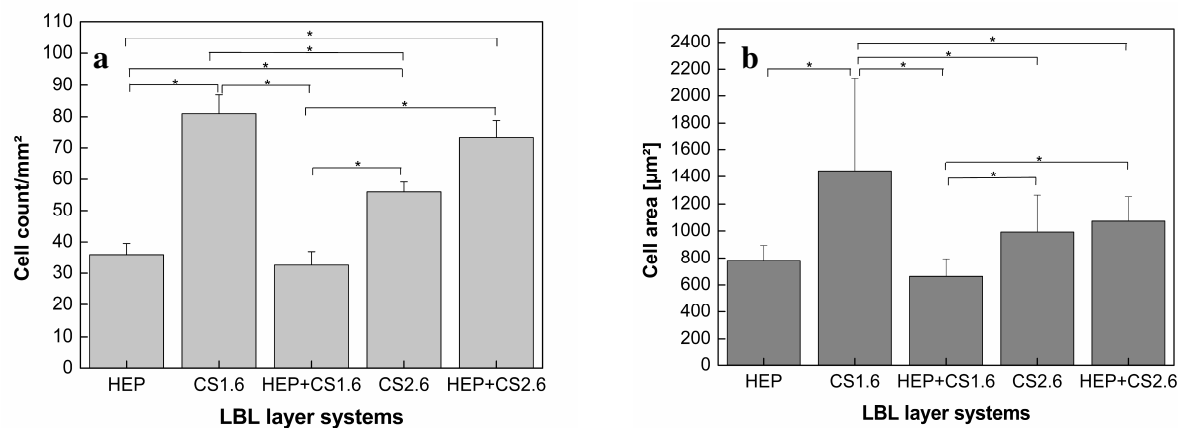


Figure 6.5: Adhesion (left, **6.5a**) and size (right, **6.5b**) of C2C12 cells plated 4 hours in DMEM with 10 % FBS on polyanion (HEP/CS1.6/HEP+CS1.6/CS2.6/HEP+CS2.6) terminated multilayers. Data represent means, standard deviations and ANOVA. Significance level of $p \leq 0.05$ is indicated by the asterisks.

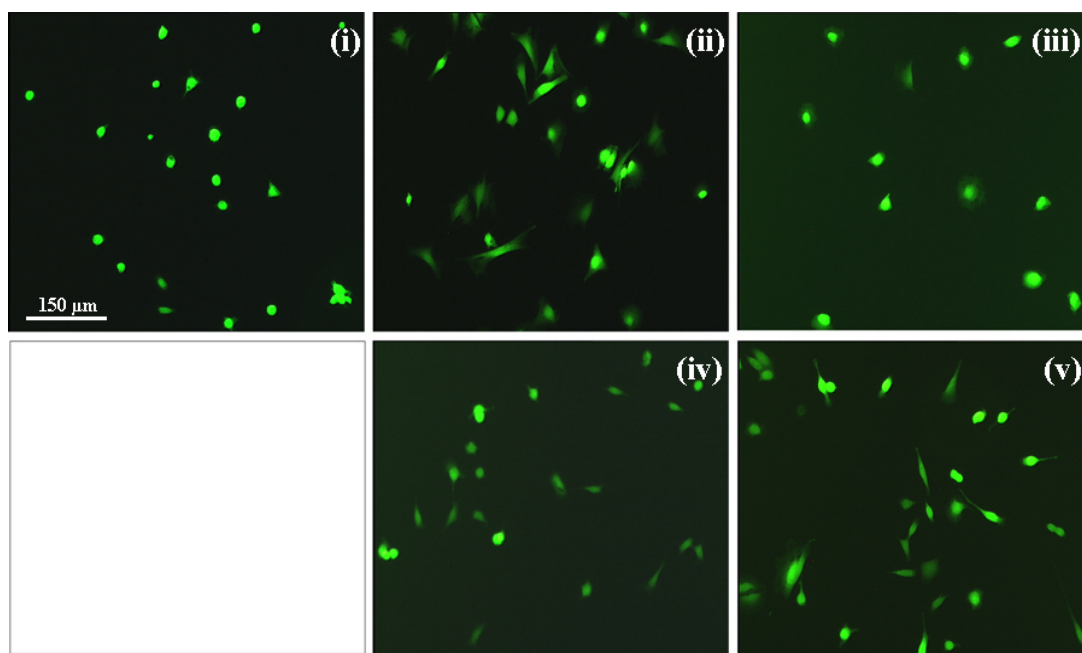


Figure 6.5c: Fluorescence images of C2C12 cells plated on (i) CHI-HEP, (ii) CHI-CS1.6, (iii) CHI-(HEP+CS1.6), (iv) CHI-CS2.6 and (v) CHI-(HEP+CS2.6) multilayers in DMEM and 10% FBS for 4 hours.

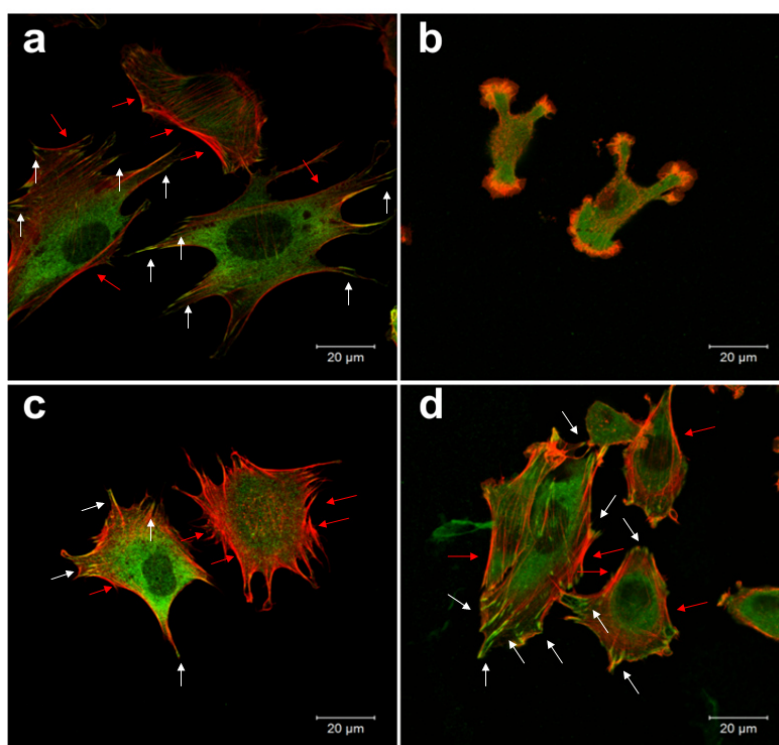


Figure 6.6: Fluorescence images of C2C12 cells plated on (a) CHI-CS1.6, (b) CHI-(HEP+CS1.6), (c) CHI-CS2.6 and (d) CHI-(HEP+CS2.6) multilayers in DMEM and

10% FBS for 4 hours. The red staining shows actin and green vinculin of cells. White arrows show focal adhesions positive for vinculin. Red arrows show actin stress fibres.

6.5. Conclusions

The preparation of polyelectrolyte multilayers via facile LBL technique offers the creation of a wide range of biomaterial coatings with potential adjustment of bioactivity towards proteins and cells. Here, we presented a comparative study on physical and biological multilayer film properties prepared from HEP, semi-synthetic CS and their blends. It was shown that blending of HEP with two different CS resulted in multilayers that differ dramatically in their bioactivity. Although HEP tended to displace major parts of both the intermediately and highly sulfated CS, the latter was obviously able to provoke a conformation of HEP that supported adsorption of adhesive proteins from serum and attachment of cells. Although the exact molecular mechanism of superior bioactivity of HEP in blends with highly sulfated CS_{2.6} was not unravelled here, but showed directions how the bioactivity of glycosaminoglycans in multilayer coatings can be tailored towards a specific type of protein and cell. Since HEP is a natural glycosaminoglycan with limited abundance, cellulose sulfates represent potential alternative materials in making bioactive surface coatings as well as diluting agent of HEP in blends, thereby merging the useful properties of natural and semi-synthetic polyelectrolytes. Overall, the blending of polyelectrolytes with different bioactivity in multilayer coatings provides additional possibilities to regulate multilayer properties and their biological response, which makes them useful for a large variety of biomedical application reaching from blood contacting surfaces to implant materials. We also propose that conformation of HEP and other polyelectrolytes in the different multilayer systems might be characterised by using detailed X-ray diffraction analysis and further details of molecular interactions and dynamics can be studied by solid state NMR in future investigations.

6.6. Acknowledgements

This work was funded partly by Deutsche Forschungsgemeinschaft under grant agreements GR1290/7-1 & GR1290/7-2, FI755/4-1 & FI755/4-2. The synthesis and characterization of cellulose sulfates by Dr. Kai Zhang from Technical University Darmstadt is highly appreciated. We are also thankful to Dr. Sofia Svedhem and Noomi Altgärde for their kind support during the QCM-D studies.

6.7. References

1. Decher G, Hong JD, Schmitt J. Buildup of ultrathin multilayer films by a self-assembly process: III. Consecutively alternating adsorption of anionic and cationic polyelectrolytes on charged surfaces. *Thin Solid Films* 1992;210–211, Part 2(0):831-835.
2. Boudou T, Crouzier T, Ren K, Blin G, Picart C. Multiple Functionalities of Polyelectrolyte Multilayer Films: New Biomedical Applications. *Advanced Materials* 2010;22(4):441-467.
3. Gribova V, Auzely-Velty R, Picart C. Polyelectrolyte Multilayer Assemblies on Materials Surfaces: From Cell Adhesion to Tissue Engineering. *Chemistry of Materials* 2011;24(5):854-869.
4. Schlenoff JB, Ly H, Li M. Charge and Mass Balance in Polyelectrolyte Multilayers. *Journal of the American Chemical Society* 1998;120(30):7626-7634.
5. Quinn JF, Johnston APR, Such GK, Zelikin AN, Caruso F. Next generation, sequentially assembled ultrathin films: beyond electrostatics. *Chemical Society Reviews* 2007;36(5):707-718.
6. Shin H, Jo S, Mikos AG. Biomimetic materials for tissue engineering. *Biomaterials* 2003;24(24):4353-4364.
7. Capila I, Linhardt RJ. Heparin - Protein interactions. *Angewandte Chemie-International Edition* 2002;41(3):391-412.
8. Powell AK, Yates EA, Fernig DG, Turnbull JE. Interactions of heparin/heparan sulfate with proteins: Appraisal of structural factors and experimental approaches. *Glycobiology* 2004;14(4):17r-30r.
9. Pike DB, Cai SS, Pomraning KR, Firpo MA, Fisher RJ, Shu XZ, Prestwich GD, Peattie RA. Heparin-regulated release of growth factors in vitro and angiogenic response in vivo to implanted hyaluronan hydrogels containing VEGF and bFGF. *Biomaterials* 2006;27(30):5242-5251.
10. Kirchhof K, Hristova K, Krasteva N, Altankov G, Groth T. Multilayer coatings on biomaterials for control of MG-63 osteoblast adhesion and growth. *Journal of Materials Science: Materials in Medicine* 2009;20(4):897-907.

11. Crouzier T, Picart C. Ion Pairing and Hydration in Polyelectrolyte Multilayer Films Containing Polysaccharides. *Biomacromolecules* 2009;10(2):433-442.
12. Franz G, Alban S. Structure-activity relationship of antithrombotic polysaccharide derivatives. *International Journal of Biological Macromolecules* 1995;17(6):311-314.
13. Groth T, Wagenknecht W. Anticoagulant potential of regioselective derivatized cellulose. *Biomaterials* 2001;22(20):2719-2729.
14. Gericke M, Doliska A, Stana J, Liebert T, Heinze T, Stana-Kleinschek K. Semi-Synthetic Polysaccharide Sulfates as Anticoagulant Coatings for PET, 1-Cellulose Sulfate. *Macromolecular Bioscience* 2011;11(4):549-556.
15. Zhang K, Peschel D, Klinger T, Gebauer K, Groth T, Fischer S. Synthesis of carboxyl cellulose sulfate with various contents of regioselectively introduced sulfate and carboxyl groups. *Carbohydrate Polymers* 2010;82(1):92-99.
16. Peschel D, Zhang K, Aggarwal N, Brendler E, Fischer S, Groth T. Synthesis of novel celluloses derivatives and investigation of their mitogenic activity in the presence and absence of FGF2. *Acta Biomaterialia* 2010;6(6):2116-2125.
17. Peschel D, Zhang K, Fischer S, Groth T. Modulation of osteogenic activity of BMP-2 by cellulose and chitosan derivatives. *Acta Biomaterialia* 2012;8(1):183-193.
18. Aggarwal N, Altgärde N, Svedhem S, Zhang K, Fischer S, Groth T. Effect of Molecular Composition of Heparin and Cellulose Sulfate on Multilayer Formation and Cell Response. *Langmuir* 2013;29(45):13853-13864.
19. Pilbat A-M, Szegletes Z, Kóta Z, Ball V, Schaaf P, Voegel J-C, Szalontai B. Phospholipid Bilayers as Biomembrane-like Barriers in Layer-by-Layer Polyelectrolyte Films. *Langmuir* 2007;23(15):8236-8242.
20. Gong X, Wang S, Moses D, Bazan GC, Heeger AJ. Multilayer polymer light-emitting diodes: White-light emission with high efficiency. *Advanced Materials* 2005;17(17):2053-+.
21. Quinn A, Such GK, Quinn JF, Caruso F. Polyelectrolyte Blend Multilayers: A Versatile Route to Engineering Interfaces and Films. *Advanced Functional Materials* 2008;18(1):17-26.

22. Crouzier T, Szarpak A, Boudou T, Auzély-Velty R, Picart C. Polysaccharide-Blend Multilayers Containing Hyaluronan and Heparin as a Delivery System for rhBMP-2. *Small* 2010;6(5):651-662.
23. Hubsch E, Ball V, Senger B, Decher G, Voegel JC, Schaaf P. Controlling the growth regime of polyelectrolyte multilayer films: Changing from exponential to linear growth by adjusting the composition of polyelectrolyte mixtures. *Langmuir* 2004;20(5):1980-1985.
24. Quinn JF, Yeo JCC, Caruso F. Layer-by-layer assembly of nanoblended thin films: Poly(allylamine hydrochloride) and a binary mixture of a synthetic and natural polyelectrolyte. *Macromolecules* 2004;37(17):6537-6543.
25. Francius G, Hemmerle J, Voegel JC, Schaaf P, Senger B, Ball V. Anomalous thickness evolution of multilayer films made from poly-L-lysine and mixtures of hyaluronic acid and polystyrene sulfonate. *Langmuir* 2007;23(5):2602-2607.
26. Sun JQ, Zou S, Wang ZQ, Zhang X, Shen JC. Layer-by-layer self-assembled multilayer films containing the organic pigment, 3,4,9,10-perylenetetracarboxylic acid, and their photo- and electroluminescence properties. *Materials Science & Engineering C-Biomimetic and Supramolecular Systems* 1999;10(1-2):123-126.
27. Kirchhof K, Andar A, Yin HB, Gadegaard N, Riehle MO, Groth T. Polyelectrolyte multilayers generated in a microfluidic device with pH gradients direct adhesion and movement of cells. *Lab on a Chip* 2011;11(19):3326-3335.
28. Aggarwal N, Altgårde N, Svedhem S, Michanetzis G, Missirlis Y, Groth T. Tuning Cell Adhesion and Growth on Biomimetic Polyelectrolyte Multilayers by Variation of pH During Layer-by-Layer Assembly. *Macromolecular Bioscience* 2013;13(10):1327-1338.
29. Aksoy EA, Hasirci V, Hasirci N, Motta A, Fedel M, Migliaresi C. Plasma Protein Adsorption and Platelet Adhesion on Heparin-Immobilized Polyurethane Films. *Journal of Bioactive and Compatible Polymers* 2008;23(6):505-519.
30. Zhang K, Brendler E, Geissler A, Fischer S. Synthesis and spectroscopic analysis of cellulose sulfates with regulable total degrees of substitution and sulfation patterns via C-13 NMR and FT Raman spectroscopy. *Polymer* 2011;52(1):26-32.
31. Patel N, Davies MC, Hartshorne M, Heaton RJ, Roberts CJ, Tendler SJB, Williams PM. Immobilization of Protein Molecules onto Homogeneous and Mixed

- Carboxylate-Terminated Self-Assembled Monolayers. *Langmuir* 1997;13(24):6485-6490.
32. Schasfoort RBM, Tudos, A. J. , editor. *Handbook of Surface Plasmon Resonance*. 1st ed. Cambridge: RSC Publishing; 2008. 128 p.
 33. Sauerbrey G. Verwendung von Schwingquarzen zur Wägung dünner Schichten und zur Mikrowägung. *Zeitschrift für Physik* 1959;155(2):206-222.
 34. Lundin M, Solaqa F, Thormann E, Macakova L, Blomberg E. Layer-by-Layer Assemblies of Chitosan and Heparin: Effect of Solution Ionic Strength and pH. *Langmuir* 2011;27(12):7537-7548.
 35. Boddohi S, Killingsworth CE, Kipper MJ. Polyelectrolyte multilayer assembly as a function of pH and ionic strength using the polysaccharides chitosan and heparin. *Biomacromolecules* 2008;9(7):2021-2028.
 36. Sui Z, Salloum D, Schlenoff JB. Effect of Molecular Weight on the Construction of Polyelectrolyte Multilayers: Stripping versus Sticking. *Langmuir* 2003;19(6):2491-2495.
 37. Koetse M, Laschewsky A, Jonas AM, Wagenknecht W. Influence of Charge Density and Distribution on the Internal Structure of Electrostatically Self-assembled Polyelectrolyte Films. *Langmuir* 2002;18(5):1655-1660.
 38. Asthagiri D, Schure MR, Lenhoff AM. Calculation of Hydration Effects in the Binding of Anionic Ligands to Basic Proteins. *The Journal of Physical Chemistry B* 2000;104(36):8753-8761.
 39. Richert L, Lavallo P, Vautier D, Senger B, Stoltz JF, Schaaf P, Voegel JC, Picart C. Cell Interactions with Polyelectrolyte Multilayer Films. *Biomacromolecules* 2002;3(6):1170-1178.
 40. Steele JG, Johnson G, Underwood PA. Role of serum vitronectin and fibronectin in adhesion of fibroblasts following seeding onto tissue culture polystyrene. *Journal of Biomedical Materials Research* 1992;26(7):861-884.
 41. Boudou T, Crouzier T, Nicolas C, Ren K, Picart C. Polyelectrolyte Multilayer Nanofilms Used as Thin Materials for Cell Mechano-Sensitivity Studies. *Macromolecular Bioscience* 2011;11(1):77-89.

42. Ballester-Beltrán J, Cantini M, Lebourg M, Rico P, Moratal D, García A, Salmerón-Sánchez M. Effect of topological cues on material-driven fibronectin fibrillogenesis and cell differentiation. *Journal of Materials Science: Materials in Medicine* 2012;23(1):195-204.
43. Kirchof K. Nanostrukturierte Biomaterialbeschichtungen zur Steuerung von Zelladhäsion und -proliferation: pH-Wert-abhängige Multischichten aus Heparin und Chitosan in diskreter und Gradientenform. Halle (Saale), Germany: Martin-Luther-University, Halle-Wittenberg, Germany; 2009.
44. Groth T, Altankov G, Kostadinova A, Krasteva N, Albrecht W, Paul D. Altered vitronectin receptor (αv integrin) function in fibroblasts adhering on hydrophobic glass. *Journal of Biomedical Materials Research* 1999;44(3):341-351.
45. Guillame-Gentil O, Semenov O, Roca AS, Groth T, Zahn R, Vörös J, Zenobi-Wong M. Engineering the Extracellular Environment: Strategies for Building 2D and 3D Cellular Structures. *Advanced Materials* 2010;22(48):5443-5462.
46. Clark EA, Hynes RO. Ras activation is necessary for integrin-mediated activation of extracellular signal-regulated kinase 2 and cytosolic phospholipase A(2) but not for cytoskeletal organization. *Journal of Biological Chemistry* 1996;271(25):14814-14818.

6.8. Supplementary Information

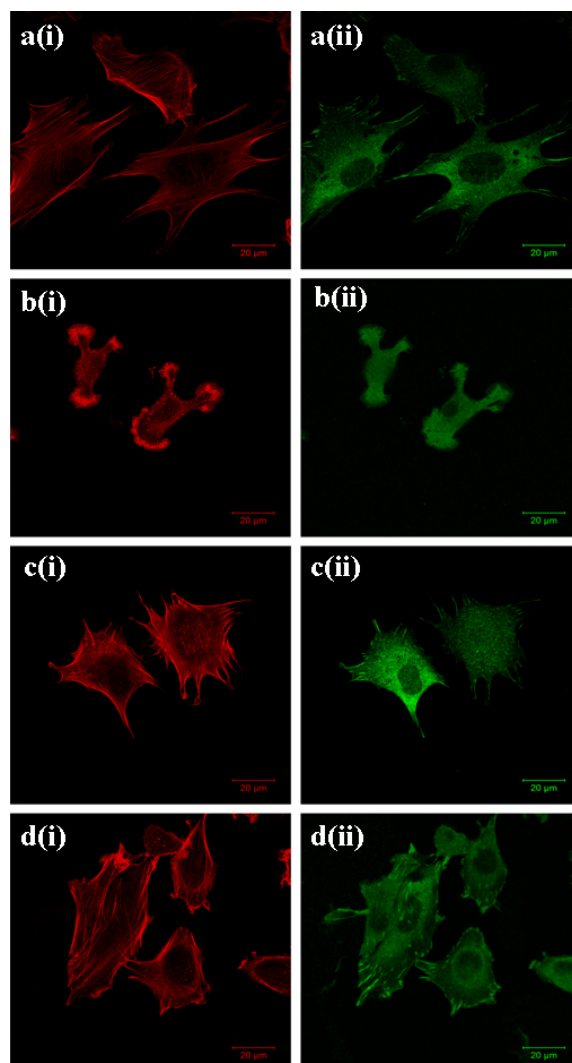


Figure S6.1: Fluorescence images of C2C12 cells plated on (a-i, ii) CHI-CS1.6, (b-i, ii) CHI-(HEP+CS1.6), (c-i, ii) CHI-CS2.6 and (d-i, ii) CHI-(HEP+CS2.6) multilayers. The left column of images show cells stained in red positive for actin while right one the green for vinculin for clear visuals of actin fibres and focal adhesions.

Chapter 7

Conclusions and Outlook

The PhD study was aimed to develop nanostructured multilayer surface coatings by exploiting distinct polyanions at different pH conditions to guide cell adhesion and growth. Here, multilayers prepared with three different polyanions (HEP, CS1.6, and CS2.6) paired with CHI as polycation, showed varying bulk and surface properties along with specific effects on cell behaviour. The selection of polyanions with varying degree of sulfation and adjustment of pH during multilayer assembly provided a tool to control multilayer properties and, with this, protein adsorption and cell interactions. The current study showed that by simple adjustment of the HEP solution pH during multilayer assembly, PEM coatings of HEP and CHI led to unique properties tailoring adhesion and growth of C2C12 cells. Additionally, pH variation also influenced the wettability of terminal layers as well as rendered differences in biomolecular mass adsorption during layer build-up and distinct surface morphology of resulting multilayers.

Semi-synthetic CS that were prepared with heparinoid features depicted their abilities to modulate growth factor-induced proliferation of 3T3 cells and even stronger mitogenic effects than HEP. Due to the remarkable bioactivity of CS, it was reasonable to use them as potential candidates for HEP substitution, since HEP is a natural GAG with limited abundance and large variation of bioactivity depending on source and isolation conditions. Thus, they were also immobilized along with HEP to assemble LBL multilayer films that were characterized physico-chemically and biologically to acquire a deeper knowledge about their construction, effect of molecular composition and bioactivity as surface coatings. Later on, the effect of changing pH values during multilayer build-up was also studied for PEM prepared with CS1.6 (middle sulfated CS). However, these layers did not show such dependency on pH value in comparison to the other systems since only low differences in properties and cell behaviour were found. Hence, these results depicted that CS is an attractive candidate for multilayer formation that does not depend strongly on pH during multilayer formation and provides an attractive substrate for cell immobilisation. Since blending of PEL is also an attractive innovation of the LBL technique that provides more opportunities to tailor the multilayer properties, it was additionally applied here by mixing CS with HEP during adsorption of polyanions. The results showed that HEP was preferentially incorporated and

tended to displace both the intermediately and highly sulfated CS. Merging of the useful properties of natural and semi-synthetic PEL and also diluting HEP as GAG with limited abundance provided additional possibilities to regulate multilayer properties and their biological response. Overall, these extensive studies showed that pH variation during multilayer deposition is a useful tool to tailor the properties and biological responses of the multilayers. Finally, semi-synthetic CS as a another very important prospective as multilayer component was investigated, which proved to be a potential alternative material in designing surface coatings and which very well promoted adhesion and growth of cells. Such multilayer systems might be useful for bioactive coatings of TE constructs and implants for regeneration of bone and other tissues.

The current work opens another end regarding the functionality of such distinct multilayers and their ability for a sustained delivery of biomolecules like growth factors. Since CS are capable of binding growth factors like FGF-2 or BMP-2 in a similar manner like HEP, it is motivative to use the HEP- and CS-based multilayers as potential reservoirs and delivery systems for growth factors and similar molecules. Preliminary experiments were performed at the end of this study to test the release potential of HEP- and CS1.6-based multilayers. For these investigations, a higher number of multilayers was deposited (up to 9 bilayers) at pH 4 because these multilayers were thicker with more absorbed molecules, which, in turn, might be able to bind more ligands and provide more efficient conditions for sustained release of growth factors. BMP-2 (Genescript, USA) was uploaded at a concentration of 250 ng ml^{-1} for 48 h on CHI/HEP and CHI/CS1.6 multilayers.

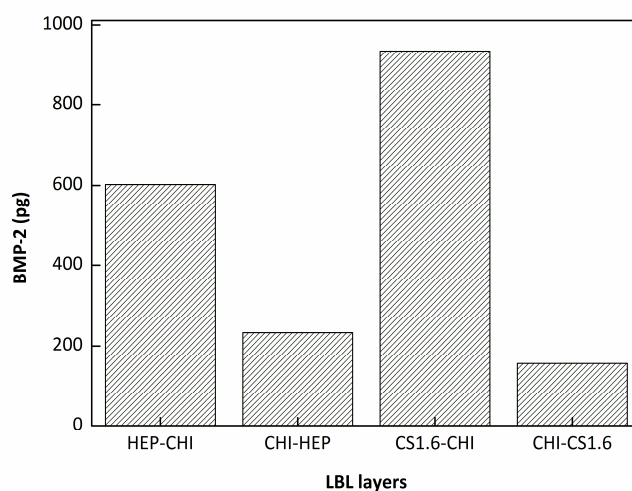


Figure 7.1: Released amounts of BMP-2 from different multilayer systems after 22 days detected and evaluated by ELISA method. HEP/CHI and CS1.6/CHI indicates the CHI

terminating layers, while CHI/HEP and CHI/CS1.6 shows the polyanion (HEP and CS1.6) terminating layers.

After loading, each well was washed once with 100 μ l PBS (pH 7.4) followed by addition 100 μ l of fresh PBS to each well and stored at 4°C on a shaker. The amount of released BMP-2 was determined after 22 days by a BMP-2 ELISA (Enzyme-linked immunosorbant assay) development kit (Peprotech GmbH, Germany). The results showed that CS-based multilayers released higher quantities of BMP-2 in comparison to the HEP ones (see figure 7.1).

It is important to note that only CHI-terminating multilayers were able to substantially release BMP-2 to a higher degree, whereas the polyanion-terminating multilayers released comparatively low amounts. However, these preliminary results require extended investigations related to the uploading and study of release kinetics of BMP-2. From this point of view and also regarding the interactions of FN with the multilayers, it is of high importance to study the conformation of PEL within the different multilayer systems by using X-ray diffraction analysis and other methods such as solid-state nuclear magnetic resonance (NMR) for further details of molecular interactions and dynamics in the future.

Acknowledgements

This PhD has been a challenging and truly a life changing experience for me. During the course of my PhD, many people have contributed and extended their help and support without which this thesis would not have been possible. I would like to convey my deepest gratitude to all of them in this acknowledgement.

I would like to express my cordial gratitude to my mentor Prof. Dr. Thomas Groth for his advice, help, constant support and guidance during the course of my PhD. He always made sure that I remain focused and encouraged me to strive for excellence and reach the set goals of my PhD. I am grateful to him for the knowledge which he imparted via stimulating scientific discussions, lectures etc. I could not have asked for a better supervisor who has helped me not only on the professional front, but also on family front.

I am greatly thankful to the collaborative work with different research groups around the globe. I extend my sincere thanks to Dr. Kai Zhang and Prof. Dr. Steffan Fisher for the synthesis of cellulose derivatives and fruitful discussions related to the ongoing work on cellulose derivatives. I would like to express my gratitude to Noomi Altgärde and Dr. Sofia Svedhem for their assistance while working with QCM-D instrument, and sharing expertise regarding QCM-D and SPR as well as with data analysis. I would also like to thank Dr. Georgios Michanetzis for assistance while working with AFM and Prof. Dr. Yannis Missirlis for providing me the opportunity to work in his lab in Patras, Greece and for fruitful discussions.

I also want to extend my thanks to Mrs. Marlis Porobin for technical support and for managing all the official things for us. I would also like to thank all the group members of Biomedical Materials Group for favours and support.

I am deeply indebted to my family and friends in Halle and worldwide for constant encouragement, help and support and creating a conducive environment for my research work.

I gratefully acknowledge the financial support from Martin-Luther-University Halle-Wittenberg, Deutsche Forschungsgemeinschaft and the European Union Seventh Framework Program (FP7/2007-2013) which enabled me to complete my PhD research.

Abbreviations

| | |
|-----------------|--|
| AFM | - Atomic force microscopy |
| AGU | - Anhydro glucose unit |
| ALP | - Alkaline phosphatase |
| BMP | - Bone morphogenic protein |
| BSA | - Bovine serum albumin |
| CHI | - Chitosan |
| CHS | - Chondroitin sulphate |
| CLSM | - Confocal laser scanning microscopy |
| CM | - Cellulose sulfate containing carboxymethyl |
| CO | - Cellulose sulfate containing carboxyl |
| COL | - Collagen |
| CS | - Cellulose sulfate |
| DA | - Degree of <i>N</i> -acetylation |
| DMAc | - Dimethylacetamide |
| DMEM | - Dulbecco's modified Eagle medium |
| DMF | - N,N-dimethylformamide |
| DMSO | - Dimethyl sulfoxide |
| DO | - Degree of oxidation |
| DP | - Degree of polymerisation |
| DS | - Dextran sulfate |
| DS _s | - Degrees of substitution with sulfate |
| ECM | - Extra cellular matrix |
| ED | - Effective dose |
| EGF | - Epidermal growth factor |
| ELISA | - Enzyme-linked immunosorbant assay |
| ERK | - Extracellular-regulated kinase |
| FA | - Focal adhesion |
| FAK | - Focal adhesion kinase |
| FBR | - Foreign body reaction |
| FBS | - Fetal bovine serum |
| FDA | - Fluorescein diacetate |

| | |
|------|-------------------------------------|
| FGF | - Fibroblast growth factor |
| FN | - Fibronectin |
| FNG | - Fibrinogen |
| GAG | - Glycosaminoglycan |
| GEL | - Gelatin |
| HEP | - Heparin |
| HA | - Hyaluronan |
| IC | - Irradiated cellulose |
| IPA | - Isopropyl alcohol |
| ITO | - Indium tin oxide |
| ITS | - Insulin-transferrin-selenium |
| LB | - Langmuir-Blodgett |
| LBL | - Layer-by-layer |
| MAP | - Mitogen activated proteins |
| MAPK | - Mitogen-activated protein kinase |
| MCC | - Microcrystalline cellulose |
| MMPs | - Matrix metalloproteinases |
| MSC | - Mesenchymal stem cells |
| MUDA | - Mercaptoundecanoic acid |
| NMR | - Nuclear magnetic resonance |
| PAA | - Poly (acrylic acid) |
| PAH | - Poly (allylamine hydrochloride) |
| PBS | - Phosphate buffered saline |
| PEG | - Poly (ethylene glycol) |
| PEL | - Polyelectrolytes |
| PEM | - Polyelectrolyte multilayers |
| PEI | - Poly (ethylene imine) |
| pFN | - Plasma fibronectin |
| PGA | - Poly (L-glutamic acid) |
| pI | - Isoelectric point |
| PIM | - Porcine intestinal mucosa |
| PLL | - Poyl-l-lysine |
| PSF | - Penicillin-streptomycin-fungizone |
| PSS | - Poly (styrene sulfonate) |

| | |
|-------|--|
| QCM-D | - Quartz crystal microbalance with dissipation |
| RGD | - Arginine-glycine-aspartate |
| Rho | - Ras homolog gene family |
| RI | - Refractive index |
| RT | - Room temperature |
| SAMs | - Self-assembled monolayers |
| SEC | - Size exclusion chromatography |
| SPR | - Surface plasmon resonance |
| TE | - Tissue engineering |
| TEMPO | - 2,2,6,6-tetramethylpiperidine-1-oxyl radical |
| TGF | - Transforming growth factor |
| VN | - Vitronectin |
| WCA | - Water contact angle |

Publication list with declaration of self contribution

1. D. Peschel, K. Zhang, N. Aggarwal, E. Brendler, S. Fischer and T. Groth

Synthesis of novel celluloses derivatives and investigation of their mitogenic activity in the presence and absence of FGF2, *Acta Biomaterialia*, 6 (2010) 2116-2125

My contribution was about 20%. I made the cytotoxicity measurements and also assisted in measurements of mitogenic effects. I contributed to the manuscript in writing the related paragraphs..

2. N. Aggarwal, N. Altgärde, S. Svedhem, G. Michanetzis, Y. Missirlis and T. Groth

Tuning Cell Adhesion and Growth on Biomimetic Polyelectrolyte Multilayers by Variation of pH During Layer-by-Layer Assembly, *Macromolecular Bioscience*, 13 (2013) 1327-1338

My contribution was about 75%. I performed all the measurements and wrote the manuscript. Ms. N. Altgärde and Dr. S. Svedhem assisted me in QCM-D measurements and also were involved in revising the manuscript draft. Dr. G. Michanetzis and Prof. Missirlis supported me during AFM measurements, which I did under their supervision. Prof. T. Groth was involved in planning the experiments, discussing results and contributed during revision of the manuscript.

3. N. Aggarwal, N. Altgärde, S. Svedhem, K. Zhang, S. Fischer and T. Groth

Effect of Molecular Composition of Heparin and Cellulose Sulfate on Multilayer Formation and Cell Response, *Langmuir*, 29 (2013) 13853-13864

My contribution was about 70%. I made all measurements and wrote the manuscript. Dr. K. Zhang synthesized and characterized the cellulose sulfates. Ms. N. Altgärde and Dr. S. Svedhem supported me in QCM-D measurements and were included in revising the manuscript. Prof. T. Groth assisted in planning all the experiments and contributed in revising the manuscript.

4. N. Aggarwal, N. Altgärde, S. Svedhem, K. Zhang, S. Fischer and T. Groth

Study on multilayer structures prepared from heparin and semi-synthetic cellulose sulfates as polyanions and their influence on cellular responses, *Colloids and Surfaces B: Biointerfaces*. "Accepted for publication – In press"

My contribution was about 70%. I conducted all experimental work except the synthesis and characterization of cellulose sulfates, which were done by Dr. K. Zhang the. Ms. N. Altgärde and Dr. S. Svedhem assisted me in QCM-D measurements and also helped in revising the manuscript. Prof. T. Groth supported the planning of experiments and and contributed during the revision of the manuscript.

5. N. Aggarwal and T. Groth

Multilayer films by blending heparin with semi-synthetic cellulose sulfates: physico-chemical characterisation and cell responses, *Journal of Biomedical Materials Research Part A*, “Accepted for publication – In press”

My contribution was about 90%. I made all the measurements and prepared the manuscript. Prof. T. Groth helped me in planning all the experiments and made some contributions during the revision of the manuscript.

Other publications that are not involved in this thesis

6. A.S. Asran, K. Razghandi, N. Aggarwal, G.H. Michler and T. Groth

Nanofibers from Blends of Polyvinyl Alcohol and Polyhydroxy Butyrate As Potential Scaffold Material for Tissue Engineering of Skin, *Biomacromolecules*, 11 (2010) 3413-3421.

Book Chapter

7. M.S. Niepel, A. Köwitsch, Y. Yang, N. Ma, N. Aggarwal, G. Guduru, T. Groth

Generic Methods of Surface Modification to Control Adhesion of Cells and Beyond, In: Taubert A, Mano JF, Rodríguez-Cabello JC (eds.), *Biomaterials Surface Science*, Chapter 15, pp. 443-468, Wiley-VCH, 2013.

Curriculum Vitae

Neha Aggarwal

Weinberg 3
06120 Halle (Saale)

Email: neha.aggarwal@pharmazie.uni-halle.de

Date of Birth: 16. Februar 1984

Place of Birth: Palwal (Haryana), India

Nationality: Indian

Academic Qualifications

02/2009 – till date **PhD Candidate** (Supervisor: Prof Dr. Thomas Groth) at
Martin-Luther-University Halle-Wittenberg, Germany

08/2005 - 08/2007 HNB Garhwal University at SBSPGI (Dehradun) Uttaranchal, India
Master of Science (M.Sc.) in Biotechnology
Dissertation: “Studies in relation to Adaptation of Thermotolerance in
Peanut (*A. hypogaea*) Suspension Culture”
Grade: First Class

07/2002 - 07/2005 Delhi University, India
Bachelor of Science (B.Sc.) in Biology
Grade: First Class

Work Experience

06/2008 - 01/2009 Trainee in Biomedical Materials Group, Institute of Pharmacy,
Martin-Luther-University Halle-Wittenberg, Halle (Saale)

09/2007 - 11/2007 Research assistant in “Centre for Science & Technology of Non-
Aligned and other developing Countries” (NAM S & T Centre),
New-Delhi, India

Awards

- | | |
|---------|--|
| 10/2011 | Student Travel Award by the German Academic Exchange Service (DAAD) |
| 10/2011 | Osborne award for Outstanding Scientific Achievements 2011", granted by the International Federation of Artificial Organs (IFAO) at 4 th Joint Congress of ESAO-IFAO in Porto, Portugal |

Halle, 08 July 2014

Neha Aggarwal

Eidesstattliche Erklärung

Ich erkläre hiermit, dass ich keine anderen als die von mir angegebenen Quellen und Hilfsmittel zur Erstellung meiner Dissertation verwendet habe. Den benutzen Werken wörtlich oder inhaltlich entnommene Stellen sind als solche gekennzeichnet.

Neha Aggarwal
Halle(Saale), 08 July 2014